Engineering Library
anal ol
DEC 3 - 1934

UNITED STATES DEPARTMENT OF COMMERCE

JOURNAL OF RESEARCH
OF THE
NATIONAL BUREAU OF STANDARDS

Vol. 13 NOVEMBER 1934 No. 5

CONTENTS

RP.	TITLE AND AUTHOR		Page
729.	Fractionation of the isotopes of hydrogen and of oxygen in a commercial electrolyzer. By Edward W. Washburn, Edgar R. Smith, and Francis A. Smith	[Price 5c]	599
730.	Relation of paper properties to register in offset lithography. Charles G. Weber	[Price 5c]	609
731.	Determination of sulphur and sulphate in wool. Ralph T. Mease	[Price 5c]	617
732.	Second spectrum of hafnium (Hf II). William F. Meggers and Bourdon F. Scribner	[Price 5c]	625
733.	Ionization of liquid carbon disulphide by X-rays. Fred L. Mohler and Lauriston S. Taylor	[Price 5c]	659
734.	Preparation of pure gallium. James I. Hoffman	[Price 5c]	665
735.	Freezing point of gallium. Wm. F. Roeser and James I. Hoffman	[Price 5c]	673
736.	A note on bactericidal effects of X-rays. Fred L. Mohler and Lauriston S. Taylor	[Price 5c]	677
737.	Gold-chromium resistance alloys. James L. Thomas	[Price 5c]	681
738.	Resistivity of sulphuric-acid solutions and its relation to viscosity and temperature. George W. Vinal and D. Norman Craig	[Price 5c]	689
739.	A temperature-control box for saturated standard cells. E. F. Mueller and H. F. Stimson	[Price 5c]	699
740.	Polymerization of olefins formed by the action of sulphuric acid on methylisopropylcarbinol. Gordon M. Kline and Nathan L. Drake	[Price 5c]	705
741.	Compression tests of structural steel at elevated temperatures. Prentiss D. Sale	[Price 5c]	713
742.	Effect of cold-rolling on the indentation hardness of copper. John G. Thompson	[Price 5c]	745

[The articles listed above may be purchased (see cover p. II) separately at the prices indicated in the table of contents]

A monthly periodical of pure and applied science published by our National Government

JOURNAL OF RESEARCH
OF THE
NATIONAL BUREAU OF STANDARDS

¶The July 1934 issue of the Journal of Research of the National Bureau of Standards begins the thirteenth semiannual volume of this periodical. The JOURNAL contains the Bureau's research papers and critical reviews in the fields of science and technology. ¶Fundamental researches always in progress in the Bureau's laboratories have their outlet in the Journal of Research of the National Bureau of Standards. If you are interested in following the new developments in science and technology, you should receive the JOURNAL. If you are already a subscriber, continue your subscription; if not, you are invited and urged to send in your subscription at once.

TECHNICAL NEWS BULLETIN

¶This is a monthly publication containing short articles reporting progress of work in the Bureau's laboratories, abstracts of papers which appear in the Journal of Research of the National Bureau of Standards, reports of scientific and technical meetings in which the Bureau has taken part, and a list of all publications by members of the staff, and other topics within the Bureau's fields. This publication is designed primarily to give its subscribers a general review of important and timely activities and accomplishments at the Bureau. The material is presented in brief but adequate form, for the information of those who are interested in the general activities of the Bureau. It is a prompt and reliable source of official information. If you are not already a subscriber to this monthly periodical you are urged to place your subscription.

ANNUAL SUBSCRIPTION	Prices	
	United States, Canada, Cuba, Mexico, Newfoundland, Republic of Panama	Other countries
Journal of Research of the National Bureau of Standards:		
12 monthly issues (2 volumes), paper covers	$2.50	$3.25
Bound volume (½ year, 1 volume), blue buckram . . .	3.00	3.50
Technical News Bulletin, 12 monthly issues	.50	.70

Research Papers, reprinted individual articles appearing in the Journal of Research, are available from the Superintendent of Documents shortly after appearance of monthly issue of the JOURNAL.

Address orders only to
Superintendent of Documents, U. S. Government Printing Office,
Washington, D.C.

UNITED STATES DEPARTMENT OF COMMERCE
DANIEL C. ROPER, Secretary
NATIONAL BUREAU OF STANDARDS
LYMAN J. BRIGGS, Director

JOURNAL OF RESEARCH
OF THE
NATIONAL BUREAU OF STANDARDS

November 1934
Vol. 13, No. 5

UNITED STATES
GOVERNMENT PRINTING OFFICE
WASHINGTON : 1934

For sale by the Superintendent of Documents, Washington, D.C. - - Price 25 cents; $2.50 per year on subscription

Beginning with the July 1934 issue of the Journal of Research of the National Bureau of Standards, the prices of the separate Research Papers appearing in the monthly issues are given on the front cover of the Journal.

A 25-percent discount is allowed when ordering 100 or more copies of any separate.

This arrangement will provide a prompt and convenient method whereby readers of the Journal of Research desiring copies of separate Research Papers appearing therein may send their orders without delay to the Superintendent of Documents, United States Government Printing Office, Washington, D.C., and will aid him in determining the number of copies to be printed for sale purposes.

U.S. DEPARTMENT OF COMMERCE NATIONAL BUREAU OF STANDARDS

RESEARCH PAPER RP729

Part of Journal of Research of the National Bureau of Standards, Volume 13, November 1934

FRACTIONATION OF THE ISOTOPES OF HYDROGEN AND OF OXYGEN IN A COMMERCIAL ELECTROLYZER[1]

By Edward W. Washburn, Edgar R. Smith, and Francis A. Smith

ABSTRACT

The electrolytic fractionation of the isotopes of hydrogen and of oxygen under the conditions prevailing in a commercial hydrogen-oxygen electrolyzer have been followed by means of measurements of density. Upon electrolysis of ordinary water, the change in its density at the beginning is caused as much by the fractionation of oxygen as of hydrogen. Curves showing the course of the fractionation of the separate isotopes are given. After an amount of water approximately equal to 10 times the volume of a commercial alkaline cell has been electrolyzed, a steady state is closely approached in which no further isotopic fractionation occurs. In this state the gases evolved have the isotopic composition existing in the water added to the cell, and the residual water left in the cell is 60 ppm heavier than ordinary water. Of this 60 ppm, 28 are contributed by the heavy isotope of hydrogen, indicating an electrolytic fractionation factor of 2.4 under the conditions described.

CONTENTS

		Page
I.	Introduction	599
II.	Description of the electrolytic cell	600
III.	The measurements	603
IV.	Fractionation of the isotopes	605
V.	Discussion	607

I. INTRODUCTION

Since the announcement of the electrolytic method for the concentration of deuterium,[2] electrolysis has become the universal method of separating deuterium and of making "heavy water". Notwithstanding the large number of papers dealing with heavy water which have already appeared, much elementary work still remains to be done for a better understanding of the electrolytic method. In the original communication,[3] it was stated that some concentration of the O^{18} isotope of oxygen also appeared possible, and in the first paper of this series [4] it was shown that the concentration of O^{18} actually occurred. In the present investigation, a study has been made of the simultaneous electrolytic fractionation of the isotopes of hydrogen and of oxygen under the conditions which prevail in a commercial cell from the time the cell is filled with fresh electrolyte until equilibrium has been reached. By equilibrium is meant the steady state which is attained after the cell has been in continuous operation with the continuous addition of ordinary water for such a length of time that the hydrogen and oxygen evolved have the same

[1] This investigation was completed and the manuscript prepared by the junior authors after the death of Dr. Edward W. Washburn on February 6, 1934.
[2] Edward W. Washburn and H. C. Urey, Proc. Nat. Acad. Sci. **18**,496(1932).
[3] See footnote 2.
[4] E. W. Washburn, E. R. Smith, and M. Frandsen, BS J.Research **11**,453(1933); RP601.

isotopic composition as they have in normal water, while the water in the cell has attained an unchanging isotopic composition richer in the heavier isotopes of hydrogen and oxygen. That such an equilibrium condition must eventually occur during the operation of a commercial hydrogen-oxygen cell is obvious [5] from the following considerations. Since the residual water in the cell is always heavier than the water formed by recombining the evolved gases, and at the beginning grows progressively denser as the electrolysis proceeds, a point will be reached where the water from the recombined gases has the same density as ordinary water. At this point ordinary water is being added to and electrolyzed from the cell at the same rate and consequently no further change occurs in the composition of the residual water. It will be seen later (fig. 2) that the evolved hydrogen attains the isotopic composition of normal hydrogen before the evolved oxygen becomes normal in composition. It is therefore of interest and importance to determine the extent of electrolysis required to produce this steady state, and the separate parts played by the hydrogen and oxygen isotopes during its attainment.

II. DESCRIPTION OF THE ELECTROLYTIC CELL

The cell used was a small electrolyzer of the filter-press type, having 56 nickel-plated cast-iron cells in series, and a capacity of 16 liters. The cell plates, which acted as anodes on one side and as cathodes on the other, were separated by asbestos cloth diaphragms, the edges of which were imbedded in rubber to form gaskets.

The electrolyte was an 18-percent solution of sodium hydroxide (5 molal), which was found in this electrolyzer to pass 12 to 15 amperes at 115 volts with a small regulating resistance in series.

Asbestos paper was fastened loosely around the outside of the cell to reduce the effect of drafts upon the temperature of the cell, its resistance, and consequently on the current and the rate of evolution of the gases. Under operating conditions the temperature of the electrolyte was about 60° C.

The cell, together with the regulating and safety devices, and the burner for recombining the gases are shown diagrammatically in figure 1. The path of the oxygen is not shown, but it follows a course similar to that indicated for the hydrogen. When operating at a normal rate, about 3 liters of hydrogen was evolved per minute. A mixture of gas and electrolyte was disgorged into the surge glasses where the continual rising and falling of the level of the liquid produced a pressure fluctuation in the delivery pipe which often amounted to ± 2 inches of water. The flow of gas from the electrolyzer was thus unsteady.

The gases passed through metal pipes surrounded by ice water to reflux as much as possible of the heavier water carried as vapor and liquid by the stream of gas. Thence the gases passed into a flask containing concentrated sulphuric acid, where they were deflected downward on the surface of the acid, depositing more water and a large part of the fog of finely divided sodium hydroxide particles.

[5] H. S. Taylor and H. Eyring, Proc. Am. Phil. Soc. 72,261(1933).

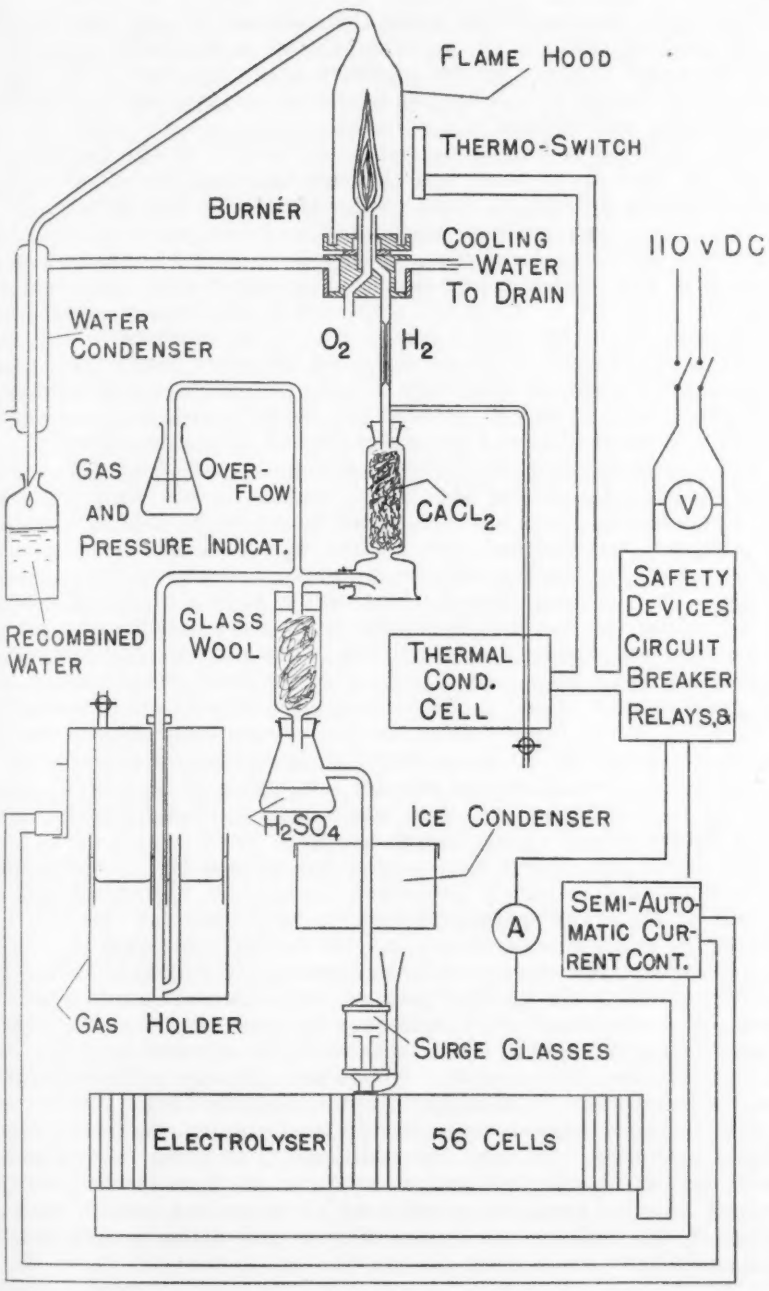

FIGURE 1.—*Electrolytic cell with regulating devices.*

The tower of fine glass wool which follows removed still more of the fog. [6]

The main streams of the gases then passed through towers of 8-mesh calcium chloride, to remove all but a negligible amount of heavier water vapor, through capillary tubes to control the rate of flow [7] and thence to the burner where the oxygen was burned in a surrounding atmosphere of hydrogen.

The water vapor formed by the recombination of the gases passed from the glass flame-hood and through the water-cooled condenser from which it dripped at room temperature into liter bottles.

The burner was made of brass and the lower part was cooled by the water from the condenser, as shown, in order to prevent overheating of the rubber connections. The upper part was separated from the lower by a "transite" disk, and made thermal contact with the burner tube over only a small area. This area was so adjusted that the upper part of the burner, and the glass flame-hood, whose rim rested in a groove filled with dibutyl phthalate, would always be well above 100° C and so prevent the condensation and consequent loss at this point of any of the water formed by combustion.

In order to prevent the fluctuating flow of gases from the electrolyzer from extinguishing the flame, and to insure that the gases delivered to the burner would at all times be in constant relative proportions, water-sealed gas holders of about 20 liters capacity were attached to the line between the glass wool and calcium chloride towers. In operation, these holders were kept near their full position by adjusting the overflow bubblers which were attached to the gas line at the same point as the holders. The purpose of the overflow bubblers was to take care of momentarily excessive pressures, and the holders maintained a nearly constant flow to the burner even though the flow in the line from the electrolyzer was reversed momentarily. Indeed, the 20 liters stored in the holders was sufficient to supply the burner at normal rate for 5 minutes, or for a much longer time at reduced rate, and thus would keep the flame lighted during short interruptions of the power supply.

The hydrogen holder also served to actuate the semiautomatic current control. During prolonged periods of voltage depression caused by abnormal demands for power elsewhere, the rate of evolution of the gases was decreased and the holder, supplying the burner at a constant rate, consequently became partly emptied. When the holder bell fell to the half-full position, a contact was made which, by means of a relay, cut out a resistance in series with the electrolyzer. The resulting increase in the current could be adjusted as desired and was usually about 2 amperes. This was ordinarily sufficient to refill the holder, which on reaching its full position broke the contact, cutting in the resistance and restoring the system to its former condition of operation. In case the additional 2 amperes proved insufficient, and the holder bell fell as much as an inch farther, another contact sounded an alarm summoning an attendant to determine the cause of the reduced evolution of gas and make proper manual adjustments.

[6] It was found that the fog could be removed almost completely by the use of electric precipitation, but this method was abandoned because the accompanying ozone caused troublesome leaks in rubber tubing used for connections.

[7] Cocks on the burner accumulated particles of the sodium hydroxide fog and repeatedly reduced the flow nearly to extinction of the flame, particularly when the burner base was not cooled. Capillaries provide equal resistance with a much larger aperture.

A small quantity of both hydrogen and oxygen was taken from their respective lines at the outlet of the calcium chloride towers and passed through a thermal conductivity cell [8] which served to detect any leakage of hydrogen into the oxygen, or vice versa, through the separators in the electrolyzer. The apparatus was so arranged that increasing contamination of either of the gases would interrupt the current through the electrolyzer and ring an alarm.

In addition, any one of several undesirable situations resulted in automatically opening the main circuit, for example, the extinction of the flame, the heat from which kept closed the contacts of a bimetallic thermostat. Insufficient heat caused the contacts to open, in turn opening the main circuit, which was equipped with a circuit breaker which had to be closed manually before the flow of current could be restored.

The level of the electrolyte was kept practically constant in the electrolyzer by adding 500-ml portions from time to time, and it was found that the ratio of volumes of the water collected to the water added to the electrolyzer during several 5-day runs was approximately 0.95. This indicates a total loss of only about 5 percent. Water vapor was lost to the sulphuric acid, calcium chloride, and at the mouth of the condenser. Gases were lost through the overflow bubblers, the thermal conductivity safety device and the condenser. The loss from the condenser could be followed visually by noting the behavior of a bit of fog which usually pulsated near the mid portion of the condenser tube when the loss was small. Some unburned gases always escaped, because when burning one gas in an atmosphere of the other, an excess of the surrounding gas is required if the first is to be completely burned. When the gases are supplied in equivalent volumes some of each escapes, and precautions should be taken against accidental ignition.

The electrolyzer was operated 24 hours a day, 5 days a week, and was capable of functioning unattended for periods as long as 12 hours. Normally, a momentary inspection was made at half-hour intervals. Thanks are due to A. R. Glasgow, C. N. Miller, and P. Schoonover, who performed this service during their night-shift work on petroleum research.

III. THE MEASUREMENTS

The water formed by recombining the gases was collected continuously in a series of 1-liter fractions at the rate of about 1 liter every 6 hours. The process was carried out at practically constant volume by adding ordinary water to the cell in 500-ml portions in pace with the volume consumed. At definite intervals the procedure was varied by collecting the liter fractions in three equal portions: (a) Oxygen from the cell combined with commercial electrolytic hydrogen, (b) hydrogen from the cell combined with commercial oxygen made from liquid air, (c) hydrogen and oxygen from the cell combined directly as usual. The differences between the densities of these samples and that of purified normal water were then measured at 25° C by the use of the differential pycnometer described in a previous paper.[9]

The commercial electrolytic hydrogen, obtained from the Southern Oxygen Co., whose cells have been in operation for several years, was

[8] See P. E. Palmer and E. R. Weaver, Tech. Pap. BS **18**, 35(1924–1925)T 249.
[9] Edward W. Washburn and Edgar R. Smith, BS J.Research **12**, 305(1934);RP656

shown to be of ordinary isotopic composition by combining it with atmospheric oxygen and comparing the density of the water thus formed with that of ordinary water. The density difference was less than 1 ppm.

The commercial oxygen was assumed at the start to be of ordinary isotopic composition. However, when the series of data was examined it was apparent that the density of the water formed by combining the gases directly from the cell differed from that of normal water by an amount greater than the sum of the differences between normal water and the samples obtained by burning the gases separately with commercial hydrogen and oxygen. That this uniform difference, amounting on the average to 2 or 3 ppm, was not due to water vapor in the commercial gases was shown by collecting and weighing water vapor from the cylinders during a combustion. The weight of water from this source amounted to only 0.05 g for each 100 ml of water formed by combustion, a quantity too small to have any detectable effect on the densities. The source of the discrepancy was finally found to lie in the assumption that commercial oxygen made by the fractionation of liquefied air has the same isotopic composition as atmospheric oxygen.[10] The error of this assumption was demonstrated in the following way: Hydrogen from the same cylinder was burned first with oxygen from the cylinder used in this investigation and then with atmospheric oxygen drawn from outside the building, to form two 400-ml samples of water. Each of these samples was thus composed of identical hydrogen combined in one case with the commercial oxygen from the fractionation of liquefied air and in the other with oxygen from the atmosphere. After purification, the densities of the two samples were compared. The sample prepared from the commercial oxygen was found heavier by 1.4 and 2.4 ppm in successive measurements. Both samples were then repurified and the difference found to be 2.8 ppm. The average of the three values was 2.2 ± 0.5 ppm. The explanation of this difference is that during the fractionation of liquid air to eliminate nitrogen, the difference in mass and vapor pressure of the oxygen isotopes causes a slight isotopic separation so that the residual oxygen compressed in the cylinders is slightly heavier than ordinary atmospheric oxygen. Neglecting the O^{17} isotope, this increase amounts to about 0.002 percent increase in the O^{18} content of the commercial oxygen and doubtless depends somewhat on the efficiency of the fractionating column. The Southern Oxygen Co., from whom the commercial oxygen was also obtained, mix their electrolytic oxygen with the liquid air oxygen but the electrolytic oxygen, which has practically the same isotopic composition as the oxygen of the normal water supplied to the electrolyzers, never amounts to more than 5 percent of the total. A correction of 2.2 ppm was applied to the density measurements on the samples obtained by burning the hydrogen from the cell with the commercial oxygen, in order to obtain the differences in density caused by changes in the isotopic composition of the hydrogen alone. Before these measurements of the slight difference in isotopic composition of atmospheric oxygen and oxygen made from liquefied air were completed, an account of measurements was reported [11] which showed that when liquefied air is fractionated

[10] E. R. Smith, J. Chem. Phys. **2**,298(1934).
[11] R. Klar and A. Krauss, Naturwissenschaften **22**,119(1934).

the oxygen escaping with the nitrogen at the top of a column is richer in the lighter isotopes of oxygen (and the residue of oxygen left in the still is richer in the O^{18} isotope) than atmospheric oxygen.

The increase in density of the water in the cell was also followed as the electrolysis progressed. This was done by stopping the electrolysis at a given point and withdrawing a sample of electrolyte for purification and measurement, after which the water was replaced in the cell and the electrolysis was continued.

When 150 liters had been collected by recombining the gases, it was found that equilibrium had been practically attained, and the hydrogen and oxygen from the cell were very close to their normal isotopic compositions. At this point the electrolysis was stopped. The increase in density of the water in the cell was then determined and its hydrogen content was normalized isotopically by successive treatments with dry ammonia gas [12] until no further decrease in density occurred. By this means an approximate measure of the isotopic composition of the water at equilibrium was obtained.

IV. FRACTIONATION OF THE ISOTOPES

The density of the water formed by recombining the gases at the beginning of the electrolysis, starting with normal water in the cell, was found to be 20.5 ppm less than normal. By burning the gases separately with normal hydrogen and with oxygen corrected to normal 13.2 ppm of this decrease was found to be contributed by the fractionation of the oxygen isotopes and 7.8 ppm by the hydrogen isotopes. At the tenth liter the respective decreases in density were 17.1, 11.0, and 6.2 ppm. The series of measurements was continued until a steady state, consisting in equilibrium water in the cell evolving isotopically normal gases, ensued. The data are given in table 1. The values given in the fourth column for the differences in density between the water formed by burning the hydrogen from the electrolyzer with oxygen corrected to normal were obtained by subtracting 2.2 ppm from the measured values, e.g., the first measured value was −5.6 ppm with the commercial oxygen which yielded water heavier than normal by 2.2 ppm and the corrected value is therefore −7.8 ppm.

TABLE 1.—*Changes in density (in* ppm)

Number of liters collected	Recombined gases	Cell O with normal H	Cell H with normal O	Residual H_2O in cell	Number of liters collected	Recombined gases	Cell O with normal H	Cell H with normal O	Residual H_2O in cell
1	−20.5	−13.2	−7.8		73				+43.0
10	−17.1	−11.0	−6.2		75	−7.3	−5.0	−2.0	
20	−14.8	−10.5	−5.6		105	−5.0	−3.0	−.1	
30	−14.1	−8.0	−5.5	+23.9	124	−3.1	−2.0	+.1	
50	−10.8	−6.3	−3.6		150	−1.5	−1.1	+.2	+57.8

The data of table 1 are shown graphically in figure 2, in which the differences in density between the samples and normal water, expressed in parts per million, are plotted as ordinates and the volumes of water electrolyzed as abscissas. The volumes plotted as abscissas, however, are expressed in terms of the total cell volume, in order to

[12] G. N. Lewis, J. Am. Chem. Soc. 55,3502(1933).

make the curves of general applicability to any commercial nickel-plated iron electrolyzer filled with alkaline electrolyte. Thus abscissa 1 means that in this case 16 liters (the total cell volume) has been electrolyzed while slightly more than 16 liters of normal water has been added to the cell to keep it full. Abscissa 10 means that a volume of water equal to 10 times the capacity of the cell has been electrolyzed, etc. Curve A shows the progressive increase in density of the unelectrolyzed water remaining in the cell, toward a limiting value of about 60 ppm. Curve B represents the portion of this

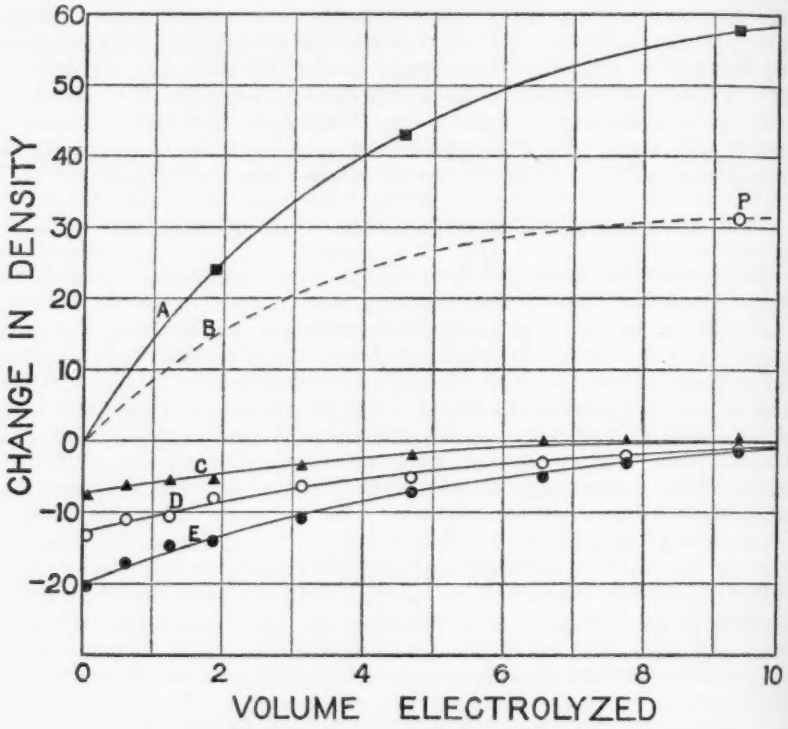

FIGURE 2.—*Progressive changes in density with continued electrolysis.*

The ordinates are values of the differences in density between the samples investigated and normal water, expressed in ppm. The abscissas represent the volumes of water electrolyzed expressed in terms of the volume of the cell. The curves represent the following: A, The change in the residual water in the cell due to fractionation of the isotopes of both hydrogen and oxygen; B, the change due to fractionation of the oxygen isotopes; C, water formed by burning hydrogen from the cell with normal oxygen; D, water formed by burning oxygen from the cell with normal hydrogen; E, water formed by recombining the gases from the cell.

progressive increase which is due to the fractionation of the oxygen isotopes. Point P on curve B was obtained by saturating and desaturating the equilibrium water, having $\Delta D = 57.8$ ppm, with ammonia gas until successive treatments produced no appreciable change in density. The remaining difference in density of 31 ppm in the equilibrium water is the portion resulting from the increased concentration of the heavier oxygen isotopes. The course of curve B between the origin and P was estimated. Curves C and D show the changes in density of the water formed by burning the electrolytic hydrogen from the cell with normal oxygen, and the electrolytic

oxygen from the cell burned with normal hydrogen, respectively. The density of the water formed by recombining the hydrogen and oxygen directly from the cell is shown by curve E.

V. DISCUSSION

It is apparent that a steady state is attained in a commercial alkaline hydrogen-oxygen electrolyzer after an amount of water approximately equal to 10 times the volume of the cell has been electrolyzed, after which no further isotopic fractionation occurs. However, the change in slope of curve A of figure 2 is not very marked at the outset, and indicates that it is economical for the electrolytic production of heavy water from ordinary water to add fresh water to the cell to keep the volume constant until two or three times the volume of the cell has been electrolyzed, before reducing the volume without the further addition of water. Curve A also shows that under the operating conditions described in this work, the density of the equilibrium water is about 60 ppm greater than that of normal water. Three samples of equilibrium water obtained from the Southern Oxygen Co., at different times between December 1931 and February 1933, had excess densities of 52.1, 53.5, and 53.3 ppm, an average of about 53 ppm. The Southern Oxygen Co., uses a 15 percent solution of potassium hydroxide as electrolyte and a current of 300 amperes. When it is considered that more water is lost by evaporation with the less efficient condensing manifold on commercially operated electrolyzers than on the small cell used in this investigation, and that this loss is replaced continually by ordinary water, it is to be expected that commercial equilibrium water should be slightly less concentrated. For this reason, the hydrogen and oxygen gases from commercial electrolyzers operating on their equilibrium water should ordinarily be slightly lighter than normal, respectively, assuming that the electrolyte volume is not allowed to fall below the average level. However, now that commercial equilibrium water is so widely used as the starting material for the production of heavy water, commercial electrolytic hydrogen and oxygen will more often be found lighter than normal because of the disposal of equilibrium water as a by-product. In the case of hydrogen, curve C shows that 8 ppm is the maximum decrease in terms of the density of water formed by burning the gas, and for oxygen curve D shows that 13 ppm is the maximum decrease to be found. These differences correspond to 40 percent less H^2 and 6 percent less O^{18} than in the normal gases. For precise work these variations can readily be determined by combining the gases with their normal complements to form water and measuring the variations in density.

Although the decrease in density of the water formed at the start by recombining the gases from the cell and the increase in density of the residual water in the cell are caused somewhat more by the fractionation of the isotopes of oxygen (curves E and B) than of hydrogen, the O^{18} isotope is present initially in tenfold larger proportion than the H^2 isotope, so that these changes represent really a smaller percentage fractionation of the oxygen than of the hydrogen isotopes. One of the next problems to be undertaken in this series of investigations is to determine how far the oxygen fractionation extends on continued electrolysis of progressively heavier water.

It has been pointed out [13] that the electrolytic fractionation factor, α, defined as the ratio of the relative abundance of the hydrogen isotopes in the solution to that in the gaseous hydrogen leaving the cell, can be readily calculated from a knowledge of the abundance ratio of the isotopes in ordinary water and of the isotopic composition of equilibrium water. In natural hydrogen the abundance ratio H^2/H^1 is probably [14] close to 2.0×10^{-4}. In the equilibrium water, about 32 of the 60 ppm increase in density is contributed by the fractionation of oxygen and 28 by the hydrogen. Dividing 28×10^{-6} by 0.10 (the approximate excess density due to the deuterium in 100 percent deuterium water) gives 2.8×10^{-4} for the increase in proportion of H^2 above that in normal water. To this figure must be added the 2.0×10^{-4} for the proportion of H^2 present in normal water to obtain 4.8×10^{-4} for the ratio H^2/H^1 in equilibrium water. The electrolytic fractionation factor is therefore the ratio 4.8/2.0, or $\alpha=2.4$ for equilibrium water under the experimental conditions of this investigation. This value is of the same order of magnitude as the ratio of the mobilities of the H^1 and H^2 ions.

WASHINGTON, August 15, 1934.

[13] H. C. Urey, Rev. Sci. Instruments, **4**,423(1933).
[14] W. Bleakney and A. J. Gould, Phys. Rev. **44**,265(1933).

U.S. DEPARTMENT OF COMMERCE NATIONAL BUREAU OF STANDARDS

RESEARCH PAPER RP730

Part of Journal of Research of the National Bureau of Standards, Volume 13, November 1934

RELATION OF PAPER PROPERTIES TO REGISTER IN OFFSET LITHOGRAPHY

By Charles G. Weber

ABSTRACT

Additional information has been obtained on the relation of fiber properties of paper to distortion and poor register in offset printing. Made-to-order papers, in the manufacture of which the fiber characteristics were carefully controlled, were tested in the laboratory and printed on a commercial offset press. Data on the closeness of register in printing were correlated with the properties of the papers and history of manufacture.

In previous studies of papers made in one mill of fibers from the same source, it was found that papers with a minimum of hydration or gelatinization of fibers and a maximum of directional difference or grain had the lowest machine direction expansion and gave best register. By the further tests on papers made in different mills of pulps from widely different sources, these findings were found to apply generally to chemical wood-fiber papers. With the chemical wood papers, best register is obtained when the machine direction coeffcient of expansion is lowest. This desirable property is obtained by manufacturing the paper with the minimum of beating and jordanning essential for the required strength and surface quality. For all-rag papers, large directional difference or pronounced grain is apparently not indicative of low expansion and good register.

CONTENTS

	Page
I. Introduction	609
II. Description and properties of papers	610
III. Register studies	611
IV. Summary and conclusions	615

I. INTRODUCTION

In previous study of the relation of paper properties to register of successive color prints in offset printing,[1] and on the influence of atmospheric changes on paper distortion,[2] the mechanical treatment of the paper fibers received in the manufacture of the paper was found to be of great importance. Paper made with a minimum of beating [3] and jordanning [4] gave best register in offset lithography. However, inasmuch as the papers used were from a single mill, and made of pulp from the same source, further studies reported herein were made to determine whether the conclusions based on the previous

[1] BS J.Research **9**,427(1932); RP480.
[2] BS J.Research **12**,53(1934); RP633.
[3] Beating is the term applied to mechanical treatment given papermaking fibers, suspended in water, to prepare them for forming a sheet on the paper machine. Beating separates, brushes, and frays the fibers, and causes them to absorb water by what is commonly termed "hydration".
[4] Jordanning is a refining process that usually follows beating to complete the preparation of papermaking fibers for forming a paper of the desired character. In the jordan, the fibers are freed from lumps and cut to the desired length.

findings relative to the relationship between fiber properties and distortion in offset printing are of general application. Special papers were prepared for this study by cooperating commercial manufacturers, and the experimental printings were made in the air-conditioned pressroom of the United States Coast and Geodetic Survey, Department of Commerce.

This is one of a series of studies made to assist the lithographers in reducing serious economic losses caused by difficulties in offset color printing. The work is being done in cooperation with the Lithographic Technical Foundation, which assists through an advisory committee composed of lithographers, paper manufacturers, and printing-equipment manufacturers appointed by the foundation.

II. DESCRIPTION AND PROPERTIES OF PAPERS

The papers used in the experiments were made according to the following specifications:

Group A.—Chemical wood offset papers made in mill "A". Fibers, 75 percent sulphite, 25 percent soda, wood pulp. Rosin sizing, 2.3 percent by weight. Finish, normal. Number 1 made with absolute minimum of beating and jordanning; no. 2 made from the same stock, with maximum of beating and jordanning commonly used in commercial practice.

Group B.—Nos. 3 and 4, duplicates of nos. 1 and 2, respectively, made in mill "B" of pulps from different sources than those used for group A papers.

Group C.—Nos. 5 and 6, duplicates of nos. 1 and 2, respectively, made in a third mill, "C", of pulps from different sources than those used in groups A and B.

Group D.—Nos. 7 and 8, 100-percent rag papers prepared like nos. 1 and 2, respectively.

Number 9.—A vegetable parchment paper. This type of paper is rendered parchment-like by gelatinizing the fibers with acid, which gives it properties somewhat comparable to a paper hydrated or gelatinized by drastic beating. It was included as being representative of the extreme as regards mechanical treatment of fibers. The test data on the papers are contained in table 1 on page 615.

The effects of increased beating on the physical properties of the papers may be observed from the data in the table by comparing the properties of the two papers in each group. The odd-numbered papers were made with minimum beating, and the even-numbered ones with the maximum. In general, increased beating decreased the machine direction [5] folding strength sharply with relatively little effect on the cross-direction strength; hence, maximum directional difference, or most pronounced grain, was associated with the minimum of beating and jordanning. The papers in group B might appear to offer an exception, but this is explained by the fact that these two papers actually differed little as regards fiber length, both having been jordanned rather hard. Apparently the difference between them may be attributed to hydration only, this being reflected also in the comparatively small difference in expansion. For all-chemical wood papers, the machine direction expan-

[5] Machine direction in paper is the direction parallel to its forward movement on the paper machine in manufacture. The direction at right angle to the machine direction is termed "cross-direction."

sion was lowest with both beating and jordanning at the minimum; a most important property since register in color printing requires a minimum of distortion in the machine direction of the paper.

Air permeability and rate of oil penetration were both greatly decreased by increased beating, indicating closing of the spaces between the fibers in the paper. The greater degree of curl with increased beating is further indication of this closing of the sheet. Beating had no significant effects on the degree of sizing or opacity.

III. REGISTER STUDIES

The special papers were subjected to experimental printings on a commercial offset press, and the closeness of register of color prints was determined for all papers by measuring with a micrometer rule.[6] The press was a 26- by 38-inch Harris offset model of late design in practically new condition. The cylinder dimensions of the press were:

	Plate	Blanket	Impression
	Inches	*Inches*	*Inches*
Bearers	16.000	16.002	15.976
Body	15.590	15.850	15.986

The press-room atmosphere was controlled with an air-conditioning system of conventional type. During the experiments, 43 ±4 percent relative humidity and 75 ±3° F were maintained.

In the first series of printings, five sheets of each paper were printed. The papers were conditioned in a cabinet type of conditioning machine in which room air is blown up through the chamber where the papers are hung. The sheets were hung in "lifts" [7] of two sheets each and left in the conditioning machine for approximately 24 hours to assure complete moisture equilibrium with the press-room air. Six-color printings were made, and the register was determined by measuring the length of each succeeding print on both back and gripper edges.

In these printing tests, the same printing pressures were used for all six colors. The pressure [8] between plate and blanket was equivalent to 0.004 inch. The impression cylinder was set up against the blanket cylinder with just sufficient pressure to give a clear print on the first color, and like pressure was used on all six colors. The register of successive prints in this series is shown graphically for the gripper and back edges of the paper in figures 1 and 2, respectively. Only the long-direction misregister is shown, because misregister in the short or around-the-cylinder direction is relatively unimportant, as it can be corrected by press adjustment.

[6] BS J.Research **9**,431(1932); RP480.

[7] By "lift" is meant the number of sheets of paper placed together in the same clips suspending the paper from the top.

[8] On the type of offset press used, the plate cylinder and blanket cylinder rest one against the other on fixed metal bands or bearers at the ends of the cylinders. When the combined heights of the cylinder bodies between the bearers is not greater than the combined heights of the bearers, the pressure between plate and blanket is zero. Pressure is introduced by placing sheet packing under the blanket and plate to bring the combined body heights of the two cylinders above their combined bearer heights. There is no convenient method of determining the actual pressure, and since it is adjusted by increasing or decreasing the amount of packing, pressure is commonly expressed as being equivalent to the difference between the combined body heights and bearer heights.

It will be noted that, of the chemical wood papers, that is groups A, B, and C, the odd-numbered paper in each group gave better register than the corresponding even-numbered papers in the respective groups. The odd-numbered papers were those prepared with a minimum of beating and jordaning, and having in consequence, the most pronounced grain or directional difference in sheet formation. Paper 9, which was a parchment paper comparable in structure to a paper made with much more drastic mechanical treatment of fibers than any of the other papers, gave correspondingly greater misregister of prints. This further emphasizes the importance of sheet formation with respect to distortion and resulting misregister of prints.

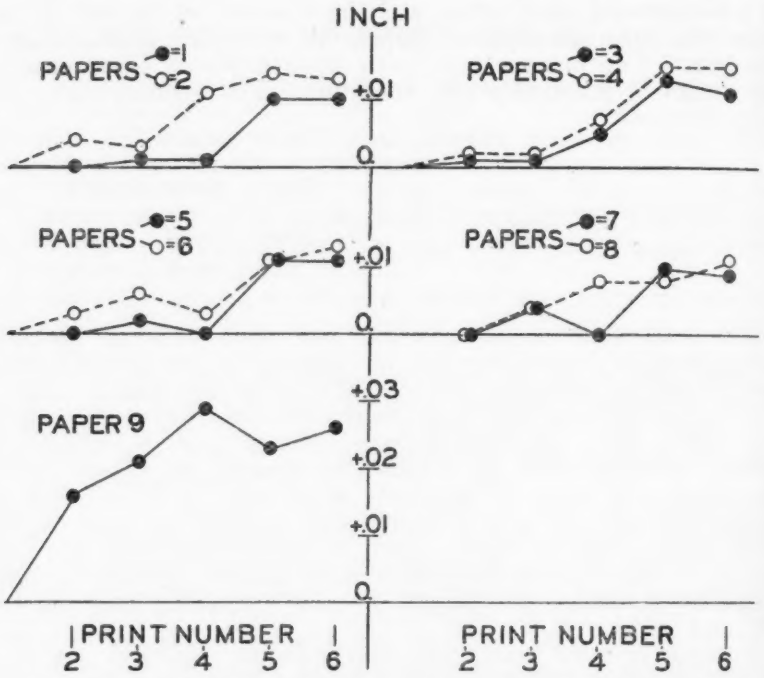

FIGURE 1.—*Relation of prints 2, 3, 4, 5, and 6 to first print length.*

Gripper edge—40-inch image.

NOTE.—Departure from 0 base equivalent to misregister with first color. Odd-numbered papers made with minimum of beating. Pressure on plate cylinder 0.004 inch for all colors.

There was no significant difference between the two rag papers in group D with respect to quality of register in these tests.

To obtain further data on these papers, a second series of printings was made under somewhat different conditions. In these tests, five sheets of each paper, with the exception of no. 9 which gave such poor register in the first printings as to require no further study, were printed. The papers were conditioned as for the first series, but were printed as part of a commercial run. The experimental papers were placed at the bottom of a pile of paper being printed on an airway map job, and were not removed for measuring until five colors had been printed. In these printings, the pressure on the plate cylinder was 0.0033 inch for each of the first two colors, and 0.0035,

0.0030, 0.0040 inch for the third, fourth, and fifth colors, respectively. Register of the fifth color with the first was determined.

As in previous tests with chemical wood papers, those made with the least drastic mechanical treatment of fibers, and having in conse-

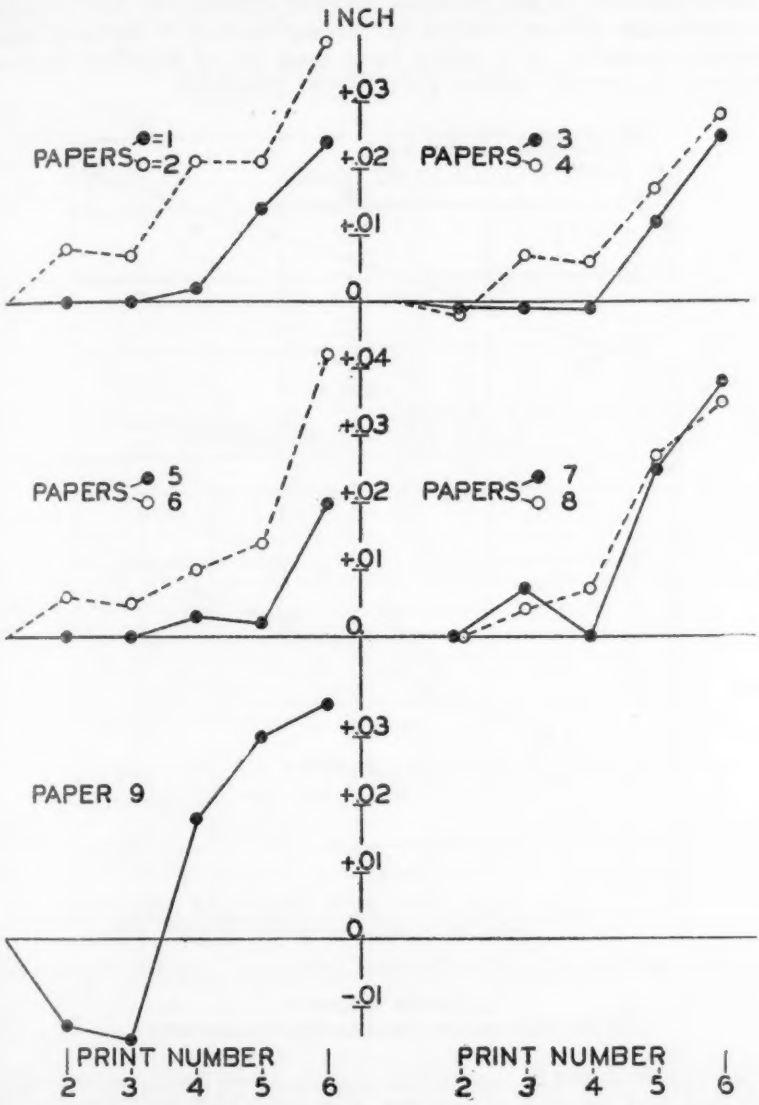

FIGURE 2.—*Relation of prints 2, 3, 4, 5, and 6 to first print length.*

Back edge—40-inch image.

NOTE.—Departure from 0 base equivalent to misregister with first color. Odd-numbered papers made with minimum of beating. Pressure on plate cylinder 0.004 inch for all colors.

quence, the lowest machine direction coefficient of linear expansion, gave the best register. The relationship between the coefficient of expansion and misregister of prints on the chemical wood papers is

shown graphically in figure 3. Separate curves show relationship for this and the preceding series of printings and it is significant that similar regularity of the curves shows that misregister increased directly with the coefficient of expansion. The rate of increase, or slope of the curve, is not the same for the 2 different series of printings because many factors such as ink areas, amount of ink and water, printing pressures, etc., which have been found to affect register[9] are never duplicated exactly for different printings.

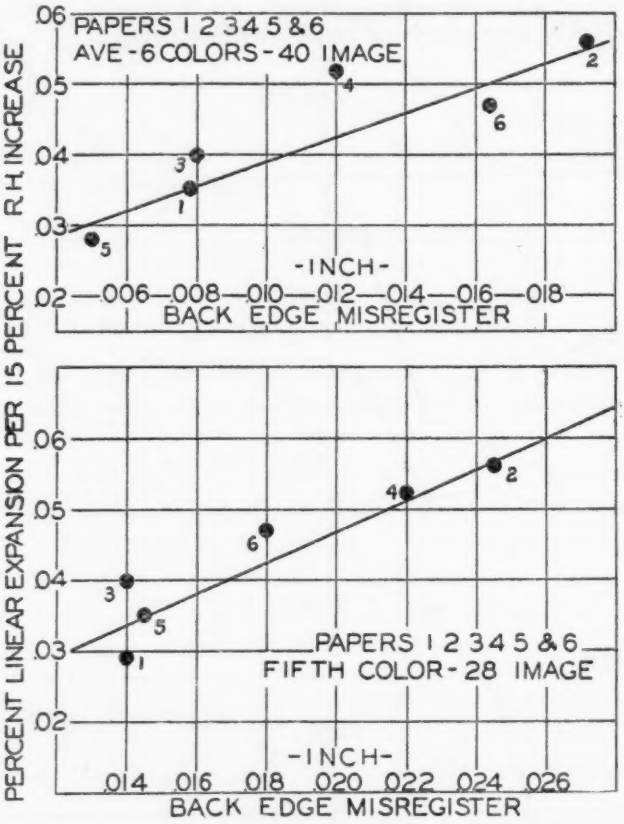

FIGURE 3.—*Relation of machine direction coefficient of expansion to misregister.*

Chemical wood papers.

NOTE.—Odd-numbered papers made with minimum beating.

Papers nos. 7 and 8, the all-rag papers made from the same stock with different degrees of beating, did not differ significantly with respect to register in either series of printings. Also, it will be noted in table 1 that while they differed as regards strength about as might be expected from the difference in mechanical treatment of the fibers, the machine direction expansion was practically the same for both. It appears, therefore, that the different manner in which rag papers respond to mechanical treatment makes the degree of beating and jordanning, so important in the case of wood fiber papers, of little

[9] BS J.Research 9,431(1932); RP480.

importance in rag papers with respect to the best sheet formation for low expansion and good register. The well known fact that cotton rag fibers fray out into threadlike fibrillas, and do not hydrate readily on beating, while the ordinary chemical wood fibers hydrate with very little fraying out, may give a clue to the reasons not clearly understood at present for the different behavior of the rag papers.

TABLE 1.—*Lithographic papers—test data* [1]

Properties	Test data on groups, and papers [2] nos.—								
	A		B		C		D		9
	1	2	3	4	5	6	7	8	
Weight (25 by 40 in., 500 sheets)..lb..	73.1	77.1	72.2	81.9	78.2	76.5	72.8	71.5	68.2
Thickness.....in..	.0054	.0054	.0055	.0058	.0054	.0050	.0051	.0049	.0039
Bursting strength.....points [9]..	26	21	22	27	31	35	26	21	45
Folding endurance [3]..machine..double folds..	52	8	11	19	480	153	71	28	5,860
Folding endurance [3]..cross.....do....	10	5	7	10	35	89	20	10	8,720
Tensile breaking strength [4]..machine.....kg..	6.6	5.7	5.6	7.8	8.8	9.8	6.2	5.5	8.5
Tensile breaking strength [4]..cross.....do....	2.9	2.8	3.3	3.2	3.8	5.2	3.0	2.6	6.2
Degree sizing (dry indicator).....sec..	45	40	47	59	65	73	20	16	300+
Air permeability [5] .cm³/sec/m²/g/cm²..	149.2	69.0	253.9	107.5	468.0	86.5	196.0	98.9	.003−
Oil permeability [6] (castor oil).....sec..	150	240	103	240	65	266	123	139	7200+
Curl [7].....degrees..	50	65	28	48	11	23	45	65	180+
Expansion [8] per 15 percent R H. increase (machine dir.).....percent..	.035	.056	.040	.052	.028	.047	.034	.038	.217
Opacity.....do....	93	95	93	94	96	94	93	93	48
Ash.....do....	7.7	11.3	8.0	10.0	5.8	8.6	8.7	9.7	0.2
Fiber composition..chemical wood..do....	100	100	100	100	100	100			
Fiber composition..rag.....do....							100	100	

[1] All tests, except curl, expansion, air and oil permeability, made by the methods of the Technical Association of the Pulp and Paper Industry.
[2] Odd-numbered papers made with minimum of beating.
[3] For test specimen 15 mm wide and 90 mm between jaws.
[4] For test specimen 15 mm wide and 100 mm between jaws.
[5] Determined with Carson permeability tester. BS J.Research **12**, 567(1934); RP681.
[6] Resistance of printing papers. Tappi Assoc. Papers [XI], no. 1(1928).
[7] Determined with Carson curl tester. Paper Trade J. **79**, 48(1924).
[8] Test specimens 44 in. long.
[9] Bursting pressure in lb/in.² through a circular orifice 1.2 in. in diameter.

IV. SUMMARY AND CONCLUSIONS

The results of trial printings of three groups of special papers made in different mills, of different pulps, confirm previous findings, and justify the following general conclusions relative to chemical wood papers for multicolor offset printing:

1. Lowest machine direction coefficient of linear expansion of paper results in the most satisfactory register of successive color prints.

2. Machine direction expansion of paper is lowest when the greatest number of fibers are parallel to that direction, and the gelatinization of fibers, commonly termed hydration, is at the minimum.

3. The sheet formation with respect to fiber orientation and hydration can be controlled by proper control of the mechanical treatment of fibers in manufacture. Fiber length should be kept at the maximum and hydration at the minimum, by keeping both beating and jordanning at the minimum required for suitable strength and surface quality.

4. The desirable sheet formation is characterized by large directional difference, or grain effect, due to fiber orientation; therefore a high ratio of machine direction to cross direction folding endurance is generally indicative of good formation for close register.

The all-rag papers did not respond in the same manner as the much more widely used type, the chemical wood papers, with respect to the relation of sheet formation to machine direction linear expansion. Hence, control of the mechanical treatment of the fibers did not in itself control expansion. With the present knowledge, the only available method of predicting the register for rag papers is by determining the coefficient of expansion.

Acknowledgment is made of the invaluable assistance of the advisory committee from the Lithographic Technical Foundation under the chairmanship of Prof. R. F. Reed; the U.S. Coast and Geodetic Survey; B. W. Scribner, chief of the paper section of the National Bureau of Standards; and the following manufacturers of the papers studied: Dill & Collins, Inc.; Oxford Paper Co.; West Virginia Pulp & Paper Co.; and Kalamazoo Vegetable Parchment Co.

WASHINGTON, September 7, 1934.

U.S. DEPARTMENT OF COMMERCE NATIONAL BUREAU OF STANDARDS

RESEARCH PAPER RP731

Part of Journal of Research of the National Bureau of Standards, Volume 13, November 1934

DETERMINATION OF SULPHUR AND SULPHATE IN WOOL

By Ralph T. Mease

ABSTRACT

Methods of known precision and accuracy for the quantitative determination of total sulphur and sulphate sulphur in wool are given in this paper and the experimental bases for them are described.

Sulphur is present in wool as an essential constituent of the wool substance, presumably in one constituent of the molecule, the amino acid, cystine. The amount varies with the type and quality of the wool and with the severity of processing. Thus cystine sulphur is of considerable practical significance. Sulphate sulphur is formed in wool through the action of light and other agencies on this sulphur and is acquired by wool from solutions used in carbonizing, dyeing, or finishing. Therefore it is necessary to distinguish between the cystine sulphur of the wool and sulphate sulphur.

The total sulphur in wool is determined by completely oxidizing a specimen in an oxygen bomb, absorbing the oxidized sulphur in ammonium carbonate solution, precipitating and weighing it as barium sulphate. The sulphate sulphur is determined by dissolving a specimen of the wool in hydrochloric acid, precipitating and weighing the sulphate as before. Under the conditions recommended, the dissolved wool does not interfere and the cystine sulphur is not precipitated.

The results reported indicate that with these methods either form of sulphur can be determined to within 2 percent of the amount present.

CONTENTS

		Page
I.	Introduction	617
II.	Preparation of wool for analysis	618
III.	Analysis of wool for total sulphur	618
IV.	Proposed method for total sulphur in wool	619
V.	Analysis of wool for sulphate	621
VI.	Proposed method for determination of sulphate in wool	623

I. INTRODUCTION

Wool protein contains from 3 to 4 percent of sulphur, all of it presumably in one constituent of the molecule, the amino acid, cystine. The amount of this sulphur has been found to vary with the type and quality of the wool. Some of the sulphur is oxidized when wool is damaged by the action of light, sulphuric acid being the end product. Wool is also liable to damage in wet processing with a loss of some of its cystine sulphur. Thus the amount of sulphur in wool has come to be regarded as of considerable practical significance.[1]

Wool may absorb sulphurous and sulphuric acid from air and from solutions used in carbonizing, dyeing, or finishing. The sulphurous acid is readily oxidized to sulphuric acid. The sulphate ion is held tenaciously and cannot be removed completely by extraction with

[1] S. G. Barker. Wool Quality, p. 209 to 223 and literature cited on p. 284 to 328(1931), His Majesty's Stationery Office, London.

water or even with dilute bases without seriously damaging the wool.[2] Therefore, it is often necessary to distinguish between the cystine sulphur of the wool and the sulphate sulphur formed from it or acquired from other sources.

Methods of known precision and accuracy for the determination of total sulphur and sulphate in wool, which are rapid and convenient, were needed in work on the analysis of wool-cotton textiles and on the system wool—sulphuric-acid—water.[3] A number of methods for the determination of the sulphur content of other organic materials have been considered. Most of them require several hours for the destruction of organic material and preparation of the oxidized sulphur for precipitation as barium sulphate. Many require the addition of nonvolatile salts which lower the rate of precipitation of barium sulphate and introduce errors by contaminating the precipitate or which necessitate reprecipitation.

This paper describes the methods for total sulphur and sulphate sulphur which have been found to be satisfactory for the analysis of wool and gives experimental results which indicate the precision and accuracy to be expected.

II. PREPARATION OF WOOL FOR ANALYSIS

The wool for the experiments was chosen from a lot which had been put through a commercial scouring process but had not been carbonized. The remaining visible foreign material was removed by hand and the wool agitated for ½ hour in a 1-percent solution of a neutral soap at 70° C. It was rinsed with distilled water at the same temperature, extracted with alcohol for 16 hours in a Soxhlet extraction apparatus and then with ether for 6 hours. It was air dried, rinsed with distilled water at 70° C, and again dried and conditioned at 70° F and 65-percent relative humidity. The fibers were cut into short lengths and mixed thoroughly.

Sulphate sulphur was introduced into some of this wool by immersing it for 20 minutes in sulphuric acid of about 72-percent concentration, at room temperature. The wool was then extracted with water in an apparatus operating similarly to a Soxhlet extraction apparatus but with the wool at room temperature at all times. The extraction was continuous for 15 hours or more with a total of about 15 liters of distilled water.

The treated wool was air dried and conditioned as before. Wool fibers thus treated lose a portion of their substance, as evidenced by a coloration of the acid solution, and retain sulphur as sulphate which is not removable by extraction with water without serious decomposition of the fiber.

III. ANALYSIS OF WOOL FOR TOTAL SULPHUR

Two methods of analysis for total sulphur in wool received special attention. The well-known Carius method [4] and the oxygen bomb method.[5] The Carius method is generally recognized to be reliable

[2] R. T. Mease and D. A. Jessup. *Analysis of wool-cotton textiles.* BS J. Research **9**,669(1932)RP498.
[3] M. Harris. *The carbonization process: A study of the system wool—sulphuric-acid—water.* BS J. Research **12**,475(1934)RP673.
[4] Ludwig Gattermann, Practical Methods of Organic Chemistry, 3d American ed. translated from 11th German ed. by William B. Schober and S. Vahan, 390 pp.(1916). The Macmillan Co., New York.
[5] F. Garelli and B. Saladini. *The determination of sulphur in organic compounds with an oxygen bomb.* Atti accad. sci. Torino (classe sci. fis.) Mat., Nat. **66**,163(1931).

for the determination of sulphur in organic compounds, and Barritt and King found it to be the best of several methods for the determination of sulphur in wool.[6]

The specimen to be analyzed by the Carius method is heated in a sealed glass tube with fuming nitric acid to destroy organic matter and to oxidize the sulphur. The nitric acid remaining after the action is complete is removed by evaporation and the sulphur is precipitated and weighed as barium sulphate. In order to obtain accurate results the nitric acid must be rémoved completely. Sulphur may be lost during the evaporation of the nitric acid through creeping of the solution up the sides of the evaporating dish and through the reducing action of particles of dust which may fall into the dish. The addition of sodium carbonate solution in excess of the amount estimated to be necessary to combine with the sulphur was found to prevent losses.

Although the Carius method is reliable and is free from errors caused by the presence of nonvolatile salts, it has the disadvantages of requiring a small specimen, unusual skill in sealing, heating, and handling the tubes, and a long time for completion of an analysis. The oxygen bomb method offered advantages in these respects.

The oxygen bomb method has been used with success by Garelli and Saladini for the analysis of a variety of organic compounds [7] and by McPherson and Cummings for the accurate determination of sulphur in rubber-sulphur compounds.[8] The specimen to be analyzed is ignited in an atmosphere of oxygen under pressure, the sulphur absorbed in a solution of ammonium carbonate, precipitated, and weighed as barium sulphate.[9]

The oxygen bomb used in this work is of an all-metal type. The combustion chamber has a diameter of approximately 6.5 cm and a depth of 11.5 cm. Too great a pressure of oxygen results in a spattering of partially-decomposed wool on the sides of the chamber where ignition is incomplete. Pressures of 150 to 180 lb/in.^{2}, were found to produce satisfactory combustion, provided the wool fibers were tightly packed in a small filter paper capsule, and so placed that on ignition the heat of combustion was not too rapidly dissipated by metal parts touching the paper container.

Table 1 gives the results of analyses for the sulphur content of the scoured and extracted wool.

The results for the two methods are in good agreement and indicate that the accuracy and precision are nearly the same for both methods.

IV. PROPOSED METHOD FOR TOTAL SULPHUR IN WOOL

Detailed instructions follow for the determination of the total sulphur content of wool in the absence of substances forming sulphates insoluble in dilute hydrochloride acid.

[6] Mease and Jessup, Analysis of wool-cotton textiles BS J. Research **9**,669(1932) RP498.
[7] F. Garelli, and B. Saladini. *The determination of sulphur in organic compounds with an oxygen bomb.* Atti accad. sci. Torino (classe sci. fis.) Mat., Nat. **66**,163(1931).
[8] Unpublished results obtained at the National Bureau of Standards.
[9] It is probable that the direct titration method described by W. C. Schneider could be applied here fo the determination of sulphate. See Ind. Eng. Chem., anal. ed., **5**,403-6(1933).

TABLE 1.—*Comparison of results obtained by Carius and oxygen-bomb methods for total sulphur in the prepared wool*

Percent sulphur	
Carius method	Oxygen-bomb method
2.95±.09	3.00±.03
2.98	3.04
3.05	3.05
3.06	3.07
3.08	3.08
3.09	3.09
3.10	3.09
3.11	3.13
Average...3.05±.03	Average...3.07±.01

Weigh accurately about 0.5 g of the dry or conditioned wool to be tested. Wrap the specimen compactly in a piece of filter paper, or in a filter-paper capsule if the specimen is in the form of loose, unspun fibers, and bind it with pure silk. Place the specimen on a rectangular piece of filter paper larger enough so that when laid on the concave side of a platinum crucible cover the four corners will rest on the rim and support the remainder of the paper free of any metal. Avoid the use of too much paper for it consumes oxygen which may be needed for complete combustion of the wool. Place the platinum cover thus loaded on the ignition platform of a calorimeter bomb. Attach the fusible ignition wire to the electric leads with which the bomb is equipped and have it touch the center of the top of the paper specimen container. Place about 50 ml of a 2-percent aqueous solution of ammonium carbonate in the bomb, fasten the cover securely in place and introduce sufficient oxygen into the bomb to produce a pressure of 150 to 180 lb/in^2. Care must be taken not to permit wetting of the paper and specimen.

Ignite the specimen and permit the bomb to stand, with occasional shaking, for 10 minutes to permit all of the sulphur to be absorbed by the ammonium carbonate solution. Open the bomb and filter the solution to remove globules of the fused ignition wire and collect the filtrate in a 300 ml beaker. Acidify the solution with concentrated hydrochloric acid (sp gr 1.18) using about 2 ml in excess, dilute to a volume of 250 ml, heat on the steam bath and add 10 ml of a 5-percent solution of barium chloride (prepared by dissolving 50 g of $BaCl_2.2H_2O$ in 1 liter of distilled water containing about 3 drops of concentrated hydrochloric acid). Allow the solution to stand, preferably overnight, until the precipitate has settled. Collect the barium sulphate by filtration through paper or other suitable filtering medium. Wash the paper and precipitate with small portions of hot distilled water until the wash water gives no test for chlorides. Transfer the precipitate and filter paper to a weighed crucible and ignite in an electric muffle or other suitable furnace, at such a rate that from 1½ to 2 hours are required to heat the crucible from room temperature to redness. Cool the precipitate in a desiccator and weigh. Then: $100\,\frac{.1314w}{W}$ is the percentage of sulphur in the specimen where w is the weight of the barium sulphate found and W the weight of the dried or conditioned specimen.

V. ANALYSIS OF WOOL FOR SULPHATE

Two convenient methods for the destruction of wool fiber without oxidation of cystine sulphur but with liberation of the sulphate sulphur preparatory to its quantitative determination seemed applicable: (1) Digestion with aqueous potassium hydroxide solution, and (2) digestion with concentrated hydrochloric acid. The first had been used by the author [10] for the purpose of sulphate determination in wool but without a critical study of its probable precision or accuracy.

Analyses of solutions of known composition were made as a basis for determining the accuracy to be expected in the determination of sulphate by these methods. A solution of known sulphur content was prepared by dissolving an accurately weighed amount of pure dry sodium sulphate in a measured volume of water. Aliquot parts were acidified and the sulphate was precipitated and determined in the usual way. The results obtained are given in table 2, experiments 1 to 5, inclusive. They serve to indicate the degree of accuracy to be expected in the absence of complicating substances. On of these is the acid which is present when the wool substance is digested in hydrochloric acid. Experiments 6 to 10 were the same as 1 to 5, except that the precipitation of barium chloride was made in the presence of the amount of hydrochloric acid necessary to dissolve wool and free the adsorbed sulphate when present. The values obtained are in reasonably good agreement with those of experiments 1 to 5. If the wool specimen were digested in potassium hydroxide solution, the potassium chloride formed when the solution is acidified would be a complicating factor. Potassium hydroxide of amount and concentration convenient to dissolve wool was added to the solutions for experiments 11 to 15 of table 2. With one exception, these results are in good agreement with those of experiments 1 to 5.

TABLE 2.—*Effect of condition of precipitating medium on* SO_4 *determination in sodium sulphate*

Experiment no.	Condition of precipitating solution	Wool present	SO_4	
			Present	Found
		g		
1	Acidified with 0.2 ml 35 percent hydrochloric acid	None	0.0847	0.0844
2		None	.0847	.0844
3		None	.0847	.0843
4		None	.0847	.0842
5		None	.000	.0001
6	Same as experiments 1 to 5, but acidified with 20 ml 30-percent hydrochloric acid.	None	.0847	.0847
7		None	.0847	.0846
8		None	.0847	.0840
9		None	.0847	.0845
10		None	.000	.0001
11	Contained 100 ml of 3½-percent potassium hydroxide and acidified with HCl with 2 ml excess.	None	.0847	.0842
12		None	.0847	.0846
13		None	.0847	.0859
14		None	.0847	.0841
15		None	.000	.0001
16	Same as 11 to 15, but contained decomposition products of wool	1.00	.0847	.0846
17		1.00	.0847	.0868
18		1.00	.0847	.0856
19		1.00	.0847	.0865
20	Same as 16 to 19, but contained no added sulphate	1.00	.000	.0015
21		1.00	.000	.0029
22		1.00	.000	.0013
23		1.00	.000	.0018
25		1.00	.000	.0019

[10] R. T. Mease and D. A. Jessup. *Analysis of wool-cotton textiles.* BS J. Research **9**,669(1932)RP498.

TABLE 2.—*Effect of condition of precipitating medium on* SO_4 *determination in sodium sulphate*—Continued

Experiment no.	Condition of precipitating solution	Wool present	SO_4	
			Present	Found
		g		
26	Same as 6 to 10, but contained decomposition products of wool	1.00	0.0847	0.0847
27		1.00	.0847	.0841
28		1.00	.0847	.0842
29		1.00	.0847	.0852
30	Same as 26 to 29, but contained no added sulphate	1.00	.000	.0001
31		1.00	.000	.0003
32		1.00	.000	.0001
33		1.00	.000	.0001
34		1.00	.000	.0001

These experiments indicate that either potassium hydroxide or hydrochloric acid may be used to dissolve the wool. However, when an alkali solution of wool is acidified preparatory to precipitation of sulphur, the organic matter present becomes colloidal. It is difficult to remove, slows filtration, and interferes with the washing of the precipitate. This may result in a loss of some of the sulphur or contamination of the precipitate by salts held by the organic matter. The predominance of the latter factor is indicated by the results of experiments 16 to 19, and a comparison of the result obtained for experiment 15 with those for 20 to 25 of table 2.

A solution of wool in hydrochloric acid is nearly clear and gives no difficulty in filtration. That it is also to be preferred for accuracy is concluded from a comparison of the results of experiments 26 to 29, and 16 to 19, also experiments 20 to 25, and 30 to 34 of table 2. The last group mentioned also shows that the cystine sulphur of wool is not precipitated with barium chloride when hydrochloric acid is used for digesting the wool for sulphate-sulphur determination.

The results given in table 3 were obtained by analyzing the sulphuric-acid-treated wool described in section II using potassium hydroxide for one group of results and hydrochloric acid for the other to dissolve the wool.

TABLE 3.—*Comparison of results obtained using the potassium-hydroxide and hydrochloric-acid methods for determining* SO_4 *in wool*

[The sulphuric-acid-treated wool described in sec. II was analyzed]

Percentage of SO_4	
Potassium hydroxide	Hydrochloric acid
7.76±.13	7.69±.05
7.92	7.84
8.09	7.83
8.26	7.86
Average...8.00±.07	Average...7.81±.03

VI. PROPOSED METHOD FOR THE DETERMINATION OF SULPHATE IN WOOL

Detailed instructions follow for the determination of the sulphate sulphur in wool in the absence of substances forming sulphates insoluble in hydrochloric acid.

Accurately weigh 1 to 1.5 g of the conditioned or dried wool to be tested and place it in a pyrex-glass test tube about 19 cm long and 75 ml capacity. Add 20 ml of a 30-percent (by weight of HCl) solution of hydrochloric acid and heat in a water bath at 95 to 100° C with occasional agitation until the wool is dissolved. Twenty to thirty minutes is usually sufficient. Cool the solution, dilute with about an equal volume of distilled water, and filter, collecting the filtrate in a 300 ml beaker. Dilute the solution to a volume of 250 ml heat on the steam bath, and add 10 ml of a 5-percent solution of barium chloride. Filter, ignite, and weigh the barium sulphate as described in section IV. Then the percentage of sulphate in the specimen is $100\,\frac{0.4115\,w}{W}$ where w is the weight of barium sulphate found and W is the weight of the dried or conditioned specimen.

WASHINGTON, September 21, 1934.

U.S. DEPARTMENT OF COMMERCE NATIONAL BUREAU OF STANDARDS

RESEARCH PAPER RP732

Part of Journal of Research of the National Bureau of Standards, Volume 13, November 1934

SECOND SPECTRUM OF HAFNIUM (Hf II)

By William F. Meggers and Bourdon F. Scribner

ABSTRACT

New data (wave-length measurements and intensity estimates) for more than 1,000 lines characteristic of singly ionized hafnium atoms, including Zeeman patterns for 207 lines, are presented. Analysis has resulted in the interpretation of 862 lines as combinations of 117 atomic energy states, most of which are grouped and identified as doublet or quartet spectral terms. The normal state of the Hf^+ ion is represented by a doublet-D term arising from the electron configuration $5d\ 6s^2$, and a tentative value of 14.8 volts is derived for the ionizing potential. Attention is called to the extraordinary similarity between La I and Hf II spectra.

CONTENTS

		Page
I.	Introduction	625
II.	Wave-length measurements and intensity estimates	626
III.	Observations of Zeeman effects	627
IV.	Classification of Hf II lines	628
V.	Structure of the Hf II spectrum	648

I. INTRODUCTION

An improved description of hafnium spectra, published in 1928 by Meggers,[1] included data on wave lengths and intensities of about 1,500 lines between the limits 2155.72 A in the ultraviolet and 9250.27 A in the infrared. The range of this list, the precision of the wave-length measurements, and especially the discrimination between lines characterizing neutral atoms (Hf I) and those due to ionized atoms (Hf II) gave the present authors an incentive to search for regularities in the first two spectra of hafnium. Such regularities were indeed found, and preliminary reports of the structures of these spectra have been published.[2] In each case relative energy levels were established which combined in such manner as to account for more than 200 spectral lines and permit the assignment of relative values of inner-quantum numbers to the levels. The absolute values of these quantum numbers were tentatively fixed on the basis of suggested identifications of the ground states; thus, from theoretical considerations and comparison with similar spectra, the lowest term for Hf I was assumed to be $(d^2s^2)^3F$, while for Hf II it was $(ds^2)^2D$. A study of the electric furnace spectrum of hafnium by King [3] confirmed our separation of Hf II from Hf I lines and indicated that our Hf I levels were correctly oriented.

At this stage it was felt that, to verify our identification of the ground states and to extend such identifications to the remaining

[1] W. F. Meggers, BS J.Research **1**,151(1928);RP51.
[2] W. F. Meggers and B. F. Scribner, J.O.S.A. & R.S.I. **17**,83(1928), Hf II. W. F. Meggers and B.F. Scribner, BS J.Research **4**,169(1930)RP139; Hf I.
[3] A. S. King, Astrophys. J. **70**,343(1929).

levels, observations on the behavior of hafnium lines in a magnetic field were indispensible. Such a study of the Zeeman effect for hafnium [4] was made possible by Dr. G. Holst, of Eindhoven, Holland, who kindly presented for this purpose a small rod of hafnium metal condensed on a tungsten filament. From this investigation we obtained new data for 280 hafnium lines (2393 to 4817 A), 70 belonging to the first and 210 to the second spectrum. Analysis of these Zeeman patterns confirmed our first suggested identifications of the low energy states, and made it possible to extend the spectral classifications, especially for Hf II lines since a larger proportion of the latter appeared in the magnetic field.

On account of the position of hafnium in the periodic table of chemical elements (immediately following the rare earth group) its spectral structures are of special interest and it is highly desirable to make these analyses as nearly complete as possible. For the Hf II analysis, it was soon found that a limitation was imposed by the restricted range for which data were available and in part by the fact that the earlier observations were made with impure materials. Thus in the work already mentioned,[5] although 2,100 lines were measured in the interval 2165 to 9250 A, more than 600 of these were discarded as evidence of columbium, zirconium, titanium, and other impurities. A more reliable and extended list of hafnium lines was finally obtained through the kind cooperation of Prof. G. von Hevesy, who, in 1932, supplied us with a sample of highly purified oxide, with which the spectra have been reobserved, and extended to 1990 A in the ultraviolet and to 10637 A in the infrared. A further extension in the ultraviolet was made by Dr. R. J. Lang of the University of Alberta, who photographed the spark spectra to 1300 A using the same electrodes which the authors employed for the study of Zeeman effects. To give a detailed account of the new experiments and to present the final results for the Hf II spectrum are the aims of the present paper. Further data and analysis of the Hf I spectrum will be published after they have been supplemented by additional observations of Zeeman effects, since the data at present available have proved insufficient for the complete identification of Hf I spectral terms.

II. WAVE-LENGTH MEASUREMENTS AND INTENSITY ESTIMATES

The new sample of hafnium oxide presented by Professor Hevesy (1932) for the continuation of our spectroscopic studies, greatly surpassed the earlier one (1925) in purity. Whereas the first sample was relatively rich in columbium, zirconium, and titanium (represented by 357, 109, and 50 lines, respectively) the last one was entirely free from titanium and showed only a spectroscopic trace of columbium, but contained considerable amounts of zirconium and nickel.

In making spectrograms with this new material, the same instruments and technic were employed as in the earlier experiments fully described elsewhere.[6] In addition to arc and spark exposures made with silver electrodes on which a portion of hafnium salt was fused, the entire range of spectrum was also investigated with very pure copper electrodes. However, in the latter case, it was found im-

[4] W. F. Meggers and B. F. Scribner, J.O.S.A. **23**,121(1933).
[5] W. F. Meggers, BS J.Research **1**,151(1928);RP151.
[6] W. F. Meggers, BS J.Research **1**,153(1928);RP151.

possible to observe the spark spectrum because of the ease with which the oxides scaled off, so stigmatic arc images were recorded full length and enhancement at the cathode was relied upon as an indication of ionization. Besides serving as a check on the observations with silver electrodes, those with copper electrodes revealed some lines which had previously been overlooked because of masking by silver lines.

The later spectrograms were, in general, stronger exposures so that it was necessary to revise the scale of estimated intensities formerly given. By using Schumann plates in the ultraviolet, the authors succeeded in extending the observations from 2155 A to 1990 A with a Hilger E_1 quartz spectrograph, and Dr. Lang recorded the spark spectrum to 1300 A with his vacuum spectrograph containing a concave grating of 2 meters radius. New photographic plates which first became available about 3 years ago permitted extension of observations in the infrared to 10637 A. Formerly no satisfactory spark exposures of hafnium were obtained for waves longer than 6000 A, but after 5 trials with the new material one was obtained which revealed enhanced lines (greater intensity in spark than in arc) up to about 7000 A. Beyond this point, lines arising from ionized atoms can only be recognized by their enhancement at the negative electrode of the arc. The same applies to lines in a portion of the ultraviolet (2000 to 2400 A) where our spark spectrograms were relatively weak. In this range, the Hf II spectrum is well developed at the arc cathode, and all lines truly enhanced in spark spectrograms probably belong to twice ionized atoms.

Our final estimates of relative intensities of halnium lines are based entirely upon the new observations, but the earlier values for wave lengths were averaged with the most recent determinations, with the hope that the final means thus derived from 4 to 7 or 8 spectrograms would be improved in precision of relative value.

III. OBSERVATIONS OF ZEEMAN EFFECTS

For the study of Zeeman effects on hafnium lines, we employed electrodes of hafnium metal condensed on a tungsten filament. The electrodes were mounted in brass supports between the pole pieces of a Weiss electromagnet made by the Geneva Society, and the spark was operated with a condensed discharge from an alternating-current transformer. After passing through a Wollaston prism of crystal quartz, the light was focused on the slit of a stigmatic concave grating spectrograph by means of a lens of fused quartz. This enabled us to photograph both parallel and perpendicular components of the transverse Zeeman effect simultaneously. Several spectrograms were made on Eastman 33 plates in the second order of a Rowland grating giving a dispersion of 1.8 A per mm, and covered the range from 2300 to 4900 A. Unfortunately, the hafnium metal oxidized and wore away rather rapidly in the atmospheric spark, so that tungsten lines finally appeared with predominating intensity and too little of the hafnium remainded for observation of Zeeman effects in the region of longer waves.

A field strength of about 33,000 gausses was maintained with a pole gap of 6 mm, the actual field strength for each exposure being determined from measurements either of calcium lines (3933, 3968 A) due

to contamination of the hafnium electrodes, or of aluminum (3944, 3962 A) or zinc lines (4680, 4722, 4810 A) impressed immediately before or after the hafnium exposure. Under the most favorable conditions of exposure and intensity distribution, we were able to resolve patterns in which the separations are about $a/8$ but the limit is more commonly around $a/5$. Patterns which are fully resolved are followed in importance by those in which the components are blended, but show typical intensity gradients. It has been customary to distinguish at least 3 different types represented by symbols A^1, A^2, and B, according as the strongest perpendicular (n) components are inside, outside, and in the center of the group, respectively. Whenever the type of unresolved pattern was obviously A, we attempted to measure the separations of the strongest components, but when no asymmetry was noticed, we assume that the measured separations apply to the centroids of the pattern. In the latter case, measurements are found to deviate about 25 percent of the total range of separations from the value for the components of greatest intensity.

IV. CLASSIFICATION OF Hf II LINES

In our preliminary account of regularities in the spark spectrum of hafnium [7] we displayed 206 combinations between 16 levels of low energy and 27 higher ones. The 2 lowest levels were tentatively named $(ds^2)^2D$, and the next 4 were regarded as $(d^2s)^4F$ but further attempts at grouping and identifying levels were considered too hazardous. As soon as the new data on Zeeman effects were available, the tentative interpretation of Hf II levels was confirmed, and the g values (splitting factors) for all of the remaining established levels were calculated from resolved patterns. This made it relatively easy to group levels into terms and configurations, which in turn indicated which terms were still missing and where they should be sought.

In this way the table of combinations was extended to include about 800 lines involving 32 levels of the first set and 70 of the second or middle set. At this point, the lines which remained unclassified were mainly faint and hazy ones, so that attention was then turned to the search for third set levels which might be expected as spectral terms forming series with the lower ones. A number of such high levels have been established but their proper grouping and interpretation are uncertain, since none of them combine strongly enough to be tested with Zeeman effects, and nothing is known at present of the structure of the Hf III spectrum, the low terms of which represent the convergence limits of Hf II series.

Soon after the already published Hf II levels were definitely identified by means of Zeeman effects and grouped into doublet and quartet terms, it was noticed that a remarkable parallelism existed between the structures of Hf II and La I spectra. Not only the relative positions of the terms but level separations and abnormalities in interval ratios and inversions are more or less faithfully duplicated (except for a scale factor) in Hf II as found [8] in La I. This close similarity of the two spectra served as a guide in the further analysis of the Hf II spectrum; it will be discussed in more detail in the last section of this paper.

[7] W. F. Meggers and B. F. Scribner, J.O.S.A. & R.S.I. **17**,83(1928).
[8] H. N. Russell and W. F. Meggers, B8 J.Research **9**,647 (1932); RP497.

Complete data for Hf II lines are presented in table 1, where measured wave lengths, estimated intensities, wave numbers in vacuum, term combinations, observed and calculated Zeeman effects appear in successive columns. Of the 1,035 lines listed in table 1 as characteristic of singly ionized hafnium atoms, 862 have been classified as combinations of 117 atomic energy levels, most of which have been grouped into doublet or quartet spectral terms. These terms combine in such a way that the simple selection rule for total angular momenta or so-called inner quantum numbers ($\Delta J=0, \pm 1$) is strictly obeyed, but there is apparently no restriction on changes in orbital momenta, ΔL (except that imposed by the ΔJ rule) and combinations occur for $\Delta L=0, \pm 1, \pm 2, \pm 3$. Intersystem combinations are very prominent and, except for more frequent intensity anomalies, follow the same rules as doublets or quartets. It is obvious that a satisfactory analysis of such a spectrum would have been impossible without the aid of Zeeman effects.

In the extreme ultraviolet only the classified lines have been quoted from Lang's observations. The unclassified lines in table 1, which are situated mainly in the ultraviolet, are relatively faint and usually hazy and unsymmetrical in the spark. Their wave lengths are derived from arc spectrograms in which they appear as electrode lines. These lines probably represent combinations with high levels which it is impossible to establish or identify from the limited data at hand.

In the last column of table 1, we have entered computed Zeeman patterns for comparison with the observed patterns reported in the preceding column. The computed patterns were obtained by applying the ordinary rules to the g values derived from the observations; they are here given in complete detail to permit a critical test of the quality and consistency of the observations, and also to facilitate comparison with tables of theoretical Zeeman effects computed by Kiess and Meggers [9] for pure *LS* coupling. The splitting factors for Hf II levels deviate so often and so widely from the Landé values that they may be regarded as a new system representative of vector coupling of a mixed or intermediate type.

TABLE 1.—*First spark spectrum of hafnium* (Hf II)

λ_{air}	Intensity		ν_{vac} cm^{-1}	Term combinations	Zeeman effects	
	Arc	Spark			Observed	Computed
9742.28	10	(?)	10261.73	$b^4F_{1\frac{1}{2}}$—$z^4D^0_{0\frac{1}{2}}$		
9453.55	2	(?)	10575.14	$b^2F_{2\frac{1}{2}}$—$z^2D^0_{1\frac{1}{2}}$		
8581.88	1	5?	11649.26	$b^4F_{2\frac{1}{2}}$—$z^4D^0_{1\frac{1}{2}}$		
8305.91	2	4	12036.32	$b^2D_{2\frac{1}{2}}$—$z^4F^0_{2\frac{1}{2}}$		
8236.13	5	10	138.29	$b^4F_{2\frac{1}{2}}$—$z^4F^0_{1\frac{1}{2}}$		
7983.66	3	5	522.14	$a^2H_{4\frac{1}{2}}$—$y^4F^0_{3\frac{1}{2}}$		
7861.22	3	8	717.18	$b^4F_{2\frac{1}{2}}$—$z^4D^0_{2\frac{1}{2}}$		
7801.53	2	6	814.48	$a^2P_{0\frac{1}{2}}$—$z^4F^0_{1\frac{1}{2}}$		
7757.89	5	15	886.56	$b^4F_{1\frac{1}{2}}$—$z^4D^0_{1\frac{1}{2}}$		
7720.72	1	2	12948.60	$b^2G_{3\frac{1}{2}}$—$z^2F^0_{3\frac{1}{2}}$		
7663.09	2	30	13045.98	$b^4F_{2\frac{1}{2}}$—$z^2D^0_{2\frac{1}{2}}$		
7634.50	1	1	094.83	$b^2P_{1\frac{1}{2}}$—$y^4P^0_{1\frac{1}{2}}$		
7565.35	—	2	214.73	$b^4P_{2\frac{1}{2}}$—$y^2D^0_{2\frac{1}{2}}$		
61.08	1	10	221.99	$b^4P_{1\frac{1}{2}}$—$z^4P^0_{2\frac{1}{2}}$		
7514.88	—	2	303.27	$b^2G_{3\frac{1}{2}}$—$y^2D^0_{2\frac{1}{2}}$		

[9] C. C. Kiess and W. F. Meggers, BS J.Research **1,641** (1928);RP23.

TABLE 1.—*First spark spectrum of hafnium* (Hf II)—Continued

λ_{air}	Intensity		ν_{vac} cm−1	Term combinations	Zeeman effects	
	Arc	Spark			Observed	Computed
7398.96	—	10	511.70	$b^2F_{2½}$—$z^2F^0_{2½}$		
7328.64	3	30	641.34	$b^4F_{2½}$—$z^4F^0_{2½}$		
7292.33	1	1	709.27	$b^2D_{1½}$—$z^4F^0_{1½}$		
78.72	—	6	734.90	$b^2D_{1½}$—$w^2D^0_{1½}$		
7277.67	5	50	736.88	$b^4F_{4½}$—$z^4D^0_{3½}$		
7189.30	1	3	905.73	$a^2P_{0½}$—$z^4D^0_{0½}$		
7164.52	1	5	13953.83	$a^2P_{1½}$—$z^4D^0_{1½}$		
7061.90	10	30?	14156.60			
30.33	30	150	220.17	$b^4F_{3½}$—$z^4D^0_{3½}$		
21.23	3	30	238.60	$b^4F_{1½}$—$z^2P^0_{0½}$		
16.99	—	6	247.20	$a^2H_{4½}$—$y^4F^0_{4½}$		
7010.68	5	10?	260.03			
6997.83	2	20	286.21	$b^2G_{4½}$—$z^4G^0_{4½}$		
80.91	100	200	320.84	$a^2F_{3½}$—$z^4F^0_{3½}$		
70.44	5	10?	342.35			
6935.16	5	50	415.31	$b^2D_{2½}$—$z^4D^0_{1½}$		
6857.03	5	10?	579.56			
55.29	7	50	583.26	$a^4P_{2½}$—$z^4F^0_{1½}$		
6850.07	20	60?	594.37			
6767.91	1	1	771.54	$b^2P_{1½}$—$z^2P^0_{0½}$		
54.61	60	100	800.63	$b^2D_{1½}$—$z^4D^0_{0½}$		
6719.40	2	50	14900.36	$b^2F_{3½}$—$z^2F^0_{3½}$		
6647.06	30	100	15040.10	$b^4F_{4½}$—$z^4F^0_{4½}$		
44.60	100	200	045.67	$b^2D_{1½}$—$z^4F^0_{2½}$		
09.20	1	8	126.25	$c^2D_{2½}$—$y^4D^0_{2½}$		
6605.91	—	1	133.79	$b^4P_{2½}$—$y^4F^0_{3½}$		
6599.76	1	4	147.89	$a^4P_{1½}$—$z^4F^0_{1½}$		
84.53	4	40	182.93	$a^2H_{5½}$—$y^4F^0_{4½}$		
67.39	6	60	222.55	$b^2G_{3½}$—$y^4F^0_{3½}$		
65.76	—	3	226.33	$b^4F_{1½}$—$z^2D^0_{1½}$		
62.86	2	10	233.06	$b^4P_{1½}$—$y^4F^0_{1½}$		
57.91	10	100	244.56	$b^4F_{3½}$—$z^4D^0_{2½}$		
50.01	1	10	262.94	$b^2F_{3½}$—$w^2D^0_{2½}$		
48.72	1	10	265.95			
48.24	2	3	267.07	$a^2H_{5½}$—$z^4G^0_{5½}$		
42.80	3	50	279.76	$a^2H_{4½}$—$z^2G^0_{4½}$		
31.66	2	30	305.82	$a^2P_{1½}$—$z^2P^0_{0½}$		
26.20	—	5	318.63	$b^2F_{2½}$—$z^4D^0_{1½}$ $b^4P_{2½}$—$y^2F^0_{2½}$		
12.61	1	10	350.59	$a^2P_{1½}$—$z^2D^0_{2½}$		
6511.62	—	6	352.93	$b^4F_{4½}$—$z^4G^0_{3½}$		
6494.58	—	5	393.21			
73.89	3	20	442.41	$b^2G_{3½}$—$y^2F^0_{3½}$		
67.90	2	2	456.71	$b^4F_{1½}$—$z^4D^0_{2½}$		
62.30	1	4	470.10	$a^2G_{3½}$—$z^2D^0_{3½}$		
6455.85	2	20	485.56	$b^4P_{1½}$—$y^2P^0_{1½}$		
6390.99	1	2	642.71			
90.32	1	2	644.35			
43.77	1	4	759.15	$b^4P_{1½}$—$y^2P^0_{0½}$		
37.76	—	1	774.09	$b^4P_{0½}$—$y^2P^0_{1½}$		
15.94	1	5	828.59	$b^2F_{2½}$—$w^2F^0_{3½}$		
6306.17	1	5	853.11	$b^4P_{2½}$—$y^4F^0_{2½}$		
6279.84	15	20	919.58	$a^4P_{2½}$—$z^4F^0_{2½}$		
71.05	1	3	941.89	$b^2G_{3½}$—$y^4F^0_{3½}$		
48.95	80	100	15998.27	$a^2F_{3½}$—$z^4F^0_{1½}$		
30.84	10	20	16044.77	$b^4F_{1½}$—$z^4G^0_{2½}$		
29.66	2	3	047.81	$b^4P_{0½}$—$y^2P^0_{0½}$		
22.81	6	10	065.47	$a^2G_{3½}$—$z^4F^0_{4½}$		
06.95	1	3	106.53	$b^2F_{3½}$—$z^2H^0_{4½}$		
6202.85	2	2	117.17	$a^4P_{0½}$—$z^4F^0_{1½}$		
6158.72	1	2	232.66	$b^2G_{3½}$—$y^2F^0_{3½}$		
56.25	3	3 d	239.17	$a^4P_{1½}$—$z^4D^0_{2½}$ $b^4F_{2½}$—$z^2P^0_{1½}$		
35.65	1	1	293.69	$a^2P_{1½}$—$z^2D^0_{1½}$		
6135.10	10	20	295.15	$b^2G_{4½}$—$y^4F^0_{4½}$		
6097.47	—	2	395.72	$b^4P_{1½}$—$y^4F^0_{2½}$		
93.15	—	2	407.34	$b^2D_{2½}$—$z^4F^0_{3½}$		

TABLE 1.—*First spark spectrum of hafnium* (Hf II)—Continued

λ_{air}	Intensity		ν_{vac} cm^{-1}	Term combinations	Zeeman effects	
	Arc	Spark			Observed	Computed
48.00	3	5	529.82	$a^2P_{0\frac{1}{2}}$—$z^4D^{\circ}_{1\frac{1}{2}}$		
41.44	2	6	547.77	$b^4F_{3\frac{1}{2}}$—$z^4F^{\circ}_{4\frac{1}{2}}$		
31.96	1	3	573.78	$b^4F_{2\frac{1}{2}}$—$y^2G^{\circ}_{3\frac{1}{2}}$		
27.57	10	20	585.85	$b^2G_{4\frac{1}{2}}$—$y^2F^{\circ}_{3\frac{1}{2}}$		
6006.39	2	2	644.34	$a^2G_{3\frac{1}{2}}$—$z^4D^{\circ}_{2\frac{1}{2}}$		
5969.38	4	5	747.53	$b^4F_{2\frac{1}{2}}$—$z^4D^{\circ}_{3\frac{1}{2}}$		
5929.35	3	5	860.59	$b^4F_{3\frac{1}{2}}$—$z^4G^{\circ}_{3\frac{1}{2}}$		
5885.58	3 Zr?	2	985.98	$b^2D_{2\frac{1}{2}}$—$z^4D^{\circ}_{3\frac{1}{2}}$		
42.23	50	80	112.02	$a^2P_{1\frac{1}{2}}$—$z^4G^{\circ}_{2\frac{1}{2}}$		
09.50	20	30	208.42	$a^4P_{0\frac{1}{2}}$—$z^4D^{\circ}_{0\frac{1}{2}}$		
5801.71	7	15	231.53	$a^2G_{3\frac{1}{2}}$—$z^4G^{\circ}_{3\frac{1}{2}}$		
5767.18	15	30	334.70	$a^2F_{3\frac{1}{2}}$—$z^4F^{\circ}_{3\frac{1}{2}}$		
5752.53	3	5	378.85			
5373.58	4	10	620.68	$b^2F_{3\frac{1}{2}}$—$z^4P^{\circ}_{2\frac{1}{2}}$		
60.40	—	1	661.71	$b^2F_{2\frac{1}{2}}$—$z^4P^{\circ}_{2\frac{1}{2}}$		
58.83	1	3	666.61	$b^2G_{3\frac{1}{2}}$—$y^4F^{\circ}_{4\frac{1}{2}}$		
5631.36	1	4	752.78	$b^2P_{1\frac{1}{2}}$—$x^2P^{\circ}_{1\frac{1}{2}}$		
5590.73	3	5	881.80	$a^2P_{0\frac{1}{2}}$—$z^2P^{\circ}_{0\frac{1}{2}}$		
65.56	2	5	17962.67	$a^2H_{4\frac{1}{2}}$—$z^2G^{\circ}_{4\frac{1}{2}}$		
47.83	—	1	18020.07	$b^2G_{4\frac{1}{2}}$—$y^4F^{\circ}_{3\frac{1}{2}}$		
24.35	40	50	096.66	$a^2F_{3\frac{1}{2}}$—$z^2D^{\circ}_{2\frac{1}{2}}$		
5514.96	1	3	127.47	$b^4P_{2\frac{1}{2}}$—$y^4D^{\circ}_{1\frac{1}{2}}$		
5493.22	1	6	199.21	$b^2F_{2\frac{1}{2}}$—$y^2G^{\circ}_{3\frac{1}{2}}$		
63.38	10?	10	298.62	$a^4P_{2\frac{1}{2}}$—$z^4D^{\circ}_{1\frac{1}{2}}$		
44.07	20	30	363.52	$b^4F_{2\frac{1}{2}}$—$z^4G^{\circ}_{3\frac{1}{2}}$		
30.06	1	4	410.90			
5420.44	2	3	443.58	$b^4F_{2\frac{1}{2}}$—$z^2F^{\circ}_{3\frac{1}{2}}$		
5391.36	6	10	543.05	$a^2P_{1\frac{1}{2}}$—$z^2P_{1\frac{1}{2}}$		
71.80	2	4	610.57	$b^4P_{2\frac{1}{2}}$—$z^2G^{\circ}_{3\frac{1}{2}}$		
61.38	1	2	646.74	$b^4P_{0\frac{1}{2}}$—$y^4D^{\circ}_{0\frac{1}{2}}$		
48.40	10	15	692.00	$a^2F_{3\frac{1}{2}}$—$z^4F^{\circ}_{4\frac{1}{2}}$		
46.30	10	40	699.34	$b^2G_{3\frac{1}{2}}$—$z^2G^{\circ}_{3\frac{1}{2}}$		
24.26	20	30	776.74	$b^2D_{1\frac{1}{2}}$—$z^2P^{\circ}_{0\frac{1}{2}}$		
5311.60	100	150	821.50	$b^2D_{1\frac{1}{2}}$—$z^2D^{\circ}_{2\frac{1}{2}}$		
5299.85	8	10	863.22	$a^4P_{1\frac{1}{2}}$—$z^4D^{\circ}_{1\frac{1}{2}}$		
98.06	80	100	869.60	$a^2P_{0\frac{1}{2}}$—$z^2D^{\circ}_{1\frac{1}{2}}$		
89.98	3	10	898.42	$a^2H_{5\frac{1}{2}}$—$z^2G^{\circ}_{4\frac{1}{2}}$		
76.39	1	3	947.09	$b^2F_{2\frac{1}{2}}$—$w^2F^{\circ}_{3\frac{1}{2}}$		
64.95	50	80	18988.26	$b^4F_{1\frac{1}{2}}$—$y^2D^{\circ}_{1\frac{1}{2}}$		
60.44	30	40	19004.54	$b^2D_{2\frac{1}{2}}$—$z^2P^{\circ}_{1\frac{1}{2}}$		
5247.10	40	60	052.86	$b^2G_{4\frac{1}{2}}$—$z^2G^{\circ}_{5\frac{1}{2}}$		
5194.57	3	6	245.53	$b^4F_{4\frac{1}{2}}$—$z^4G^{\circ}_{4\frac{1}{2}}$		
87.75	20	30	270.83	$a^2F_{3\frac{1}{2}}$—$z^4D^{\circ}_{2\frac{1}{2}}$		
64.56	3	8	357.36	$b^4P_{2\frac{1}{2}}$—$y^4D^{\circ}_{2\frac{1}{2}}$		
56.06	1	5	389.17	$b^4F_{1\frac{1}{2}}$—$y^4D^{\circ}_{1\frac{1}{2}}$		
28.53	10	20	493.35	$a^2G_{4\frac{1}{2}}$—$z^4D^{\circ}_{3\frac{1}{2}}$		
27.08	--	1	498.87	$b^4P_{0\frac{1}{2}}$—$z^2S^{\circ}_{0\frac{1}{2}}$		
5110.61	--	7	561.70	$c^2D_{2\frac{1}{2}}$—$z^2F^{\circ}_{3\frac{1}{2}}$		
5080.44	2	10	677.87	$b^4P_{0\frac{1}{2}}$—$y^4D^{\circ}_{1\frac{1}{2}}$		
79.65	40	60	680.92	$b^4F_{1\frac{1}{2}}$—$z^2F^{\circ}_{2\frac{1}{2}}$		
75.92	10	20	695.39	$a^4P_{2\frac{1}{2}}$—$z^2D^{\circ}_{2\frac{1}{2}}$		
71.23	6	8	713.60	$a^2F_{2\frac{1}{2}}$—$z^4D^{\circ}_{1\frac{1}{2}}$		
58.18	8	10	764.46	$b^2D_{1\frac{1}{2}}$—$z^2D^{\circ}_{1\frac{1}{2}}$		
57.03	20	30	768.96	$b^4F_{3\frac{1}{2}}$—$z^2F^{\circ}_{3\frac{1}{2}}$		
40.82	100	150	832.53	$a^4P_{0\frac{1}{2}}$—$z^4D^{\circ}_{1\frac{1}{2}}$		
5034.33	4	8	858.09	$a^2F_{3\frac{1}{2}}$—$z^4G^{\circ}_{3\frac{1}{2}}$		
4999.69	30	40	19995.68	$b^2D_{1\frac{1}{2}}$—$z^4D^{\circ}_{2\frac{1}{2}}$		
84.78	1	3	20055.49	$a^2P_{1\frac{1}{2}}$—$y^2D^{\circ}_{1\frac{1}{2}}$		
45.38	7	10	215.27	$a^4P_{1\frac{1}{2}}$—$z^2P^{\circ}_{0\frac{1}{2}}$		
34.46	50	60	260.00	$a^4P_{1\frac{1}{2}}$—$z^2D^{\circ}_{2\frac{1}{2}}$		
26.99	6	8	290.72	$a^4P_{2\frac{1}{2}}$—$z^4F^{\circ}_{3\frac{1}{2}}$		
20.97	2	5	315.54			
07.34	1	3	371.97	$b^4F_{2\frac{1}{2}}$—$z^4P^{\circ}_{2\frac{1}{2}}$		
4904.51	10	30	383.72	$b^4P_{2\frac{1}{2}}$—$y^4D^{\circ}_{2\frac{1}{2}}$		
4885.75	1	6	461.99	$a^2H_{4\frac{1}{2}}$—$z^2F^{\circ}_{3\frac{1}{2}}$		

TABLE 1.—*First spark spectrum of hafnium* (Hf II)—Continued

λ_{air}	Intensity		ν_{vac} cm^{-1}	Term combinations	Zeeman effects	
	Arc	Spark			Observed	Computed
83.26	—	4	472.42	$b^3G_{3½}$—$y^4D^0_{3½}$		
65.43	5	10	547.45	$b^3G_{3½}$—$x^3D^0_{2½}$		
60.54	1	3	568.12	$a^2P_{1½}$—$z^4P^0_{½}$		
48.46	4	20	619.36	$b^4P_{1½}$—$y^4D^0_{2½}$		
44.00	10	15	638.35	$a^4P_{2½}$—$z^3D^0_{1½}$		
34.84	—	2	677.45	$b^3F_{3½}$—$v^3D^0_{2½}$		
17.22	20	80	753.08	$b^4F_{3½}$—$z^4G^0_{4½}$	(0.00 w) 1.09	(0.03, 0.09, 0.15, 0.21) **0.86**, 1.02, 1.08, 1.14, 1.20, 1.26, 1.32, 1.38
09.18	4	6	787.77	$a^2G_{3½}$—$z^4G^0_{3½}$		
4807.14	15	20	796.60	$a^2G_{4½}$—$z^4F^0_{4½}$		
4790.72	15	40	867.87	$a^2G_{3½}$—$z^2F^0_{2½}$		
65.78	2	12	977.08	$b^4P_{0½}$—$x^2D^0_{1½}$		
60.59	4	20	20999.95	$b^4P_{0½}$—$z^4S^0_{1½}$		
49.39	—	1	21049.47	$b^2F_{2½}$—$x^4D^0_{1½}$		
35.75	—	10	110.10	$a^2G_{4½}$—$z^4G^0_{5½}$		
35.67	(?)	20	110.45	$a^2F_{3½}$—$z^2D^0_{2½}$		
33.74	—	2	119.06	$a^2P_{0½}$—$z^2P^0_{1½}$		
31.36	20	40	129.68	$b^2D_{3½}$—$z^4G^0_{3½}$		
19.10	20	30	184.57	$a^4P_{0½}$—$z^2P^0_{½}$		
14.99	—	3	203.04	$a^4P_{1½}$—$z^2D^0_{1½}$		
13.47	1	1	209.88	$b^2D_{2½}$—$z^2F^0_{2½}$		
4703.62	3	10	254.29	$b^4F_{4½}$—$y^4F^0_{3½}$		
4699.72	15	40	271.93	$b^4F_{3½}$—$z^2F^0_{3½}$		
82.68	—	8	349.34	$a^2H_{4½}$—$w^2F^0_{3½}$		
75.45	—	10	382.35	$b^2G_{3½}$—$z^2G^0_{4½}$		
64.14	100	150	434.20	$a^4P_{1½}$—$z^4D^0_{2½}$	(0.18, 0.51) **0.80**, 1.12	(0.18, 0.56) **0.76**, 1.04, 1.50, 1.88
59.22	4	4	456.83	$a^4P_{2½}$—$z^4G^0_{2½}$		
55.65	—	3	473.29			
40.14	8	20	545.06	$b^4F_{4½}$—$y^2F^0_{3½}$		
26.41	6 Zr?	6	609.00	$b^4F_{1½}$—$z^4P^0_{½}$		
22.71	30	100	626.29	$b^4F_{3½}$—$y^2D^0_{2½}$	(0.00 w) 1.06	(0.04, 0.10, **0.18**) 0.90, 0.98, **1.04**, 1.12, 1.18
13.74	10	50	668.34	$a^2H_{4½}$—$z^2H^0_{4½}$	(0.00) 1.04	(0.01, 0.03, 0.05, 0.07, **0.09**) 0.96, 0.98, 1.00, 1.02, **1.04**, 1.06, 1.08, 1.10, 1.12
4605.79	20	30	705.74	$a^2F_{3½}$—$z^4F^0_{3½}$		
4599.46	6	40	735.61	$b^2G_{4½}$—$z^2G^0_{4½}$		
86.25	4	10	798.22	$a^2F_{3½}$—$z^4D^0_{3½}$		
73.81	6	20	857.50	$b^2D_{2½}$—$z^4P^0_{1½}$		
70.70	2	30	872.38	$b^4P_{2½}$—$y^4P^0_{1½}$	(0.00) 1.45	(0.04, 0.10) **1.40**, 1.48, 1.54, 1.62
63.81	—	8 h	905.40			
46.34	—	2	21989.57	$x^2D^0_{1½}$—5		
41.31	10	20	22013.93	$b^2D_{1½}$—$z^2P^0_{1½}$		
39.76	3	3	021.44	$a^4P_{1½}$—$z^4G^0_{2½}$		
35.38	6	30	042.71	$b^4F_{2½}$—$y^4F^0_{2½}$		
33.18	30	40	053.41	$a^2F_{2½}$—$z^2D^0_{1½}$	(0.00 w) 1.13 A[2]	(0.07, 0.21) 0.77, 0.91, 1.05, **1.19**
24.74	3	30	094.54	$a^2H_{4½}$—$y^2G^0_{3½}$		
4519.02	—	10 h	122.51			
4490.60	2	20	262.51	$b^4F_{3½}$—$y^2F^0_{2½}$	(0.00 W) 1.69 h	(0.14, 0.42, 0.70) 0.53, 0.81, 1.09, 1.37, 1.65, **1.93**
86.65	1	20	282.11	$c^2D_{2½}$—$w^2D_{2½}$	(0.00 w) 1.18	(0.03, 0.09, **0.15**) 1.06, 1.12, **1.18**, 1.24, 1.30
86.14	20	30	284.65	$a^2F_{2½}$—$z^4D^0_{2½}$		
83.29	—	5	298.81	$c^2D_{2½}$—$x^2P^0_{1½}$		
66.41	6	30	383.09	$b^4F_{2½}$—$y^4F^0_{1½}$	(0.00 W) 1.69	(0.22, 0.66) 0.35, 0.79, 1.23, **1.67**
52.70	—	10	452.00	$b^2G_{3½}$—$x^2F^0_{2½}$	(0.00) 0.91	(0.00) 0.92
43.07	15	20	500.66			
26.18	3	9	586.52	$b^4P_{2½}$—$w^2D^0_{1½}$		
22.76	20	150	603.98	$a^2H_{3½}$—$z^2H^0_{4½}$	(0.00 w) 1.28 A[2]?	(0.04, 0.10, 0.18, 0.24, 0.32) 0.78, 0.86, 0.92, 1.00, 1.06, 1.14, 1.20, 1.28, 1.34, **1.42**
4417.37	40	100	631.57	$a^2P_{3½}$—$y^2D^0_{1½}$	(0.00) **0.78**	(0.03) 0.77, **0.83**
4397.15	—	3 h	735.64			

TABLE 1.—*First spark spectrum of hafnium* (Hf II)—Continued

λ_{air}	Intensity		ν_{vac} cm^{-1}	Term combinations	Zeeman effects	
	Arc	Spark			Observed	Computed
85.52	—	5	795.93	$a^3G_{3\frac{1}{2}}$—$z^4P^0_{2\frac{1}{2}}$		
70.95	60	100	871.92	$a^2F_{2\frac{1}{2}}$—$z^4G^0_{3\frac{1}{2}}$	(0.00) 0.98	(0.01, 0.03, **0.05**) 0.95, 0.97, **0.99**, 1.01, 1.03
67.90	30	40	887.89	$a^4P_{2\frac{1}{2}}$—$z^2P^0_{1\frac{1}{2}}$	(0.00) 1.50	(**0.06**, 0.16) 1.26, 1.36, 1.48, **1.58**
65.73	—	5	899.26			
50.52	30	150	22979.32	$b^4F_{4\frac{1}{2}}$—$y^4F^0_{4\frac{1}{2}}$	(0.34) 1.28 B	(0.04, 0.12, 0.20, 0.28, **0.36**) 0.95, 1.03, 1.11, 1.19, **1.27**, 1.35, 1.43, 1.51, 1.59
36.66	40	200	23052.76	$b^4F_{3\frac{1}{2}}$—$y^2F^0_{3\frac{1}{2}}$	(0.26) 1.19	(0.04, 0.10, 0.18, **0.24**) 0.98, 1.06, 1.12, **1.20**, 1.26, 1.34, 1.40
35.15	5	5	060.79	$a^4F_{3\frac{1}{2}}$—$z^4F^0_{4\frac{1}{2}}$		
34.65	10	30	063.45	$b^4F_{4\frac{1}{2}}$—$z^4G^0_{5\frac{1}{2}}$	(0.00) 1.16	(**0.02**, 0.06, 0.10, 0.14, 0.18) **1.09**, 1.13, 1.17, 1.21, 1.25, 1.29, 1.33, 1.37, 1.41, 1.45
27.55	?	4	101.29	$a^2F_{3\frac{1}{2}}$—$z^4F^0_{4\frac{1}{2}}$		
21.36	2	30	134.38	$b^4P_{1\frac{1}{2}}$—$y^4P^0_{1\frac{1}{2}}$	(0.00 w) 1.70	(0.09, **0.27**) 1.49, **1.67**, 1.85
20.69	15	40	137.97	$b^2D_{2\frac{1}{2}}$—$z^4P^0_{2\frac{1}{2}}$	(0.35) 1.37 B w	(0.08, 0.24, **0.40**) 1.05, 1.21, **1.37**, 1.53, 1.69
4319.51	1	8	144.29	$a^2P_{0\frac{1}{2}}$—$z^4P^0_{1\frac{1}{2}}$		
4272.85	20	60	397.02	$a^4P_{2\frac{1}{2}}$—$z^4D^0_{3\frac{1}{2}}$	(0.00) 1.36	(**0.02**, **0.04**, 0.08) **1.32**, 1.34, 1.38, 1.40, 1.44, 1.46
69.67	10	20	414.45	$a^2F_{3\frac{1}{2}}$—$z^4G^0_{3\frac{1}{2}}$	(0.00) 1.00?	(0.02, 0.08, 0.12, **0.18**) 0.94, **0.98**, 1.04, **1.08**, 1.14, 1.18, 1.24
68.10	—	5	423.06	$b^4P_{0\frac{1}{2}}$—$y^4P^0_{1\frac{1}{2}}$		
62.72	4	10	452.62	$a^4P_{1\frac{1}{2}}$—$z^2P^0_{1\frac{1}{2}}$		
52.61	?	1	508.38	$z^2G^0_{3\frac{1}{2}}$—3		
49.33	10	30	526.52	$b^2D_{1\frac{1}{2}}$—$y^2D^0_{1\frac{1}{2}}$	(0.37) 0.86 B	(0.12, **0.34**) 0.68, **0.92**, 1.14
45.84	8	20	545.86	$b^4F_{3\frac{1}{2}}$—$y^4F^0_{2\frac{1}{2}}$	(0.12) 0.98	(0.02, 0.04, **0.08**) 0.94, 0.96, **1.00**, 1.02, 1.06
41.93	1	7	567.56	$c^2D_{2\frac{1}{2}}$—$w^2P^0_{1\frac{1}{2}}$		
32.43	30	60	620.46	$b^4F_{1\frac{1}{2}}$—$y^4F^0_{1\frac{1}{2}}$	(0.14) 0.52	(0.06, **0.16**) 0.40, **0.52**, 0.62
31.61	—	2 Zr?	625.04	$b^4P_{1\frac{1}{2}}$—$z^2F^0_{2\frac{1}{2}}$		
18.84	(?)	1	696.55	$a^2G_{3\frac{1}{2}}$—$z^2F^0_{3\frac{1}{2}}$		
07.39	—	2	761.03	$a^2H_{4\frac{1}{2}}$—$y^2G^0_{4\frac{1}{2}}$		
06.59	30	80	765.55	$b^4F_{2\frac{1}{2}}$—$y^2F^0_{3\frac{1}{2}}$	(0.00) 1.02	(0.03, 0.09, **0.15**) 0.86, 0.92, **0.98**, 1.04, 1.10
4201.76	(?)	1	792.87	$b^4P_{2\frac{1}{2}}$—$z^2F^0_{3\frac{1}{2}}$		
4187.68	5	8	872.87	$b^4F_{1\frac{1}{2}}$—$y^2P^0_{1\frac{1}{2}}$		
79.55	1	10	919.30	$b^2F_{2\frac{1}{2}}$—$w^2D^0_{2\frac{1}{2}}$	(0.00) 0.92	
77.50	10	20	931.04	$a^2P_{1\frac{1}{2}}$—$y^2D^0_{2\frac{1}{2}}$	(0.00) 1.06	(**0.02**, 0.06) **1.02**, 1.06, 1.10 1.14
70.41	2	2	971.72	$a^2P_{0\frac{1}{2}}$—$z^4P^0_{1\frac{1}{2}}$		
66.64	—	3	23993.41	$b^2P_{1\frac{1}{2}}$—$u^2D^0_{1\frac{1}{2}}$		
63.43	1	5	24011.91	$b^4F_{4\frac{1}{2}}$—$z^2G^0_{3\frac{1}{2}}$		
62.40	10	50	017.85	$a^2G_{4\frac{1}{2}}$—$z^2F^0_{3\frac{1}{2}}$	(0.00) 1.13	(**0.00**, 0.01, 0.02, 0.03) 1.09, 1.10, 1.11, 1.12, 1.13, 1.14, 1.15, **1.16**
58.90	5	30	038.07	$b^2D_{2\frac{1}{2}}$—$z^2F^0_{3\frac{1}{2}}$	(0.00 w) 0.86 h	(**0.08**, 0.26, 0.42) **0.70**, 0.86, 1.04, 1.20, 1.38, 1.54
56.74	(?)	4	050.56	$a^2G_{3\frac{1}{2}}$—$y^2D^0_{2\frac{1}{2}}$		
41.84	(?)	5	137.08	$b^4P_{0\frac{1}{2}}$—$w^2D^0_{1\frac{1}{2}}$		
40.21	(?)	2	146.58	$b^4F_{1\frac{1}{2}}$—$y^2P^0_{0\frac{1}{2}}$		
38.70	(?)	3	155.39	$b^4P_{2\frac{1}{2}}$—$w^2D^0_{2\frac{1}{2}}$		
27.80	10	40	219.17	$b^2D_{1\frac{1}{2}}$—$z^2F^0_{2\frac{1}{2}}$	(0.00 w) 0.72 A[1]	(0.07, 0.21) **0.68**, 0.82, 0.96, 1.00
25.10	(?)	5	235.02	$b^2G_{4\frac{1}{2}}$—$z^2F^0_{3\frac{1}{2}}$		
23.54	1	10	244.19	$b^2G_{3\frac{1}{2}}$—$w^2D^0_{2\frac{1}{2}}$		
4113.58	15	20	302.89	$a^2F_{2\frac{1}{2}}$—$z^2P^0_{1\frac{1}{2}}$	(**0.18**, 0.54) **0.44**, 0.79, 1.14	(**0.16**, 0.50) **0.48**, 0.82, 1.14, 1.48, 1.80
4097.21	3?	8	399.99	$a^4P_{2\frac{1}{2}}$—$y^2D^0_{1\frac{1}{2}}$		
93.16	120	150	424.13	$a^4F_{1\frac{1}{2}}$—$z^4F^0_{1\frac{1}{2}}$	(0.08) 0.47	(0.04, **0.10**) 0.42, **0.48**, 0.56
82.67	—	1	486.89	$b^4F_{3\frac{1}{2}}$—$y^4F^0_{3\frac{1}{2}}$		
80.44	30	60	500.27	$a^4F_{2\frac{1}{2}}$—$z^4F^0_{2\frac{1}{2}}$	(0.00) 1.07	(0.01, 0.03, **0.05**) 1.03, 1.05, **1.07**, 1.09, 1.11
71.22	3	6	555.75	$b^4F_{2\frac{1}{2}}$—$y^2F^0_{2\frac{1}{2}}$		
50.67	2	7	680.33	$a^2G_{3\frac{1}{2}}$—$z^4G^0_{4\frac{1}{2}}$	(0.00 w) 1.69 h	(**0.12**, 0.38, 0.62, 0.88) 0.30, 0.54, 0.80, 1.04, 1.30, 1.54, 1.80, **2.04**
49.44	4	10	687.82	$a^2P_{1\frac{1}{2}}$—$y^4F^0_{1\frac{1}{2}}$	(0.86) 0.31, **0.86**, 1.39	(0.28, **0.82**) 0.30, **0.84**, 1.40
48.46	(?)	3	693.80	$a^2H_{4\frac{1}{2}}$—$z^2H^0_{5\frac{1}{2}}$		

TABLE 1.—*First spark spectrum of hafnium* (Hf II)—Continued

λ_{air}	Intensity		ν_{vac} cm^{-1}	Term combinations	Zeeman effects	
	Arc	Spark			Observed	Computed
47.96	4	50	696.85	$a^3H_{3½}$—$y^3G^0_{4½}$	(0.00) 1.16	(**0.01**, 0.03, 0.05, 0.07, 0.09) 1.01, 1.03, 1.05, 1.07, 1.09, 1.11, 1.13, 1.15, 1.17, 1.19
33.88	1	6	783.05	$b^4F_{1½}$—$y^4F^0_{1½}$	(**0.26**, 0.80) 1.30, **1.84**	(**0.26**, 0.78) 0.20, 0.72, 1.24, **1.76**
29.16	4	10	812.08	$a^3F_{2½}$—$z^4D^0_{3½}$	(**0.21**, 0.61) 2.39	(**0.20**, 0.62, 1.02) 0.36, 0.78, 1.20, 1.60, 2.00, **2.42**
20.25	5?	5	867.07	$b^3D_{1½}$—$z^4P^0_{1½}$		
08.46	2?	8	940.21	$a^3P_{1½}$—$y^3P^0_{1½}$	(0.14) 1.15	(0.06, **0.18**) 1.06, 1.18, 1.30
4007.36	2?	10	24947.06	$b^4P_{2½}$—$x^4P^0_{1½}$	(0.00) 1.58	(**0.04**, 0.14) 1.38, 1.46, 1.56, **1.64**
3998.51	1?	6 d	25002.27	$a^3G_{4½}$—$z^4G^0_{4½}$	(0.24) 1.15	(0.02, 0.06, 0.10, 0.14, **0.18**) 0.99, 1.03, 1.07, 1.11, **1.15**, 1.19, 1.23, 1.27, 1.31
96.80	1?	5	012.97	$a^4P_{2½}$—$z^4G^0_{3½}$		
84.85	1	5	087.98	$b^3G_{2½}$—$z^2H^0_{1½}$	(0.18 h) 1.34 h	(**0.06**, 0.16, 0.28, 0.38) 0.64, 0.76, 0.86, 0.98, 1.08, 1.20, 1.30, **1.42**
84.03	3	8	093.14	$a^4P_{2½}$—$z^2F^0_{2½}$	(1.40) 1.20	(0.26, 0.80, **1.32**) 0.10, 0.62, **1.16**, 1.68, 2.22
79.40	4	40	122.34	$b^3G_{4½}$—$w^2F^0_{3½}$	(0.00 w) 0.62 A[1]	(**0.06**, 0.18, 0.30, 0.42) **0.64**, 0.76, 0.88, 1.00, 1.12, 1.24, 1.36, 1.48
75.15	—	4	149.26	$b^3D_{2½}$—$y^4F^0_{1½}$		
64.96	5	15	213.83	$a^3P_{1½}$—$y^3P^0_{0½}$	(0.29) 0.86, **1.42**	(0.28) 0.84, **1.40**
46.00	—	7 h	334.97	$b^3F_{3½}$—$z^3F^0_{2½}$	(0.00 h) 1.28 h	
45.36	—	10 h	339.08	$c^2D_{2½}$—$v^3D^0_{1½}$	(0.00 h) 1.24 h	(0.09, 0.27, **0.45**) 0.88, 1.06, **1.24**, 1.42, 1.60
35.64	7	20	401.66	$b^3D_{2½}$—$y^3P^0_{1½}$	(0.00) 1.33	(**0.02**, 0.08) 1.22, 1.26, 1.32, **1.36**
33.65	30	40	414.51	$a^4F_{4½}$—$z^4F^0_{3½}$	(0.00 w) 1.47	(**0.04**, 0.10, 0.18, 0.24), 1.08 1.16, 1.22, 1.30, 1.36, **1.44**, **1.50**, **1.58**
33.18	—	1	417.55	$b^4P_{1½}$—$w^2D^0_{2½}$		
32.40	3	10	422.59	$a^2F_{3½}$—$z^4P^0_{2½}$		
31.96	—	1	425.44	$b^4P_{2½}$—$w^4D^0_{1½}$		
29.53	3 Zr	3	441.16	$b^3G_{4½}$—$z^2H^0_{4½}$		
23.91	15	40	477.60	$a^4P_{1½}$—$z^4P^0_{0½}$	(0.47) **1.22**, 2.16	(0.47) **1.22**, 2.16.
18.10	60	100	515.38	$a^4F_{1½}$—$z^4D^0_{0½}$	(0.00) 0.41	(0.04) **0.41**, 0.49.
17.47	4	20	519.48	$b^4F_{3½}$—$z^2G^0_{3½}$	(0.63) 1.12 Bw	(0.10, 0.30, 0.50, **0.70**) 0.53, 0.73, 0.93, **1.13**, 1.33, 1.53, 1.73.
3900.64	2	20	629.59	$a^2H_{5½}$—$z^2H^0_{5½}$	(0.00) 1.08	(0.01, 0.03, 0.05, 0.07, 0.09, **0.11**) 0.99, 1.01, 1.03, 1.05, 1.07, **1.09**, 1.11, 1.13, 1.15, 1.17, 1.19.
3883.77	6	20	740.91	$a^4P_{2½}$—$z^4P^0_{1½}$	(0.00w) 1.18	(**0.13**, 0.39) **1.03**, 1.29, 1.55, 1.81.
82.23	—	3 h	751.12	$a^2H_{4½}$—$y^3G^0_{3½}$		
80.82	30	40	760.48	$a^4F_{1½}$—$z^4F^0_{2½}$	(**0.32**, 0.95) 0.78, 1.42, **2.06**	(**0.32**, 0.94) 0.14, 0.76, 1.40, **2.02.**
77.11	5	40	785.12	$b^4F_{4½}$—$y^4D^0_{3½}$	(0.00) 1.26	(**0.03**, 0.09, 0.15, 0.21) **1.10**, 1.16, 1.22, 1.28, 1.34, 1.40, 1.46, 1.52.
72.55	7	20	815.49	$a^2F_{2½}$—$y^2D^0_{1½}$	(0.00 w) 1.21 A[3]	(**0.09**, 0.27) 0.71, 0.89, **1.07**, **1.25.**
67.32	4	15	850.40	$a^2P_{1½}$—$y^4F^0_{2½}$	(0.00 w) 0.82 A[1]	(**0.07**, 0.21) **0.77**, 0.91, 1.05, 1.19.
64.75	2	20	867.59	$b^2G_{4½}$—$y^2G^0_{3½}$	(0.00 w) 0.45 A[1]	(**0.07**, 0.21, 0.35, ') **0.57**, 0.71, 0.85, 0.99, 1.13, 1.27, 1.41, 1.55.
49.52	7	25	25969.93	$a^2G_{3½}$—$y^4F^0_{3½}$	(0.00) 0.83	(**0.03**, 0.09, 0.15) **0.77**, 0.83, 0.89, 0.95, 1.01, 1.07.
38.37	1	3	26045.36	$b^4P_{1½}$—$x^4P^0_{0½}$	(0.38) 1.31	(0.41) 0.41, **1.35.**
23.53	1	4	146.45	$b^4P_{2½}$—$x^4D^0_{3½}$		

TABLE 1.—*First spark spectrum of hafnium* (Hf II)—Continued

λ_{air}	Intensity		ν_{vac} cm^{-1}	Term combinations	Zeeman effects	
	Arc	Spark			Observed	Computed
19.90	—	2 h	171.30			
17.20	6	20	189.81	$a^3G_{3½}$—$y^2F^0_{3½}$	(0.00) 0.87	(0.02, 0.04, 0.08) **0.84**, 0.88, 0.90, 0.94, 0.96, 1.00.
10.59	2	10	235.24	$b^3G_{3½}$—$x^4D^0_{3½}$	(**0.19**, 0.58, 0.96) 0.00 Wus	(**0.19**, 0.57, 0.95)—**0.03**, +0.35, 0.73, 1.11, 1.49, 1.87.
06.07	6	40	266.39	$b^4F_{3½}$—$y^4D^0_{3½}$	(0.00 w) 1.04 A[1]	(**0.05**, 0.15, 0.25) 0.98, 1.08, 1.18, 1.28, 1.38, 1.48.
3800.39	40?	5	305.65	$a^4P_{1½}$—$z^4P^0_{1½}$	(0.00) 1.69	(0.00) 1.68, **1.70**.
3799.51	—	3	311.74	$b^2D_{2½}$—$y^4F^0_{1½}$		
97.95	5	10	322.55	$a^2F_{3½}$—$z^2F^0_{3½}$	(0.00) 1.12	(0.00, 0.01, 0.02, **0.03**) 1.08, 1.09, 1.10, **1.11**, 1.12, 1.13, 1.14.
93.37	40	60	354.33	$a^2D_{2½}$—$z^4F^0_{2½}$	(0.22) 1.13	(0.05, 0.15, **0.25**) 0.93, 1.03, **1.13**, 1.23, 1.33.
82.78	4	8	428.11	$a^2F_{2½}$—$z^4G^0_{3½}$	(0.00) 1.18	(0.04, 0.12, 0.20) 0.86, 0.94, 1.02, 1.10, 1.18, 1.26.
80.09	3	7	446.91	$a^4P_{0½}$—$z^4P^0_{½}$	(0.00) 2.62	(0.01) 2.62.
72.83	—	1	497.80	$b^4P_{0½}$—$x^4P^0_{1½}$		
71.36	3	8	508.13	$a^2F_{2½}$—$z^2F^0_{2½}$	(0.24) 0.96	(0.04, 0.14, **0.22**) 0.76, 0.84, 0.94, 1.02, 1.12.
70.64	—	3	513.19	$b^4P_{2½}$—$x^4P^0_{1½}$		
66.92	10	50	539.37	$b^4F_{2½}$—$y^4D^0_{1½}$	(0.00 w) 0.85 A[1]	(**0.08**, 0.22) **0.78**, 0.94, 1.08, 1.24.
62.51	2	25	570.48	$a^2H_{4½}$—$x^4D^0_{3½}$	(0.00 w) 0.81 A[1]	(**0.04**, 0.10, 0.18, 0.24) **0.80**, 0.88, 0.94, 1.02 1.08, 1.16, 1.22, 1.30.
58.04	—	3	602.08	$b^2G_{3½}$—$x^4P^0_{2½}$		
47.48	3	7	677.04	$a^2F_{3½}$—$y^2D^0_{2½}$	(0.00) 1.10	(**0.02**, **0.04**, 0.08) 1.04, 1.06, 1.10, 1.12, 1.16, **1.18**.
45.78	—	1	689.15	$a^2G_{3½}$—$y^4F^0_{3½}$		
44.98	3	15	701.91	$b^4F_{4½}$—$z^2G^0_{4½}$	(0.64) 1.20 Bw	(0.08, 0.22, 0.38, 0.52, **0.68**) 0.64, 0.78, 0.94, 1.08, **1.24**, 1.38, 1.54, 1.68, 1.84.
37.88	5	15	745.56	$b^4F_{1½}$—$y^4D^0_{½}$	(0.00) 0.44	(0.00) 0.46.
19.27	50	70	879.38	$a^4F_{2½}$—$z^4D^0_{1½}$	(0.00 w) 0.85 A[1]	(**0.08**, 0.24) **0.82**, 0.98, 1.14, 1.30.
05.40	5	15	26979.99	$a^3G_{3½}$—$y^2F^0_{2½}$	(0.64) 1.01 Bw	(0.12, 0.36, 0.60, **0.84**) 0.32, 0.56, 0.80, **1.04**, 1.28, 1.52, 1.76.
02.36	—	2	27002.14	$b^3F_{3½}$—$v^3F^0_{3½}$		
3701.15	15	40	010.97	$a^3G_{4½}$—$y^4F^0_{3½}$	(0.00) 1.02 A[1]	(**0.02**, 0.08, 0.12, 0.18) **0.96**, 1.00, 1.06, 1.10, 1.16, 1.20, 1.26, 1.30.
3699.72	10	25	021.41	$a^4P_{2½}$—$z^4P^0_{2½}$	(0.00) 1.42	(0.02, 0.04, 0.08) 1.38, 1.40, **1.44**, 1.46, 1.50.
99.56	1?	3	022.58	$b^4F_{2½}$—$z^2G^0_{3½}$		
98.39	3	10	031.13	$b^2D_{2½}$—$y^4F^0_{3½}$	(0.00 w) 1.02 A[1]	(**0.06**, 0.16, 0.28) **0.90**, 1.02, 1.12, 1.24, 1.34, 1.46.
81.39	2	4	155.95	$a^3F_{2½}$—$z^4P^0_{1½}$		
78.05	—	3	180.61	$b^3G_{3½}$—$y^2G^0_{4½}$		
66.79	—	2	264.08	$a^3P_{0½}$—$y^4F^0_{½}$		
63.35	8	20	274.78	$a^4P_{0½}$—$z^4P^0_{1½}$	(0.48) **1.12**, 2.08	(0.46) **1.22**, 2.14.
61.73	—	2	301.75	$a^3G_{4½}$—$y^2F^0_{3½}$		
61.05	5	12	306.82	$a^3F_{3½}$—$z^4G^0_{4½}$	(0.00 w) 1.37 A[2]	(**0.03**, 0.09, 0.15, 0.21) 0.96, 1.02, 1.08, 1.14, 1.20, 1.26, 1.32, **1.38**
59.02	2	4	321.97	$b^2D_{2½}$—$y^2F^0_{2½}$	(0.00 w) 1.02 h	(**0.06**, **0.20**, 0.32) **0.84**, 0.96, 1.10, 1.22, 1.36, 1.48
56.64	—	2	339.75	$b^2P_{1½}$—$u^2D^0_{2½}$		
48.35	4	6	401.87	$b^2D_{1½}$—$y^2D^0_{2½}$	(0.00) 1.14	(**0.02**, 0.08) 1.00, 1.06, 1.10, **1.16**
47.48	—	2	408.41	$b^4P_{1½}$—$z^4D^0_{2½}$		
44.35	50	60	431.95	$a^4F_{3½}$—$z^4F^0_{3½}$	(0.00) 1.25	(0.04, 0.08, **0.10**) 1.14, 1.18, 1.22, **1.24**, 1.28, 1.30, 1.34
42.54	—	1	445.58	$y^4F^0_{3½}$—5		
33.19	2	4	516.21	$a^3P_{0½}$—$y^2P^0_{½}$	(0.25) 1.50	(0.25) 0.99, **1.49**

TABLE 1.—*First spark spectrum of hafnium* (Hf II)—Continued

λ_{air}	Intensity		ν_{vac} cm^{-1}	Term combinations	Zeeman effects	
	Arc	Spark			Observed	Computed
30.86	157	2	533.86	$b^2G_{4½}$—$y^2G^0_{4½}$		
24.00	6	10	585.98	$a^4P_{1½}$—$z^4P^0_{½}$	(**0.11**, 0.34) 1.14 A[1]	(**0.12**, 0.36) **1.09**, 1.33, 1.57, 1.81
22.46	1	4	597.71	$b^4F_{1½}$—$z^2S^0_{½}$	(0.62) 0.16	(0.61)− **0.15**, +1.07
3600.07	1	4	769.34	$b^4F_{2½}$—$y^4D^0_{½}$		
3599.16	—	3	776.36	$b^4F_{1½}$—$y^4D^0_{½}$	(0.38, **1.12**) 0.00, **0.80**, 1.56	(0.35, **1.05**) 0.11, **0.81**, 1.51
97.42	5	10	789.80	$a^2P_{0½}$—$y^2P^0_{½}$	(0.00) 0.66	(0.09) 0.65
94.42	—	2	812.99	$a^2P_{1½}$—$y^4D^0_{½}$		
91.11	—	1	838.63	$b^4F_{2½}$—$z^2D^0_{1½}$		
80.46	1	3	27921.43	$a^4P_{2½}$—$z^2F^0_{2½}$		
69.03	50	80	28010.85	$a^4F_{3½}$—$z^4D^0_{2½}$	(0.00) 1.10	(**0.04**, 0.14, 0.22) **1.00**, 1.10, 1.18, 1.28, 1.36, 1.46
61.65	70	80	068.89	$a^2D_{1½}$—$z^4F^0_{1½}$	(0.13, 0.39) 0.37, **0.62**, 0.88	(0.14, **0.42**) 0.38, **0.66**, 0.94
52.70	30	40	139.60	$a^4F_{1½}$—$z^4D^0_{½}$	(0.40, **1.19**) 0.00, **0.79**, 1.59	(0.38, **1.16**) 0.06, **0.84**, 1.60
50.27	—	1	158.85	$b^2D_{1½}$—$y^4F^0_{1½}$		
44.78	—	2	202.47	$b^4F_{3½}$—$z^2G^0_{4½}$		
35.54	50	80	276.17	$a^4F_{3½}$—$z^2D^0_{2½}$	(0.00) 1.05	(0.00, 0.01, **0.02**) 1.03, 1.04, **1.05**, 1.06, 1.07
18.75	6	15	411.09	$b^2D_{1½}$—$y^2P^0_{1½}$	(0.26) 1.14	(0.10, **0.32**) 0.92, **1.14**, 1.34
18.38	—	3	414.08	$a^2G_{3½}$—$y^4F^0_{1½}$		
15.62	—	1	436.38	$a^2F_{2½}$—$z^4P^0_{2½}$		
11.88	1	4	466.66	$b^2G_{4½}$—$z^2H^0_{5½}$		
3505.22	50	150	520.75	$a^4F_{4½}$—$z^4D^0_{3½}$	(0.00) 1.22	(**0.03**, 0.09, 0.15, 0.21) **1.12**, 1.18, 1.24, 1.30, 1.36, 1.42, 1.48, 1.54
3495.94	3	10	596.46	$a^2F_{3½}$—$y^4F^0_{3½}$	(0.00 w) 1.29 A[2]	(**0.06**, 0.18, 0.32) 0.78, 0.92, 1.04, 1.18, 1.30, **1.44**
95.75	12	20	598.01	$a^4F_{3½}$—$z^4G^0_{2½}$	(**0.11**, 0.32, 0.54) 1.57, **1.80**	(**0.12**, 0.34, 0.58) 0.66, 0.88, 1.12, 1.34, 1.58, **1.80**
87.57	4	8	665.08	$a^2P_{1½}$—$z^2S^0_{½}$	(0.25) **0.86**, 1.35	(0.28) **0.84**, 1.40
85.16	2	3	684.91	$b^2D_{1½}$—$y^2P^0_{½}$		
79.29	30	40	733.30	$a^2D_{2½}$—$z^4D^0_{1½}$	(0.00) 1.14	(**0.02**, 0.06) **1.12**, 1.16, 1.20, 1.24
78.98	8	30	735.86	$a^2G_{4½}$—$y^4F^0_{4½}$	(0.42) 1.20 Bw	(0.05, 0.15, 0.25, 0.35, **0.45**) 0.78, 0.88, 0.98, 1.08, **1.18**, 1.28, 1.38, 1.48, 1.58
75.85	—	2	761.74	$z^4D^0_{3½}$—1		
69.23	1	2	816.62	$a^2F_{3½}$—$y^2F^0_{3½}$		
68.86	2	2	819.69	$a^2G_{4½}$—$z^4G^0_{5½}$		
65.92	1	2	844.14	$a^2P_{1½}$—$y^4D^0_{½}$		
62.65	10	15	28871.37	$a^4F_{2½}$—$z^4F^0_{3½}$	(0.00 w) 1.75 A[2]	(**0.10**, 0.30, 0.50) 0.76, 0.96, 1.16, 1.36, 1.56, **1.76**
43.42	—	1	29032.60	$a^4P_{2½}$—$y^4F^0_{1½}$		
38.24	10	15+Zr	076.34	$b^4F_{1½}$—$z^4D^0_{½}$		
28.37	15	20	160.05	$a^2D_{1½}$—$z^4D^0_{½}$	(0.12) 0.72, 0.96	(0.14) 0.67, 0.94
21.45	3	4	219.02	$a^4F_{2½}$—$z^2D^0_{1½}$		
13.74	3	8	285.01	$a^4P_{2½}$—$y^2P^0_{1½}$	(0.00 w) 1.62 A[2]	(**0.09**, 0.27) 1.15, 1.33, 1.51, **1.69**
10.18	15	40	315.58	$a^2F_{3½}$—$y^4F^0_{3½}$	(0.24) 1.14 Bw	(0.04, 0.10, 0.18, **0.24**) 0.94, 1.00, 1.08, **1.14**, 1.22, 1.28, 1.36
3407.76	7	15	336.40	$a^2F_{2½}$—$z^2F^0_{3½}$	(0.00 w) 1.32 A[2]	(0.07, 0.21, 0.35) 0.77, 0.91, 1.05, 1.19, 1.33, **1.47**
3399.80	100	150	405.09	$a^2D_{1½}$—$z^4F^0_{1½}$	(**0.14**, 0.41) 1.21, **1.48**	(**0.14**, 0.42) 0.66, 0.94, 1.22 **1.50**
94.99	6	30	446.75	$a^2G_{3½}$—$z^2G^0_{3½}$	(0.23) 0.99	(0.06, 0.16, 0.28, **0.38**) 0.64, 0.76, 0.86, **0.98**, 1.08, 1.20, 130
94.58	10	25	450.30	$a^4F_{2½}$—$z^4D^0_{3½}$	(0.64) 1.16 B	(0.13, 0.39, **0.65**) 0.67, 0.93, **1.19**, 1.45, 1.71
89.83	40	70	491.57	$a^4F_{1½}$—$z^2P^0_{½}$	(0.00) 0.49	(0.08) 0.37, **0.53**
86.10	—	2	524.05	$b^2G_{4½}$—$y^2G^0_{3½}$		
85.22	—	2	531.73			
84.70	10	20	536.27	$a^4F_{1½}$—$z^2D^0_{2½}$	(0.29, 0.87) 0.80, 1.40, **2.00**	(**0.30**, 0.90) 0.15, 0.75, 1.35, **1.95**

TABLE 1.—*First spark spectrum of hafnium* (Hf II)—Continued

λ_{air}	Intensity		ν_{vac} cm^{-1}	Term combinations	Zeeman effects	
	Arc	Spark			Observed	Computed
84.14	5	10	541.15	$b^3D_{1\frac{1}{2}}-y^2F^0_{2\frac{1}{2}}$	(0.00) 1.01	(**0.04**, 0.12) **0.83**, 0.91, 0.99, 1.07
76.68	1	4	606.42	$a^2F_{3\frac{1}{2}}-y^2F^0_{3\frac{1}{2}}$		
70.69	—	5	659.03	$b^2G_{3\frac{1}{2}}-v^2D^0_{2\frac{1}{2}}$		
67.09	1	2	690.74	$a^2F_{2\frac{1}{2}}-y^2D^0_{2\frac{1}{2}}$		
65.80	—	2	702.12			
58.30	3	8	768.45	$a^2G_{4\frac{1}{2}}-z^2G^0_{3\frac{1}{2}}$		
56.05	4	6+Zr	788.40	$b^2D_{2\frac{1}{2}}-z^2G^0_{3\frac{1}{2}}$		
52.06	40	80	823.86	$a^4F_{4\frac{1}{2}}-z^4F^0_{4\frac{1}{2}}$	(0.00) 1.34	(0.00, 0.01, 0.02, 0.03, **0.04**) 1.29, 1,30, 1.31, 1.32, **1.33**, 1.34, 1.35, 1.36,1.37
49.17	—	5	849.59	$a^4P_{1\frac{1}{2}}-y^2P^0_{1\frac{1}{2}}$		
33.49	—	2	29989.99	$b^2G_{3\frac{1}{2}}-x^4D^0_{3\frac{1}{2}}$		
28.21	15	20	30037.57	$a^4F_{2\frac{1}{2}}-z^4G^0_{2\frac{1}{2}}$	(0.00 w) 1.07	(0.03, 0.09, **0.15**) 0.91, 0.97, **1.03**, 1.09, 1.15
24.18	2	6	073.98	$a^2P_{1\frac{1}{2}}-y^4D^0_{2\frac{1}{2}}$		
23.35	4	20	081.50	$b^4F_{4\frac{1}{2}}-w^2F^0_{3\frac{1}{2}}$	(0.00 w) 1.74 A^2	(**0.06**, 0.20, 0.32, 0.46) 0.86, 0.98, 1.12, 1.24, 1.38, 1.50, 1.64, **1.76**
18.74	1	1	123.28	$a^4P_{1\frac{1}{2}}-y^2P^0_{0\frac{1}{2}}$		
17.99	15	20	130.09	$a^2D_{2\frac{1}{2}}-z^2D^0_{2\frac{1}{2}}$	(0.29) 1.12	(0.06, 0.20, **0.32**) 0.86, 0.98, **1.12**, 1.24, 1.38
17.24	—	2	136.90	$a^4F_{4\frac{1}{2}}-z^4G^0_{3\frac{1}{2}}$		
14.03	—	2	166.09	$a^2P_{1\frac{1}{2}}-z^4S^0_{1\frac{1}{2}}$		
3310.85	2	6	195.06	$a^4P_{2\frac{1}{2}}-y^4F^0_{2\frac{1}{2}}$		
3294.68	—	3	343.25	$b^2G_{4\frac{1}{2}}-x^4D^0_{3\frac{1}{2}}$		
89.74	2	3	388.82	$a^2P^0_{0\frac{1}{2}}-y^4D^0_{0\frac{1}{2}}$		
83.39	3	6	447.58	$a^2F_{2\frac{1}{2}}-y^4F^0_{1\frac{1}{2}}$		
79.98	20?	20	479.24	$a^4F_{1\frac{1}{2}}-z^2D^0_{1\frac{1}{2}}$	(0.57) 0.28, **0.63**, 0 98	(0.20, **0.58**) 0.26, **0.64**, 1.04
73.66	6?	6	538.08	$a^4F_{2\frac{1}{2}}-z^4D^0_{2\frac{1}{2}}$		
66.53	—	2	604.73	$b^2D_{2\frac{1}{2}}-x^2D^0_{1\frac{1}{2}}$		
56.15	—	1	702.29	$b^4F_{3\frac{1}{2}}-x^2F^0_{3\frac{1}{2}}$		
55.28	15	25	710.50	$a^4F_{1\frac{1}{2}}-z^4D^0_{2\frac{1}{2}}$	(**0.45**, 1.34) 0.93, 1.81, **2.70**	(**0.44**, 1.30) 0.02, 0.88, 1.76, **2.62**
53.70	30	80	725.41	$a^2D_{2\frac{1}{2}}-z^4F^0_{3\frac{1}{2}}$	(0.00) 1.38	(**0.04**, 0.12, 0.20) 1.06, 1.14, 1.22, 1.30, 1.38, 1.46.
50.07	—	1	759.73	$a^4P_{1\frac{1}{2}}-y^4F^0_{2\frac{1}{2}}$		
43.00	1	6	826.78	$b^4F_{4\frac{1}{2}}-y^2G^0_{3\frac{1}{2}}$	(0.00) 1.57	(**0.06**, 0.16, 0.28, 0.38) 0.92, 1.04, 1.14, 1.26, 1.36, 1.48, 1.58, **1.70**
33.80	1	4	914.48	$a^4P_{2\frac{1}{2}}-y^4F^0_{3\frac{1}{2}}$		
27.00	2	4	979.62	$a^4P_{1\frac{1}{2}}-y^2F^0_{2\frac{1}{2}}$		
25.04	1	4	30998.45	$b^4F_{2\frac{1}{2}}-w^2D^0_{1\frac{1}{2}}$		
20.66	10	50	31040.60	$a^2F_{3\frac{1}{2}}-y^4F^0_{4\frac{1}{2}}$	(0.00 w) 1.55 A^2	(**0.06**, 0.18, 0.30, 0.42) 0.81, 0.93, 1.05, 1.17, 1.29, 1.41, 1.53, **1.65**
18.20	2	8	064.33	$b^4F_{3\frac{1}{2}}-w^2D^0_{2\frac{1}{2}}$		
17.30	20	25	073.02	$a^2D_{2\frac{1}{2}}-z^2D^0_{1\frac{1}{2}}$	(**0.16**, 0.48) 1.66 A^2	(**0.17**, 0.51) 0.67, 1.01, 1.35, **1.69**
15.29	—	1	092.44	$a^4P_{0\frac{1}{2}}-y^2P^0_{0\frac{1}{2}}$		
06.77	1	4	175.05	$a^2P_{1\frac{1}{2}}-x^2D^0_{2\frac{1}{2}}$	(0.00) 1.36	(**0.07**, 0.21) 1.05, 1.19, 1.33, **1.47**
03.67	3	10	205.21	$a^4P_{2\frac{1}{2}}-y^2F^0_{3\frac{1}{2}}$	(0.00 w) 0.76	(**0.13**, 0.39, 0.65) **0.51**, 0.77, 1.03, 1.29, 1.55, 1.81
3202.16	1	4	219.93	$a^2G_{3\frac{1}{2}}-y^4D^0_{3\frac{1}{2}}$		
3199.99	6	30	241.10	$a^2P_{0\frac{1}{2}}-z^2S^0_{0\frac{1}{2}}$	(0.48) 1.22	(0.47) 1.21
98.33	—	2	257.31	$y^2F^0_{2\frac{1}{2}}-9$		
95.63	4	8	283.72	$b^2D_{1\frac{1}{2}}-y^4D^0_{0\frac{1}{2}}$	(0.26) 1.33	(0.28) 0.75, **1.31**
94.47	1	5	295.08	$a^2G_{3\frac{1}{2}}-x^2D^0_{2\frac{1}{2}}$		
94.19	50	100	297.82	$a^4F_{1\frac{1}{2}}-z^4G^0_{2\frac{1}{2}}$	(**0.27**, 0.81) 0.76, 1.30, **1.83**	(**0.28**, 0.82) 0.18, 0.72, 1.28, **1.82**
93.53	30	40	304.29	$a^2D_{2\frac{1}{2}}-z^4D^0_{2\frac{1}{2}}$	(0.35) 1.24 B w	(0.07, 0.21, **0.35**) 0.97, 1.11, **1.25**, 1.39, 1.53
85.32	—	3	384.98	$z^2F^0_{2\frac{1}{2}}-5$		
83.67	—	1	401.24	$y^4F^0_{3\frac{1}{2}}-10$		
81.76	1	3	420.09	$a^2P^0_{0\frac{1}{2}}-y^4D^0_{1\frac{1}{2}}$		
76.85	40	50	468.65	$a^4F_{3\frac{1}{2}}-z^2P^0_{1\frac{1}{2}}$	(0.00 w) 0.74 A^1	(**0.12**, 0.38) **0.68**, 0.94, 1.18, 1.44
67.46	1	3	561.94	$b^2D_{2\frac{1}{2}}-y^4D^0_{1\frac{1}{2}}$		

TABLE 1.—*First spark spectrum of hafnium* (Hf II)—Continued

λ_{air}	Intensity		ν_{vac} cm^{-1}	Term combinations	Zeeman effects	
	Arc	Spark			Observed	Computed
62.61	5?	40	610.33	$a^3F_{3½}-y^4F^0_{4½}$	(0.00) 0.96	(0.00) 0.98
59.93	—	2	637.14	$b^3D_{2½}-x^3D^0_{3½}$		
45.32	20	25	784.09	$a^3D_{1½}-z^4D^0_{1½}$		
40.77	7	15	830.14	$a^3F_{2½}-y^3F^0_{3½}$	(0.00) 0.99	(0.02, 0.04, 0.08) 0.90, 0.94, 0.96, 1.00, 1.02
39.67	10	15	841.29	$a^4F_{3½}-z^4F^0_{3½}$	(0.00 w) 1.50	(0.06, 0.16, 0.28, 0.38) 0.96, 1.06, 1.18, 1.28, 1.40, 1.50, 1.62, 1.72
34.72	70	150	891.56	$a^3D_{2½}-z^4G^0_{3½}$	(0.44) 1.09 B w	(0.09, 0.27, 0.45) 0.73, 0.91, 1.09, 1.27, 1.45
33.50	1	4 Zr?	903.98	$y^3D^0_{2½}-6$		
33.10	1	4	908.05	$b^4F_{3½}-z^3H^0_{3½}$		
26.27	3	6	31977.76	$a^4F_{2½}-z^4D^0_{3½}$		
16.95	3	8	32073.37	$a^3F_{3½}-z^3G^0_{3½}$	(0.00) 1.10	(0.04, 0.12, 0.20, 0.28) 0.83, 0.91, 0.99, 1.07, 1.15, 1.23, 1.31
11.49	—	2	129.66	$a^3G_{3½}-z^3G^0_{4½}$		
10.87	10	40	136.06	$b^3D_{1½}-z^3S^0_{1½}$	(0.32) 0.72	(0.32) 0.70, 1.36
09.11	50	150	154.25	$a^4F_{3½}-z^4G^0_{3½}$	(0.59) 1.14 B w	(0.08, 0.26, 0.42, 0.60) 0.64, 0.80, 0.98, 1.14, 1.32, 1.48, 1.66
07.83	—	2	167.49	$z^4G^0_{5½}-3$		
3101.39	40	100	234.28	$a^4F_{3½}-z^3F^0_{3½}$	(0.14, 0.43, 0.72) 2.15 A^2	(0.17, 0.51, 0.85) 0.38, 0.72, 1.06, 1.40, 1.74, 2.08
3099.13	—	3	257.79	$z^3F^0_{3½}-6$		
92.26	6	20	329.45	$a^3F_{2½}-y^4F^0_{3½}$	(0.00 w) 1.70 A^2	(0.10, 0.30, 0.50) 0.68, 0.88, 1.08, 1.28, 1.48, 1.68
91.79	1	5	334.37	$b^4F_{2½}-y^3G^0_{3½}$		
83.65	1	3	419.72			
80.64	20	100	451.39	$a^3G^0_{4½}-z^3G^0_{4½}$	(0.00) 1.15	(0.02, 0.04, 0.08, 0.10, 0.14) 1.02, 1.06, 1.08, 1.12, 1.14, 1.18, 1.20, 1.24, 1.26
76.70	1	4	492.95	$b^4F_{4½}-y^3G^0_{4½}$		
70.00	—	4	563.86	$a^3H_{4½}-z^3F^0_{3½}$		
69.66	—	2 Cb?	567.46	$b^4F_{2½}-w^3D^0_{2½}$		
66.53	—	3	600.70	$z^4D^0_{3½}-4$		
64.68	7	20	620.38	$a^3F_{2½}-y^3F^0_{3½}$	(0.00 w) 1.46 A^2	(0.09, 0.27, 0.45) 0.71, 0.89, 1.07, 1.25, 1.43, 1.61
64.38	—	5	623.58	$y^3F^0_{3½}-14$		
55.43	4	9	719.13	$a^3P_{0½}-z^3D^0_{1½}$	(0.00 w) 1.33	(0.24) 0.98, 1.44
54.52	6	15	728.88	$a^4F_{1½}-z^3P^0_{1½}$		
46.03	5	20	820.10	$a^3F_{3½}-y^4D^0_{2½}$	(0.00 w) 0.75	(0.11, 0.33, 0.55) 0.56, 0.78, 1.00, 1.22, 1.44, 1.66
35.28	—	3	936.33	$z^3P^0_{1½}-2$		
31.16	60	120	32981.10	$a^4F_{2½}-y^5D^0_{1½}$	(0.13, 0.38) 1.42 A^2	(0.13, 0.39) 0.67, 0.93, 1.19, 1.45
25.29	10	20	33045.09	$a^4F_{4½}-z^3F^0_{3½}$	(0.00 w) 1.96 A^2	(0.10, 0.32, 0.52, 0.64) 0.60, 0.80, 1.02, 1.22, 1.44, 1.64 1.86, 2.06
24.78	3	15	050.66	$b^3D_{2½}-y^4P^0_{1½}$	(0.00 w) 0.89 A^1	(0.14, 0.44) 0.86, 1.14, 1.44 1.72
24.35	—	2	055.36	$b^4F_{2½}-x^4D^0_{2½}$		
22.11	1	4	079.86	$a^3P_{1½}-z^3F^0_{2½}$		
16.94	5	6	136.54	$a^3D_{1½}-z^3P^0_{2½}$		
14.98	—	3	158.09	$z^4P^0_{2½}-6$		
12.90	50	100	180.98	$a^3D_{1½}-z^3D^0_{2½}$	(0.00 w) 1.37 A^2	(0.12, 0.38) 0.68, 0.92, 1.18, 1.42
12.19	—	4	188.79	$a^4P_{2½}-y^4D^0_{1½}$		
11.24	3	20	199.27	$a^3G_{3½}-z^3F^0_{2½}$	(0.00) 1.06	(0.00) 0.92
04.77	—	3	270.75			
01.85	—	4	303.11	$a^3P_{1½}-w^3D^0_{1½}$		
3000.09	25	40	322.65	$a^3D_{2½}-z^3P^0_{1½}$	(0.00 w) 1.04 A^1	(0.06, 0.20) 0.98, 1.12, 1.24, 1.38
2996.76	—	3	359.67	$b^4F_{2½}-x^4P^0_{1½}$		
93.45	—	2	396.56			
90.83	1	7	425.81	$b^4F_{4½}-z^3H^0_{4½}$		
84.38	—	3	498.05	$y^4F^0_{4½}-11$		
80.21	1	4	544.92	$b^3D_{1½}-y^4D^0_{½}$		
77.59	6	25	574.44	$a^4P_{1½}-z^3S^0_{1½}$	(0.00) 1.68	(0.00) 1.68, 1.70
77.13	—	5	579.62			

TABLE 1.—*First spark spectrum of hafnium* (Hf II)—Continued

λ_{air}	Intensity		ν_{vac} cm^{-1}	Term combinations	Zeeman effects	
	Arc	Spark			Observed	Computed
75.89	70	150	593.62	$a^4F_{2\frac{1}{2}}$—$z^4G^0_{3\frac{1}{2}}$	(0.00) 1.04	(0.00) 1.06
74.09	1	6	613.95	$b^2D_{1\frac{1}{2}}$—$x^2D^0_{1\frac{1}{2}}$		
70.60	—	2	653.44			
68.94	5	15	672.25	$a^4P_{2\frac{1}{2}}$—$z^2G^0_{3\frac{1}{2}}$		
68.82	60	120	673.61	$a^4F_{2\frac{1}{2}}$—$z^2F^0_{2\frac{1}{2}}$	(0.43) 0.97 Bw	(0.08, 0.26, **0.42**) 0.64, 0.80, **0.98**, 1.14, 1.32
67.24	10	30	691.54	$a^4P_{0\frac{1}{2}}$—$y^4D^0_{0\frac{1}{2}}$	(1.09) 1.55	(1.07) 1.54
63.75	—	2	731.21			
61.80	6	40	753.42	$a^4P_{1\frac{1}{2}}$—$y^4D^0_{1\frac{1}{2}}$	(0.67) 1.44 Bw	(0.26, **0.80**) 0.90, **1.42**, 1.96
60.83	2	15	764.48	$b^2D_{2\frac{1}{2}}$—$w^2D^0_{1\frac{1}{2}}$	(0.00 w) 1.50 A[2]	(**0.10**, 0.28) 1.00, 1.20, 1.38, **1.58**
59.17	—	4	783.42	$z^4D^0_{3\frac{1}{2}}$—3		
56.01	—	1	819.53	$b^4F_{1\frac{1}{2}}$—$x^4D^0_{1\frac{1}{2}}$		
53.65	2	4	846.55	$a^2F_{2\frac{1}{2}}$—$y^4D^0_{2\frac{1}{2}}$		
52.53	—	1	859.39	$z^4D^0_{1\frac{1}{2}}$—1		
49.62	—	6	892.79	$z^2G^0_{3\frac{1}{2}}$—17		
47.14	4	12	33921.31	$a^2F_{2\frac{1}{2}}$—$z^2D^0_{2\frac{1}{2}}$	(0.00 w) 0.86	(0.08, 0.22, 0.38) **0.74**, 0.88, 1.04, 1.18, 1.34, 1.48
40.26	—	2	34000.68	$b^4F_{2\frac{1}{2}}$—$y^2G^0_{3\frac{1}{2}}$		
37.79	50	120	029.27	$a^4F_{4\frac{1}{2}}$—$z^4G^0_{3\frac{1}{2}}$	(0.60) 1.24 Bw	(0.08, 0.24, 0.40, 0.56, **0.72**) 0.61, 0.77, 0.93, 1.09, **1.25**, 1.41, 1.57, 1.73, 1.89
30.60	—	7 h	112.75			
29.63	70	80	124.05	$a^2D_{1\frac{1}{2}}$—$z^2D^0_{1\frac{1}{2}}$	(0.00) 0.82	(**0.02**, 0.06) 0.78, **0.82**, 0.86
26.33	2	4	162.53	$a^4F_{2\frac{1}{2}}$—$z^4P^0_{2\frac{1}{2}}$		
26.06	—	5	165.68			
19.59	40	90	241.39	$a^4F_{1\frac{1}{2}}$—$y^2D^0_{1\frac{1}{2}}$	(0.54) 0.30, **0.60**, 0.90	(0.18, **0.52**) 0.28, **0.62**, 0.98
17.51	3	12	265.80	$a^2P_{1\frac{1}{2}}$—$x^4D^0_{0\frac{1}{2}}$		
13.21	1	7	316.37	$b^2G_{3\frac{1}{2}}$—$v^2F^0_{3\frac{1}{2}}$		
12.79	1	3	321.32	$a^4F_{2\frac{1}{2}}$—$z^4P^0_{1\frac{1}{2}}$		
09.91	20	30	355.29	$a^2D_{1\frac{1}{2}}$—$z^4D^0_{2\frac{1}{2}}$	(0.30) 2.02	(**0.26**, 0.78) 0.54, 1.06, 1.58, **2.10**
08.86	1	15	367.69	$z^4G^0_{3\frac{1}{2}}$—2		
06.63	—	1	394.05	$z^2F^0_{3\frac{1}{2}}$—10		
04.51	?	10	419.16	$a^4P_{2\frac{1}{2}}$—$y^4D^0_{3\frac{1}{2}}$		
2903.57	—	3	430.30			
2898.71	15	60	488.02	$a^4P_{2\frac{1}{2}}$—$x^2D^0_{1\frac{1}{2}}$	(0.00w) 1.73A[2]	(**0.10**, 0.32) 1.10, 1.32, **1.52**, **1.74**
94.01	1	4	544.03	$a^4P_{0\frac{1}{2}}$—$z^2S^0_{0\frac{1}{2}}$		
92.31	—	4	564.33			
89.01	1	6	603.81	$a^2F_{2\frac{1}{2}}$—$y^4D^0_{1\frac{1}{2}}$		
86.91	—	2	628.98	$a^2G_{3\frac{1}{2}}$—$z^2F^0_{3\frac{1}{2}}$		
85.47	4	20	646.26	$b^2D_{1\frac{1}{2}}$—$x^2D^0_{2\frac{1}{2}}$	(0.00) 1.44	(**0.12**, 0.34) 0.92, 1.14, 1.38, **1.60**
80.24	—	2	709.17			
79.75	—	6	715.08			
79.12	5	20	722.67	$a^4P^0_{0\frac{1}{2}}$—$y^4D^0_{1\frac{1}{2}}$		
76.33	10	100	756.35	$a^2F_{3\frac{1}{2}}$—$z^2G^0_{4\frac{1}{2}}$	(0.00) 1.29	(**0.02**, 0.08, 0.12, 0.18) 0.98, 1.04, 1.08, 1.14, 1.18, 1.24, 1.28, **1.34**
70.78	—	2	823.54	$y^2D^0_{2\frac{1}{2}}$—12		
69.82	15	20	835.19	$a^2D_{2\frac{1}{2}}$—$y^2D^0_{1\frac{1}{2}}$		
65.57	—	4	886.85	$a^2P_{1\frac{1}{2}}$—$x^4D^0_{2\frac{1}{2}}$		
61.69	80	160	934.15	$a^4F_{1\frac{1}{2}}$—$z^2F^0_{2\frac{1}{2}}$	(**0.22**, 0.67) 0.63, 1.09, **1.54**	(**0.22**, 0.66) 0.23, 0.67, 1.11, **1.55**
61.01	60	100	942.45	$a^2D_{1\frac{1}{2}}$—$z^4G^0_{2\frac{1}{2}}$	(0.00 w) 1.20A[2]	(**0.10**, 0.30) 0.70, 0.90, 1.10, **1.50**
60.32	2	15	950.88	$a^2G_{4\frac{1}{2}}$—$x^2F^0_{3\frac{1}{2}}$	(0.00) 1.06	(**0.02**, 0.06, 0.10, 0.14) **0.99**, 1.03, 1.07, 1.11, 1.15, 1.19, 1.23, 1.27
58.68	—	3	970.93	$b^2D_{2\frac{1}{2}}$—$x^2F^0_{3\frac{1}{2}}$		
57.65	3	20	983.54	$a^4P_{1\frac{1}{2}}$—$y^4D^0_{2\frac{1}{2}}$		
56.99	—	4	34991.62	$a^2G_{3\frac{1}{2}}$—$w^2D^0_{2\frac{1}{2}}$		
52.02	10	40	35052.59	$a^4P_{1\frac{1}{2}}$—$x^4D^0_{1\frac{1}{2}}$	(0.75) 1.49	(0.24, **0.72**) 0.97, **1.45**, 1.94
51.22	20	60	062.43	$a^4F_{3\frac{1}{2}}$—$z^2F^0_{3\frac{1}{2}}$	(0.39) 1.18B	(0.06, 0.16, 0.28, **0.38**) 0.84, 0.96, 1.06, **1.18**, 1.28, 1.40, 1.50
50.15	4	15	075.59	$a^4P_{1\frac{1}{2}}$—$z^4S^0_{1\frac{1}{2}}$		
49.21	20	100	087.16	$a^2F_{3\frac{1}{2}}$—$z^2G^0_{3\frac{1}{2}}$	(0.00) 1.14	(**0.02**, 0.08, 0.12) 0.90, 0.96, 1.00, 1.06, 1.10, **1.16**
47.70	—	2	105.76			
47.08	—	2	113.41	$y^2F^0_{3\frac{1}{2}}$—16		

TABLE 1.—*First spark spectrum of hafnium* (Hf II)—Continued

λ_{air}	Intensity		ν_{vac} cm^{-1}	Term combinations	Zeeman effects	
	Arc	Spark			Observed	Computed
46.40	—	6	121.80			
45.15	—	3	137.23			
41.95	—	10 hl	176.79			
41.20	—	1	186.07	$z^3D^\circ_{1½}$—2		
38.79	—	2	215.94			
35.18	—	5 h	260.78	$y^3D^\circ_{1½}$—8		
32.59	—	2	293.02			
29.33	4	20	333.68	$b^3D_{2½}$—$w^3D^\circ_{2½}$	(0.00) 1.16	(0.13, 0.39, **0.65**) 0.64, 0.90, **1.16**, 1.42, 1.68
28.51	—	3	343.93			
28.15	1	4	348.43	$b^3D_{2½}$—$x^4D^\circ_{1½}$		
23.42	—	2	407.64			
22.68	40	100	416.92	$a^4F_{2½}$—$y^3D^\circ_{2½}$	(0.00w) 1.52 A[1]	(0.08, 0.22, 0.38) 0.86, 1.00, **1.16**, 1.30, 1.46, **1.60**
20.43	3	10	445.18	$a^4P_{2½}$—$y^4D^\circ_{2½}$		
20.23	100	200	447.69	$a^2D_{2½}$—$z^4G^\circ_{3½}$	(0.00w) 0.88A[1]	(**0.06**, 0.18, 0.30) 0.76, 0.88, 1.00, 1.12, 1.24, 1.36
19.23	—	2	460.26			
18.03	—	3	475.36			
16.90	—	2	489.59	$b^4P_{1½}$—$v^2F^\circ_{2½}$		
16.08	2	12	499.92	$a^2P_{1½}$—$y^4P^\circ_{2½}$		
14.77	6	40	516.45	$a^2G_{3½}$—$w^2F^\circ_{3½}$		
14.48	15	80	520.10	$a^4P_{2½}$—$x^2D^\circ_{2½}$	(0.36) 1.33B	(0.08, 0.24, **0.40**) 1.02, 1.18, **1.34**, 1.50, 1.66
13.87	40	70	527.80	$a^2D_{2½}$—$z^2F^\circ_{2½}$	(0.68) 1.13 Bw	(0.14, 0.44, **0.72**) 0.46, 0.74, **1.04**, 1.32, 1.62
10.23	—	3	573.82			
09.61	1	3	581.67	$a^4F_{1½}$—$z^4P^\circ_{1½}$		
08.00	30	80	602.07	$a^4F_{2½}$—$z^4P^\circ_{2½}$	(0.84) 1.30B	(0.20, 0.58, **0.98**) 0.48, 0.86, **1.26**, 1.64, 2.04
2807.53	—	4	608.03	$z^4D^\circ_{2½}$—5		
2799.77	—	4	706.72	$z^4F^\circ_{1½}$ —4		
98.50	—	6 h	722.92			
94.11	—	1	779.04	$y^3D^\circ_{1½}$—6		
93.62	—	3	785.32	$z^2P^\circ_{1½}$—7		
92.81	1	4	795.70	$b^4F_{1½}$—$x^4D^\circ_{2½}$		
90.44	1	5	826.10	$a^2F_{3½}$—$x^2F^\circ_{3½}$		
89.81	3	20	834.19	$a^2F_{2½}$—$y^4D^\circ_{1½}$		
89.73	10	60	835.22	$a^2G_{3½}$—$z^2H^\circ_{4½}$	(0.00) 1.15	(**0.06**, 0.16, 0.28, 0.38) 0.64, 0.76, 0.86, 0.98, 1.08, 1.20, 1.30, **1.42**
89.51	7	50	838.04	$a^2G_{4½}$—$w^2F^\circ_{3½}$	(0.00) 1.07	(**0.02**, 0.08, 0.12, 0.18) **0.96**, 1.00, 1.06, 1.10, 1.16, 1.20, 1.26, 1.30
87.92	—	2	858.48	$b^2D_{2½}$—$w^2F^\circ_{3½}$		
86.31	2	12	879.20	$a^2P_{0½}$—$w^2D^\circ_{1½}$		
85.89	—	2	884.61			
84.47	—	3	902.91	$a^2F_{2½}$—$x^2D^\circ_{1½}$		
77.31	—	3	35995.46			
75.27	4	15	36021.92	$a^4P_{0½}$—$x^2D^\circ_{1½}$		
74.02	15	60	038.15	$a^4F_{4½}$—$y^4F^\circ_{3½}$	(0.00w) 1.83A[2]	(0.08, 0.22, 0.38, 0.52) 0.80, 0.96, 1.10, 1.26, 1.40, 1.56, 1.70, **1.86**
73.50	5	20	044.91	$a^4P_{0½}$—$z^4S^\circ_{1½}$		
73.36	50	250	046.72	$a^4F_{3½}$—$z^4G^\circ_{4½}$	(0.00) 1.09	(0.03, 0.09, 0.15, 0.21) **0.96**, 1.02, 1.08, 1.14, 1.20, 1.26, 1.32, 1.38
72.34	4	20	059.99	$b^2D_{1½}$—$y^4P^\circ_{1½}$		
70.44	6	30	084.72	$a^4P_{1½}$—$z^2D^\circ_{2½}$		
69.69	—	3	094.49			
67.34	1	8	125.14	$b^2D_{2½}$—$z^4P^\circ_{1½}$		
64.89	1	10	157.14	$a^2G_{4½}$—$z^2H^\circ_{4½}$		
64.48	—	2	162.51	$b^4F_{1½}$—$z^4P^\circ_{2½}$		
61.20	—	6	205.46	$b^2G_{3½}$—$u^2D^\circ_{2½}$		
59.09	—	2	233.15			
56.92	5	30	261.66	$a^2G_{3½}$—$y^2G^\circ_{3½}$		
53.84	—	1	302.22	$z^2D^\circ_{2½}$—4		
53.61	—	10 h	305.25			
52.57	—	7 h	318.97			

TABLE 1.—*First spark spectrum of hafnium* (Hf II)—Continued

λ_{air}	Intensity		ν_{vac} cm^{-1}	Term combinations	Zeeman effects	
	Arc	Spark			Observed	Computed
51.81	20	80	329.00	$a^4F_{4½}$—$y^2F^3_{3½}$	(0.00w) 1.82A[2]	(**0.08**, 0.26, 0.42, 0.60) 0.74, 0.90, 1.08, 1.24, 1.42. 1.58, 1.76, **1.92**
51.21	—	3	336.92	$b^2G_{4½}$—$v^2F^3_{3½}$		
48.70	—	2	370.10			
48.41	—	2	373.94	$a^2D_{1½}$—$z^2P^1_{1½}$		
40.42	—	7	479.98	$b^4F_{3½}$—$v^2D^2_{2½}$		
39.08	—	3	497.83			
38.77	60	150	501.96	$a^4F_{3½}$—$z^2F^3_{3½}$	(0.00) 1.19	(**0.03**, 0.09, 0.15) 0.97, 1.03, 1.09, 1.15, 1.21, **1.27.**
35.76	—	4	542.12	$z^2D^1_{1½}$—3		
35.12	1	7	550.67	$b^2D_{1½}$—$x^2F^2_{2½}$		
32.98	—	20 h	579.29	$z^2F^2_{2½}$—9		
32.68	3	15	583.30	$a^2G_{4½}$—$y^2G^3_{4½}$		
31.16	2	10	603.66	$b^2D_{2½}$—$y^2G^3_{3½}$		
29.47	—	5	626.32			
28.25	—	2	642.70			
27.18	—	4	657.08			
18.51	40?	50	773.98	$b^2D_{1½}$—$w^2D^1_{1½}$	(0.00) 1.08	(0.04, **0.10**) 0.90, **1.06**, 1.14.
17.90	—	10	782.23	$z^4D^2_{3½}$—6 $z^2D^2_{2½}$—5		
14.60	—	2	826.94	$z^2P^2_{0½}$—5		
13.51	—	10	841.74	$a^2P_{0½}$—$x^4D^1_{0½}$		
12.43	20	60	856.40	$a^4F_{2½}$—$y^2D^2_{2½}$	(0.00) 1.08	(0.01, 0.03, **0.05**) 1.03, 1.05, **1.07**, 1.09, 1.11.
12.13	1	15	860.48	$a^2F_{2½}$—$y^4D^3_{3½}$		
11.96	2	20	862.79	$a^2P_{1½}$—$x^4D^2_{1½}$		
10.65	—	5	880.61			
10.00	—	8	889.45	$z^4F^3_{3½}$—3		
06.71	10	100	934.29	$a^4P_{2½}$—$y^4P^1_{1½}$	(0.00 w) 1.16 A[1]	(**0.08**, 0.24) **1.18**, 1.34, 1.50, 1.66.
03.18	1	10	982.52	$a^2G_{3½}$—$x^4D^2_{3½}$		
02.52	—	3	36991.55			
01.55	—	1	37004.83	$y^4F^4_{4½}$—19		
2700.98	—	4 h	012.50			
2687.22	—	5 h	202.15			
86.55	—	2	211.43			
85.72	—	3	222.93	$z^2F^2_{2½}$—10		
85.22	4	30	229.86	$a^2P_{1½}$—$x^4P^2_{2½}$	(0.00) 1.27	(**0.04**, 0.14) 1.08, 1.16, 1.26, **1.34.**
84.02	1	7	246.50	$a^2P_{1½}$—$x^2P^1_{1½}$		
83.35	40	150	255.80	$a^2F_{2½}$—$x^2F^2_{2½}$	(0.18) 1.14	(0.03, 0.09, 0.15, **0.21**) 0.96, 1.02, 1.08, **1.14**, 1.20, 1.26, 1.32.
82.99	—	2	260.80			
78.42	2	10	324.37	$b^2D_{2½}$—$x^4D^3_{3½}$		
77.95	—	2	330.92			
77.56	2	10	336.36	$a^4F_{3½}$—$y^4F^3_{3½}$		
76.63	2	20	349.33	$a^2G_{3½}$—$x^4P^2_{2½}$		
75.21	—	2	369.15			
74.52	—	1	378.80	$b^4P_{1½}$—$u^2D^2_{2½}$		
72.05	—	1	413.34	$z^4G^4_{4½}$—16		
71.25	7	15	424.55	$a^4P_{2½}$—$x^2F^2_{2½}$		
70.33	—	3	437.44	$z^2F^2_{2½}$—11		
69.57	2	7	448.10	$b^4F_{1½}$—$w^2P^1_{1½}$		
69.01	20	25	455.95	$a^2D_{2½}$—$z^4P^3_{2½}$		
67.53	—	6 h	476.74			
67.15	—	2 h	482.07			
66.95	—	2 h	484.88	$z^2D^2_{2½}$—3		
65.98	15	50	498.52	$a^4P_{1½}$—$y^4P^1_{1½}$	(0.00) 1.63	(0.06, **0.16**) 1.52, **1.64**, 1.74.
64.03	—	2	525.97	$z^4D^1_{1½}$—2		
61.89	30	100	556.14	$a^4F_{3½}$—$y^3F^2_{2½}$	(0.00 W) 1.72 A[2]	(**0.14**, 0.42, 0.70) 0.53, 0.81, 1.09, 1.37, 1.65, **1.93.**
60.53	—	3	575.33	$z^4F^1_{1½}$—1		
59.69	—	4 h	587.20			
57.85	20	50	613.22	$a^4F_{3½}$—$y^4F^4_{4½}$		
57.50	7	20	618.17	$a^2F_{3½}$—$w^2D^3_{3½}$		
55.68	—	3 h	643.95			
55.41	—	4	647.78	$a^4P_{2½}$—$w^2D^1_{1½}$		
55.06	—	2 h	652.74			

TABLE 1.—*First spark spectrum of hafnium* (Hf II)—Continued

λ_{air}	Intensity		ν_{vac} cm^{-1}	Term combinations	Zeeman effects	
	Arc	Spark			Observed	Computed
53.06	—	2 h	681.12			
52.86	—	4	683.96	$z^3F^0_{3½}$—5		
52.33	—	5	691.49	$b^3D_{2½}$—$x^4P^0_{2½}$		
51.79	—	1	699.17	$z^4D^0_{½}$—4		
51.17	10	40	707.98	$b^3D_{2½}$—$x^2P^0_{1½}$	(0.00) 1.22	(**0.04**, 0.14) **1.14**, 1.24, 1.34 1.44.
50.28	—	6 h	720.65			
49.15	5	20	736.73	$b^3D_{1½}$—$x^4D^0_{½}$		
48.06	—	3 h	752.27			
47.30	60	200	763.10	$a^4F_{4½}$—$y^4F^0_{4½}$	(0.40) 1.28 Bw	(0.05, 0.15, 0.25, 0.35, **0.45**) 0.88, 0.98, 1.08, 1.18, **1.28**, 1.38, 1.48, 1.58, 1.68.
44.46	—	3	803.65	$z^4D^0_{3½}$—7		
41.41	100	400	847.31	$a^4F_{4½}$—$z^4G^0_{5½}$	(0.00) 1.14	(**0.03**, 0.09, 0.15, 0.21, 0.27) **1.00**, 1.06, 1.12, 1.18, 1.24, 1.30, 1.36, 1.42, **1.48**, 1.54.
38.71	80	200	886.03	$a^3D_{1½}$—$y^3D^0_{1½}$	(0.00) 0.81	(0.00) 0.80.
37.53	—	2	902.98			
36.69	—	2	915.05	$y^3D^0_{1½}$—10		
35.79	6	30	928.00	$a^3G_{3½}$—$y^3G^0_{4½}$	(0.00 w) 1.61 A[2]	(**0.08**, **0.24**, 0.40, 0.56) 0.52, 0.68, 0.84, 1.00, 1.16, 1.32, **1.48**, **1.64**.
32.02	—	4	982.32	$b^4F_{3½}$—$z^3D^0_{3½}$		
31.52	—	1	37989.54	$a^4P_{1½}$—$x^3F^0_{2½}$		
30.18	—	4	38008.89			
29.77	—	2	014.82			
29.52	—	4	018.43			
27.83	—	1	042.88	$y^3D^0_{1½}$—16		
26.96	10	20	055.48	$a^4F_{3½}$—$y^4F^0_{3½}$		
25.56	2	10	075.77	$a^3P_{0½}$—$z^4P^0_{0½}$		
24.83	1?	3 h	086.36	$z^4G^0_{5½}$—12		
22.75	50	150	116.56	$a^4F_{1½}$—$y^3D^0_{2½}$	(**0.34**, 0.96) 1.49, **2.11**	(**0.32**, 0.94) 0.14, 0.76, 1.40, **2.02**.
21.81	—	5 h	130.22	$y^3D^0_{1½}$—11		
20.96	1	5	142.59	$a^3F_{3½}$—$w^3F^0_{3½}$		
17.17	—	1	197.82			
14.30	3	10	239.75	$a^3P_{0½}$—$x^4P^0_{1½}$		
13.61	20	100	249.85	$a^3G_{4½}$—$y^3G^0_{4½}$	(0.18) 1.10 B	(0.02, 0.08, 0.12, 0.18, **0.22**) 0.90, 0.96, 1.00, 1.06, **1.10**, 1.16, 1.20, 1.26, 1.30
11.65	—	1	278.55			
09.29	—	4	313.17	$b^4F_{2½}$—$x^4D^0_{3½}$		
07.26	5	20	343.00	$b^3D_{1½}$—$w^3D^0_{2½}$		
7.03	50	150	346.38	$a^4F_{3½}$—$y^3F^0_{3½}$	(0.26) 1.14	(0.04, 0.10, 0.18, 0.24) 0.98, 1.06, 1.12, **1.20**, 1.26, 1.34 1.40
06.38	40	100	355.94	$a^3D_{2½}$—$z^3F^0_{3½}$	(0.00) 1.02	(**0.03**, 0.09, 0.15) **0.97**, 1.03, 1.09, 1.15, 1.21, 1.27
03.50	1	1	398.37	$a^3D_{1½}$—$z^4P^0_{2½}$		
2600.30	—	4	445.62			
2599.20	6	25	461.89	$a^3F_{3½}$—$z^2H^0_{4½}$		
98.84	—	3	467.22	$a^4P_{0½}$—$y^4P^0_{1½}$		
96.68	—	5 h	499.21			
96.37	—	4 h	503.81			
95.61	1	8	515.08	$a^3P_{1½}$—$w^3P^0_{1½}$		
93.40	—	3	547.90			
91.32	15	30	578.84	$a^3D_{1½}$—$z^3F^0_{2½}$		
90.97	—	1	584.05	$z^4P^0_{2½}$—15 $z^2F^0_{2½}$—13		
87.51	—	2	635.64			
86.81	—	2	646.10			
86.27	—	2	654.16			
84.05	—	2	687.37			
82.90	—	3	704.60			
82.51	25	60	710.44	$a^3D_{2½}$—$y^3D^0_{2½}$		
81.70	—	1	722.59	$z^4G^0_{5½}$—6		
81.22	—	1	729.79	$y^4F^0_{3½}$—19		
80.09	—	3	746.75			
79.08	—	4 h	761.92			

TABLE 1.—*First spark spectrum of hafnium* (Hf II)—Continued

λ_{air}	Intensity		ν_{vac} cm^{-1}	Term combinations	Zeeman effects	
	Arc	Spark			Observed	Computed
78.15	20	60	775.90	$a^4F_{2\frac{1}{2}}$—$y^4F^0_{2\frac{1}{2}}$		
77.53	—	2	785.23	$z^2P^0_{1\frac{1}{2}}$—9		
76.83	20	80	795.76	$a^4F_{4\frac{1}{2}}$—$z^2G^0_{3\frac{1}{2}}$		
75.50	—	15 h	815.80	$z^4G^0_{3\frac{1}{2}}$—14		
74.28	2?	8	834.19			
73.91	25	100	839.77	$a^3F_{3\frac{1}{2}}$—$x^3F^0_{2\frac{1}{2}}$	(0.16) 1.00	(0.03, 0.09, **0.15**) 0.83, 0.89, **0.95**, 1.01, 1.07
72.95	3	8	854.26	$a^4P_{2\frac{1}{2}}$—$x^2F^0_{3\frac{1}{2}}$		
71.68	30	150	873.45	$a^4F_{1\frac{1}{2}}$—$y^4F^0_{1\frac{1}{2}}$	(0.18) 0.51	(0.06, **0.18**) 0.39, **0.51**, 0.63
71.13	—	5	881.76	$z^4D^0_{1\frac{1}{2}}$—3		
70.71	3	10	888.12	$a^2F_{3\frac{1}{2}}$—$y^2G^0_{3\frac{1}{2}}$		
67.46	—	10 h	937.34			
66.63	—	6 h	949.93			
65.24	—	2	971.03	$b^2D_{1\frac{1}{2}}$—$x^4P^0_{0\frac{1}{2}}$		
64.87	—	1	976.65	$b^2D_{2\frac{1}{2}}$—$w^2P^0_{1\frac{1}{2}}$		
63.61	30	50	38995.81	$a^4F_{2\frac{1}{2}}$—$y^3F^0_{2\frac{1}{2}}$	(0.00w) 1.03	(0.06, 0.16, **0.28**) 0.78, 0.90, **1.00**, 1.12, 1.22
62.81	—	3	39007.98			
61.81	—	3	023.21	$z^2D^0_{1\frac{1}{2}}$—8 $z^2P^0_{0\frac{1}{2}}$—7		
60.74	—	20 h	039.51			
59.20	10	30	063.00	$a^2F_{2\frac{1}{2}}$—$w^2D^0_{1\frac{1}{2}}$	(0.00) 0.86	(**0.06**, 0.18) **0.80**, 0.92, 1.04, 1.16
56.40	—	3 h	105.79			
55.33	—	3 h	122.16			
55.10	—	2	125.68	$a^4F_{1\frac{1}{2}}$—$y^2P^0_{1\frac{1}{2}}$		
53.73	—	2 h	146.67			
52.36	—	8 h	167.68			
51.85	3	10	175.51	$a^4P_{1\frac{1}{2}}$—$x^4D^0_{0\frac{1}{2}}$		
51.40	40	150	182.42	$a^2G_{4\frac{1}{2}}$—$z^2H^0_{5\frac{1}{2}}$		
49.14	—	4	217.15	$a^4P_{2\frac{1}{2}}$—$w^2D^0_{2\frac{1}{2}}$		
48.97	—	3	219.77	$b^4F_{1\frac{1}{2}}$—$e^2D^0_{2\frac{1}{2}}$		
48.52	1	3	226.69	$a^2D_{1\frac{1}{2}}$—$z^4P^0_{1\frac{1}{2}}$		
48.20	10	30	231.62	$a^4P_{2\frac{1}{2}}$—$x^4D^0_{1\frac{1}{2}}$		
44.82	—	6 h	283.72			
43.93	—	2	297.46	$z^4P^0_{2\frac{1}{2}}$—16		
43.13	—	3 h	309.82	$z^4D^0_{2\frac{1}{2}}$—6		
37.34	20	30	399.52	$a^4F_{1\frac{1}{2}}$—$y^2P^0_{0\frac{1}{2}}$		
34.33	—	10	446.31			
32.97	6	8	467.49	$a^2D_{2\frac{1}{2}}$—$y^4F^0_{1\frac{1}{2}}$		
31.19	30	50	495.24	$a^4F_{2\frac{1}{2}}$—$y^4F^0_{2\frac{1}{2}}$		
29.78	—	5 h	517.25			
28.24	—	3 h	541.32	$z^2D^0_{1\frac{1}{2}}$—6		
26.28	—	3 h	572.00			
23.89	—	1	609.47	$a^2F_{3\frac{1}{2}}$—$z^4D^0_{2\frac{1}{2}}$		
23.64	—	10 h	613.39			
21.72	—	5 h	643.47	$z^2F^0_{3\frac{1}{2}}$—17		
21.49	10	20	647.16	$a^2P_{1\frac{1}{2}}$—$w^2P^0_{0\frac{1}{2}}$		
20.41	—	6 h	664.15			
16.88	60	150	719.78	$a^2D_{2\frac{1}{2}}$—$y^2P^0_{1\frac{1}{2}}$	(0.00) 1.14	(0.03, 0.09) **1.09**, 1.15, 1.21, 1.27.
15.49	10	30	741.73	$a^4P_{2\frac{1}{2}}$—$w^2F^0_{3\frac{1}{2}}$		
13.02	25	80	780.78	$a^4F_{3\frac{1}{2}}$—$y^4F^0_{4\frac{1}{2}}$	(0.00) 1.21	(0.00) 1.23.
12.68	20	60	786.17	$a^4F_{2\frac{1}{2}}$—$y^2F^0_{3\frac{1}{2}}$	(0.00) 1.36	(**0.05**, 0.15, 0.25) 0.91, 1.01[8] 1.11, **1.21**, 1.31, 1.41.
10.36	—	4	822.93	$a^3P_{0\frac{1}{2}}$—$x^2P^0_{1\frac{1}{2}}$		
05.17	—	3 h	905.43	$z^4F^0_{3\frac{1}{2}}$—2		
01.34	—	2	966.53	$z^2D^0_{2\frac{1}{2}}$—8		
2500.75	10	25	39975.95	$a^2F_{3\frac{1}{2}}$—$z^4P^0_{2\frac{1}{2}}$		
2498.56	—	4 h	40010.99	$z^2P^0_{0\frac{1}{2}}$—8		
96.99	30	60	036.15	$a^4F_{1\frac{1}{2}}$—$y^4F^0_{2\frac{1}{2}}$		
94.37	—	10 h	078.20	$z^4F^0_{4\frac{1}{2}}$—4		
90.23	—	2	144.82	$a^4P_{0\frac{1}{2}}$—$x^4D^0_{0\frac{1}{2}}$		
86.08	—	1	211.83	$z^2P^0_{1\frac{1}{2}}$—12		
85.83	—	3	215.87	$z^4G^0_{5\frac{1}{2}}$—9		
83.34	10	20	256.19	$a^4F_{1\frac{1}{2}}$—$y^2F^0_{2\frac{1}{2}}$		

TABLE 1.—*First spark spectrum of hafnium* (Hf II)—Continued

λ_{air}	Intensity		ν_{vac} cm^{-1}	Term combinations	Zeeman effects	
	Arc	Spark			Observed	Computed
82.49	—	2	269.98	$a^2F_{2½}$—$x^2F^0_{3½}$		
81.44	10	25	287.02	$a^2P_{1½}$—$v^2D^0_{2½}$		
78.56	10	15	333.82	$b^2D_{1½}$—$x^4D^0_{2½}$		
76.05	—	3 h	374.71	$z^4D^0_{1½}$—7		
74.09	1	5	406.69	$a^2G_{3½}$—$v^2D^0_{2½}$		
73.90	8	20	409.79	$a^4P_{1½}$—$x^4P^0_{½}$		
72.54	—	2	432.02	$z^4D^0_{3½}$—14		
71.78	—	2 h	444.45			
71.21	—	3 h	453.78			
69.17	40	60	487.20	$a^4P_{2½}$—$y^2G^0_{3½}$		
67.96	20	20	507.04	$a^2D_{1½}$—$z^4P^0_{½}$		
65.06	10	25	554.69	$a^2F_{3½}$—$y^2G^0_{4½}$		
64.19	60	100	569.01	$a^4F_{4½}$—$y^4D^0_{3½}$	(0.00) 1.30	(0.02, 0.06, 0.10, 0.14) 1.19, 1.23, 1.27, 1.31, 1.35, 1.39, 1.43, 1.47
63.96	10?	20	572.80	$a^4P_{1½}$—$x^4P^0_{1½}$		
62.77	—	3 h	592.40	$z^4G^0_{5½}$—15		
61.73	1	25 h	609.95	Hf III?		
60.49	70	80	630.01	$a^2D_{2½}$—$y^4F^0_{3½}$		
59.46	3	4	647.03	$a^2F_{2½}$—$z^4D^0_{1½}$		
56.97	—	2 h	688.22			
56.65	—	3 h	693.52	$z^2F^0_{3½}$—18		
55.20	5	5	717.55	$b^2D_{1½}$—$z^2P^0_{1½}$		
53.98	4	15	737.79	$a^2G_{3½}$—$x^4D^0_{2½}$		
53.34	10	40	748.42	$b^2D^0_{2½}$—$v^2D^0_{2½}$		
52.47	—	15	762.87	Hf III?		
52.30	10	12	765.70	$a^4F^0_{½}$—$x^4D^0_{1½}$		
50.05	—	3 h	803.13	$z^4D^0_{½}$—5 $z^4D^0_{3½}$—9		
49.43	30	40	813.47	$a^4F_{1½}$—$z^2G^0_{2½}$		
47.25	40	50	849.81	$a^2D_{2½}$—$y^2F^0_{2½}$		
46.72	—	2	858.66	$a^4G^0_{2½}$—10		
45.58	—	2 h	877.70			
43.25	—	2	916.69			
41.05	1	10 hl	40953.56			
36.16	—	2	41035.75			
34.76	10	20	059.35	$a^2G_{4½}$—$x^4D^0_{3½}$		
33.87	—	3 h	074.36	$z^4G^0_{3½}$—11		
33.56	30	50	079.59	$b^2D_{2½}$—$x^4D^0_{2½}$		
32.86	—	2 h	091.41	$a^2P_{½}$—$w^2P^0_{½}$		
30.16	—	1	137.06	$b^4F_{3½}$—$v^2F^0_{2½}$		
28.99	20	30	156.87	$a^2F_{2½}$—$w^2F^0_{3½}$		
26.86	—	6 h	193.00			
25.98	50	70	207.94	$a^4P_{2½}$—$x^4D^0_{2½}$		
24.01	1	8 h	241.42	$z^4F^0_{½}$—2		
22.86	—	2 h	261.00	$z^4F^0_{2½}$—3		
20.76	2	4	296.79	$a^4F_{4½}$—$v^2F^0_{3½}$		
20.21	—	2?	306.17	$z^4G^0_{3½}$—16		
17.69	70	80	349.22	$a^2D_{2½}$—$y^4F^0_{3½}$		
17.23	—	6	357.09			
17.03	—	2	360.51			
16.88	—	2 h	363.08	$z^4D^0_{½}$—8		
15.95	15	20	379.00	$a^4P_{0½}$—$x^4P^0_{½}$		
13.86	—	2?	414.82	$z^4F^0_{½}$—4		
13.33	4	15	423.92	$a^2F_{2½}$—$z^4P^0_{½}$		
12.04	—	2	446.07	$z^4D^0_{2½}$—10		
10.13	40	60	478.91	$a^4F_{4½}$—$z^2G^0_{3½}$		
09.53	—	2 h	489.24			
06.43	30	50	542.68	$a^4P_{0½}$—$x^4P^0_{1½}$		
05.42	60	100	560.13	$a^4F_{3½}$—$y^4D^0_{3½}$	(0.00) 1.12	(0.05, 0.15, 0.25) 0.98, 1.08, 1.18, 1.28, 1.38, 1.48
04.56	10	20	574.99	$a^4P_{2½}$—$x^4P^0_{2½}$		
03.60	6	10	591.59	$a^4P_{2½}$—$x^2P^0_{1½}$		
02.02	—	3 h	618.95	$z^4F^0_{4½}$—16		
2400.79	40	50	640.27	$a^2D_{2½}$—$y^2F^0_{3½}$		
2397.20	—	2 h	702.62			
96.01	—	1	723.33	$z^2F^0_{3½}$—19		
94.96	—	2 h	741.62			
93.83	80	100	761.33	$a^2D_{1½}$—$y^2D^0_{2½}$	(0.00 w) 1.44 A^2	(0.14, 0.42) 0.66, 0.94, 1.22, 1.50

TABLE 1.—*First spark spectrum of hafnium* (Hf II)—Continued

λ_{air}	Intensity		ν_{vac} cm^{-1}	Term combinations	Zeeman effects	
	Arc	Spark			Observed	Computed
93.36	50	80	769.53	$a^4F_{2\frac{1}{2}}$—$y^4D^{\circ}_{1\frac{1}{2}}$	(0.00) 1.00	(0.05, 0.15) 0.91, 1.01, 1.11, 1.21
93.17	20	40	772.84	$a^4P_{1\frac{1}{2}}$—$x^4D^{\circ}_{\frac{1}{2}}$		
92.00	—	3 h	793.27			
86.32	—	3?	892.74	$z^2D^{\circ}_{1\frac{1}{2}}$—11		
85.78	—	3	902.22	$a^3F_{2\frac{1}{2}}$—$y^2G^{\circ}_{3\frac{1}{2}}$		
85.18	—	4 h	912.76			
84.57	—	2 h	923.48			
81.51	—	1 h	977.35	$z^2D^{\circ}_{2\frac{1}{2}}$—9		
81.00	20	40	986.34	$b^2D_{1\frac{1}{2}}$—$w^2P^{\circ}_{1\frac{1}{2}}$		
80.30	30	60	41998.68	$a^4F_{1\frac{1}{2}}$—$y^4D^{\circ}_{0\frac{1}{2}}$		
78.81	—	2 h	42024.99	$z^4F^{\circ}_{3\frac{1}{2}}$—10		
77.97	—	7	039.83			
72.33	3	4	139.77	$a^4P_{1\frac{1}{2}}$—$x^4P^{\circ}_{2\frac{1}{2}}$		
71.93	—	3 h	146.87			
71.40	6	8	156.29	$a^4P_{1\frac{1}{2}}$—$x^2P^{\circ}_{1\frac{1}{2}}$		
68.47	—	4 h	208.44	$z^4D^{\circ}_{1\frac{1}{2}}$—15		
67.63	2	3	223.41	$a^3F_{0\frac{1}{2}}$—$w^3P^{\circ}_{0\frac{1}{2}}$		
65.98	8	10	252.86	$a^4F_{2\frac{1}{2}}$—$z^3G^{\circ}_{3\frac{1}{2}}$		
62.32	—	2	318.31			
51.21	100	150	518.26	$a^2D_{1\frac{1}{2}}$—$y^4F^{\circ}_{1\frac{1}{2}}$		
49.33	—	2 h	552.28	$z^4G^{\circ}_{3\frac{1}{2}}$—17		
47.44	80	120	586.54	$a^4F_{1\frac{1}{2}}$—$y^4D^{\circ}_{2\frac{1}{2}}$		
45.41	4	5	623.39	$a^3F_{2\frac{1}{2}}$—$z^4D^{\circ}_{2\frac{1}{2}}$		
43.32	60	80	661.41	$a^4F_{3\frac{1}{2}}$—$z^3D^{\circ}_{2\frac{1}{2}}$		
40.39	—	8 h	714.80			
38.23	—	10 h	754.26	$z^4F^{\circ}_{2\frac{1}{2}}$—7		
37.59	—	3 h	765.97			
37.33	30	30	770.73	$a^2D_{1\frac{1}{2}}$—$y^2P^{\circ}_{1\frac{1}{2}}$		
35.50	1	1	804.24	$b^4F_{2\frac{1}{2}}$—$y^2F^{\circ}_{3\frac{1}{2}}$		
35.24	—	2	809.00	$z^4F^{\circ}_{2\frac{1}{2}}$—12		
33.79	—	4 h	835.60	$z^2D^{\circ}_{2\frac{1}{2}}$—11		
32.95	40	50	851.02	$a^4F_{1\frac{1}{2}}$—$z^2S^{\circ}_{\frac{1}{2}}$		
32.44	7	10	860.39	$a^4P_{2\frac{1}{2}}$—$w^2P^{\circ}_{1\frac{1}{2}}$		
32.18	2		865.16	$z^4F^{\circ}_{2\frac{1}{2}}$—17		
29.09	2	2 h	922.03	$z^4D^{\circ}_{3\frac{1}{2}}$—16		
25.40	1	?	990.13	$a^3F_{2\frac{1}{2}}$—$x^4P^{\circ}_{2\frac{1}{2}}$		
24.89	40	80	42999.56	$a^4F_{2\frac{1}{2}}$—$y^4D^{\circ}_{2\frac{1}{2}}$		
24.50	20	40	43006.78	$a^3F_{2\frac{1}{2}}$—$x^2P^{\circ}_{1\frac{1}{2}}$		
23.25	40	60	029.91	$a^4F_{1\frac{1}{2}}$—$y^4D^{\circ}_{1\frac{1}{2}}$		
22.47	60	60	044.36	$a^2D_{1\frac{1}{2}}$—$y^2P^{\circ}_{0\frac{1}{2}}$		
21.14	50	60	069.03	$a^4F_{2\frac{1}{2}}$—$z^2D^{\circ}_{1\frac{1}{2}}$		
18.49	8	10	118.25	$b^2D_{1\frac{1}{2}}$—$w^2P^{\circ}_{0\frac{1}{2}}$		
16.49	10	20	155.47			
05.34	6	8	364.18	$a^2F_{2\frac{1}{2}}$—$x^4D^{\circ}_{3\frac{1}{2}}$		
04.50	3	3 h	379.98			
03.21	4	4 h	404.28	$z^2D^{\circ}_{2\frac{1}{2}}$—12		
2302.11	5	6	425.01	$a^4P_{1\frac{1}{2}}$—$w^4P^{\circ}_{1\frac{1}{2}}$		
2298.78	6	8	487.91	$a^2P_{1\frac{1}{2}}$—$u^2D^{\circ}_{1\frac{1}{2}}$		
98.33	25	50	496.43	$a^4F_{3\frac{1}{2}}$—$z^2G^{\circ}_{4\frac{1}{2}}$		
96.13	5	6 h	538.10	$z^4F^{\circ}_{3\frac{1}{2}}$—14		
92.77	3	3 h	601.90	$z^4G^{\circ}_{3\frac{1}{2}}$—18		
92.34	2	2 h	610.07			
91.64	30	40	623.39	$a^2D_{2\frac{1}{2}}$—$y^4D^{\circ}_{1\frac{1}{2}}$		
88.63	5	6	680.76	$a^2D_{1\frac{1}{2}}$—$y^4F^{\circ}_{2\frac{1}{2}}$		
85.43	6	6 h	741.92	$z^4F^{\circ}_{2\frac{1}{2}}$—8		
84.60	20	30	757.81	$b^2D_{1\frac{1}{2}}$—$v^2D^{\circ}_{2\frac{1}{2}}$		
81.81	5	6 h	811.30			
77.16	150	150	900.76	$a^2D_{1\frac{1}{2}}$—$y^2F^{\circ}_{2\frac{1}{2}}$		
76.43	4	4 h	914.83	$z^4F^{\circ}_{4\frac{1}{2}}$—18		
74.64	15	20	949.39	$b^2D_{2\frac{1}{2}}$—$u^2D^{\circ}_{1\frac{1}{2}}$		
73.15	40	60	43978.19	$a^4F_{4\frac{1}{2}}$—$z^2F^{\circ}_{3\frac{1}{2}}$		
71.14	2	2 h	44017.11	$z^4D^{\circ}_{1\frac{1}{2}}$—10		
70.68	6	7	026.03	$a^4F_{2\frac{1}{2}}$—$y^4D^{\circ}_{2\frac{1}{2}}$		
69.86	8	8 h	041.93			
68.47	2	2 h	068.92			

TABLE 1.—*First spark spectrum of hafnium* (Hf II)—Continued

λ_{air}	Intensity		ν_{vac} cm^{-1}	Term combinations	Zeeman effects	
	Arc	Spark			Observed	Computed
67.91	3	3 h	079.80			
67.58	3	3 h	086.21			
67.35	3	3 h	090.68	$z^4F^1_{1/2}$—7		
66.83	60	80	100.79	$a^4F_{2/2}$—$z^2D^2_{3/2}$		
66.52	30	40	106.82	$a^2D_{2/2}$—$z^2G^2_{3/2}$		
63.36	2	2 h	168.40	$z^4D^1_{3/2}$—17		
61.54	3	3 h	203.94			
60.25	2	2 h	229.17			
58.68	15	20	259.91	$a^4F_{1/2}$—$y^4D^1_{3/2}$		
57.89	10	15	275.39	$a^4F_{2/2}$—$w^2P^1_{1/2}$		
56.26	1	2	307.37	$b^4F_{2/2}$—$v^2F^2_{3/2}$		
55.15	40	60	329.18	$a^4F_{1/2}$—$x^2D^1_{3/2}$		
54.00	60	80	351.80	$a^4F_{1/2}$—$z^4S^1_{3/2}$		
51.85	8	9	394.14	$a^4P_{0/2}$—$w^2P^1_{1/2}$		
49.82	5	5 h	434.19			
44.23	4	4 h	544.85			
43.18	15	20	565.70	$a^4F_{2/2}$—$x^2F_{3/2}$		
39.86	5	6	631.75	$a^4P_{2/2}$—$v^2D_{3/2}$		
36.34	4	4 h	702.00			
35.41	3	20 h	720.59	Hf III?		
31.41	3	3 h	800.75	$z^4D^1_{3/2}$—12		
28.78	7	8	853.61	$a^2D_{2/2}$—$y^4D_{3/2}$		
28.45	4	4 h	860.25			
28.18	6	8	865.69	$a^4F_{1/2}$—$w^2F^2_{3/2}$		
25.35	6	7	922.74	$a^2D_{2/2}$—$x^2D^1_{3/2}$		
24.29	10	10 H	944.14	$z^4F^1_{3/2}$—19		
23.36	4	5	44962.94	$a^4P_{2/2}$—$z^4D^1_{3/2}$		
20.48	7	8 h	45021.25			
18.37	10	15	064.07	$a^2G_{3/2}$—$v^2F^2_{3/2}$		
17.66	2	2h	078.50	$z^4F^1_{3/2}$—8		
12.45	25	30	184.64	$a^4F_{1/2}$—$z^2H^1_{3/2}$		
11.86	5	6	196.69	$a^4P_{1/2}$—$v^2D^2_{3/2}$		
10.82	2	2 h	217.95	$z^4D^1_{3/2}$—18		
06.59	2	2 h	304.62			
06.11	10	10 h	314.47	$z^4F^1_{3/2}$—15		
03.85	3	3	360.94	$a^4F_{1/2}$—$z^2D^1_{3/2}$		
02.99	3	3 h	378.64	$z^4D^1_{3/2}$—13		
2201.67	3	3	405.85	$b^2D_{2/2}$—$v^2F^2_{3/2}$		
2199.84	4	4 h	443.62			
99.57	8	8 h	449.19	$z^4D^2_{3/2}$—16		
99.40	7	8	514.78	$a^4F_{2/2}$—$y^4P^1_{1/2}$		
91.79	10	15	610.51	$a^4F_{1/2}$—$y^2G^2_{3/2}$		
91.27	5	5 h	621.33			
90.22	30	30	643.20	$a^2D_{1/2}$—$y^4D^2_{3/2}$		
88.87	5	6 h	671.34			
84.95	6	6 h	753.27	$z^4F^2_{3/2}$—9		
84.31	6	8	766.68	$b^4F_{1/2}$—$u^2D^2_{3/2}$		
81.94	3	3 h	816.38			
80.22	2	2 h	852.52			
78.90	60	80	880.30	$a^2D_{2/2}$—$y^4D^2_{3/2}$		
75.36	25	30	954.95	$a^2D_{2/2}$—$z^2D^2_{3/2}$		
73.44	15	20	45995.54	$a^4F_{2/2}$—$x^2F^2_{3/2}$		
72.96	5	5 h	46005.70	$a^4F_{2/2}$—$z^2F^2_{3/2}$		
71.89	6	6 h	028.36	$z^4F^2_{3/2}$—16		
70.22	20	30	063.78	$a^2P_{0/2}$—$u^2D^1_{3/2}$		
62.48	15	15	228.63	$a^4F_{2/2}$—$w^2D^1_{3/2}$		
61.61	10	10 h	247.24	$z^4D^1_{3/2}$—19		
58.12	15	15 h	322.02			
56.44	25	35	358.10	$a^4F_{2/2}$—$w^2D^2_{3/2}$		
55.51	1	1	378.10	$a^2F_{2/2}$—$x^4D^2_{3/2}$		
54.66	4	4 h	396.39	$z^4F^2_{3/2}$—10		
50.30	10	10 h	490.45			
50.07	5	5	495.43	$a^2D_{1/2}$—$z^2S^1_{3/2}$		
49.86	6	6 h	499.97			
44.73	3	3 h	611.18	$z^4F^2_{3/2}$—11		
44.17	6	6 h	623.31	$z^2D^2_{3/2}$—16		
41.84	20	20	674.06	$a^2D_{1/2}$—$y^4D^1_{3/2}$		
39.24	30	40	730.78	$a^2G_{3/2}$—$v^2F^1_{3/2}$		
37.22	6	6	774.95	$a^4F_{1/2}$—$y^4P^1_{1/2}$		
34.53	15	20	833.89	$a^2P_{1/2}$—$u^2D^2_{3/2}$		

TABLE 1.—*First spark spectrum of hafnium* (Hf II)—Continued

λ_{air}	Intensity		ν_{vac} cm^{-1}	Term combinations	Zeeman effects	
	Arc	Spark			Observed	Computed
33.36	4	4 h	859.57			
32.28	9	10	883.30	$a^4F_{3\frac{1}{2}}$—$w^2F^0_{3\frac{1}{2}}$		
30.09	8	8 h	931.50			
29.10	60	100	953.32	$a^2G_{2\frac{1}{2}}$—$u^2D^0_{2\frac{1}{2}}$		
27.50	5	5 h	46988.62			
26.61	7	8 h	47008.28			
24.59	50	80	052.97	$a^2G_{4\frac{1}{2}}$—$v^2F^0_{3\frac{1}{2}}$		
23.68	40	40	073.13	$b^2D_{2\frac{1}{2}}$—$v^2F^0_{2\frac{1}{2}}$		
22.94	15	15 h	089.54	$z^4F^0_{1\frac{1}{2}}$—9		
17.95	5	5 h	200.47	$a^4F_{3\frac{1}{2}}$—$z^2H^0_{4\frac{1}{2}}$		
16.80	4	(?)	226.11			
15.61	4	(?)	252.67			
15.02	20	20	265.85	$a^4F_{1\frac{1}{2}}$—$x^2F^0_{2\frac{1}{2}}$		
14.62	2	(?)	274.79	$z^4F^0_{3\frac{1}{2}}$—17		
10.42	15	15	368.86	$a^2D_{2\frac{1}{2}}$—$y^4P^0_{1\frac{1}{2}}$		
08.50	15	10 h	411.99			
2107.47	60	60	435.15	$a^4F_{2\frac{1}{2}}$—$x^2F^0_{1\frac{1}{2}}$		
2098.91	2	(?)	628.59	$a^4F_{3\frac{1}{2}}$—$y^2G^0_{4\frac{1}{2}}$		
96.18	100	150	690.61	$a^2F_{3\frac{1}{2}}$—$v^2F^0_{3\frac{1}{2}}$		
94.33	3	(?)	732.73	$z^4F^0_{1\frac{1}{2}}$—10		
93.22	7	(?)	758.04	$z^4F^0_{2\frac{1}{2}}$—13		
90.83	40	40	812.63	$a^4F_{2\frac{1}{2}}$—$x^4D^0_{1\frac{1}{2}}$		
89.95	30	30	832.76	$a^4P_{2\frac{1}{2}}$—$u^2D^0_{1\frac{1}{2}}$		
89.38	3	(?)	845.80			
88.77	50	50	859.77	$a^2D_{2\frac{1}{2}}$—$x^2F^0_{2\frac{1}{2}}$		
87.66	4	(?)	885.22			
86.80	8	4	904.95	$a^2D_{1\frac{1}{2}}$—$y^4D^0_{2\frac{1}{2}}$		
86.29	12	(?)	916.66			
84.94	1	(?)	947.68	$z^4F^0_{1\frac{1}{2}}$—11		
84.45	2	(?)	956.65			
83.80	40	30	973.91	$a^2D_{1\frac{1}{2}}$—$x^2D^0_{1\frac{1}{2}}$		
82.80	15	8	47996.94	$a^2D_{1\frac{1}{2}}$—$z^4S^0_{1\frac{1}{2}}$		
79.72	3	(?)	48068.01			
79.11	3 d	(?)	082.11	$a^2D_{2\frac{1}{2}}$—$w^2D^0_{1\frac{1}{2}}$		
76.70	3	(?)	137.90			
76.04	4	(?)	153.21			
68.84	20	4 h	320.77			
68.76	3	(?)	322.63	$a^4F_{2\frac{1}{2}}$—$w^2F^0_{3\frac{1}{2}}$		
68.58	5	(?)	326.85			
66.20	2	(?)	382.50			
65.55	2	(?)	397.72	$a^4P_{1\frac{1}{2}}$—$u^2D^0_{1\frac{1}{2}}$		
64.78	15	4	415.77	$b^2D_{1\frac{1}{2}}$—$v^2F^0_{2\frac{1}{2}}$		
64.43	2	(?)	423.98			
63.23	3	(?)	452.13	$a^4F_{1\frac{1}{2}}$—$x^4D^0_{2\frac{1}{2}}$		
61.39	4	(?)	495.38			
60.49	7	(?)	516.55	$z^4F^0_{2\frac{1}{2}}$—12		
57.39	3	(?)	589.65	$a^4F_{2\frac{1}{2}}$—$x^4P^0_{1\frac{1}{2}}$		
55.30	4	(?)	639.05			
54.86	2	(?)	48649.47			
39.08	6	2	49025.90			
37.32	2	(?)	068.25	$a^4F_{2\frac{1}{2}}$—$y^2G^0_{3\frac{1}{2}}$		
36.24	3	(?)	094.27	$z^4F^0_{3\frac{1}{2}}$—13		
29.88	5	(?)	248.07	$a^2F_{2\frac{1}{2}}$—$u^2D^0_{1\frac{1}{2}}$		
28.18	25	15	289.34	$a^4P_{2\frac{1}{2}}$—$v^2F^0_{2\frac{1}{2}}$ $a^2D_{2\frac{1}{2}}$—$x^2F^0_{3\frac{1}{2}}$		
23.36	2	(?)	406.74			
20.07	3	(?)	487.20			
13.38	2	(?)	651.61	$a^2D_{2\frac{1}{2}}$—$w^2D^0_{2\frac{1}{2}}$		
2012.78	10	4	49666.41	$a^2D_{2\frac{1}{2}}$—$z^4D^0_{1\frac{1}{2}}$		
λ_{vac}						
2005.99	—	1	49851	$a^4F_{1\frac{1}{2}}$—$x^4P^0_{1\frac{1}{2}}$		
1993.10	—	3	50173	$a^4F_{2\frac{1}{2}}$—$x^2P^0_{1\frac{1}{2}}$		
64.23	—	15	911	$a^2D_{1\frac{1}{2}}$—$x^2F^0_{2\frac{1}{2}}$		
63.75	—	9	923	$a^2D_{2\frac{1}{2}}$—$y^2G^0_{3\frac{1}{2}}$		
62.44	—	5	50957	$a^4P_{2\frac{1}{2}}$—$v^2F^0_{3\frac{1}{2}}$		

TABLE 1.—*First spark spectrum of hafnium* (Hf II)—Continued

λ_{air}	Intensity		ν_{vac} cm^{-1}	Term combinations	Zeeman effects	
	Arc	Spark			Observed	Computed
55.66	—	12	51134	$a^3D_{1½}$—$w^3D^0_{1½}$		
22.74	—	12	52009	$a^3D_{2½}$—$x^4P^0_{2½}$		
22.11	—	9	026	$a^3D_{2½}$—$z^3P^0_{1½}$		
19.52	—	20	096	$a^3D_{1½}$—$x^4D^0_{½½}$		
09.46	—	4	371	$a^3F_{2½}$—$v^3F^0_{3½}$		
1901.40	—	6	593	$a^3F_{2½}$—$u^3D^0_{2½}$		
1897.51	—	3	52701	$a^3D_{1½}$—$w^3D^0_{2½}$		
69.24	—	7	53498	$a^3D_{1½}$—$z^3P^0_{1½}$		
16.26	—	4	55058	$a^3D_{1½}$—$x^4P^0_{2½}$		
16.05	—	3	065	$a^3D_{2½}$—$v^3D^0_{3½}$		
1815.71	—	9	55075	$a^3D_{1½}$—$x^3P^0_{1½}$		
1774.81	—	10	56344	$a^3D_{1½}$—$w^3P^0_{1½}$		
1716.23	—	6	58267	$a^3D_{2½}$—$u^3D^0_{1½}$		
1679.58	—	3	59538	$a^4F_{2½}$—$v^3F^0_{3½}$		
1628.91	—	12	61390	$a^3D_{2½}$—$v^3F^0_{3½}$		
1623.06	—	12	61612	$a^3D_{2½}$—$u^3D^0_{2½}$		

V. STRUCTURE OF THE Hf II SPECTRUM

In the process of atom building as first outlined by Bohr [10] the group of 14 rare-earth elements occurring between lanthanum (57) and hafnium (72) is accounted for by the successive addition of *f*-type electrons in the shell with total quantum number 4 while the (remaining) valence electrons $5d$ and $6s^2$ remain unchanged. Thus the first $4f$ electron appears in cerium (58), the shell of 14 such electrons is filled in lutecium (71), and the addition of $5d$ electrons is resumed in hafnium (72) so that its configuration of valence electrons may be presumed to be $5d^26s^2$. If the hafnium atom is ionized by the removal of one of its *d* electrons the outer structure is identical with that of neutral lanthanum, and except for a scale factor due to difference in nuclear charge the Hf II and La I spectra may be expected to be similar in structure. In this case the *displacement law* of spectroscopy can be tested with a displacement of 15 units in atomic number, much like the comparison of Zr II with La I, which is a displacement of 17 units in the other direction. When the structures of Hf II and La I spectra are compared they are found to exhibit the most striking similarity that has ever been observed in comparisons of this type. This is illustrated in figures 1 and 2, which are energy diagrams of these 2 spectra. The diagram for La I (fig. 1) is reproduced from the paper by Russell and Meggers [11], while the diagram for Hf II (fig. 2) is similarly constructed except that the ordinates are doubled in numerical value. For a comparison of details, however, it is necessary to refer to the term tables for these two spectra. The chief differences will be found to consist (1) of a group of low terms (associated with d^3 electrons) which has been established for Hf II but not for La I, and (2) more middle terms involving an *f* electron are found in La I than in Hf II.

The modern theory of spectral structure [12] which correlates spectral terms with configurations of valence electrons indicates that for 3

[10] N. Bohr, Z. Physik, 9,1(1922).
[11] H. N. Russell and W. F. Meggers, BS J.Research 9,647(1932); RP497.
[12] F. Hund, Linienspektren und periodisches System der Elemente, Julius Springer, Berlin(1927).

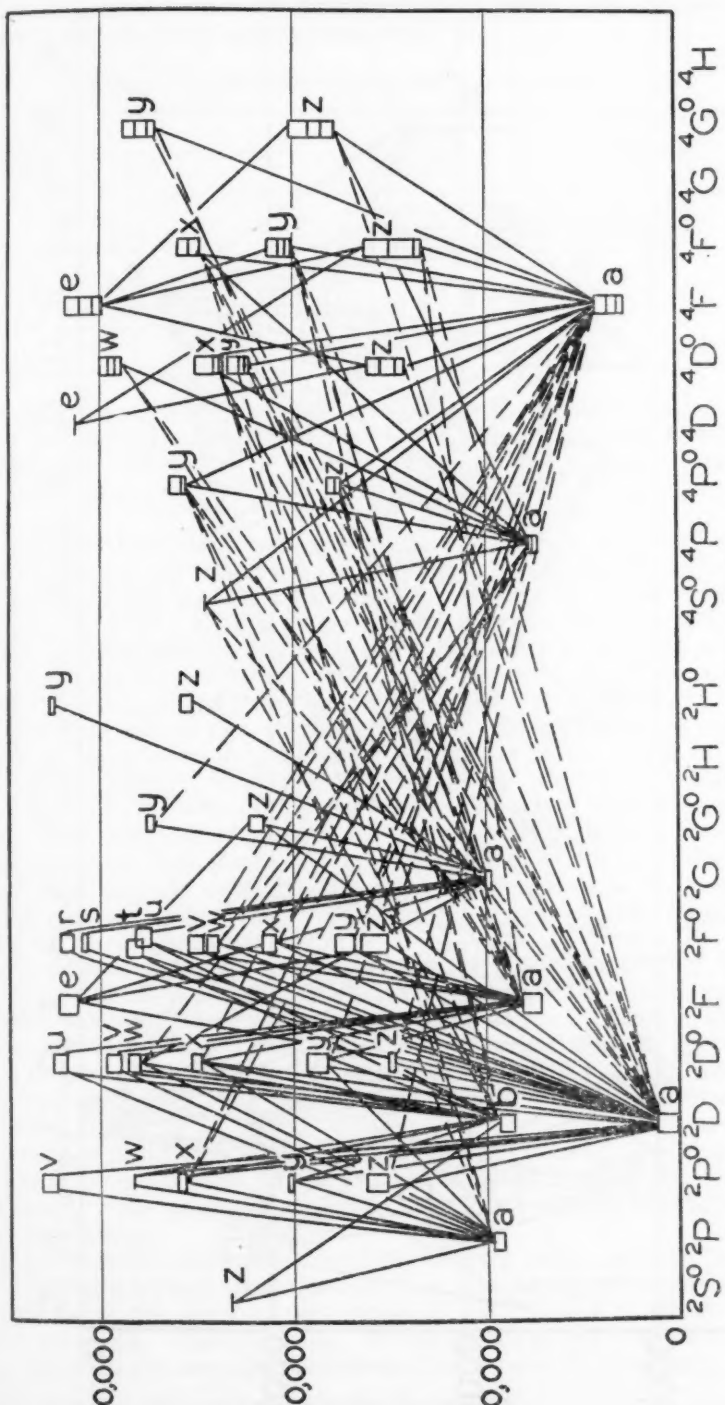

FIGURE 1.—*Terms and combinations of the* La I *spectrum.*

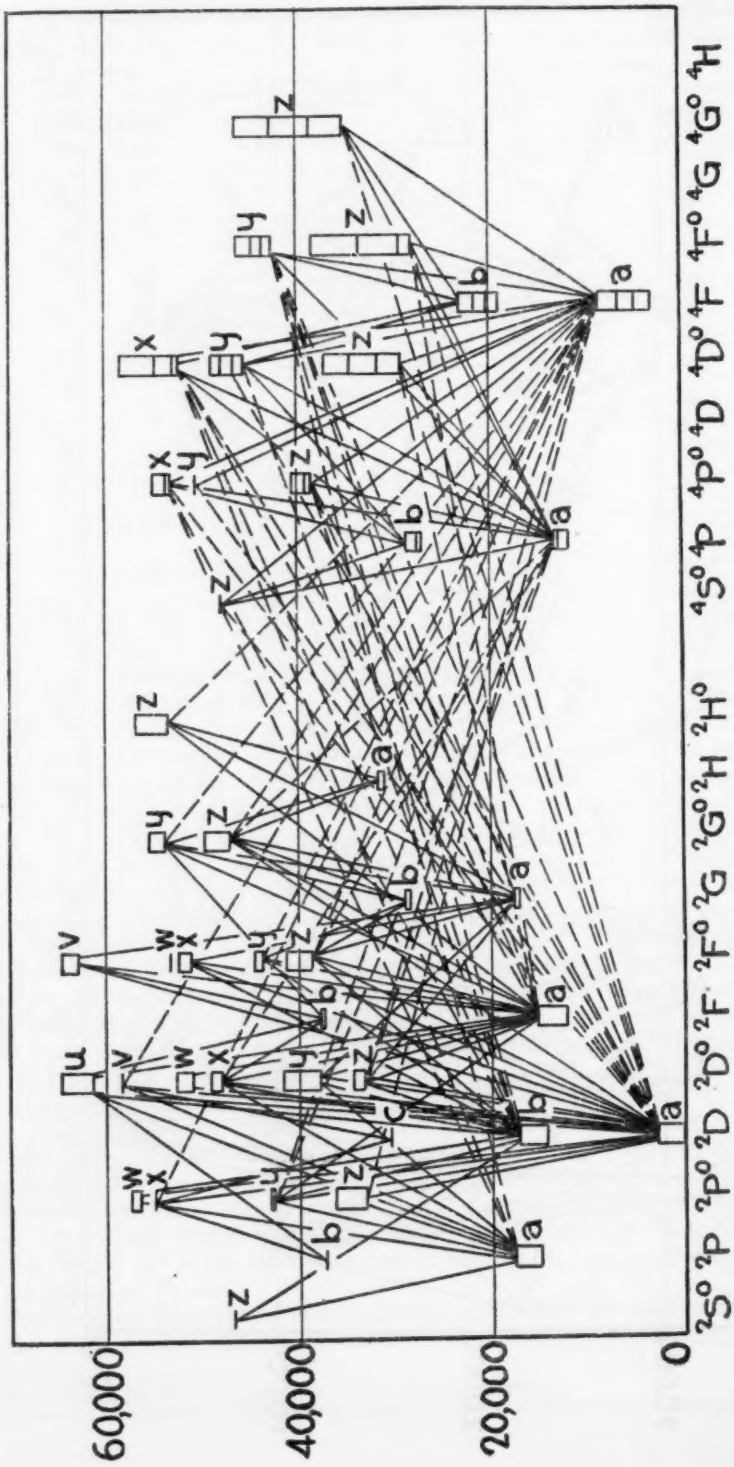

FIGURE 2.—*Terms and combinations of the* Hf II *spectrum.*

electron spectra such as Hf II, etc., one may expect to find the terms listed in table 2 as the most prominent.

TABLE 2.—*Theoretical terms in the* Hf II *spectrum*

Electron configuration	Spectral terms	Electron configuration	Spectral terms
$5d\,6s^2$	^2D	$5d^3\,6p$	$^2D^0, {}^2F^0, {}^2G^0, {}^4D^0, {}^4F^0, {}^4G^0$ $^2S^0, {}^2P^0, {}^2D^0, {}^4S^0, {}^4P^0, {}^4D^0$ $^2F^0, {}^2G^0, {}^2H^0$ $^2P^0, {}^2D^0, {}^2F^0$
$5d^2\,6s$	$^2S, {}^2D, {}^2G, {}^2P, {}^2F, {}^4P, {}^4F$		
$5d^3$	$^2D, {}^2P, {}^2D, {}^2F, {}^2G, {}^2H, {}^4P, {}^4F$	$5d^3\,7s$	$^2P, {}^2F, {}^4P, {}^4F$ $^2S, {}^2D, {}^2G$
$5d\,6s\,6p$	$^2P^0, {}^2D^0, {}^2F^0, {}^4P^0, {}^4D^0, {}^4F^0$ $^2P^0, {}^2D^0, {}^2F^0$	Etc.	

Substitution of an *f*-type electron for any of the above would yield a great variety of additional terms[13] which may be expected to be more important in the spectra of so-called "rare-earth elements", although the first terms of this sort have actually been found in La and Hf spectra.

The first three configurations in table 2 produce 16 terms of low energy content (including the normal state); 14 (all but ^2S ($5d^26s$) and the first ^2D(d^3)) have been identified for Hf II. The next two configurations involve a *p*-type electron and are responsible for a host of higher (middle) states which combine with the low even set to account for a large majority of the observed lines, including all of the stronger ones. Additional odd terms may be expected if an electron of type 4*f* ever appears among the valence group. Terms of this type or fragments of them have indeed been found in La I, La II and in Hf II spectra. Normally, there is no 4*f* electron in the La atom and the filled *f* shell in Hf is inactive. But in excited states these atoms may exhibit a 4*f* electron, because in the former case the stage is set for its appearance, while in the latter the displacement of one from the completed shell has the same spectroscopic consequences as the presence of a single one. These terms appear to be somewhat more prominent in La than in Hf spectra.

A total of seventy-odd terms has been established for Hf II. These combine with the low even terms and thus formally account for approximately 900 lines characteristic of singly ionized hafnium atoms. These odd terms also combine with higher even terms forming series with the low ones, but combinations of this sort are always weak so that it is difficult to verify and identify the higher members of series. We have found 19 levels belonging to the high even set, but have experienced great difficulty with their interpretation. Owing to the lack of sufficient criteria for the grouping of these high levels, we shall not essay, at the present time, to go beyond a tentative identification of some of them.

A spectroscopic determination of the ionizing potential of Hf^+ atoms presupposes a correct identification of series forming terms and also a knowledge of the lower energy states of Hf^{++} atoms to which these series converge. Unfortunately, we are unable at the present time to offer more than a tentative interpretation of some of the highest levels

[13] R. C. Gibbs, D. T. Wilber, and H. E. White, Phys. Rev. **29**, 790(1927).

which have been found, and are ignorant of the structure of the Hf III spectrum. However, the remarkable parallelism between Hf II and La I spectra leads us to believe that the structure of Hf III will resemble that of La II when plotted on ordinates having double the numerical value of those for La II. If we make this assumption, and also assume that e^2D and e^4F form series with a^2D and a^4F, respectively, tentative values for the series limits may be calculated. Such calculations lead to an approximate value of 120,000 units for the separation of $a^2D_{1½}$ (Hf II) from a^3F_2 (Hf III), so that 14.8 volts may be adopted tentatively as the ionization potential for Hf^+ atoms.

The observed Zeeman effects on hafnium lines have been most helpful in identifying the spectral terms, although most of the patterns are unrecognizable by direct comparison with those of the Landé theory [14] which assumes simple (*LS*) coupling.

It is obvious that the departures from theoretical values derived either from strict (*LS*) or from pure (*JJ*) coupling indicate some intermediate form of vector coupling in hafnium atoms. The Zeeman effect analysis was carried out in the following manner. First, all the magnetic splitting factors (g values) which could be derived from fully resolved patterns were calculated, and averaged when more than one value was obtained for a given level. These constitute the g values of highest weight. Next the patterns marked A^1 or A^2 (occurring when $\Delta J = \pm 1$) or B (occurring when $\Delta J = 0$) were exploited for the calculation of further g values, and then the formulas of Shenstone and Blair [15] were applied to the unresolved blends for the calculation of g values for the remaining levels. The final g values thus derived from the experimental data were used in calculations of the complete patterns which might be expected for each of the lines actually observed in the magnetic field, and these results were placed in the last column of table 1 where they are readily compared with the actual observations, or with patterns resulting from LS coupling.[16]

TABLE 3.—*Relative terms in the* Hf II *spectrum*

Electron configurations	Terms	Level values	Level separations	g values		Combinations
				Observed	Landé	
$5d\ 6s^2$	$a^2D_{1½}$	0.0	3050.9	0.80	0.80	$z^4F°$, $z^4D°$, $z^4G°$, $z^4P°$, $y^4F°$, $y^4D°$, $z^4S°$, $z^4D°$, $y^4P°$, $z^4P°$, $z^2D°$, $z^2P°$, $z^2F°$, $y^2D°$, $y^2P°$, $y^2F°$, $z^2S°$, $z^2G°$, $x^2D°$, $x^2F°$, $w^2D°$, $x^2P°$, $v^2D°$, $w^2P°$, $u^2D°$, $v^2F°$.
	$a^2D_{2½}$	3050.9		1.18	1.20	
$5d^2\ 6s$	$a^4F_{1½}$	3644.5	1260.4	0.45	0.40	$z^4F°$, $z^4D°$, $z^4G°$, $z^4P°$, $y^4F°$, $y^4D°$, $z^4S°$, $z^4D°$, $y^4P°$, $z^4P°$, $z^2D°$, $z^2P°$, $z^2F°$, $y^2D°$, $y^2P°$, $y^2F°$, $z^2S°$, $z^2G°$, $x^2D°$, $x^2F°$, $w^2D°$, $y^2G°$, $w^2F°$, $x^2P°$, $z^2H°$, $v^2F°$.
	$a^4F_{2½}$	4904.9	1439.5	1.06	1.03	
	$a^4F_{3½}$	6344.4	2017.4	1.23	1.24	
	$a^4F_{4½}$	8361.8		1.33	1.33	
$5d^26s$	$a^4P_{½}$	11951.7	969.2	2.61	2.67	$z^4F°$, $z^4D°$, $z^4G°$, $z^4P°$, $y^4F°$, $y^4D°$, $z^4S°$, $z^4D°$, $y^4P°$, $z^4P°$, $z^2D°$, $z^2P°$, $z^2F°$, $y^2D°$, $y^2P°$, $y^2F°$, $z^2S°$, $z^2G°$, $x^2D°$, $x^2F°$, $w^2D°$, $y^2G°$, $w^2F°$, $x^2P°$, $z^2D°$, $w^2P°$, $u^2D°$, $v^2F°$.
	$a^4P_{1½}$	12920.9	564.6	1.69	1.73	
	$a^4P_{2½}$	13485.5		1.42	1.60	
$5d^2\ 6s$	$a^2F_{2½}$	12070.5	3013.7	0.98	0.86	$z^4F°$, $z^4D°$, $z^4G°$, $z^4P°$, $y^4F°$, $y^4D°$, $x^4D°$, $x^4P°$, $z^2D°$, $z^2P°$, $z^2F°$, $y^2D°$, $w^2F°$, $y^2F°$, $z^2G°$, $x^2D°$, $x^2F°$ $w^2D°$, $y^2G°$, $z^2H°$, $w^2P°$, $u^2D°$, $v^2F°$.
	$a^2F_{3½}$	15084.2		1.11	1.14	

[14] A. Landé, Zeit. f. Phys. **5**, 231(1921); **15**, 189(1923).
[15] A. G. Shenstone and H. A. Blair, Phil. Mag. **8**,765(1929); H. N. Russell, Phys. Rev. **36**, 1590(1930).
[16] C. C. Kiess and W. F. Meggers, BS J. Research **1**, 641(1928); RP23.

TABLE 3.—*Relative terms in the* Hf II *spectrum*—Continued

Electron configurations	Terms	Level values	Level separations	g values		Combinations
				Observed	Landé	
$5d^2\,6s$	$b^3D_{1½}$	14359.5	3009.4	1.03	0.80	$z^4F°$, $z^4D°$, $z^4G°$, $z^4P°$, $y^4F°$, $y^4D°$, $x^4D°$, $y^4P°$, $x^4P°$, $z^2D°$, $z^2P°$, $z^2F°$, $y^2D°$, $y^2P°$, $y^2F°$, $z^2S°$, $z^2G°$, $z^2D°$, $x^2F°$, $w^2D°$, $y^2G°$, $z^2P°$, $v^2D°$, $w^2P°$, $u^2D°$, $v^2F°$.
	$b^3D_{2½}$	17368.9		1.29	1.20	
$5d^2\,6s$	$a^3P_{0½}$	15254.4	2576.0	0.74	0.67	$z^4D°$, $z^4G°$, $z^4P°$, $y^4F°$, $y^4D°$, $z^4S°$, $x^4D°$, $y^4P°$, $x^4P°$, $z^2D°$, $z^2P°$, $y^2D°$, $y^2P°$, $z^2S°$, $x^2D°$, $z^2F°$, $w^2D°$, $x^2P°$, $v^2D°$, $w^2P°$, $u^2D°$, $v^2F°$.
	$a^3P_{1½}$	17830.4		1.12	1.33	
$5d^2\,6s$	$a^3G_{3½}$	17710.7	−321.6	0.92	0.89	$z^4F°$, $z^4D°$, $z^4G°$, $z^4P°$, $y^4F°$, $y^4D°$, $x^4D°$, $x^4P°$, $z^2D°$, $z^2F°$, $y^2D°$, $y^2F°$, $z^2G°$, $x^2D°$, $x^2F°$, $w^2F°$, $w^2D°$, $z^2H°$, $y^2G°$, $v^2D°$, $u^2D°$, $v^2F°$.
	$a^3G_{4½}$	17389.1		1.13	1.11	
$5d^3$	$b^4F_{1½}$	18897.7	1237.3	0.46	0.40	$z^4F°$, $z^4D°$, $z^4G°$, $z^4P°$, $y^4D°$, $x^4D°$, $x^4P°$, $z^2D°$, $z^2P°$, $z^2F°$, $y^2D°$, $y^2P°$, $y^2F°$, $z^2S°$, $z^2G°$, $x^2D°$, $x^2F°$, $w^2F°$, $w^2D°$, $y^2G°$, $z^2H°$, $v^2D°$, $w^2P°$, $u^2D°$, $v^2F°$.
	$b^4F_{2½}$	20135.0	1502.8	1.01	1.03	
	$b^4F_{3½}$	21637.8	1507.9	1.23	1.24	
	$b^4F_{4½}$	23145.7		1.29	1.33	
$5d^3$	$b^4P_{0½}$	26996.5	288.6			$z^4P°$, $y^4F°$, $y^4D°$, $z^4S°$, $x^4D°$, $y^4P°$, $x^4P°$, $y^2D°$, $y^2P°$, $y^2F°$, $z^2S°$, $z^2G°$, $z^2D°$, $x^2F°$, $w^2D°$, $w^2F°$, $u^2D°$, $v^2F°$.
	$b^4P_{1½}$	27285.1	1262.0	1.76	1.73	
	$b^4P_{2½}$	28547.1		1.51	1.60	
$5d^3$	$b^2G_{3½}$	28458.2	−353.3	0.92	0.89	$z^4G°$, $y^4F°$, $y^4D°$, $x^4D°$, $x^4P°$, $z^2F°$, $y^2D°$, $y^2F°$, $z^2G°$, $x^2D°$, $x^2F°$, $w^2D°$, $w^2F°$, $z^2H°$, $y^2G°$, $v^2D°$, $u^2D°$, $v^2F°$.
	$b^2G_{4½}$	28104.9		1.05	1.11	
$5d^3$	$a^2H_{4½}$	31877.8	−935.7	1.05	0.91	$z^4G°$, $y^4F°$, $x^4D°$, $z^2G°$, $x^2F°$, $w^2F°$, $z^2H°$, $y^2G°$, $v^2F°$.
	$a^2H_{5½}$	30942.1		1.10	1.09	
$5d$	$c^2D_{1½}$	—		1.15	1.20	$y^4D°$, $x^4P°$, $x^2F°$, $x^2P°$, $v^2D°$, $w^2P°$.
	$c^2D_{2½}$	32778.1				
$5d^3$	$b^2P_{0½}$	—				$x^4D°$, $y^4P°$, $x^2P°$, $u^2D°$.
	$b^2P_{1½}$	37324.6				
$5d^3$	$b^2F_{2½}$	37398.6	40.9			$x^4D°$, $x^4P°$, $x^2D°$, $x^2F°$, $w^2F°$, $y^2G°$, $z^2H°$, $y^2G°$, $v^2D°$, $w^2P°$, $u^2D°$, $v^2F°$.
	$b^2F_{3½}$	37439.5				
$5d\,6s\,6p$ $a^3D.p$	$z^4F°_{1½}$	28068.8	1336.4	0.52	0.40	a^2D, a^4F, a^4P, a^2F, b^2D, a^2P, a^2G, b^4F, 1, 2, 3, 4, 7, 8, 9, 10, 11, 12, 13, 14, 15, 16, 17, 18, 19.
	$z^4F°_{2½}$	29405.2	4371.1	1.08	1.03	
	$z^4F°_{3½}$	33776.3	4409.4	1.26	1.24	
	$z^4F°_{4½}$	38185.7		1.34	1.33	
$5d\,6s\,6p$ $a^3D.p$	$z^4D°_{½}$	29160.1	2624.2	0.53	0.00	a^2D, a^4F, a^4P, a^2F, b^2D, a^2P, a^2G, b^4F, 1, 2, 3, 4, 5, 6, 7, 8, 9, 10, 12, 13, 14, 15, 16, 17, 18, 19.
	$z^4D°_{1½}$	31784.3	2570.8	1.22	1.20	
	$z^4D°_{2½}$	34355.1	2527.4	1.32	1.37	
	$z^4D°_{3½}$	36882.5		1.39	1.43	
$5d\,6s\,6p$ $a^1D.p$	$z^2D°_{1½}$	34124.0	−943.0	0.84	0.80	a^2D, a^4F, a^4P, a^2F, b^2D, a^2P, a^2G, b^4F, 2, 3, 4, 5, 6, 8, 9, 11, 12
	$z^2D°_{2½}$	33181.0		1.05	1.20	
$5d\,6s\,6p$ $a^3D.p$	$z^2P°_{½}$	33136.3	3237.1	0.29	0.67	a^2D, a^4F, a^4P, a^2F, b^2D, a^2P, b^4F, 2, 5, 7, 8, 9, 12.
	$z^2P°_{1½}$	36373.4		1.31	1.33	
$5d^2\,6p$ $a^3F.p$	$z^4G°_{2½}$	34942.4	3556.1	1.00	0.57	a^2D, a^4F, a^4P, a^2F, b^2D, a^2P, a^2G, b^4F, b^2G, a^2H, 1, 2, 3, 6, 9, 10, 11, 12, 14, 15, 16, 17, 18.
	$z^4G°_{3½}$	38498.5	3892.5	1.06	0.98	
	$z^4G°_{4½}$	42391.0	3818.1	1.17	1.17	
	$z^4G°_{5½}$	46209.1		1.27	1.27	

TABLE 3.—*Relative terms in the* Hf II *spectrum*—Continued

Electron configurations	Terms	Level values	Level separations	g values		Combinations
				Observed	Landé	
$5d\ 6s\ 6p$ $a^3D.p$	$x^4P_{5/2}$	38398.6	827.8	2.63	2.67	a^2D, a^4F, a^4P, a^2F, b^2D, a^2P, a^2G, b^4F, b^4P, 6, 12, 15, 16.
	$x^4P_{3/2}$	39226.4	1280.4	1.68	1.73	
	$x^4P_{1/2}$	40506.8		1.45	1.60	
$5d\ 6s\ 6p$ $a^3D.p$	$y^2D_{5/2}$	37886.0	3875.3	0.80	0.80	a^2D, a^4F, a^4P, a^2F, b^2D, a^2P, a^2G, b^4F, b^4P, b^2G, 6, 8, 10, 11, 12, 16.
	$y^2D_{3/2}$	41761.3		1.08	1.20	
$5d\ 6s\ 6p$ $a^3D.p$	$z^2F_{5/2}$	38578.7	2828.3	0.89	0.86	a^2D, a^4F, a^4P, a^2F, b^2D, a^2G, b^4F, b^2G, 5, 6, 9, 10, 11, 13, 15, 17, 18, 19.
	$z^2F_{7/2}$	41407.0		1.12	1.14	
$5d^2\ 6p$ $a^3F.p$	$y^4F_{5/2}$	42518.2	1162.5	0.57	0.40	a^2D, a^4F, a^4P, a^2F, b^2D, a^2P, a^2G, b^4F, b^4P, b^2G, a^2H, 5, 10, 11, 19.
	$y^4F_{3/2}$	43680.7	719.3	0.98	1.03	
	$y^4F_{5/2}$	44400.0	1725.0	1.18	1.24	
	$y^4F_{7/2}$	46125.0		1.23	1.33	
$5d\ 6s\ 6p$ $a^1D.p$	$y^2P_{3/2}$	43044.3	−273.7	0.56	0.67	a^2D, a^4F, a^4P, b^2D, a^2P, b^4F, b^4P.
	$y^2P_{1/2}$	42770.6		1.24	1.33	
$5d\ 6s\ 6p$ $a^1D.p$	$y^2F_{5/2}$	43900.6	790.2	0.95	0.86	a^2D, a^4F, a^4P, a^2F, b^2D, a^2G, b^4F, b^4P, b^2G, 9, 14, 16.
	$y^2F_{7/2}$	44690.8		1.16	1.14	
$5d^2\ 6p$ $a^3F.p$	$y^4D_{5/2}$	45643.1	1031.4	0.47	0.00	a^2D, a^4F, a^4P, a^2F, b^2D, a^2P, b^4F, b^4P, b^2G, c^2D.
	$y^4D_{7/2}$	46674.5	1229.9	1.16	1.20	
	$y^4D_{3/2}$	47904.4	1026.4	1.33	1.37	
	$y^4D_{1/2}$	48930.8		1.37	1.43	
$5d^2\ 6p$ $a^3P.p$	$z^4S_{3/2}$	46495.4		1.68	2.00	a^2D, a^4F, a^4P, b^2D, a^2P, b^4F, b^4P.
$5d^2\ 6p$ $a^3F.p$	$z^2G_{9/2}$	47157.7	2682.9	1.03	0.89	a^2D, a^4F, a^4P, a^2F, b^2D, a^2G, b^4F, b^4P, b^2G, a^2H, 3, 17.
	$z^2G_{7/2}$	49840.6		1.16	1.11	
$5d^2\ 6p$ $b^1D.p$	$x^2D_{3/2}$	47973.4	1032.5	1.21	0.80	a^2D, a^4F, a^4P, a^2F, b^2D, a^2P, a^2G, b^4F, b^4P, b^2G, b^2F, 5.
	$x^2D_{5/2}$	49005.9		1.26	1.20	
$5d^2\ 6p$ $a^3P.p$	$z^4S_{5/2}$	47996.4				a^2D, a^4F, a^4P, a^2P, b^4P.
f^1	$y^4P_{5/2}$	50419.6		1.58	1.73	a^2D, a^4F, a^4P, b^2D, b^4P, b^2P.
$5d^2\ 6p$ $a^3F.p$	$x^2F_{5/2}$	50910.0	1420.7	0.92	0.86	a^2D, a^4F, a^4P, a^2F, b^2D, a^2P, a^2G, b^4F, b^4P, b^2G, a^2H, c^2D, b^2F.
	$x^2F_{7/2}$	52339.7		1.17	1.14	
$5d^2\ 6p$ $a^3F.p$	$w^2D_{5/2}$	51133.5	1569.3	1.10	0.80	a^2D, a^4F, a^4P, a^2F, b^2D, a^2P, a^2G, b^4F, b^4P, b^2G, b^2F.
	$w^2D_{3/2}$	52702.8		1.03	1.20	
$5d^2\ 6p$ $b^1D.p$	$w^2F_{5/2}$	53227.2		1.18	1.14	a^4F, a^4P, a^2F, b^2D, a^2G, b^4F, b^4P, b^2G, a^2H, b^2F.
$5d^2\ 6p$ $a^3P.p$	$x^4D_{5/2}$	52096.5				a^2D, a^4F, a^4P, a^2F, b^2D, a^2P, a^2G, b^4F, b^4P, b^2G, a^2H, b^2F.
	$x^4D_{7/2}$	52717.1	620.6			
	$x^4D_{1/2}$	54693.2	1976.1	1.30	1.37	
	$x^4D_{3/2}$	58448.1	3754.9	1.12	1.14	
$5d^2\ 6p$ $a^3P.p$	$x^4P_{5/2}$	53330.7		2.58	2.67	a^2D, a^4F, a^4P, a^2F, b^2D, a^2P, a^2G, b^4F, b^4P, b^2G, c^2D, b^2F.
	$x^4P_{3/2}$	53494.1	163.4	1.42	1.73	
	$x^4P_{1/2}$	55060.1	1566.0	1.21	1.60	

TABLE 3.—*Relative terms in the* Hf II *spectrum*—Continued

Electron configurations	Terms	Level values	Level separations	g values		Combinations
				Observed	Landé	
$5d^3\,6p$ $a^1G.p$	$z^2H^0_{11/2}$	53546.0	3025.5	1.03	0.91	a^4F, a^2F, a^2G, b^4F, b^2G, a^2H, b^2F.
	$z^2H^0_{9/2}$	56571.5		1.08	1.09	
$5d^3\,6p$ $a^1G.p$	$y^2G^0_{9/2}$	53972.5	1666.2	1.20	0.89	a^2D, a^4F, a^4P, a^2F, a^2G, b^4F, b^2G, a^2H, b^2F.
	$y^2G^0_{7/2}$	55638.7		1.08	1.11	
$5d^3\,6p$ $b^1D.p$	$x^2F^0_{7/2}$	55076.9		1.38	1.33	a^2D, a^4F, a^4P, a^2F, b^2D, a^2P, b^4P, c^2D, b^2P.
$5d^3\,6p$ $a^3P.p$	$w^2P^0_{3/2}$	57477.6	−1131.9			a^2D, a^4P, a^2F, b^2D, a^2P, b^4F, c^2D, b^2F.
	$w^2P^0_{1/2}$	56345.7				
f	$v^2D^0_{5/2}$	58117.3		1.20	1.20	a^2D, a^4P, b^2D, a^2P, a^2G, b^4F, b^2G, c^2D, b^2F.
$5d^3\,6p$ $a^3P.p$	$u^2D^0_{3/2}$	61318.2	3345.9			a^2D, a^4P, a^2F, b^2D, a^2P, a^2G, b^4F, b^4P, b^2G, b^2P.
	$u^2D^0_{5/2}$	64664.1				
$5d^3\,6p$ $a^1G.p$	$v^2F^0_{7/2}$	62775.0	1667.1			a^2D, a^4F, a^4P, a^2F, b^2D, a^2P, a^2G, b^4F, b^4P, b^2G, a^2H, b^2F.
	$v^2F^0_{5/2}$	64442.1				
	$1_{3/2}$	65643.9				$z^4F°$, $z^4D°$, $z^4G°$.
	$(c^4F?)2_{1/2}$	69310.2	1355.8			$z^4F°$, $z^4D°$, $z^4G°$, $z^2D°$, $z^2P°$.
	$(c^4F?)3_{3/2}$	70666.0				$z^4F°$, $z^4D°$, $z^4G°$, $z^2D°$, $z^2G°$.
	$4_{3/2}$	69483.3				$z^4F°$, $z^4D°$, $z^2D°$.
	$(c^2D?)5_{1/2}$	69963.2	3701.8			$z^4D°$, $y^4F°$, $z^2D°$, $z^2P°$, $z^2F°$, $x^2D°$.
	$(c^2D?)6_{3/2}$	73665.0				$z^4D°$, $z^4G°$, $z^2D°$, $z^2F°$, $y^2D°$.
	$7_{1/2}$	72159.2				$z^4F°$, $z^4D°$, $z^2P°$.
	$8_{1/2}$	73147.3				$z^4F°$, $z^4D°$, $z^2D°$, $z^2P°$, $y^2D°$.
	$9_{1/2}$	75158.4				$z^4F°$, $z^4D°$, $z^4G°$ $z^2D°$, $z^2P°$, $z^2F°$, $y^2F°$.
	$10_{3/2}$	75801.5				$z^4F°$, $z^4D°$, $z^4G°$, $y^4F°$, $z^2F°$, $y^2D°$.
	$11_{1/2}$	76016.5				$z^4F°$, $z^4G°$, $y^4F°$, $z^2D°$, $z^2F°$, $y^2D°$.
	$12_{3/2}$	76585.2				$z^4F°$, $z^4D°$, $z^4G°$, $z^2D°$, $z^2P°$, $y^2D°$.
	$13_{1/2}$	77163.0				$z^4F°$, $z^4D°$, $z^2F°$.
	$14_{3/2}$	77314.5				$z^4F°$, $z^4D°$, $z^4G°$, $y^2F°$.
	$15_{3/2}$	79090.8				$z^4F°$, $z^4D°$, $z^4G°$, $z^4P°$.
	$(c^2G?)16_{3/2}$	79804.6	1246.4			$z^4F°$, $z^4D°$, $z^4G°$, $z^4P°$, $y^2D°$, $y^2F°$.
	$(c^2G?)17_{1/2}$	81051.0				$z^4F°$, $z^4D°$, $z^4G°$, $z^2F°$, $z^2G°$.
	$18_{3/2}$	82100.5				$z^4F°$, $z^4D°$, $z^4G°$, $z^2F°$.
	$19_{3/2}$	83129.8				$z^4F°$, $z^4D°$, $z^4G°$, $y^4F°$, $z^2F°$.

All data relating to the established Hf II spectral terms are summarized in table 3 where electron configurations, term symbols, level values, level separations, observed and Landé g values, and combinations appear in successive columns. The symbols associated with energy levels are those now in general use for spectral line classifications.[17]

[17] Phys. Rev. 33, 900(1929).

TABLE 4.—*Zeeman effect* Hf II: *Sums of observed and Landé g values*

Electrons	Terms	J = 4½ Observed	J = 4½ Landé	J = 3½ Observed	J = 3½ Landé	J = 2½ Observed	J = 2½ Landé	J = 1½ Observed	J = 1½ Landé	J = 0½ Observed	J = 0½ Landé	Sum Observed	Sum Landé
$5d\ 6s^3$	a^2D					1.18	1.20	0.80	0.80			1.98	2.00
$5d^2\ 6s$	a^4F	1.33	1.33	1.23	1.24	1.06	1.03	0.45	0.40			4.07	4.00
	a^4P					1.42	1.60	1.69	1.73	2.61	2.67	5.72	6.00
	a^2G	1.13	1.11	0.92	0.89							2.05	2.00
	a^2F			1.11	1.14	0.98	0.86					2.09	2.00
	b^2D					1.29	1.20	1.03	0.80			2.32	2.00
	a^2P							1.12	1.33	0.74	0.67	1.86	2.00
	^2S									(2.00)	2.00	(2.00)	2.00
Sum low terms		2.46	2.44	3.26	3.27	5.93	5.89	5.09	5.06	5.35	5.34	22.09	22.00
$5d\ 6s\ 6p$	$z^4F°$	1.34	1.33	1.26	1.24	1.08	1.03	0.52	0.40			4.20	4.00
	$z^4D°$			1.39	1.43	1.32	1.37	1.22	1.20	0.53	0.00	4.46	4.00
	$z^4P°$					1.45	1.60	1.68	1.73	2.63	2.67	5.76	6.00
	$z^2F°$			1.12	1.14	0.89	0.86					2.01	2.00
	$z^2D°$					1.08	1.20	0.80	0.80			1.88	2.00
	$z^2P°$							1.31	1.33	0.29	0.67	1.60	2.00
	$y^2F°$			1.16	1.14	0.95	0.86					2.11	2.00
	$z^2D°$					1.05	1.20	0.84	0.80			1.89	2.00
	$y^2P°$							1.24	1.33	0.56	0.67	1.80	2.00
Sum odd terms		1.34	1.33	4.93	4.95	7.82	8.12	7.61	7.59	4.01	4.01	25.71	26.00

The so-called "g-sum rule" of Pauli [18] is expected to be valid for all spectra no matter what the nature of the vector coupling may be. This rule may be stated as follows: If among all terms arising through the coupling of one electron, those terms with the same inner quantum number J be grouped, the sum of the g values of the terms in each group must have a value independent of the nature of the coupling, and consequently is, among others, equal to the sum of the Landé g values for a similar group. This rule is tested in table 4 where the observed and Landé g sums are displayed for all groups for which the data are complete. On the whole, the agreement is very satisfactory, the one outstanding discrepancy which occurs for $J=2\frac{1}{2}$ in the *dsp* configuration remaining unexplained for the present.

In conclusion, we wish to make a statement regarding the spark *raie ultime* of hafnium, i.e., the most persistent spectral line for revealing the presence of ionized hafnium atoms.

Recent progress in analysis of spectral structure and correlation with electron configurations has enabled us to formulate a new rule governing the selection of the *raie ultime* in any spectrum. This rule has been tested in a large number of spectra (which will be detailed in another publication), and is believed to be more fundamental and general than any heretofore proposed for such lines. It may be briefly stated as follows: A *raie ultime* in any spectrum originates with a simple interchange of a single electron between s and p states, usually preferring configurations in which only one electron occurs in such states. In accordance with this rule it may be said that the transition $(5d^26s)\ a^4F_{4\frac{1}{2}}-(5d^26p)\ z^4G^0_{5\frac{1}{2}}$, corresponding to the line of wave length 2641.41 A, represents the true *raie ultime* of the Hf II spectrum. It is undoubtedly the most intense line in this spectrum and appears also to be the strongest line ascribable to hafnium in spark spectra of zirconium containing hafnium as an impurity.

WASHINGTON, August 8, 1934

[18] W. Pauli, Zeit. f. Phys. 16, 155(1923).

U.S. DEPARTMENT OF COMMERCE NATIONAL BUREAU OF STANDARDS

RESEARCH PAPER RP733

Part of Journal of Research of the National Bureau of Standards, Volume 13, November 1934

IONIZATION OF LIQUID CARBON DISULPHIDE BY X-RAYS

By Fred L. Mohler and Lauriston S. Taylor

ABSTRACT

The ionization was measured in a layer of liquid between flat aluminum disks with spacings of 1 and 0.3 mm. Fields up to 60 kv per cm were used and the current voltage curve rose continuously but at a decreasing rate in this range. A plot of the reciprocal of the current against the reciprocal of the field is a straight line above 20 kv and can be extrapolated to infinite field. The form of curve is consistent with the theory of columnar recombination and the intercept at infinite field gives the rate of production of ions. Comparison with the radiation in roentgens gives the ionization per unit volume in liquid carbon disulphide as 2,600 times that of air under standard conditions. The absorption is 1,910 times that of air and the energy of ionization per ion pair about 0.75 times that of air. The shape of the curve and the columnar theory give the diameter of the columns as 5.8×10^{-6} cm and the density of ionization in the columns as 2.3×10^{16} ions per cm^3.

CONTENTS

		Page
I.	Introduction	659
II.	Ionization chambers	660
III.	Purification of liquid	660
IV.	Radiation	661
V.	Electrical measurements	661
VI.	The current voltage curve	661
VII.	Comparison with air ionization	662
VIII.	Columnar ionization	663
IX.	Conclusions	664

I. INTRODUCTION

The ionization of dielectric liquids by X-rays was discovered by J. J. Thomson [1] in 1895 and the related case of ionization by gamma rays was studied in detail by Jaffé [2] and his associates in the period 1906 to 1913. The properties of ionized liquids are comparable to those of very dense gases. The mobility of the ions and their rate of recombination are very small (in liquid carbon disulphide both are about 10^{-4} of the values for air at one atmosphere).[3] The current voltage curves rise rapidly toward saturation with fields up to 1,000 volts per cm but with further increase in field the current continues to increase and in the range 1,000 to 5,000 volts the increase is nearly linear. Some of Jaffé's experiments seemed to indicate that this linear increase was absent in very pure liquids but his later papers reject this result. In a comprehensive theoretical paper [4] he was able to show that Langevin's theory of columnar recombination could

[1] J. J. Thomson, Nat., **53**,378(1895).
[2] Jaffé, Ann. der Phys., **25**,257(1908);**28**,326(1909).
[3] Van der Bijl, Ann. der Phys., **39**,170(1912).
[4] Jaffé, Ann. der Phys., **42**,303(1913).

account for the lack of saturation in liquids and gases ionized by alpha and gamma rays. The absorption of a quantum of X-rays or gamma rays gives rise to a single high-speed electron. This traverses the gas or liquid leaving a dense trail of ions and these may be so close together that the highest fields will not separate them before some of them recombine. Insofar as the ions from separate columns do not recombine with each other, the current will be proportional to the number of quanta absorbed but will be less than the total production of ion pairs. Jaffé estimated that in liquids ionized by gamma rays only a tenth of the ions are removed from the column while from alpha ray tracks only one in a thousand escapes. These estimates are based on the assumption that the average energy expended per ion pair is the same as in air. Published results obtained with fields of less than 5,000 v/cm give no basis for an experimental value of the actual number of ions produced in a liquid. It has been our purpose to extend current voltage curves to much higher fields in an attempt to measure the actual production of ions by X-rays in liquids. Jaffé's results and our preliminary experiments indicated that carbon disulphide was a promising liquid for the experiment.

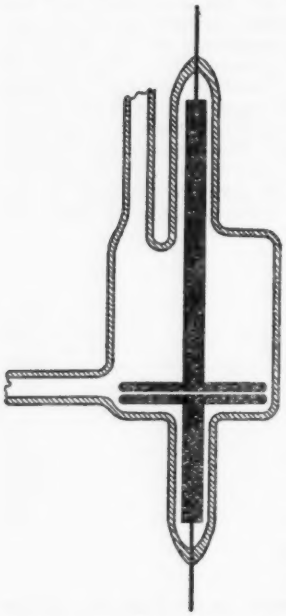

FIGURE 1.—*Ionization chamber.*

II. IONIZATION CHAMBERS

The attainment of high fields requires smooth rounded surfaces close together and we have used a simple two-electrode chamber sealed in a pyrex glass bulb as illustrated in figure 1. The electrodes are aluminum disks 4.5 cm in diameter with the edges rounded. Plate separations of 1 and 0.3 mm were used. This bulb construction is adapted to obtaining pure dry liquid in the chamber, but it was not possible to evaluate accurately the radiation flux through the end of the bulb.

For quantitative comparison of liquid and air ionization the following chamber was made. Two plates of aluminum were separated by mica rings of 8 cm outside diameter and 4 cm inside diameter. These rested in a crystallizing dish. A mica cover limited evaporation and a lead ring restricted the vertical X-ray beam to the 4-cm hole in the mica spacers. Here the radiation flux could be closely estimated and the ionized volume of liquid is not subject to edge corrections.

III. PURIFICATION OF LIQUID

Commercial carbon disulphide has a high conductivity and must be purified. The conducting impurities are probably water and hydrogen sulphide. The procedure was to pour the liquid into a bulb containing quicklime and hold it at liquid air temperature in high vacuum while baking out the ionization chamber. Then the liquid was slowly distilled in vacuum through phosphorus pentoxide into a

trap, and finally into the ionization chamber. The resulting liquid had a specific resistance of more than 10^{14} ohms. This gives a leak of less than 1 percent of the ionization current but very much higher resistance can be obtained with elaborate precautions.[5] In using the open chamber, this was first dried by warming and the purified liquid poured in. The leak here was about 10 times that in the vacuum chamber though the experiments were made in cold dry winter weather.

IV. RADIATION

Slightly filtered X-rays from a tungsten target tube operated at 120 kv constant potential and a current of 5 ma or less, passed through the chamber normal to the electrodes at a distance of about 50 cm from the target. The ionization in the liquid was compared with air ionization by replacing the chamber by a roentgenometer calibrated to read in roentgens for the quality of radiation used. The quality of radiation expressed in terms of the true effective wave length in aluminum was 0.44 A outside the chamber and 0.27 in the liquid.[6]

The ionization in a small chamber depends on the wall material as well as the ionized medium. For carbon disulphide and aluminum the effect is small for both have comparable X-ray absorption so that the loss of electrons by the liquid nearly compensates for the gain from the metal. Taking the difference in ionization with different electrode spacings should eliminate the wall effect, but because of the increased experimental error this procedure was not used.

V. ELECTRICAL MEASUREMENTS

The voltage source for the ionization chamber was a very steady constant potential X-ray generator. The leads to the chamber were covered and shielded to avoid corona and air ionization. Currents were of a magnitude to measure with a sensitive galvanometer. The response upon admitting or cutting off the radiation was nearly instantaneous, but the dark current dropped at a decreasing rate for minutes every time the voltage was increased. This comes in part from electrical clean-up of the liquid and in part from polarization. With fields up to 20 or 30 kv per cm the dark current is small. At higher fields it rapidly becomes large and unsteady, and above 60 kv the measurements are too inaccurate to be useful. The maximum field strength was about the same for plate separations of 1 or 0.3 mm for dry liquid in vacuum and for the liquid exposed to air.

VI. THE CURRENT VOLTAGE CURVE

All results reduced to the same current scale are included in figure 2. Open circles give measurements with a 1 mm spacing and crosses apply to the 0.3 mm spacing with a current correspondingly smaller. Tests with different intensities of radiation showed that above 2 kv per cm the current is proportional to the intensity. Hence we conclude

[5] Van der Bijl, Ann. der Phys., **39**,170(1912).

[6] The roentgen is the quantity of radiation which will give in 0.001293 g of air 1 esu of ion pairs. The true effective wave length is the wave length of homogeneous radiation which will be reduced in the same ratio by an infinitesimal layer of aluminum. In media comparable with aluminum in atomic number (and only in these) the radiation can be treated as a homogeneous radiation of this wave length. L. S. Taylor, BS J.Research **5**,517(1930);RP212.

that above this point the form of the curve is not influenced by intercolumnar recombination. There was no observable difference between the curves obtained in the pure liquid and in the liquid exposed to air. This result does not support the view that traces of impurity modify the form of the curve.[7]

Jaffé [8] has derived a general expression for the fraction of ions I_X/I_∞ drawn from a column by a field X when the ion pairs are initially distributed in a cylinder of diameter d with a density of N pairs per cm of column length.

$$\frac{I_\infty}{I_X}=1+\frac{\alpha N}{7.85\,duX\,F(X)} \tag{1}$$

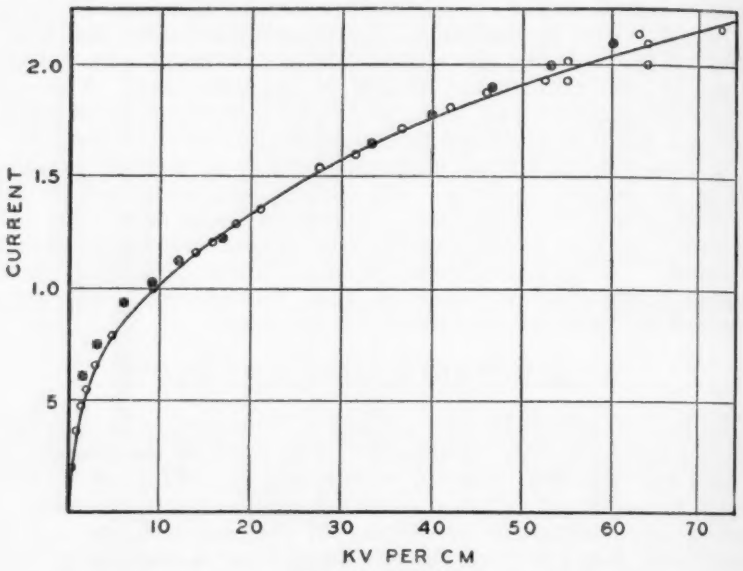

FIGURE 2.—*Current voltage curve in liquid carbon disulphide.*
Circles with 1 mm between electrodes, crosses 0.3 mm.

Here α is the recombination coefficient, 9×10^{-10}, and u the mobility of the ions, 0.66×10^{-3} cm per sec, per volt per cm. $F(X)$ is a complicated function which approaches 1 for high fields (over 10^4 volts per cm). The form of the equation indicates that a plot of $1/I_X$ versus $1/X$ will be nearly linear. Figure 3 gives the curve of figure 2 on this scale and the resulting curve conforms to the theoretical prediction. In view of the theory it is safe to make a linear extrapolation from the observed points to $1/X=0$. The intercept gives (in arbitrary units) the reciprocal of the current at infinite voltage and is a measure of the actual rate of production of ions by the X-rays. Measurements at the highest fields gave about three-quarters of the saturation current.

VII. COMPARISON WITH AIR IONIZATION

The ionization produced in the open chamber with 1 mm spacing was compared with the reading of the roentgenometer. The radiation flux corrected for absorption in the top plate of the liquid chamber

[7] Jaffé, Ann. der Phys., **28**, 326(1909).
[8] Jaffé, Ann. der Phys., **42**, 303(1913).

was 0.129 roentgens per sec (0.129 esu per cm^3 of free air under standard conditions). The current in the liquid extrapolated to infinite field was 1.12×10^{-7} amp per cm^3 or 336 esu per cm^3 per sec. Hence the ionization per unit volume in liquid carbon disulphide is 2,600 times that in air.

The ionization in any medium is proportional to the energy absorbed divided by the average energy required to produce an ion pair or $\mu\rho/E$ where μ is the mass absorption coefficient, ρ the density and E the energy per ion pair. Thus

$$\frac{(\mu\rho/E) \text{ for } CS_2}{(\mu\rho/E) \text{ for air}} = 2{,}600$$

The experimental value of μ for air for radiation of this quality is 0.35.[9] The value μ for CS_2 computed from the monochromatic values for C and S at 0.27 A (the effective wave length in Al for the radiation) is 0.67. The density ratio is 1,000. Taking the average energy expended per ion pair in air as 33 electron volts we find the average energy in liquid carbon disulphide is 24 volts. A published value [10] of the ionization of carbon disulphide vapor by X-rays indicates a value of 26 electron volts. We conclude that within the range of experimental uncertainty the energy required to ionize carbon disulphide is the same in the liquid phase as in the gas phase.

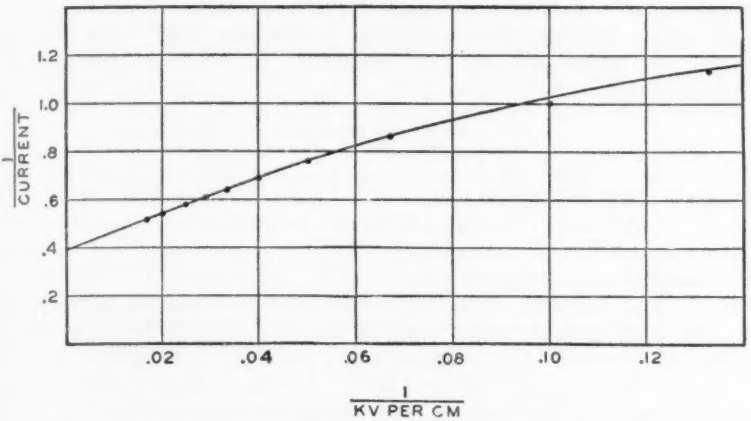

FIGURE 3.—*Curve of figure 2 plotted with reciprocal of current versus reciprocal of voltage.*

VIII. COLUMNAR IONIZATION

As noted above, the process of ionization consists in the ejection of a high-speed electron which traverses the liquid and produces a dense column of ions. On the basis of our experimental data and Jaffé's theory the process can be described in more detail. The secondary electrons will have an average energy of 46,000 electron volts (corresponding to 0.27 A). These will go a distance of 3.2×10^{-3} cm [11]

[9] L. S. Taylor, BS J. Research, **6**, 219(1931); RP271.
[10] J. J. Thomson, Conduction of Electricity in Gases, **2**, 238(1933).
[11] Rutherford Chadwick and Ellis, Radiation from Radioactive Substances, 422(1930).

through the liquid and produce in this distance 1,900 ion pairs giving an average density of 6×10^5 pairs per cm of path. At high voltages equation 1 becomes

$$\frac{I_\infty - I_x}{I_x} = \frac{\alpha N}{7.85\, duX}$$

where N is the ion density evaluated above, and all other quantities are known except d, the diameter of the column. The slope of the curve in figure 3 gives the value of d as 5.8×10^{-6} cm. (The distance between ion pairs $(1/N)$ is 1.7×10^{-6} cm). The physical significance of d is probably as follows: The secondary electrons produce positive ions and tertiary electrons of about 10 volts energy which move away until they become attached to molecules to form heavy negative ions. The constant d is (apart from a small geometrical factor) the distance the electron goes before attaching. This distance is a characteristic of the liquid and an important but unpredictable factor in determining the yield of ions under a given field.

The values for the dimensions of a column lead to a value of $2.3+10^{16}$ ion pairs per cm^3 in a column. From the recombination equation in the form

$$\frac{1}{n} - \frac{1}{n_o} = \alpha t$$

it is found that this ionization will be reduced to a fifth of its initial value in 2×10^{-7} sec. About a fifth of the ions escape in zero field so this time is the life of the column. In our experiment X-ray quanta were absorbed and columns produced at the rate of 3.7×10^8 per cm^3 per sec. Thus about 74 columns per cm^3 existed at any instant. From the conductivity produced by X-rays at low voltage and the mobility of the ions one estimates the average concentration of ion pairs in zero field as 1.1×10^{10} per cm^3. Upon cutting off the radiation this will drop to half value by recombination in 0.2 sec.

IX. CONCLUSIONS

The above numerical values for the elementary processes are of interest only as an illustration of the deductions that can be drawn from the constants of the current voltage curve. The results support the assumption that the number of ions produced in a liquid by the absorption of a quantum is about the same as in a gas and that the current resulting from the ionization is greatly reduced by intracolumnar recombination.

The application of liquid ionization chambers to the measurement of X-rays and gamma rays is not new, but its possibilities are not generally appreciated.[12] With fields of the order of 20 kv per cm the current in carbon disulphide is perfectly steady and strictly proportional to the intensity and it is over 1,000 times the current from an equal volume of air. The comparison of radiations of different quality would require further research. The columnar recombination theory indicates that the degree of saturation for a given field will depend on the quality because of the variation in the number of ions per unit length of the column.

WASHINGTON, September 13, 1934.

[12] Stahel, Strahlentherapie, **31**, 582(1929).

U.S. DEPARTMENT OF COMMERCE NATIONAL BUREAU OF STANDARDS

RESEARCH PAPER RP734

Part of Journal of Research of the National Bureau of Standards, Volume 13, November 1934

PREPARATION OF PURE GALLIUM

By James I. Hoffman

ABSTRACT

A method is described for the preparation of pure gallium. The principal operations consist in (1) preparing a hydrochloric-acid solution of the metal and extracting the gallium, molybdenum, gold, iron, and thallium, together with small amounts of other elements, with ether; (2) precipitating antimony, arsenic, bismuth, cadmium, copper, germanium, gold, mercury, silver, and tin, and most of the lead, molybdenum, and rhenium, with hydrogen sulphide in an acid solution of the ether extract; (3) precipitating iron and thallium with sodium hydroxide and filtering; (4) depositing the gallium electrolytically from the alkaline filtrate; and (5) eliminating the remaining impurities by fractional crystallization of the metal. Indium and lead are the most persistent impurities, but the last traces can be removed by fractional crystallization.

Gallium (at least 99.999 percent pure) containing only very faint traces of iron, lead, and calcium, and having a melting point of $29.780 \pm 0.005°C$, was obtained.

CONTENTS

	Page
I. General considerations and experiments	665
II. Method for the preparation of pure gallium	667
1. Outline of the procedure	667
2. Preparation of the solution for electrolysis	668
3. Electrolysis	669
4. Fractional crystallization	669
III. Test of the procedure outlined	670
IV. Purity and yield	670
V. Recovery of residual gallium	671

I. GENERAL CONSIDERATIONS AND EXPERIMENTS

To provide metallic gallium of the highest purity for use as an alloying element in the cadmium-vapor arc lamp[1] and for researches in spectroscopy, and also for a study of its physical properties, a quantity of crude gallium, containing 5 percent of indium, 0.1 percent of lead, and smaller amounts of silver, tin, and zinc, was carefully purified. In order that the method of purification devised might be of general use, the separations employed were so chosen that additional impurities, such as aluminum, antimony, arsenic, beryllium, bismuth, cadmium, calcium, chromium, copper, germanium, gold, magnesium, mercury, molybdenum, rhenium, thallium, tungsten, uranium, and vanadium would be eliminated.

For the preliminary separation of gallium from most of the other elements, extraction of the chloride with ether is quite satisfactory.

[1] F. J. Bates, BS Sci. Pap. **16**, 45 (1920); S371

Gallium, molybdenum, and tervalent gold, thallium, and iron in hydrochloric acid solution are almost quantitatively extracted by ether, together with small amounts of germanium, arsenic, and antimony. All of the other elements likely to be present remain almost quantitatively in the acid solution. If thallium and iron are reduced to the univalent and bivalent stages, respectively, they likewise remain in the acid solution, but their reduction is recommended only if they are present in large amount; small amounts are more easily eliminated by precipitating them in the tervalent form with sodium hydroxide. Silver (and some univalent thallium when present in large amount) is precipitated as chloride and must be removed by filtration in order to obtain a clear solution for the ether extraction. Germanium and arsenic can be removed by precipitating them as sulphides and filtering, or by distilling them as chlorides ($GeCl_4$ and $AsCl_3$). If these are not previously eliminated, they will probably be volatilized when the ether extract is evaporated. Precipitation as sulphides followed by filtration also serves to remove antimony, bismuth, cadmium, copper, gold, mercury, silver, and tin, and most of the lead, molybdenum, and rhenium.

In the method described, gallium is deposited electrolytically from a strongly alkaline solution (10 percent NaOH). Consequently, the possibility of partial purification by fractional deposition from such a solution was investigated. Solutions containing indium, lead, and gallium were electrolyzed with a current of 2 to 5 amperes at 4 to 5 volts, and the deposited metal obtained at various stages of the electrolysis was tested for impurities. There was so little difference in the amounts of indium and lead in the fractions that this means of purification was abandoned. Preliminary tests also showed that electrolysis in such solutions did not yield complete separations of silver, bismuth, indium, molybdenum, rhenium, lead, tin, thallium, iron, calcium, and magnesium. Calcium and magnesium were shown spectrochemically to be present in the deposited metal only in faint traces, no greater than those found in material obtained in a similar way when calcium and magnesium were not added to the electrolyte. It may be inferred, therefore, that calcium and magnesium were not deposited electrolytically, but that sufficient of these to give a spectrochemical test was derived from the dust of the air. Probably dust was also the source of the faint trace of iron found in nearly all of the samples of gallium that were tested spectrochemically.[2]

A more comprehensive test was then made to determine the efficacy of the precipitation of iron, thallium, etc., with sodium hydroxide followed by electrolysis of the alkaline filtrate. To a slightly acid solution of gallium chloride, containing 4 g of gallium, were added 10 mg each of aluminum, antimony, arsenic, beryllium, bismuth, cadmium, calcium, chromium, copper, germanium, gold, indium, lead, magnesium, mercury, molybdenum, rhenium, silver, thallium, tin, tungsten, uranium, vanadium, and zinc. These were added as solutions of the chlorides or sulphates because nitrates must be

[2] In an attempt to eliminate calcium and magnesium, a portion of metal was recrystallized 10 times in a small closed room that was entirely lined (floor, sides, and ceiling) with tinned steel. Spectrochemical tests showed that calcium and magnesium were eliminated but that there was a notable increase in the amount of iron. Close examination of the surface of the galvanized steel showed that it contained many small rust pits. Dust from these was probably responsible for the increase in the amount of iron. Chemical analysis showed that the iron content had increased from 0.00008 to 0. 00015 percent during the 10 crystallizations.

avoided in alkaline solutions from which gallium is to be electrolyzed.[3] Sodium hydroxide was then added until an excess of 10 g per 100 ml was present. After standing overnight, the solution was filtered and the clear filtrate electrolyzed. The deposited gallium was definitely contaminated by zinc, copper, silver, thallium, indium, tin, and lead, and showed traces of rhenium, bismuth, and molybdenum. Of these, copper, silver, tin, and bismuth can be completely removed by treatment with hydrogen sulphide prior to electrolysis, and the others can best be eliminated by fractional crystallization of the deposited metal.

Lecoq de Boisbaudran [4] obtained crystals of the metal, and later T. W. Richards and S. Boyer [5] made use of fractional crystallization for the final purification of gallium. Recently F. M. Jaeger, P. Terpstra, and H. E. K. Westenbrink [6] have made a study of the crystal structure of gallium. These authors have shown that rather large ditetragonal-bipyramidal crystals are formed from strongly undercooled molten metal, whereas smaller and very flat crystals are the rule when crystallization takes place slowly from metal that is only slightly undercooled. These two types of crystals were observed in this work, and a photograph of the largest and most perfect crystal of the first type is reproduced in figure 1.

In order to determine the efficacy of fractional crystallization, a portion of metallic gallium containing traces of indium and lead was recrystallized five times by the procedure given in section II–4, page 669. Spectrochemical tests showed a decided improvement in the purity, and 15 additional recrystallizations entirely freed the crystals from indium and lead. Further tests on a portion of gallium containing silver, gold, indium, lead, platinum, tin, thallium, and zinc showed that fractional crystallization tends to eliminate all of these, but that faint traces of platinum and gold, especially the latter, often are very difficult to remove. Fortunately, gold is easily removed by a preliminary precipitation with hydrogen sulphide, but platinum must be considered as a possible contaminating element in the deposited metal because of attack on the electrodes during electrolysis.

II. METHOD FOR THE PREPARATION OF PURE GALLIUM

1. OUTLINE OF THE PROCEDURE

On the basis of the foregoing considerations, the procedure outlined below has been adopted for the preparation of pure gallium. The steps and the effect of the various operations, if applied successively to a solution containing gallium, aluminum, antimony, arsenic, beryllium, bismuth, cadmium, calcium, chromium, copper, germanium, indium, iron, lead, magnesium, mercury, molybdenum, rhenium, silver, tin, tungsten, uranium, vanadium, zinc, and tervalent gold, iron, and thallium, are as follows: (1) The first ether separation concentrates gallium, molybdenum, and tervalent iron, thallium, and gold in the ether; small quantities of all of the others may also be expected to accompany the gallium. (2) Precipitation by hydrogen sulphide in acid solution followed by filtration removes all of the cadmium, copper, silver, tin, germanium, antimony, bismuth, arsenic,

[3] H. S. Uhler, Am. J. Sci. [4]43, 81(1917).
[4] Compt. rend. 83,1044(1876).
[5] J. Am. Chem. Soc. 43,281(1921).
[6] Koninklijke Akad. Wetenschappen Amsterdam, Proc. of Section of Sciences, 29,1193(1926).

mercury, gold, and most of the lead, molybdenum, and rhenium. The solution, in addition to gallium, may now contain small quantities of indium, iron, zinc, calcium, aluminum, magnesium, thallium, uranium, beryllium, chromium, vanadium, tungsten, lead, molybdenum, and rhenium. The last three may remain because of incomplete precipitation by hydrogen sulphide. (3) A second ether extraction more completely removes elements other than molybdenum and tervalent thallium and iron. (4) Precipitation by sodium hydroxide and filtration removes iron, thallium, and probably the traces of uranium and chromium which may still remain, and may leave the gallium associated with traces of indium, zinc, calcium, aluminum, magnesium, beryllium, vanadium, tungsten, lead, molybdenum, and rhenium. (5) Electrolysis in a 10 percent solution of sodium hydroxide deposits gallium, indium, zinc, lead, and possibly traces of molybdenum and rhenium. (6) Fractional crystallization of the metal frees it from the remaining impurities.

2. PREPARATION OF THE SOLUTION FOR ELECTROLYSIS

If a quantity of gallium other than that specified in the directions which follow is used at the start, corresponding changes in the volumes of solutions and quantities of reagents should be made.

Dissolve 60 g of the impure metal in a mixture of 200 ml of water and 100 ml of hydrochloric acid. Use a covered 1.5-liter beaker and set it in a vessel containing cold water to retard the rapid initial reaction. Add 100 ml of hydrochloric acid to the resulting solution and evaporate to a sirup. Again add 100 ml of hydrochloric acid and evaporate to a sirup. Transfer the sirupy solution of gallium chloride to a 2-liter separatory funnel with the aid of not more than 150 ml of diluted hydrochloric acid (1+1).[7] Add 1 liter of ether, cool, shake cautiously at first and then vigorously for 2 or 3 minutes. After the contents of the funnel have separated into two distinct layers, withdraw the acid solution, and wash the ether by adding 50 ml of cool diluted hydrochloric acid (1+1), shaking thoroughly, and withdrawing the acid layer. Repeat the washing 7 times, and reserve the combined washings and acid solution. Now withdraw the ether extract and allow it to stand in a warm place until most of the ether has evaporated. Concentrate this solution as far as possible on the steam bath and add an excess of hydrogen peroxide (30 percent) to oxidize organic compounds. Destroy the excess of hydrogen peroxide by heating on the steam bath for about 1 hour, and then dilute the solution to 3-liters with diluted hydrochloric acid (2+98).

Heat the solution nearly to boiling and treat it with a rapid stream of hydrogen sulphide. Allow it to stand overnight, filter through a paper of close texture, and wash the paper and precipitate with diluted hydrochloric acid (2+98) saturated with hydrogen sulphide. Add 400 ml of hydrochloric acid to the filtrate, and evaporate it to a volume of 1 liter. Treat the solution with hydrogen sulphide, and filter if a precipitate appears. Evaporate the filtrate to a sirup, oxidize with hydrogen peroxide, and heat to destroy the excess of peroxide. Repeat the ether extraction and washing of the ether as previously described.

[7] This denotes one volume of hydrochloric acid, specific gravity 1.18, diluted with 1 volume of water. Diluted hydrochloric acid (2+98) means 2 volumes of the acid, specific gravity 1.18, diluted with 98 volumes of water. If no dilution is specified, the concentrated acid is intended.

FIGURE 1.—*Crystal of gallium, weighing 2.2 grams.*
Approximately 4 times actual size.

UNIV. OF MICH.

Cautiously expel the ether from this second ether extract, and oxidize organic compounds by heating with hydrogen peroxide. Dilute the solution to about 500 ml, add a 50-percent solution of sodium hydroxide until the solution is just alkaline to litmus, and then 200 ml in excess. Adjust the volume of the solution to 1 liter, digest on the steam bath for ½ hour, and allow it to stand overnight at room temperature. Filter through a paper of close texture, wash with a 1-percent solution of sodium hydroxide, and nearly fill a 1-liter platinum dish with the filtrate. (The small portion of filtrate and washings remaining is reserved to be added to the dish later).

3. ELECTROLYSIS

Electrolyze at 2 to 5 amperes and 4 to 5 volts, using the platinum dish as the anode and a platinum helix as the cathode. Immerse a 25-ml beaker under the helix in the electrolyte to receive the globules of gallium as they drop from the cathode. After most of the gallium has been deposited (30 to 40 hours), discontinue the current, and evaporate the electrolyte in the platinum dish on the steam bath to such a volume as will permit the addition of the reserved alkaline filtrate. Add the reserved solution and continue the electrolysis until no more gallium is deposited (30 to 40 hours).

A no. 18 (B. & S. gage) platinum wire, twisted into a helix, serves satisfactorily as a cathode. The total length of wire immersed in the electrolyte should be from 8 to 10 cm, but may be less. The small amount of gallium that remains attached to the cathode is preferably dissolved in hydrochloric acid and combined with other residual gallium for further purification. (See sec. V.)

At the end of the electrolysis, transfer the gallium from the beaker to a small Erlenmeyer flask. To remove most of the alkali, wash the metal 10 times by shaking it in the small flask with hot water and then decanting the water. In a similar way wash 3 or 4 times with ethyl alcohol. Remove the last of the alcohol by drying over sulphuric acid in a desiccator or by drawing a stream of clean dry air through the flask. Stopper the flask and reserve the gallium for further purification by fractional crystallization.

4. FRACTIONAL CRYSTALLIZATION

To the gallium in the small flask add sufficient distilled water to cover the metal to a depth of about 0.5 cm, warm to about 50° C, and then add 5 to 10 drops of hydrochloric acid. Transfer the contents of the flask to a 50-ml beaker, set the beaker in ice water, and, when the crystals appear, pick them out of the molten metal with the aid of glass-tipped tweezers. Continue picking out the crystals until only a small globule (0.5 to 1.0 g) of metal remains. Combine and melt the crystals, and by the same process repeat the crystallization until crystals of the desired purity are obtained. Reserve the hydrochloric acid solution and the small globules of uncrystallized metal for further purification. During the last crystallization, drop the crystals into cold alcohol and wash two or three times with alcohol by decantation. Dry the crystals by drawing clean dry air over them or by placing them in a desiccator over sulphuric acid. Preserve the crystallized metal in a stoppered flask.

If economy of metal is no object and it is desired to obtain a small portion of very pure crystals, the metal may be crystallized in 4 approximately equal portions and only the first 2 portions taken for the next crystallization. If this process is repeated many times, the yield is small, but pure crystals are obtained in less time than by the method just outlined.

III. TEST OF THE PROCEDURE OUTLINED

The procedure was tested by applying it to a hydrochloric-acid solution of gallium to which had been added sufficient zinc and indium to correspond to an impurity of 1 percent of each, sufficient lead, cadmium, copper, thallium, tin, aluminum, calcium, magnesium, germanium, antimony, bismuth, arsenic, and molybdenum to correspond to an impurity of 0.1 percent of each, and sufficient gold, silver, mercury, rhenium, beryllium, chromium, vanadium, uranium, and tungsten to correspond to an impurity of 0.01 percent of each. The spectrochemical report on the metal as obtained by following all the steps of the procedure except fractional crystallization showed: calcium, trace; indium, trace; lead, trace; silver, faint trace?; magnesium, faint trace; and iron, faint trace. Ten crystallizations of this metal eliminated practically all indium, magnesium, lead, and silver, but 20 to 25 recrystallizations were necessary to eliminate indium and lead so completely that they could not be detected with the apparatus used by the spectroscopy section of the National Bureau of Standards.

IV. PURITY AND YIELD

Tests of the purity of the metal at the various stages were made spectrochemically by B. F. Scribner of the spectroscopy section. A stigmatic concave spectrograph was used,[8] and the spectra were examined for the sensitive lines of Ag, Al, As, Au, Ba, Be, Bi, Ca, Cb, Cd, Co, Cr, Fe, Ge, Hf, Hg, In, Ir, K, Li, Mg, Mn, Mo, Na, Ni, Os, Pb, Pd, Pt, Re, Rh, Ru, Sb, Si, Sn, Sr, Ta, Th, Ti, U, V, W, Zn, and Zr. In most cases the evidence for silver in the samples was questionable because of the presence of this element in the copper electrodes. In all cases the scale used in qualitatively designating the amounts of impurities is: *trace*, *very weak*, *weak*, *moderate*, *strong*, and *very strong*. The designation "*faint trace*" is used only when the most sensitive lines of the impurity appear near the limit of visibility.

Gallium originally containing 5 percent of indium, approximately 0.1 percent each of lead, zinc, and silver, and traces of calcium and tin was subjected to all of the treatments described in the foregoing procedure. Ten crystallizations of the electrolytically deposited metal yielded crystals which by spectrochemical tests showed only weak lines of indium and calcium and faint traces of lead and silver. Fifteen additional crystallizations yielded crystals in which *very faint traces* of only iron, lead, and calcium were detected. This metal showed a melting point[9] of $29.780 \pm 0.005°$ C.

The quantity of iron was determined chemically by treating a chloride solution of 3 g of this gallium with potassium thiocyanate,

[8] Described by W. F. Meggers, C. C. Kiess, and F. J. Stimson, BS Sci. Pap. 18, 244 (1922);S444, and by W. F. Meggers and Keivin Burns, BS Sci. Pap. 18, 191 (1922); S441.

[9] Determination described in J. Research, NBS 13,673(1934);RP735.

shaking with amyl alcohol, and comparing the color in the amyl alcohol with that obtained by treating a very dilute standard solution of iron in a similar way. Only 0.00009 percent of iron was found. No attempt was made to determine calcium because it was considered that the amount was too small for detection by chemical means. In order to eliminate the uncertainties concerning the presence of silver and copper and to get an approximation of the amount of platinum, 23 g of the metal was dissolved, and the resulting dilute-acid solution treated with hydrogen sulphide. After standing 3 days, more hydrogen sulphide was added, and the sulphides and sulphur were collected on a filter paper. This was gently ignited in a porcelain crucible, digested with hydrochloric acid, diluted to 25 ml, and treated with hydrogen sulphide as before. The small precipitate was collected on a filter paper, gently ignited, and weighed. The weight was only 0.2 mg more than that obtained on a blank on the reagents. This shows that the combined percentages of platinum, silver, and copper was less than 0.001. These tests indicate that the metal was at least 99.999 percent pure.

A lot of 53 g similarly prepared at a later time from impure metal from a different source was equally pure and had the same melting point (29.780° C).

By the procedure outlined it is not possible to obtain all of the gallium in the highest state of purity. An example will show approximately how the gallium is distributed. In the last preparation of pure gallium, 65 g of impure metal containing about 3 percent of indium was taken at the start. Of this 4.5 g passed into the acid extract and washings from the first ether extraction, 4.3 g passed into the acid extract and washings from the second ether extraction, and 2 g remained in the electrolyte. The metal obtained by electrolysis weighed 52 g. This was recrystallized 20 times and yielded 35 g of pure crystals and 17 g of uncrystallized metal. Even the latter was sufficiently pure for most purposes, as is shown by the fact that spectrochemically only the following impurities were reported: Indium, moderate; silver, trace; and faint traces of gold,[10] calcium, and lead.

V. RECOVERY OF RESIDUAL GALLIUM

As has already been stated, a certain amount of gallium remains in the acid during ether extractions, some remains in the electrolyte, and some remains as uncrystallized globules in the process of fractional crystallization. The procedure for the recovery of gallium from the acid solutions obtained in the ether separations depends upon the impurities in the original material. If considerable quantities of such elements as zinc, magnesium, manganese, nickel, or cobalt are present, precipitating the gallium with a slight excess of ammonium hydroxide and filtering will eliminate a large proportion of all of these. If elements such as gold, silver, copper, antimony, tin, etc., are present, these are removed by precipitating with hydrogen sulphide and filtering. If indium is the preponderant impurity (as is usually the case), most of it is eliminated by precipitating it with an excess of sodium hydroxide and filtering. If the amount of indium is large, the precipitate should be dissolved and the precipitation and filtration repeated. After the preliminary separations of the impurities

[10] Derived from the dish in which the electrolysis was made.

have been made as indicated, the gallium is converted to the chloride, which is then ready for purification by the procedure already described. The volumes of the solutions at the various stages are kept proportionately smaller in accordance with the quantity of gallium. Usually it is more convenient to set these solutions aside and add them to the hydrochloric acid solution of the next portion of gallium to be purified.

The gallium in the electrolyte is recovered by acidifying the solution, precipitating with a slight excess of ammonium hydroxide, and filtering. The precipitate is washed with hot water and dissolved in hydrochloric acid. The solution needs no further purification and may be electrolyzed as described in the procedure but in a correspondingly smaller volume. In practice, it is usually set aside and added to the next portion of solution that is to be electrolyzed.

The uncrystallized globules may be united and partially purified by fractional crystallization, or they may be dissolved and again put through the whole process of purification.

Acknowledgment is made to F. J. Bates for furnishing the gallium with which the work was done, to B. F. Scribner for making the spectrochemical tests, and to G. E. F. Lundell for much helpful advice.

WASHINGTON, September 7, 1934.

U.S. DEPARTMENT OF COMMERCE NATIONAL BUREAU OF STANDARDS

RESEARCH PAPER RP735

Part of Journal of Research of the National Bureau of Standards, Volume 13, November 1934

FREEZING POINT OF GALLIUM

By Wm. F. Roeser and James I. Hoffman

ABSTRACT

The temperature of equilibrium between liquid and solid gallium was found to be 29.780±0.005° C. Four determinations on two different lots of metal all yielded the same result. Difficulties ascribed to the undercooling and low thermal conductivity of the gallium prevented a satisfactory determination from ordinary heating and cooling curves. The temperature of equilibrium between the liquid and solid phases of the metal was obtained by measuring the temperature of an intimate mixture of the solid and the liquid. It was found that the presence of the oxide did not affect the freezing temperature, indicating that the oxide is not appreciably soluble in the metal.

CONTENTS

	Page
I. Introduction	673
II. Present work	674
1. Preliminary discussion	674
2. Procedure	674
3. Results	675
III. Summary of previous work	676

I. INTRODUCTION

The preparation by one of the authors [1] of a considerable quantity of gallium of exceptional purity afforded an opportunity of determining the melting or freezing temperature of this metal. Variations in the values previously determined suggest that impure metal was used in some of these cases, or that experimental difficulties have resulted in errors many times larger than those which can be ascribed to temperature measurements.

The usual method of determining the temperature of equilibrium between the liquid and solid phases of a metal is to immerse the actuating element of a thermometric device in the material and use the absorption or evolution of heat as a criterion of the change in state. However, in reviewing the literature only one determination [2] was found in which this method was used. In this case, the bulb of a liquid-in-glass thermometer was immersed in the gallium and the melting temperature obtained by running heating curves. In the other determinations, the temperature of a bath was measured at the time a sample of the metal in the bath was observed to melt, or at the time melting or freezing was indicated by the contraction or expansion of the metal in a dilatometer.

[1] J. Research NBS 13,665(1934)RP734.
[2] T. W. Richards and S. Boyer, J. Am. Chem. Soc. 43,274(1921)

II. PRESENT WORK

1. PRELIMINARY DISCUSSION

In the present work it was found that the usual method of determining the freezing temperature from time-temperature cooling curves did not give satisfactory results. The difficulties encountered in these attempts to obtain the freezing temperature from cooling curves are ascribed to the extreme undercooling and apparently low thermal conductivity of gallium. In running an ordinary cooling curve the liquid gallium undercooled [3] as much as 15° C. When the liquid gallium was brought to a temperature below its freezing point and crystallization was started by adding a crystal of the pure metal, freezing proceeded slowly from the added solid, while the liquid apparently remained in an undercooled state. The temperature in various parts of the liquid depended upon the distance from the solid and upon the temperature of the bath. Similar difficulties may account for the fact that no determinations using cooling curves were found in the literature.

No attempt was made to obtain heating curves as it was believed that they would not have given very satisfactory results because of the apparently low thermal conductivity of gallium.

2. PROCEDURE

The procedure followed in the present work was only slightly different from the usual method of running heating and cooling curves. The crystals of gallium were placed in a pyrex-glass tube having an inside diameter of about 1 cm. To prevent the loss of gallium in case the tube should break and to reduce the rate of heat transfer, the pyrex tube was placed inside a slightly larger glass tube. After the gallium was melted, the assembly was placed in a stirred water bath controlled at a temperature of about 29.5° C. Crystallization was started by adding several crystals of gallium which were stirred into the liquid. A five-junction copper-constantan thermocouple, protected by a small thin-wall pyrex-glass tube, was immersed in the gallium to the desired depth and held in place by means of corks. The temperature of the bath was maintained below the freezing point until about one-half of the metal was frozen. The emf of the thermocouple in the gallium was then measured both when the bath was adjusted to the same temperature as that of the gallium and as the temperature of the bath was varied above and below that of the gallium. It was found that the temperature of the gallium was constant to 0.0005° C (the precision of the measurements) while the temperature of the bath was raised and lowered nearly a tenth of a degree above and below the temperature of the gallium. The temperature of the bath was maintained both above and below the freezing temperature for at least an hour without any change in the temperature of the metal. This constant temperature was taken as the temperature of equilibrium between liquid and solid gallium.

The temperature corresponding to the observed emf of the thermocouple at the freezing point was determined after each series of measure-

[3] This is not in agreement with the statement "It was found that gallium when quite pure shows little of the tendency toward supercooling which is so characteristic of impure gallium", by W. M. Craig and G. W. Drake, J. Am. Chem. Soc. 56,584(1934).

ments. The thermocouple was placed in the bath which was completely surrounded by a thermostated water jacket, and the temperature adjusted until the thermocouple yielded the same emf as obtained when immersed in the gallium during freezing and melting. The temperature of the bath, and consequently the freezing point of the gallium, was then measured with a standard platinum resistance thermometer. The freezing temperature was thus referred to the international temperature scale. We are indebted to R. S. Jessup for the calorimeter used as a bath and for assistance in controlling and measuring the temperatures.

The first two determinations were made on a 15-g portion of gallium prepared from crude metal from Bartlesville, Okla. During the first determination, no precautions were taken to prevent the metal from oxidizing, and consequently an appreciable amount of oxide was present. The second determination was made on the same lot of metal after the oxide had been removed. The oxide was dissolved by shaking the molten metal in the glass tube with dilute hydrochloric acid. As soon as the metal appeared clean and bright, the acid was decanted and replaced by recently boiled water. The protecting layer of water which contained a trace of acid prevented oxidation of the metal during the determination.

In order to ascertain whether the heat of reaction between the trace of acid remaining in the protecting solution and the gallium had an appreciable effect on the temperature measurement, the difference between the temperature of the bath and that of the liquid metal covered with the protecting solution was measured when the bath was maintained at a constant temperature above the freezing point of the gallium. The temperature of the metal under these conditions was less than 0.003° C higher than that of the bath.

The other two determinations were made on a 35-g portion of gallium in order to obtain a greater depth of immersion of the thermocouple. This metal was prepared from impure gallium originating from many different sources. The first determination was made after the oxide had been removed from the metal with hydrochloric acid as previously described, and the other on the same metal after removing the oxide and then replacing the hydrochloric acid with liquid petrolatum.

3. RESULTS

Each of the 4 separate determinations on the 2 different lots of metal yielded the same result, 29.780° C, for the temperature of equilibrium between liquid and solid gallium. The uncertainty in this determination is believed to be not greater than ± 0.005° C. The fact that the presence of oxide did not affect the results indicates that the oxide is insoluble in the metal.

It is estimated that the gallium on which these determinations were made contained less than 0.001 percent of impurities. The preparation and purity are discussed elsewhere in this journal, Research Paper RP 734. Spectrochemical tests indicated that no contamination occurred during the freezing point determinations.

III. SUMMARY OF PREVIOUS WORK

The various determinations of the melting point of gallium found in the literature together with the value reported in this paper are summarized in table 1.

TABLE 1.—*Determinations of the melting point of gallium*

Author	References	Methods used	Reported values
			°C
Lecoq de Boisbaudran	Compt. rend. **82**, 1036(1876)	Not given	29.5
Do	Compt. rend. **83**, 611(1876)	do	30.15
A. Guntz and W. Broniewski.	Compt. rend. **147**, 1474(1908)	Measured change in specific resistance.	29
P. E. Browning and H. S. Uhler.	Am. J. Sci. **41**, 351(1916)	Observed temperature at which a disk of gallium fell through a platinum ring.	29.5
T. W. Richards and S. Boyer.	J. Am. Chem. Soc. **41**, 133(1919)	Observed crystal at bottom of a test tube or suspended in a ring.	30.8
S. Boyer, reported by P. W. Bridgman.	Contrib. Jeff. Phys. Lab. **14**, 107(1919–20)	Not given	29.85
T. W. Richards and S. Boyer.	J. Am. Chem. Soc. **43**, 274(1921)	Heating curves; thermometer with small Beckmann apparatus.	29.752
Do	J. Am. Chem. Soc. **43**, 274(1921)	Dilatometer	29.75
W. M. Craig and G. W. Drake.	J. Am. Chem. Soc. **56**, 584(1934)	do	29.755
W. F. Roeser and J. I. Hoffman.	Present work	Temperature of equilibrium between solid and liquid.	29.780

WASHINGTON, September 14, 1934.

U.S. DEPARTMENT OF COMMERCE NATIONAL BUREAU OF STANDARDS

RESEARCH PAPER RP736

Part of Journal of Research of the National Bureau of Standards, Volume 13, November 1934

A NOTE ON BACTERICIDAL EFFECTS OF X-RAYS

By Fred L. Mohler and Lauriston S. Taylor

ABSTRACT

The effects of X-rays in liquids are localized in columns of ionization along the path of each high-speed electron. It is assumed that biological effects are produced in these columns and experimental results of Wyckoff and Rivers on killing of colon bacilli by cathode rays and X-rays are expressed in terms of the effective collision area of the column and bacillus for killing. Cathode rays of 155 kv give an area of 0.68×10^{-10} cm². X-rays of wave lengths ranging from 0.56 to 4 A give values between 0.72×10^{-10} and 2.6×10^{-10} cm². As the area of the bacillus is about 10^{-8} cm² passage of a column through the bacillus is in general not fatal. The column must pass through a particular point to cause death.

When an X-ray is absorbed by matter the entire energy of the X-ray quantum is given to a single electron. This high-speed secondary electron traverses the medium and produces a dense path of ion pairs. The energy of the secondary electron is related to the wave length of the X-rays by the quantum relation.

$$V \text{ (electron volts)} = 12340/\lambda \text{ (angstroms)} \qquad (1)$$

The number of ion pairs in air is about $V/35$. The length x of the electron path depends on the density of the medium and is given with fair approximation by the relation

$$x\rho = v^4/.505\times10^{43} \qquad (2)$$

where ρ is the density and v the electron velocity.[1] The path is crooked and the average distance the electron goes is less than x. These general relations should be applicable to liquids and solids as well as gases. In a medium of density one the electron path will be reduced to about one eight-hundredth of its value in air and the ion density will be correspondingly greater. Experiments [2] on the ionization of liquid carbon disulphide by X-rays (effective wave length 0.27 A) have given roughly quantitative information concerning these columns of ionization. The number of ions produced per quantum in the liquid is about the same as in the gaseous phase. The volume ionized by each quantum is equal to a cylinder of length equal to the electron path (3×10^{-3} cm) and of cross section 0.28×10^{-10} cm². This dense column of ionization disappears by recombination in less than a millionth of a second and only a small fraction of the ions diffuse into the surrounding medium.

[1] A. H. Compton, *X-rays and Electrons*, p. 256(1928).
[2] Mohler and Taylor, J. Research NBS 13,659(1934);RP733.

It is attractive to assume that biological effects of X-rays are produced exclusively in these columns of ionization and that the chance of producing a given effect on a cell depends on the chance of a column passing either through the cell or through a particular part of the cell. This view is not new. Wyckoff [3] has discussed his experimental results on destruction of bacteria by X-rays in these terms. His computations are however made on a somewhat different basis. In the following we will treat his results from a purely columnar viewpoint.

Experiments on the destruction of bacteria by cathode rays of 155 kv were made by Wyckoff and Rivers.[4] Separate bacteria spread on a surface of agar were exposed to a beam of cathode rays of measured intensity and the fraction surviving after a time t was determined by counting the clusters developed after an incubation period. They show that this survival ratio is given by the relation

$$A(t)/A_0 = e^{-at} = e^{-bnt} \tag{3}$$

where n is the number of cathode rays per cm^2 per sec and b gives the fraction of bacteria killed per cathode ray and a the fraction per sec. As they point out this exponential relation is consistent with the view that killing depends simply on the cathode ray striking a given area in the bacillus. Consider this area, σ, associated with the cathode ray. Then an area $n\sigma$ is sterilized when n rays pass through the surface and we see that σ is to be identified with the constant b. In their experiments with colon bacilli a current of 1.65×10^9 electrons per sec gave a value of a of 0.112 per sec. Hence $\sigma=0.68\times10^{-10}$ cm^2. Their experiments with *Bacillus aertryke* gave an identical effective area. *Staphylococcus aureus* gave an area half as great. The colon bacillus is a rod about 2×10^{-4} cm long and 0.5×10^{-4} cm in diameter and hence has a cross section of about 10^{-8} cm^2 in any direction. The fatal area is very much smaller than the area of the bacillus.

Wyckoff [5] carried out comparable experiments on the destruction of colon bacilli by X-rays of different wave lengths. The X-rays were predominantly the characteristic radiations listed in table 1. The experimental data are the air ionization in roentgens per sec and the constant a of eq 3 determined from measurements of survival ratios. The energy of the secondary electrons in electron volts (eq 1) divided by 35 gives the number of ion pairs produced per quantum, and from the measured air ionization one derives the number of quanta absorbed in air per cm^3 per sec. The rate of absorption of quanta and production of columns, n, in the agar is taken to be 780 times this. The volume sterilized by each column is σx where x is given by eq 2 and $n\sigma x$ is the volume sterilized per sec which is equated to the constant a of eq 3. The last column of table 1 gives the computed values of σ for the different radiations. The physical basis for these computations becomes uncertain for the longest wave lengths since eq 2 giving the range x has not been tested in this range.

[3] Wyckoff, J. Exp. Med., 52,769(1930).
[4] Wyckoff and Rivers, J. Exp. Med., 51,921(1930).
[5] Wyckoff, J. Exp. Med., 52,435(1930).

TABLE 1.—*Killing of colon bacilli by X-rays*

Radiation	λ(A)	Energy of electrons	Range of electrons	Quanta absorbed in agar	Rate of killing (a)	Effective areea σ
		kv	*cm*	*Per sec per cm³*		*cm²*
AgK	0.564	22	1.2×10^{-3}	1.9×10^{11}	0.0174	0.76×10^{-10}
MoK	.710	17.4	$.75 \times 10^{-3}$	3.1×10^{11}	.0167	$.72 \times 10^{-10}$
CuK	1.537	8.0	1.6×10^{-4}	12.4×10^{11}	.0370	1.9×10^{-10}
CrK	2.29	5.4	$.72 \times 10^{-4}$	29×10^{11}	.0413	2.0×10^{-10}
AgL	3.98	3.1	2.4×10^{-5}	25×10^{11}	.0159	2.6×10^{-10}
Cathode rays		155	1.8×10^{-2}			$.68 \times 10^{-10}$

The important conclusion from these computations is that the effective area is nearly the same for cathode rays and secondary electrons produced by X-rays and that this area is very much smaller than the cross section of a bacillus. On the view that there is a sensitive spot in the bacillus through which the column of ionization must pass, the effective area may be expressed as

$$\sigma = \pi (a_1 + a_2)^2$$

where a_1 is the radius of the column and a_2 the radius of the spot. The experimental values of σ are of the same magnitude as the cross section of the column of ionization computed for the particular case of carbon disulphide ionized by X-rays. If the columns in agar are of comparable size the area of the hypothetical spot may be indefinitely less than σ.

Wyckoff has expressed the effectiveness of both cathode rays and X-rays in terms of the fraction absorbed by a single bacillus. From a purely columnar viewpoint the absorption does not enter at all in evaluating the effectiveness of cathode rays; while in the case of X-rays it is the absorption coefficient of the bacillus and of the surrounding medium which is significant. It is to be emphasized that in the present state of knowledge there is little question of right or wrong in either viewpoint.

The density of ionization in a column decreases with increasing speed of the electron and is nearly 15 times as great for the AgL secondaries as for the 155 kv cathode rays. If the effectiveness of X-rays depended solely on the volume of the columns of ionization then σ would remain constant and the effect per roentgen would decrease with increasing wave lengths. For Wyckoff's experimental data the values of σ increase somewhat with increasing wave length and the effect per roentgen decreases but not as much as for a pure volume effect. It is doubtful whether this variation in σ is significant and it is certain that no general conclusion as to biological effectiveness of X-rays can be drawn from a single series of experiments.

Although σ may be expected to vary with the biological material and the quality of the radiation, nevertheless the columnar viewpoint seems to offer a logical starting point for theory. The known physical effects of X-rays in liquids and solids are limited to the columns of ionization produced by high-speed electrons. The numerical value of σ is a convenient expression for the bactericidal effectiveness of the columns whether or not one takes the view that killing depends on striking a certain spot in the cell.

WASHINGTON, September 13, 1934.

U.S. DEPARTMENT OF COMMERCE NATIONAL BUREAU OF STANDARDS

RESEARCH PAPER RP737

Part of Journal of Research of the National Bureau of Standards, Volume 13, November 1934

GOLD-CHROMIUM RESISTANCE ALLOYS

By James L. Thomas

ABSTRACT

The addition of from 1.6 to 2.4 percent or more of chromium to gold produces alloys having very small temperature coefficients of electrical resistance. In particular, 2.1 percent of chromium in gold gives an alloy whose resistance has been made independent of temperature, to a few parts in 10 million, in at least the interval 20 to 30° C. These alloys are also exceptionally stable in resistance. They, however, have a thermoelectric power against copper which is 3 or 4 times as large as that of manganin. The preparation and heat treatment of some of these alloys are described.

CONTENTS

	Page
I. Introduction	681
II. Preparation of gold-chromium alloys	682
III. Properties of the alloys	682
1. Temperature coefficient of resistance	682
2. Stability	685
3. Miscellaneous properties	687
IV. Conclusions	688

I. INTRODUCTION

The electrical characteristics of alloys of gold with small amounts of other metals has recently been investigated by Linde.[1] As part of this investigation he prepared an alloy having 2 percent of chromium by weight and found it to have a zero temperature coefficient of resistance at about −50° C, and a slightly lower resistance at 100° C than at −50° C. These results suggested that a slightly smaller amount of chromium added to the gold might give a zero temperature coefficient of resistance at room temperatures.

An investigation of the electrical properties of pure metals [2] has shown that pure gold is very stable in electrical resistance. It was thought that the addition of a small amount of chromium would have little effect upon this stability. To test this, several alloys were prepared, and the preliminary data indicated that they were very stable in resistance. It also was found possible to choose the composition and heat treatment so as to obtain a practically zero temperature coefficient of resistance.

[1] J. O. Linde, Annalen der Physik **402**,52(1931); **407**,219(1932).
[2] J. L. Thomas, BS J.Research **12**,313(1934);RP657.

II. PREPARATION OF GOLD-CHROMIUM ALLOYS

No information seemed to be available as to the proper technique to be employed in alloying chromium with gold. Preliminary attempts to prepare the alloys in a vacuum or in an atmosphere of dry hydrogen were not very successful. However, it was found that they could be very readily prepared by melting the gold and chromium together in graphite crucibles, under a heavy coating of borax. The graphite crucibles were heated by means of an induction furnace. When at a temperature of about 1,200° C the alloys were poured into graphite molds.

The ingots were first hot-forged into the form of rods 5 or 6 mm square. They were then cold-rolled and swaged to a diameter of 0.75 mm, after which they were drawn down to the required size through sapphire dies. The material was annealed 4 or 5 times during the rolling and swaging, but the wire was not annealed during the drawing.

Nine of these gold-chromium alloys were prepared and investigated. They contained from 1.6 to 2.5 percent of chromium by weight, as shown by chemical analyses. With 30 grams of gold it was found that there was a loss of nearly one-fifth of the chromium in the melting. The characteristics of these alloys are given in the following sections.

III. PROPERTIES OF THE ALLOYS

1. TEMPERATURE COEFFICIENT OF RESISTANCE

For these gold-chromium alloys the relation between resistance and temperature in the interval 20 to 30° C was found to be represented with sufficient accuracy by the equation:

$$R_t = R_{25}\,[1+\alpha\,(t-25)+\beta\,(t-25)^2]$$

where R_t is the resistance at t° C and R_{25} is the resistance at 25° C. Both α and β were found to be functions of the percentage of chromium, but the magnitude of α could be changed by baking at comparatively low temperatures.

The dependence of α upon the composition and the annealing is shown in figure 1. The percentages of chromium by weight were plotted as abscissas, while the values of α in the interval 20 to 30 °C were plotted as ordinates. The upper curve is for hard-drawn wire, while the lower is for wire annealed[3] in vacuo at about 500° C.

These curves suggested that a zero value for α could be obtained in either of two ways. An alloy could be prepared which contained 1.8 percent chromium by weight and annealed at 500° C, or an alloy containing more chromium could be prepared and annealed at a lower temperature. This latter procedure was tried experimentally. A 10-ohm coil of the hard-drawn wire containing 2.35 percent chromium was baked in air at 150° C for several days. The resistance and value of α were measured at frequent intervals during this baking. The results obtained are shown by figure 2. From this figure it was found that α could be made as small as was desired by properly choosing the amount of baking at 150° C. Actually this coil was baked until

[3] This annealing was done in an evacuated quartz-tube furnace. About 1½ hours were required to raise the temperature to 500° C, after which the heating current was cut off and approximately the same length of time was required for the furnace to cool.

α was made slightly negative. It was sealed in a container filled with oil, and is 10-ohm coil no. 23 for which data are given later.

Figure 2 also shows the effect of baking upon the resistance of this coil. The resistance of the coil increased as a result of the baking, while the value of α decreased. There was a linear relation between

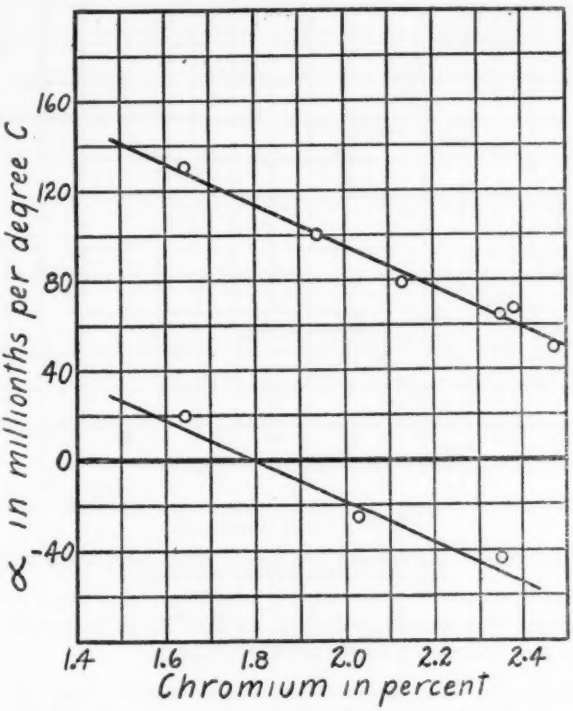

FIGURE 1.—*Values of α for gold-chromium alloys.*

Upper curve is for hard-drawn wire, while lower curve is for wire annealed in vacuo at 500° C.

the change in the resistance and the change in the value of α. A change of 1 percent in the resistance was accompanied by a change of 26 parts per million per degree C in α. This relation facilitated the adjustment of α to a zero value. The changes in resistance were comparatively large, and could be very readily measured, so the magnitude of α could be adjusted with a comparatively few determinations of its value.

In order to see whether the value of β was dependent upon the amount of chromium, 5 of the alloys were drawn down into wire 0.43 mm in diameter. After measuring the resistivity, 10-ohm coils were constructed from these wires and baked for a sufficient time to make α fairly small. The values of β were then determined in the interval 20 to 30° C, and plotted against the chromium content as shown in figure 3. They were again baked so as to change the values of α by small amounts. No measurable change in the β's resulted from this second baking.

From this curve it was evident that a gold-chromium alloy having about 2.1 percent of chromium would have a zero value for β, that is

to say, the temperature-resistance curve would be linear. With the proper baking the value of α, i.e., the slope of the temperature-resistance curve, could be made zero at least in the interval 20 to 30° C.

One of the alloys had a chromium content which was very nearly 2.1 percent. It was therefore investigated in detail. A 10-ohm coil

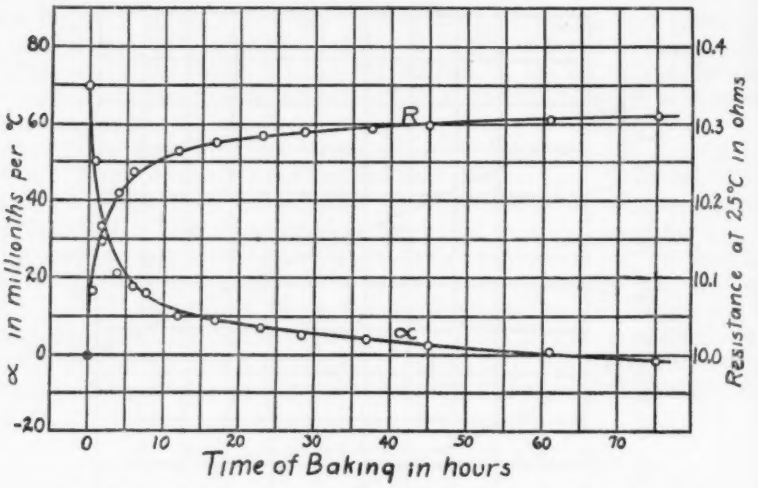

FIGURE 2.—*Effects of baking at 150°C upon gold-chromium alloys containing 2.35 percent chromium.*

Curve R shows how the resistance increased with time of baking, while the temperature coefficient decreased, as shown by curve marked α.

of this material was carefully baked at 200° C to bring its value of α to zero, and the following data were obtained:

Temperature	Resistance
°C.	
20	9.99561_2
22.5	9.99561_2
25	9.99561_1
27.5	9.99561_0
30	9.99561_1

Within the limits of error of the resistance measurements (a few parts in 10^7), the resistance of this coil was independent of temperature throughout the entire interval of 20 to 30° C. With manganin a minimum variation of about 10 parts per million would have been expected in this temperature interval, which is nearly 100 times that reported above. It might be pointed out that the copper lead wires contributed somewhat to the temperature coefficient of this coil. This means that for the resistance material alone, the value of α is slightly negative.

Two 100-ohm coils were made from the same melt, of wire drawn down to a diameter of 0.2 mm. Each of these 100-ohm coils required between 9 and 10 meters of wire, that is, about 6 g of the alloy.

Although the value of α was not as accurately adjusted as for the above-described 10-ohm coil, no measurable curvature was found in the temperature-resistance curves. This indicated that the magnitude of β did not depend upon the size of the wire, but only upon the chromium content.

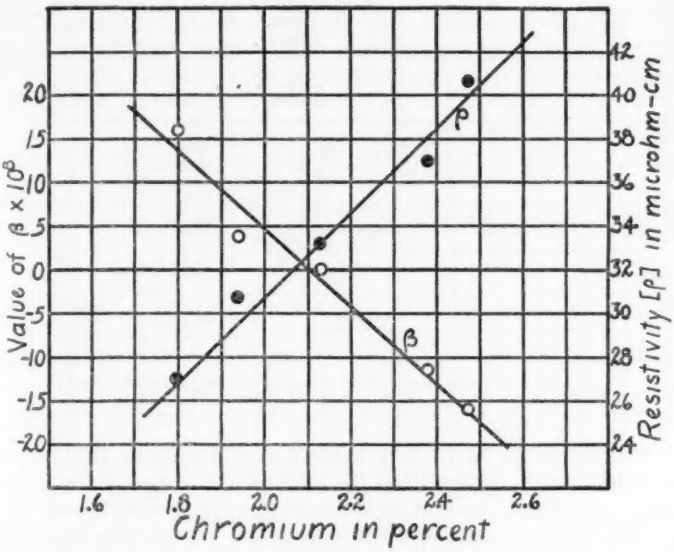

FIGURE 3.—*Resistivity and curvature of temperature-resistance curves for gold-chromium alloys.*

Curves for which β is positive are concave upward, while if β is negative they are concave downward.

2. STABILITY

Tests of the stability of these alloys were started before the best composition from the viewpoint of temperature coefficient had been determined. Two compositions were investigated, one having more and the other less chromium than 2.1 percent. While it will require a number of years to fully test the stability of these gold-chromium resistance alloys, the results so far obtained are remarkably promising. Table 1 shows the data obtained for four resistance standards. The coils were wound with bare wire on silk-covered brass tubes, spaced with silk thread, shellacked and baked in air at comparatively low temperatures and mounted in oil-filled containers of the Rosa [4] type.

TABLE 1.—*Data on resistance standards*

Items	No. 3938	No. 3937	No. 23	No. 3936
Percent chromium	1.64	2.35	2.35	2.35
Baking temperature, °C	140	150	150	140
Time of baking (hours)	67	21	138	20
α in millionths/°C	45	2	−4	−4

[4] E. B. Rosa, BS Sci. Pap. **107** (1908).

TABLE 1.—*Data on resistance standards*—Continued

RESISTANCE AT 25° C. IN OHMS

Date	No. 3938	No. 3937	No. 23	No. 3936
Jan. 22, 1934	9.99564			
Jan. 23, 1934	9.99564			
Jan. 24, 1934	9.99563			
Jan. 26, 1934	9.99563			
Jan. 30, 1934	9.99563			
Feb. 5, 1934	9.99564			
Feb. 8, 1934	9.99564	9.99550		
Feb. 14, 1934				99.9533
Feb. 15, 1934				99.9534
Feb. 16, 1934		9.99550		99.9534
Feb. 19, 1934	9.99564	9.99550		99.9534
Mar. 1, 1934	9.99563	9.99549		99.9534
Mar. 6, 1934	9.99564	9.99550		99.9535
Mar. 19, 1934	9.99563	9.99552	9.99540	99.9535
Mar. 22, 1934	9.99564	9.99551	9.99543	99.9535
Mar. 23, 1934		9.99550	9.99544	99.9535
Mar. 26, 1934		9.99551	9.99545	99.9535
Apr. 3, 1934	9.99564	9.99549	9.99544	99.9534
Apr. 17, 1934		9.99549	9.99543	99.9535
May 25, 1934	9.99564	9.99551	9.99542	99.9535
July 20, 1934	9.99564	9.99547	9.99541	99.9534

The resistances given in this table are in terms of the Washington unit as maintained since 1910 by means of a group of ten 1-ohm manganin standards. The resistances were determined by comparing with 10-ohm or 100-ohm manganin standards which in turn were occasionally compared with the reference group of 1-ohm standards. These 10- and 100-ohm standards were not entirely constant in resistance between comparisons with the reference group. Some of the changes in the values obtained for the resistances of the gold-chromium coils could be attributed to changes in the secondary manganin standards.

In considering the stability of these new alloys one must bear in mind the fact that the coils were baked at fairly low temperatures, and that they were mounted in oil-filled containers of the Rosa type. No other resistance material is known which will give a comparable stability when the coils are baked and mounted in this way, although 1-ohm manganin standards give a similar performance when coils of large-sized wire are annealed at 550° C and mounted in double-walled containers.[5]

In order to compare the stability of the gold-chromium alloys with that of manganin, the data from the preceding table are plotted in figure 4, together with typical curves obtained for manganin 10- and 100-ohm standards. The gold-chromium coils were constructed with bare wire wound on silk-insulated brass tubes, while double-silk-covered manganin wire was used. For all the curves the time is plotted beginning with the first measurements immediately after baking.

When manganin is used in the construction of resistance standards, the coils are usually kept for a year or more after they are baked in order to reach a reasonably stable condition. In the case of the coils made of gold-chromium alloys, this aging appeared to be

[5] J. L. Thomas, BS. J. Research 5, 295(1930); RP201.

unnecessary. While it does not necessarily follow from this that the gold-chromium alloys will be stable in resistance over long periods of time, it is to be expected.

3. MISCELLANEOUS PROPERTIES

All the gold-chromium alloys were very easy to work into wire. While no hardness tests were made, all of these alloys seemed to be comparable with pure gold. The chromium oxidized slightly on the surface when the ingots were annealed and this oxide was removed

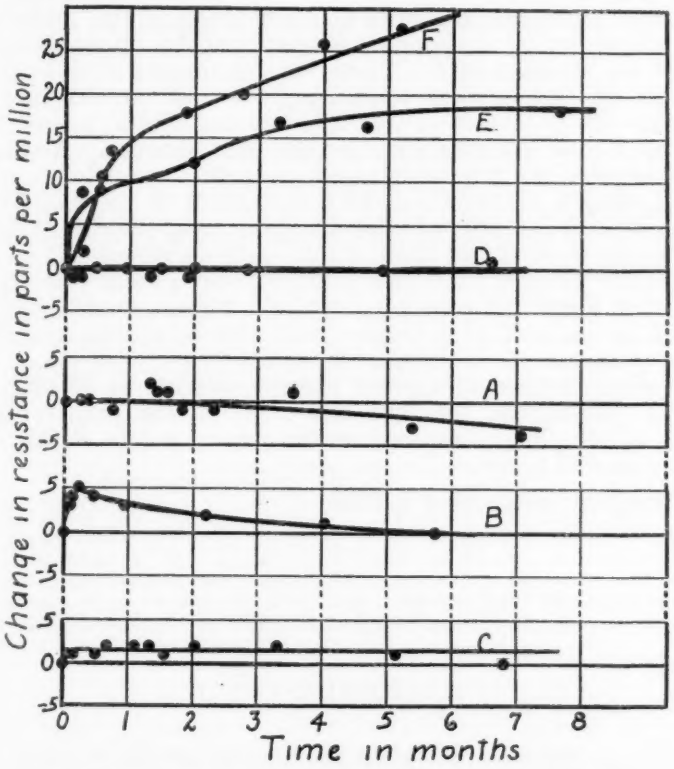

FIGURE 4.—*Stability of gold-chromium resistance alloys.*

Curve A for 10-ohm coil no. 3837; curve B for 10-ohm coil no. 23; curve C for 100-ohm coil no. 3936; curve D for 10-ohm coil no. 3938; curve E for 10-ohm manganin coil baked at 120° C; and curve F for 100-ohm manganin coil baked at 140° C.

by pickling in aqua-regia. Little hot working was required and the material was worked cold after a little initial forging.

The thermoelectromotive force of these gold-chromium alloys against copper was 7 or 8 microvolts per degree C at 25° C, as compared with 2 or 3 microvolts per degree C for manganin against copper. This, however, did not prevent the resistance of the coils from being measured to parts in a million when immersed in a well-stirred oil bath. It would be more troublesome in low-resistance coils, but the cost of the material probably precludes its use in constructing such coils.

The resistivity of the 2.13-percent alloy was found to be about 15 times that of pure gold at 20° C. Its value is 33 microhm-cm as compared with about 45 microhm-cm for manganin. The curve marked ρ in figure 3 shows how the resistivity depends upon the percentage of chromium.

IV. CONCLUSIONS

In the preceding sections it has been shown that the addition of 2.1 percent by weight of chromium to gold produced an alloy having exceptional electrical characteristics. By baking at comparatively low temperatures the resistance of a coil made of this material was made independent of temperature over at least the interval 20 to 30° C.

While the stability of the 2.1-percent chromium alloy or the stability of its temperature coefficient was not investigated, coils made from alloys containing slightly more and slightly less chromium appeared to be exceptionally stable in resistance. A thorough investigation of the 2.1-percent alloy is to be made.

In choosing a material for the construction of standards for the maintenance of the unit of resistance, the most important factor is undoubtedly that of stability. If the gold-chromium alloys are as stable as the preliminary results indicate, they should yield valuable information about the constancy of the manganin standards used in maintaining the unit of resistance, and may even replace manganin for this purpose.

The author wishes to express his appreciation to W. F. Roeser and J. G. Thompson for their assistance in the preparation and working of the alloys described in this paper, and to R. M. Fowler for the chemical analyses.

WASHINGTON, September 5, 1934.

U.S. DEPARTMENT OF COMMERCE NATIONAL BUREAU OF STANDARDS

RESEARCH PAPER RP738

Part of Journal of Research of the National Bureau of Standards, Volume 13, November 1934

RESISTIVITY OF SULPHURIC-ACID SOLUTIONS AND ITS RELATION TO VISCOSITY AND TEMPERATURE

By George W. Vinal and D. Norman Craig

ABSTRACT

The resistivity of sulphuric-acid solutions ranging from 15 to 45 percent acid has been measured at temperatures of +30 to −40° C, except as the measurements of some solutions were limited by their freezing points. The resistivity of these solutions at 0° C is about 1.7 times that at +30° C, but at −40° C the resistivity is 5.5 times as great. The composition of solutions having minimum resistivity (maximum conductivity) was found to depend on the temperature. At 18 °C the solution having minimum resistivity was found to be 30.4 percent, as previously determined by Kohlrausch, but at −25° C the solution of minimum resistivity contains only 26.5 percent acid. Values of resistivity for each interval of 5 percent in composition and 5° C in temperature are given. An empirical relation between resistivity, kinematic viscosity, and absolute temperature was found to hold for concentrated solutions over a temperature range from +30 to −40° C.

CONTENTS

		Page
I.	Introduction	689
II.	The apparatus	690
III.	Experimental results	692
IV.	Solutions having minimum resistivity	693
V.	Relation between resistivity, kinematic viscosity, and temperature	695
VI.	Comparison with previous determinations	697
VII.	Accuracy of the measurements	697

I. INTRODUCTION

In a paper [1] on the viscosity of sulphuric-acid solutions it was stated that both resistivity and viscosity of battery electrolytes are important factors in determining the amount of electrical energy which can be delivered by a battery under specified conditions of temperature and rate of discharge. Storage batteries are now used under such widely differing temperature conditions that an extension of our knowledge of the basic properties of sulphuric-acid solutions became necessary. In the viscosity paper, measurements on solutions ranging in concentration from 10 to 50 percent H_2SO_4 were reported for temperatures between +30 and −50° C. The present paper reports resistivities of similar solutions between +30 and −40° C, insofar as the temperatures are above the freezing points of the solutions.

[1] Vinal and Craig, BS J.Research **10**,781(1933);RP566. We shall have occasion to refer to this paper frequently and it will be called the "viscosity paper", without further specific reference.

We have chosen to express the results as resistivities rather than as conductivities, because the resistivity of the solutions is more conveniently used in engineering problems. Corresponding conductivities can be calculated readily by taking reciprocals of the values for resistivity.

Data previously available for conductivity and resistivity of sulphuric-acid solutions have served as a basis for values reported in the International Critical Tables,[2] but no data for the resistivity of sulphuric-acid solutions below 0° C have been found. In a later section of the present paper comparison is made between our determinations and the data which are given in the International Critical Tables. Such a comparison is limited, however, to few values, since our work covered relatively concentrated solutions at low temperatures, while previous work was confined for the most part to measurements of dilute solutions at higher temperatures.

Much of the apparatus for controlling and measuring the temperature of the condutivity cells was the same as that described in the viscosity paper. For many details of the present work, reference is made to that paper, the results of the resistivity measurements being presented as briefly as possible.

II. THE APPARATUS

Two conductivity cells, similar in design to the Washburn type C cells, were employed. The electrodes in these cells were platinized platinum, about 1.5 cm in diameter. The small size of electrodes in our cells was made possible by the use of a two-stage amplifier in the detector circuit. This arrangement afforded ample sensitivity, although the current through the cells was very small. The heating effect of the test current was negligible.

We employed a Parker solution[3] of 76.627_6 g of purified potassium chloride per kilogram of distilled water to determine the constants of the cells. Five determinations at 25° C were made on each cell and a correction of 0.01 ohm was made for the leads. This correction was calculated and subsequently verified by filling the cells with mercury. The mean values of the constants were found to be:

Cell no. 1	73.37_3
Cell no. 2	17.64_8

Since the constant for cell no. 1 is more than four times that of cell no. 2 measurements were made to show that these cells gave concordant results when measuring a particular solution of sulphuric acid over a wide range of temperatures. The ratio of the observed resistance with the two cells is given in table 1. The agreement of results obtained is within 0.1 percent on the average.

[2] International Critical Tables 6,241(1929).
[3] International Critical Tables 6,230(1929).

TABLE 1.—*Comparison of measurements with cells, nos. 1 and 2*

Temperature	Solution	Ratio of resistance—cell 1:cell 2	Difference from KCl ratio	Differences
°C	*Percent*			*Percent*
25	KCl (Parker)	4.158		
30	H_2SO_4 31.22	4.153	0.005	−0.12
25	H_2SO_4 31.22	4.158	.000	0.00
20	H_2SO_4 31.22	4.156	.002	−0.05
18	H_2SO_4 31.22	4.155	.003	−0.07
15	H_2SO_4 31.22	4.151	.007	−0.17
10	H_2SO_4 31.22	4.156	.002	−0.05
5	H_2SO_4 31.22	4.166	.008	+0.19
0	H_2SO_4 31.22	4.163	.005	+0.12
15	H_2SO_4 29.52	4.159	.001	+0.02
10	H_2SO_4 29.52	4.157	.001	−0.02
5	H_2SO_4 29.52	4.158	.000	0.00
Average				±0.07

The change with temperature in the constant for type C cells has been calculated to be less than 0.02 percent at 0° C on the basis of data given by Washburn.[4] At −40° C this error should not amount to more than 0.05 percent. No corrections for change in cell constant have been necessary in calculating our results.

The bridge which was employed in making the measurements was designed particularly for measuring the resistance of storage-battery separators and will be described in detail in a forthcoming publication on that subject. Briefly, it consisted of two equal ratio arms having resistances of 10 ohms. Precision resistance coils were used in these arms. The third arm of the bridge included a decade resistance box having 0.1-ohm steps in the last dial. The fourth arm included the conductivity cell. Between the resistance box and the cell was a slide wire about 50 cm long having a resistance of slightly more than 0.05 ohm. The test current for the bridge was supplied by a 1,000-cycle oscillator and the detector circuit included a two-stage audio amplifier.

The bridge was balanced approximately by moving a contact of the detector circuit along the slide wire. Then the adjustment of a small mutual inductance, which coupled the telephone detector circuit to the bridge circuit, permitted balancing any out-of-phase component of potential difference in the bridge. Following this, the contact to the slide wire was again moved until the final balance of the bridge was obtained. For this very satisfactory device for balancing the bridge the authors are indebted to Dr. F. Wenner of this Bureau. Details of it have been published by him.[5] Settings of the bridge could be made and repeated to within 0.1 percent.

The temperature control for the conductivity cells was similar to that described in the viscosity paper. It is unnecessary to describe it further. No attempt was made to carry the resistivity measurements to as low temperatures as those in the viscosity work because the mercury contacts of the cells would have frozen.

[4] J. Am. Chem. Soc. **38**, 2455(1916).
[5] BS J. Research **5**,714(1930);RP223.

III. EXPERIMENTAL RESULTS

The composition of each solution was determined by titrating 2 weighed portions.

The concentration of acid was then expressed as the percentage of H_2SO_4. The percentages so obtained were 14.68, 21.41, 28.13, 29.52, 30.43, 31.22, 33.89, 40.17, and 45.45. As a check on these determinations, the specific gravity of each solution was measured with calibrated hydrometers which could be read to 0.0005. From these measurements the percentage of H_2SO_4 was calculated by using data in the International Critical Tables. The average difference between the results of the titrations and the specific-gravity measurements was less than 0.1 percent of sulphuric acid, excepting the one case of 45.45 percent acid for which the difference amounted to 0.2 percent. The results given in this paper are based entirely on the values determined by titration.

Some of these solutions are the same as those used for the viscosity determinations, but we have added three solutions in the middle range, since the percent composition of solutions having minimum resistivity changes with temperature.

Experimental curves showing the relation between the measured resistance of the cell (85 to 650 ohms for cell no. 1 and 25 to 90 ohms for cell no. 2) and the temperature were plotted on a large scale, but the curvature made it difficult to interpolate values with the accuracy which we desired. We resorted, therefore, to a plot similar to that of figure 3 of the viscosity paper. After several trials it was found that plotting the function $\frac{1}{\log\ (6 \times \text{resistivity})}$ against the temperature yielded a nearly linear relation throughout the range of temperature from +30 to −40° C. Interpolation and, in a few cases, extrapolation over a few degrees could be accomplished easily and accurately. Individual points which were plotted were in some cases the mean result of as many as 6 or 8 determinations. After reading from the curves the values of $\frac{1}{\log\ (6 \times \text{resistivity})}$ for each 5-degree interval, isothermal curves were plotted for the logarithmic function against percentage composition of the acid. These curves, however, could not be used as advantageously for determining resistivities at even percentages of the acid as when the resistivities, calculated from the values of the function were plotted. The curves of the logarithmic function against percent composition had one great advantage, however, in determining the points of minimum resistivity since the curvature is accentuated in this region.

We have used both sets of curves, that is, resistivity against percent composition and the logarithmic function against percent composition, in determining the values for resistivity of sulphuric-acid solutions given in table 2. One set of curves has been used as a check on the other. In no case was any large discrepancy noted between the results from the two curves, but we have given the greater weight to determinations based on the plot of resistivity against percent composition, because the curvature of these is less than for the others.

Table 2 gives the complete results of our measurements. In rounding off values, we have followed the same rule as in the viscosity determinations, that is, four significant figures are given for values

less than 2.500 which are at or above 0° C. Three figures are given for the remainder.

TABLE 2.—*Resistivity of sulphuric-acid solutions*

Temperature	15 percent	20 percent	25 percent	30 percent	35 percent	40 percent	45 percent
°C	ohm-cm	ohm-cm	ohm-cm	ohm-cm	ohm-cm	ohm-cm	ohm-cm
+30	1.596	1.313	1.180	1.131	1.140	1.203	1.312
25	1.689	1.396	1.261	1.214	1.231	1.301	1.422
20	1.800	1.494	1.357	1.311	1.334	1.415	1.549
18	1.852	1.541	1.401	1.355	1.380	1.467	1.608
15	1.932	1.613	1.470	1.426	1.454	1.549	1.702
10	2.090	1.755	1.606	1.563	1.602	1.710	1.885
5	2.279	1.922	1.768	1.727	1.782	1.906	2.104
0	2.51	2.128	1.961	1.930	1.998	2.146	2.371
−5	2.79	2.38	2.20	2.18	2.27	2.44	2.70
−10	----------	2.69	2.50	2.49	2.60	2.81	3.10
−15	----------	----------	2.87	2.88	3.01	3.27	3.63
−20	----------	----------	3.35	3.39	3.57	3.86	4.31
−25	----------	----------	----------	4.09	4.32	4.65	5.21
−30	----------	----------	----------	5.00	5.29	5.73	6.35
−35	----------	----------	----------	6.20	6.59	7.18	7.90
−40	----------	----------	----------	----------	8.39	9.09	9.89

Figure 1 shows the results graphically and also the relation of resistivity to the specific gravity of the solutions.

IV. SOLUTIONS HAVING MINIMUM RESISTIVITY

It has long been known that solutions of about 30 percent sulphuric acid have minimum resistivity. The Kohlrausch solution having minimum resistivity at 18° C was specified by him [6] as 30 percent H_2SO_4, having a density of 1.223 at 18° C. The specified percentage is not entirely consistent with the density. His table on page 157 shows that a density of 1.223 at 18° C corresponds to 30.3 percent H_2SO_4 and later tables [7] indicate that 30.4 percent (30.36 percent) is more nearly correct. Our table 3 shows that we also have found the solution, which has the maximum conductivity at 18° C, to contain 30.4 percent acid.

The conductivity of the solution which has the maximum conductivity at 25° C is given in table 3 as 0.8243 reciprocal ohm-centimeters. This is in close agreement with the value given in the International Critical Tables [8] 0.8242, which is based on the work of Eastman.[9] It is not entirely certain, however, that the percentage composition of his solution was precisely the same as ours. A variation of a few tenths of a percent in composition of the solution makes an exceedingly small change in conductivity in the region of maximum conductivity. It is probable that the difference between Eastman's result at 25° C and ours is not less than 1 nor more than 4 parts in 8,200.

[6] Kohlrausch und Holborn, Das Leitvermögen der Elektrolyte 75 (1916).
[7] International Critical Tables 3,56(1928).
[8] International Critical Tables 6,230(1929).
[9] J. Am. Chem. Soc. 46,333(1924).

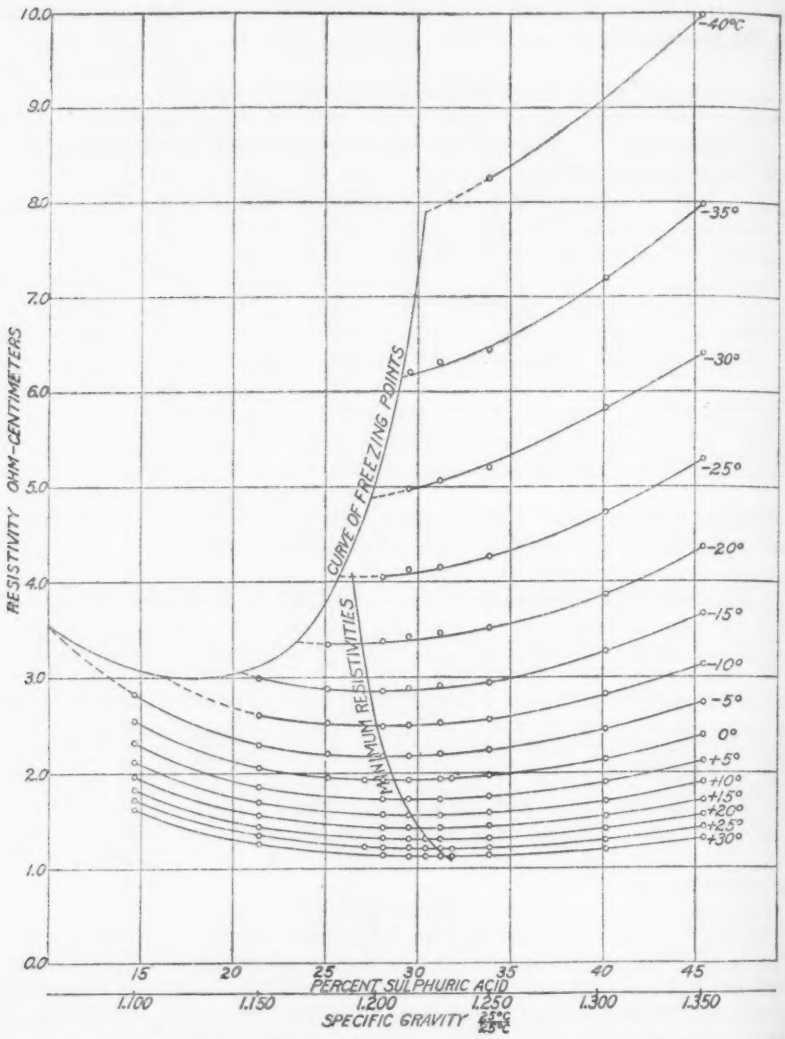

FIGURE 1.—*Resistivity of sulphuric-acid solutions.*

TABLE 3.—*Concentration of solutions having minimum resistivity at various temperatures*

Temperature	Concentration	Resistivity	Conductivity	Temperature	Concentration	Resistivity	Conductivity
°C	*Percent*	*ohm-cm*	*1/ohm-cm*	°C	*Percent*	*ohm-cm*	*1/ohm-cm*
+30	31.5	1.129	0.8855	0	28.8	1.928	0.5187
25	31.1	1.213	0.8243	−5	28.4	2.17	0.461
20	30.6	1.310	0.7635	−10	27.9	2.48	0.403
18	30.4	1.353	0.7388	−15	27.4	2.86	0.350
15	30.2	1.425	0.7015	−20	26.9	3.34	0.299
10	29.8	1.562	0.6402	−25	26.5	4.05	0.247
5	29.3	1.726	0.5794				

Our results show clearly that the composition of the solution having minimum resistivity (maximum conductivity) is not the same for all temperatures. As the temperature is lowered, the percentage of H_2SO_4 must be decreased slightly to obtain minimum resistivity. Thus, at +30° C we find the solution having least resistivity to contain 31.5 percent H_2SO_4 and at −25° C the solution to contain 26.5 percent acid.

Table 3 gives the percentage composition of solutions having minimum resistivity for each 5° C interval between +30 and −25° C. In this table we have included also the conductivities of the respective solutions for comparison with existing data.

V. RELATION BETWEEN RESISTIVITY, KINEMATIC VISCOSITY, AND TEMPERATURE

In the third section of this paper it was stated that an approximately linear relation between a function of resistivity of the sulphuric-acid solutions and temperature was obtained by plotting the function

$$\frac{1}{\log\,(6\times\text{resistivity})}$$

against the temperature. This function, which we shall call "function A" for convenience, was obtained empirically. The relation between function A and the temperature was more nearly linear in the case of the higher concentrations than for the lower concentrations (21.4 and 14.7 percent H_2SO_4). The slight curvature of the plotted lines for these caused no inconvenience in interpolating values, but may have been of some significance in the computations which follow, particularly as the curvature was most pronounced at the higher temperatures. The unit of resistivity which we employ in the following discussion is the ohm-centimeter as in table 2.

A similar linear relationship was shown to exist between temperature and the function

$$\frac{1}{\log\,(20\times\text{kinematic viscosity})}$$

The plot of this was shown in figure 3 of the viscosity paper. We shall call this function of viscosity "function B." The unit of kinematic viscosity employed here is the same as that which we used in the viscosity paper, namely, the centistoke.

The existence of these two linear relationships suggested the possibility of finding a simple relation between resistivity, kinematic viscosity, and temperature. By purely empirical methods, we have found that the ratio of function A to function B divided by the square root of the absolute temperature, T, gives a constant for solutions ranging from 28 to 45 percent H_2SO_4 over the wide range of temperature from +30 to −40° C. The relation is less exact for the lower concentrations, 21.4 and 14.7 percent H_2SO_4. The reason for this may be the greater departure from a linear relation between function A and temperature or may involve the constitution of the solutions, since these

particular solutions are on the dilute side of the region of minimum resistivity. The relation is expressed as follows:

$$\frac{\text{Function } A}{\sqrt{T}\,\text{Function } B}=\text{constant}$$

or

$$\frac{\text{Function } A}{\text{Function } B}=\text{constant}\ \sqrt{T}$$

Table 4 gives the complete data for calculating the ratio of function A to function B. The table shows that this ratio is proportional to the square root of the absolute temperature, at least for solutions of 45.5, 40.2, 33.9, and 28.1 percent H_2SO_4. In the last column of the table we have given the computed value of the constant of equation 1. The average deviation of a single value from the mean value of this constant is 1 percent for the more concentrated solutions and 5 percent if all the determinations are included. It is perhaps significant in the case of the more dilute solutions that the value of the constant approached more nearly to the average value for all when these solutions were at the lowest temperatures. It was in the region of lowest temperatures that the relation between function A and temperature was more nearly linear for these two solutions.

TABLE 4.—*Relation between resistivity, kinematic viscosity, and absolute temperature*

Concentration	Temperature		Function A	Function B	A/B	$\sqrt{T}$	$\frac{A}{B\sqrt{T}}$
Percent	° *C*	*Abs.*					
45.5	30	303	1.1110	0.6312	1.76	17.4	0.101
	15	288	.9868	.5791	1.70	17.0	.100
	0	273	.8641	.5245	1.65	16.5	.100
	−15	258	.7444	.4692	1.59	16.1	.099
	−30	243	.6299	.4116	1.53	15.6	.098
	−40	233	.5654	.3727	1.52	15.3	.099
40.2	30	303	1.1644	.6558	1.77	17.4	.102
	15	288	1.0316	.5985	1.73	17.0	.102
	0	273	.9000	.5396	1.67	16.5	.101
	−15	258	.7722	.4802	1.61	16.1	.100
	−30	243	.6504	.4204	1.55	15.6	.099
	−40	233	.5706	.3802	1.50	15.3	.098
33.9	30	303	1.1992	.6853	1.75	17.4	.101
	15	288	1.0665	.6220	1.71	17.0	.101
	0	273	.9320	.5580	1.67	16.5	.101
	−15	258	.7997	.4944	1.62	16.1	.101
	−30	243	.6711	.4306	1.56	15.6	.100
	−40	233	.5870	.3880	1.51	15.3	.099
28.1	30	303	1.1956	.7127	1.68	17.4	.097
	15	288	1.0708	.6424	1.67	17.0	.098
	0	273	.9404	.5738	1.64	16.5	.099
	−15	258	.8094	.5066	1.60	16.1	.099
	−30	243	.6792	.4397	1.55	15.6	.099
21.4	30	303	1.1368	.7442	1.53	17.4	.088
	15	288	1.0293	.6676	1.53	17.0	.090
	0	273	.9155	.5944	1.54	16.5	.093
	−15	258	.7978	.5238	1.52	16.1	.093
14.7	30	303	1.0122	.7738	1.31	17.4	.075
	15	288	.9330	.6916	1.35	17.0	.080
	0	273	.8441	.6128	1.38	16.5	.084

Average (omitting 21.4 and 14.7 percent)	0.100
Average deviation (omitting 21.4 and 14.7 percent)	±.001
Average (all observations)	.097
Average deviation (all observations)	±.005

VI. COMPARISON WITH PREVIOUS DETERMINATIONS

Comparatively few of our values can be compared directly with the values previously published. The International Critical Tables [10] give values of conductivity for solutions at 18° C ranging in concentration from 4,000 to 11,000 milliequivalents per liter. These values are compared with ours in table 5. In only one case is the difference as large as 0.5 percent, and the average difference is 0.24 percent.

VII. ACCURACY OF THE MEASUREMENTS

Sources of error in determining the composition of the solution, the temperature and the resistance of the solution in the conductivity cell, all affect the accuracy of the measurements. Systematic errors in determining the composition of the solution have been avoided by checking the results of titrations by measurements of specific gravity. The greatest difference observed between these determinations could affect the values given by as much as 0.2 percent in the case of only 1 out of 9 solutions.

Accidental errors in measuring the temperature of the solution were probably the same as in the viscosity measurements. In the viscosity paper it was stated that above −1° C the error in temperature measurement of a single determination did not exceed 0.05° C. This would correspond to about 0.1 percent in the resistivity. Below −1° C the errors of temperature measurement may have amounted to 0.2° C. Between −25 and −30° C this would correspond to 0.8 percent in the resistivity. The electrical measurements could be repeated to 0.1 percent.

TABLE 5.—*Comparison of values of resistivity with data from International Critical Tables*

(Ohm-centimeters at 18° C)

Concentration	I.C.T. values (reciprocals)	Observed values (this paper)	Difference	Concentration	I.C.T. values (reciprocals)	Observed values (this paper)	Difference
Millieq/liter			*Percent*	*Millieq/liter*			*Percent*
4,000	1.661	1.661	0.00	9,000	1.375	1.380	0.36
5,000	1.486	1.492	.40	10,000	1.423	1.430	.49
6,000	1.399	1.402	.21	11,000	1.500	1.496	.27
7,000	1.361	1.361	.00				
8,000	1.354	1.357	.22	Average			.24

In view of the preceding statements and the comparison of our results with existing data at 18° C, it seems probable that the results given in table 2 are not in error by more than 0.2 or 0.3 percent for measurements above −1° C nor by more than 1 percent between −1 and −20° C. Below −20° C the error may increase to 2 percent at the lowest temperatures.

WASHINGTON, July 18, 1934.

[10] International Critical Tables 6, p. 241.

U.S. DEPARTMENT OF COMMERCE NATIONAL BUREAU OF STANDARDS

RESEARCH PAPER RP739

Part of Journal of Research of the National Bureau of Standards, Volume 13, November 1934

A TEMPERATURE-CONTROL BOX FOR SATURATED STANDARD CELLS

By E. F. Mueller and H. F. Stimson

ABSTRACT

In order to meet the need for a portable standard of electromotive force somewhat better than the unsaturated standard cell, a semiportable temperature-control box for a group of saturated cells was constructed, and is described here. The apparatus provides an adequate solution for the problem of maintaining a working standard of emf for those purposes for which the unsaturated cell is not good enough.

CONTENTS

	Page
I. Introduction	699
II. Design and construction	700
III. Performance	702
IV. Conclusion	704

I. INTRODUCTION

The unsaturated cadmium standard cell has been very generally used as a working standard of electromotive force, even in precise potentiometric measurements, having been preferred to the saturated cadmium cell principally on account of its portability and very low temperature coefficient.

It is commonly recognized that temperature gradients in the unsaturated cell may cause appreciable changes in its emf, but the effect known as "hysteresis" may also at times be an unsuspected but significant source of error. This hysteresis is a temporary change of emf, resulting from a change in the cell temperature, and tends to become more pronounced as the cells age. Its magnitude is uncertain and appreciable effects may persist for some days.[1]

The saturated cell is more constant in emf but suffers from the disadvantage of having a rather large negative temperature coefficient, about 40 microvolts per degree C at 20° and nearly 60 microvolts per degree at 35° C. When used for precise work, either its temperature must be determined with considerable accuracy in order that corrections may be applied, or it must be placed in a thermostat, at some sacrifice of portability.

In precise calorimetry, a potentiometer is used to measure the power supplied to an electric heater, used to add definite quantities of heat to the calorimetric system. It was suspected that irregularities in the emf of unsaturated cells due to hysteresis may have been responsible

[1] J. H. Park. *Effect of service temperature conditions on the electromotive force of unsaturated portable standard cells.* BS J. Research **10**,89(1933);RP518.

for occasional calorimetric errors, as large as 0.05 percent, and a convenient means of keeping saturated cells at constant temperature was therefore sought.

II. DESIGN AND CONSTRUCTION

The type of temperature controller having metal cases rather than a stirred liquid bath to distribute the heat was chosen on account of its simplicity and portability. The aim in the design was to control the cell temperature within $\pm 0.01°$ C and to make it uniform to 0.001° C. Commercially pure aluminum was used for the cases on account of its lightness and high thermal conductivity. In this control box the temperature of an outer aluminum case is automatically controlled by a conventional mercury-in-glass thermoregulator. A second aluminum case, inside the first and thermally well insulated from it, contains the standard cells. The inner case will assume a temperature very nearly the time average of that of the outer case. The temperature oscillations of the inner case, resulting from the operation of the thermoregulator, can be attenuated to any reasonable degree by suitable choice of the heat capacity of the inner case and of the amount of thermal insulation between the two cases.

The box constructed provides space for five standard cells. The inner case is 3⅜ inches long, 2¾ inches wide, and 4 inches deep inside. This case is a casting with walls ¼ inch thick and bottom ⅜ inch thick. The cover, secured with numerous screws to improve thermal contact, is of sheet aluminum, ¼ inch thick. The inner case is spaced within the outer one with balsa wood ½ inch thick on all six faces. The outer case is also a casting, with side walls ⅜ inch thick and bottom ½ inch thick. The cover of sheet aluminum ⅜ inch thick is also secured with screws. The end walls of the casting are plane on the inside and cylindrical on the outside, the thickness at the edges being ⅜ inch, and ¾ inch at the middle, this extra thickness providing space for a vertical hole $^{15}/_{32}$ inch in diameter and 6 inches deep to accommodate the thermoregulator at one end and a smaller hole to accommodate a thermometer at the other end.

The outer case is insulated with a layer of balsa wood 1 inch thick on the sides and bottom, and 2 inches thick on the top. The pieces of balsa wood fit neatly into an outer wooden box. This box is long enough to provide a compartment at one end to contain a transformer, relay, and binding posts for the necessary connections. These accessories are mounted on a wooden panel which slides in vertical grooves in the sides of the box. The outside dimensions of the box are 8 by 13 inches, by 10 inches deep, and its weight, complete, is 22 pounds. A horizontal section of the control box is shown in figure 1.

The standard cells in the inner case were mounted on a simple support cut to appropriate shape from a piece of balsa wood. Connections to the cell terminals were made with no. 28 (0.013 inch) insulated copper wire, a length of about 4 feet being used for each terminal. About one-third of this length is in the form of a helix inside the inner case and another third is between the inner and outer cases. The wires were brought through the cases in smoothed saw cuts in the upper edges of the sides, and were insulated additionally with silk and glyptal lacquer, thus affording good thermal

contact with the metal cases, as well as adequate electric insulation (many thousands of megohms). These thermal tie-downs, and the considerable lengths of wire, reduce heat conduction from the outside along the wires to the cells to a negligible amount. Sheets of mica were placed on the surfaces of the aluminum cases, adjacent to the connecting wires, to protect them against accidental electrical grounding. Outside the outer case the wires were brought to binding posts supported on a hard-rubber strip set into the outer wooden box, the positive terminals being on one side of the box, the negative on the other.

The thermoregulator is of the adjustable mercury-in-glass type with a bulb 4 inches long and nearly $^{15}/_{32}$ inch in diameter. The total length of the regulator is 8 inches. It fits rather closely into the hole in the outer case, and a coating of grease serves to improve the thermal contact. A part of the stem of the thermoregulator was

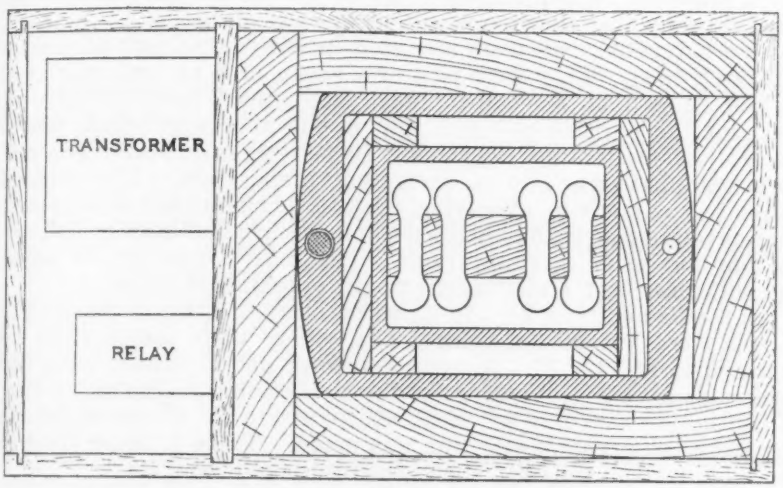

FIGURE 1.—*Horizontal section of temperature-control box.*

purposely left projecting above the outer aluminum case to compensate for changes in room temperature. The changes in room temperature alter the temperature of the projecting stem which in turn alters the temperature at which the regulator makes contact, in the proper sense to compensate for the displacement of its mean temperature due to the attendant changes in the relative lengths of the heating and cooling periods.

The heating resistor is no. 38 (0.004 inch) constantan and has a resistance of about 70 ohms. It is wound in about four turns, on the sides and ends of the outer aluminum case over silk fabric, the wire being spaced so as to distribute the heat as well as practicable. One turn is near the top edge and one near the bottom edge.

A small quick-acting alternating-current relay is used. It operates well on 12 volts at about 0.05 ampere although rated for 24 volts. Power for the relay and heater is supplied by a bell-ringing transformer rated at 50 watts, with secondary voltages from 4 to 24 in steps of 4 volts. The relay is operated on 12 volts and the heater

on 20. If the regulator should fail to shut off the current, the temperature of the cells would not rise more than 20 degrees above room temperature.

III. PERFORMANCE

Before the cells were installed, a bare resistance thermometer was temporarily mounted in the inner case. No oscillations traceable to the operation of the thermoregulator were detectable, although the sensitivity of the equipment used would have made it possible to detect changes of less than 0.001° C. The temperature oscillation in the outer case amounted to a few hundredths of a degree. The temperature of the inner compartment wandered slowly and irregularly, since the regulator did not maintain an entirely constant average temperature. The range of the wanderings was of the order of 0.01° C in the course of a week. A change of 15 degrees in room temperature produced no appreciable effect on the temperature in the inner case, showing that the compensation was adequate.

Four saturated cells were mounted in the control box at the end of March 1933. They were part of a group of 6 neutral cells made at the Bureau in November 1932. Redistilled new mercury was used for the positive electrode and in the amalgam, which was an electrolytic preparation containing 10 percent cadmium. The mercurous sulphate was also an electrolytic preparation. The cadmium sulphate was made by dissolving electrolytic cadmium metal in nitric acid, precipitating with redistilled sulphuric acid and heating, followed by four successive crystallizations. The glass blanks were of American soft glass with a minimum amount of sealing-in glass.

All 6 cells had been kept in an oil bath at 28° C up to the time the 4 cells were put in the control box, where their temperature was maintained at 32.8° C. A temperature of 35° C. would have been preferable for use in Washington during the summer, but as the effect of continuous exposure to temperatures above 28° C was not known, the more conservative selection was made. Table 1, taken from the record of tests of the cells, shows the results obtained.

TABLE 1.—*Electromotive force of cells in temperature-control box*

[International volts at 32.8° C]

Date	No. 773	No. 775	No. 776	No. 778
Apr. 7, 1933	1.017645	1.017642	1.017642	1.01764
Apr. 15, 1933	44	41	40	3
Apr. 22, 1933	40	39	38	3
May 6, 1933	35	36	34	2
May 20, 1933	31	34	33	2
Jan. 11, 1934	19	19	20	2
May 7, 1934	22	21	21	2

Each value recorded is representative of a group of observations made on several successive days. The data given above are not corrected for temperature, which in all cases was that maintained by the regulator.

The changes in emf of these cells, reported in table 1, are comparable with those of the remainder of the group which have been maintained at lower temperatures. Differences in emf from the

value for Weston normal cells at the respective temperatures, calculated on the basis of the international formula for the temperature coefficient of the Weston normal cell, are shown in table 2.

TABLE 2.—*Comparison of changes in* emf *of cells in the control box with those of similar cells maintained at lower temperature*

Cell number	Temperature	Differences from Weston normal cell		Total change
		Apr. 1933	May 1934	
		μv	μv	μv
773	In box 32.8° C	0	−23	−23
774	In oil bath 28° C	+3	−18	−21
775	In box 32.8° C	−3	−24	−21
776	do	−3	−24	−21
777	In oil bath 28° C	−1	−15	−14
778	In box 32.8° C	−3	−13	−10
Average change, 4 cells in box at 32.8° C				−19
Average change, 2 cells in oil bath at 28° C				−18

The changes shown in table 2 appear to be of the same magnitude and kind as those reported by Vinal and Howard [2] for a group of 14 neutral cells. The results therefore indicate that a temperature as high as 33° C has not been harmful to the cells.

Although the changes in the emf of the cells have been discussed in some detail, it is evident that the entire change would have been negligible, even in precise potentiometric measurements, under all ordinary circumstances. Only in case such a group of cells were used to maintain a reference standard of emf would it be necessary to take account of changes of the magnitude observed. It therefore appears that the portable control box, even at 33° C is adequate to control reference standards of emf to very nearly the precision attainable with the more elaborate baths in which the primary standards are kept.

When the prospective change from the international volt to the absolute volt shall have been made, the emf assigned to these cells will be about 1.0180 volts, a value within the range of the standard cell dials of most potentiometers now made. The low value is at present a minor inconvenience.

No provision was made for a thermometer to indicate the temperature of the inner case, as it was considered desirable to minimize the thermal connection between the two cases. It is possible, therefore, if the power fails for some time and comes on again an hour or two before observations are begun, that the thermometer in the outer case will indicate the proper temperature, while that of the cells may still be considerably too low. Such failure will be evident, however, if a synchronous electric clock of the type which stops when the power goes off is connected to the same line. Except on occasions when the power failed or the room temperature has exceeded 32° C, the regulator has operated continuously without failure for 17 months.

[2] *Effect of glass containers on the electromotive force of Weston normal cells*, BS J. Research **11**,263(1933);RP588

IV. CONCLUSION

The temperature-control box provides an adequate solution for the problem of maintaining a standard of emf for those purposes for which the unsaturated cell is not good enough. A box of this type is ideally adapted for controlling the temperature of any small apparatus in which little or no heat is developed. A similar control box, much smaller in size, has been used successfully for nearly 2 years to control the temperature of the coils of a Wheatstone bridge for resistance thermometry, where the maximum power developed in the coils is a few milliwatts.

We are indebted to Geo. W. Vinal, for the four very excellent cells used as well as for the test data and comparisons showing their performance.

WASHINGTON, July 17, 1934.

U.S. DEPARTMENT OF COMMERCE NATIONAL BUREAU OF STANDARDS

RESEARCH PAPER RP740

Part of Journal of Research of the National Bureau of Standards, Volume 13, November 1934

POLYMERIZATION OF OLEFINS FORMED BY THE ACTION OF SULPHURIC ACID ON METHYLISOPROPYLCARBINOL

By Gordon M. Kline and Nathan L. Drake

ABSTRACT

The action of 75 percent sulphuric acid on methylisopropylcarbinol at 80° C results in the formation of 2 isomeric decenes, namely, 3,4,5,5-tetramethylhexene-2 and 3,5,5-trimethylheptene-2. The theory proposed by Whitmore for the polymerization of olefins does not explain the formation of the above products without the postulation of a complicated rearrangement. A theory is proposed for the polymerization of olefins, based on the apparent activation of the olefin molecule, causing it to behave as 2 fragments which then add to the double bond of another olefin molecule in the usual manner. This behavior is analogous to the addition of RMgX to a carbonyl group $=C=O$ to yield $=C(R)-OMgX$. From a consideration of the relative calorie strengths of bonds, it is predicted that a C–C bond would be broken more readily than a C–H bond during the addition of the activated olefin molecule to another olefin molecule; thus the products to be expected differ markedly in many cases from those predicted on the basis of a labile hydrogen mechanism. This activation theory for the polymerization of olefins furnishes a simple mechanism for the diisoamylenes studied and for the formation of the known di– and triisobutylenes from isobutylene.

CONTENTS

	Page
I. Introduction	705
II. Experimental	706
III. Discussion of results	708
1. Application of Whitmore's polymerization theory	708
2. Proposed activation mechanism	709
3. Application of the activation mechanism to diisobutylene	710
4. Application of the activation mechanism to triisobutylene	710
5. Possible tautomeric equilibrium	711
6. Labile hydrogen theory	711

I. INTRODUCTION

The formation of products of high molecular weight by the action of polymerizing agents on olefins is well known. This reaction has important industrial applications in the manufacture of lubricating oils[1] and synthetic resins.[2] [3]

The extensive literature on the polymerization of ethylene has been reviewed by Stanley [4] and Carothers.[5] Mignonac and Saint-Aunay [6] succeeded in isolating butene-1 and hexene-1 as the first products

[1] Ind. Eng. Chem. **23**, 604 (1931).
[2] Ind. Eng. Chem. **24**, 1125 (1932).
[3] Carleton, Ellis, Synthetic Resins and Their Plastics, Chemical Catalog Co., Inc., 1923.
[4] J. Soc. Chem. Ind. **49**, 349T (1930).
[5] Chem. Rev. **8**, 353 (1931).
[6] Bul. soc. chim. **47**, 522 (1930).

formed in the action of the silent discharge on ethylene. Pease [7] found butene-1 in the products of thermal polymerization of ethylene and from a study of the kinetics has concluded that this is a chain reaction. Carothers states that in effect at least this reaction involves at the first step the addition of ethylene, as $H+CH=CH_2$, to the double bond of another molecule of ethylene, and then a similar addition to the butylene so formed.

The isomers in diisobutylene prepared by the action of sulphuric acid on tertiary butyl alcohol were found by Whitmore and his students [8] to be 2,4,4-trimethylpentene-1 and -2, in approximately the ratio of 4:1, which confirms the previous work of McCubbin and Adkins.[9]

A mechanism for the polymerization of olefins by acid catalysts has been proposed by Whitmore.[10] He postulates as the first step the addition of a hydrogen ion to the extra electron pair in the double bond to form a positively charged group which then adds to another olefin molecule to form a second positively charged group. This latter group may then liberate a hydrogen ion to form a new olefin molecule. The process is, therefore, catalyzed by any substance which gives hydrogen ions. On the basis of this theory, Whitmore has predicted that the most probable products in the diisoamylenes should be 3,5,5-trimethylheptene-2 and -3, 2,3,4,4-tetramethylhexene-1 and -2, and 2-ethyl-4, 4-dimethylhexene-1.

The purpose of the present work was to determine the structure of the diisoamylenes prepared by the action of sulphuric acid on methylisopropylcarbinol in order to add further to our knowledge of the mechanism of polymerization of simple olefins to complex oils and resins.

II. EXPERIMENTAL

Methylisopropylcarbinol was prepared from isopropyl bromide and acetaldehyde by means of the Grignard reaction as described by Drake and Cooke.[11] The carbinol was treated with one and one-half moles of 75 percent sulphuric acid at 80° C for 20 minutes. This treatment has been shown by Cooke [12] to give the best yield of the unsaturated dipolymer having the empirical formula $C_{10}H_{20}$. The purified decene was fractionated in a 250-cm chain-packed distilling column [13] at the National Bureau of Standards through the courtesy of the late E.W. Washburn and S.T. Schicktanz. This still had been found to give an efficient separation of a 50 mole percent mixture of benzene and ethylene chloride, which have boiling points differing by only 3.42° C. Distillation of 1,820 ml of decene gave 28 fractions varying in volumes from 46 to 71 ml and a residue of 210 ml, representing 97.5 percent recovery. The boiling points and refractive indices of the various fractions indicated that the distilled material consisted primarily of 2 substances having approximately the following physical properties:

1st decene.....bp −215 mm=110.8° C $n_D^{25}=1.4340$
2nd decene.....bp −215 mm=116.8° C $n_D^{25}=1.4375$

[7] J. Am. Chem. Soc. **53**, 1158 (1930).
[8] J. Am. Chem. Soc. **53**, 3136 (1931); **54**, 3706, 3710 (1932).
[9] J. Am. Chem. Soc. **52**, 2547 (1930).
[10] Ind. Eng. Chem. **26**, 94 (1934).
[11] Organic Syntheses, **12**, 48.
[12] Thesis for Ph.D. degree, University of Maryland, 1929.
[13] BS J.Research 7,852(1931); 11,89(1933).

The first decene, when ozonized, yields acetaldehyde and a ketone boiling at 147.2° C at 766 mm, the semicarbazone of which melts at 147.6–8° C. The second decene, when ozonized, yields acetaldehyde and a ketone boiling at 154.4° C at 768 mm, the semicarbazone of which melts at 169.5° C. Thorough examination of fractions 2,5,13,19,25 and the residue failed to reveal the presence of any other decene. It was concluded that there are only 2 isomeric decenes formed, and that these isomers are present in equal proportions since the curve obtained by plotting the refractive index against the percentage distilled shows at approximately the midpoint a sharp rise between the 2 plateaus corresponding to the 2 decene isomers.

Inasmuch as acetaldehyde is formed by ozonolysis of both decenes, the group $=C=CH(CH_3)$ is present. Both ketones give the Hofmann test characteristic of methyl ketones, thereby extending the known portion of the decene molecules to $-C(CH_3)=CH(CH_3)$.

Oxidation of the methyl ketone obtained from the second decene to a seven-carbon acid with sodium hypobromite took place with good yields. The amide of the seven-carbon acid melts at 76.5° C. There are 17 possible structurally isomeric saturated seven-carbon acids. Beilstein lists the amides of 13 of these, only one of which melts in the neighborhood of the unknown amide. This acid is methyldiethylacetic acid whose amide has been reported by Haller and Bauer [14] to melt at 78–79° C. This acid was synthesized by the Grignard reaction from methyldiethylcarbinyl chloride and carbon dioxide, and was found to boil at the same temperature as the unknown seven-carbon acid, namely 104° C, at 13 mm. The amide melts at 78.5° C; a mixed melting point, however, shows a depression of approximately 30 degrees, indicating that the 2 acids are different.

Twelve of the seventeen possible structurally isomeric saturated eight-carbon methyl ketones are described in the literature. The boiling point of one of these and the melting point of its semicarbazone are very close to those of the unknown ketone. This is 3-methyl-3-ethylpentanone-2, which has been found by Nyberg [15] to boil at 153.5 to 154° C at 756 mm and to yield a semicarbazone melting at 168° C. This methyl ketone should yield on oxidation with sodium hypobromite the same seven-carbon acid that had already been synthesized by us. In view of the remarkable similarity in physical constants of the two ketones and acids, 3-methyl-3-ethylpentanone-2 was synthesized in order to check a possible rearrangement during the preparation of the acid. The method of Nyberg was used for the synthesis, involving the reduction of methylethylketone with magnesium amalgam and rearrangement of the symmetrical pinacol to the pinacolone with sulphuric acid at −10° C. The semicarbazone of the ketone fraction boiling from 153 to 155° C melts at 167.5° C; when mixed with the unknown semicarbazone the melting point shows a depression of about 30 degrees. Hence the two semicarbazones and the ketones are different substances.

Inspection of the data in the literature revealed that there were only three 8-carbon methyl ketones whose semicarbazones or derived seven-carbon acid amides were unknown. One of these three, namely 4,5-dimethylhexanone-2, has been made by Wheeler [16] and its

[14] Compt.rend. **148**,127(1909).
[15] Ber. Deut. Chem. Ges. **55B**,1960(1922).
[16] Thesis for M.S. degree, University of Maryland, 1931.

semicarbazone found to melt at 159 to 160.5° C. There remained only the following possible methyl ketones: 3,4,4-trimethylpentanone-2 and 4,4-dimethylhexanone-2. Evidence accumulated in the meantime by W. Gordon Rose [17] indicated that the ketone obtained from the lower boiling decene is 3,4,4-trimethylpentanone-2. It remained to prove that the second ketone is 4,4-dimethylhexanone-2.

The ketone was converted into the oxime by treatment with hydroxylamine and the resulting ketoxime was subjected to the Beckmann rearrangement by treatment with phosphorus pentachloride. The rearrangement proceeded with a 20 percent yield of a substituted acetamide, which was then hydrolyzed by a 1:1 aqueous syrupy phosphoric acid solution in a sealed tube at 230 to 240° C. Solid derivatives of the resultant amine were prepared with picryl chloride and benzenesulphonyl chloride. The picramide melts at 88 to 88.5° C. and the benzenesulphonamide at 59.5° C. The picramide and benzenesulphonamide of 1-amino-2,2-dimethylbutane were prepared synthetically in the following manner. Dimethylethylacetic acid was made through the Grignard reaction from tertiary amyl chloride and carbon dioxide. The acid was converted into the chloride with thionyl chloride and then into the amide by treatment with ammonium hydroxide. The amide was dehydrated with phosphorus pentoxide to form the nitrile which was then reduced to the amine with sodium and alcohol. The picramide and benzenesulphonamide were prepared in the usual manner. The picramide melts at 88 to 88.5° C and the benzenesulphonamide at 59.5° C. Mixed melting points with the derivatives obtained from the unknown ketone gave no depressions of the melting points. Hence the second ketone is 4,4-dimethylhexanone-2.

The action of 75 percent sulphuric acid on methylisopropylcarbinol at 80° C results, therefore, in the formation of 2 isomeric decenes, namely, 3,4,5,5-tetramethylhexene-2 and 3,5,5-trimethylheptene-2:

$$CH_3CH(CH_3)CHOHCH_3 \xrightarrow{H_2SO_4} CH_3C(CH_3)_2CH(CH_3)C(CH_3)=CHCH_3 + CH_3CH_2C(CH_3)_2CH_2C(CH_3)=CHCH_3$$

Details regarding the experimental procedure and analyses of the compounds are given elsewhere.[18]

III. DISCUSSION OF RESULTS

1. APPLICATION OF WHITMORE'S POLYMERIZATION THEORY

According to the theory of Whitmore [19] for the dehydration of alcohols, methylisopropylcarbinol would lose the hydroxyl group and become a positive organic ion, $CH_3CH(CH_3)\overset{+}{C}HCH_3$ (1). This positive fragment may lose a hydrogen ion from the isopropyl group to form trimethylethylene, $CH_3C(CH_3)=CHCH_3$ (2), or from the methyl group adjacent to the positive carbon to form isopropylethylene, $CH_3CH(CH_3)CH=CH_2$ (3). If the positive carbon of (1) has a greater attraction for electrons than the adjacent secondary

[17] Thesis for Ph.D. degree, University of Maryland, 1934.
[18] G. M. Kline. Thesis for Ph.D. degree, University of Maryland, 1934.
[19] J. Am. Chem. Soc. **54**, 3274 (1932).

carbon, the hydrogen may shift with its electrons to form a new positive ion, $CH_3\overset{+}{C}(CH_3)CH_2CH_3$ (4). A shift of a methyl group in the case of (1) would not result in any change in structure of the positive ion. A loss of hydrogen from the newly formed ethyl group would produce trimethylethylene (2); loss of hydrogen from the adjacent methyl group would produce 1-methyl-1-ethylethylene, $CH_2=C(CH_3)-CH_2CH_3$ (5). Inasmuch as the carbon having the most electronegative groups attached to it has the least attraction for electrons, (4) would be expected to predominate rather than (1).

Union of (4) with (5) would yield a new positive organic ion, $CH_3CH_2C(CH_3)_2CH_2\overset{+}{C}(CH_3)CH_2CH_3$ (6). Loss of a hydrogen ion from the ethyl group would be expected as in the case of methylethylneopentylcarbinol,[20] and would form 3,5,5-trimethylheptene-2, $CH_3CH_2C(CH_3)_2CH_2C(CH_3)=CHCH_3$ (7), observed as one of the products. Union of (4) with (2) would yield another positive ion, $CH_3CH_2C(CH_3)_2CH(CH_3)\overset{+}{C}(CH_3)_2$ (8). In order to account for the 3,4,5,5-tetramethylhexene-2 observed as the second product of the reaction investigated, (8) would have to undergo a shift of a methyl group to form $CH_3CH_2\overset{+}{C}(CH_3)CH(CH_3)C(CH_3)_2CH_3$ and then loss of hydrogen from the ethyl group to yield the observed olefin, $CH_3CH=C(CH_3)CH(CH_3)C(CH_3)_2CH_3$ (9). However, the evidence accumulated by Whitmore in his investigation of the dehydration of various alcohols indicates that a positive fragment such as (8) would liberate the hydrogen ion adjacent to the positive carbon to form 2,3,4,4-tetramethylhexene-2.

2. PROPOSED ACTIVATION MECHANISM

If the explanation of the formation of the above products is sought in a theory somewhat analogous to that proposed by Rice [21] for the thermal decomposition of organic compounds from the standpoint of free radicals, the mechanism is much simpler. In effect at least the molecule of trimethylethylene behaves as though it were activated in the following manner: $CH_3^- \ ^+C(CH_3)=CH(CH_3)$. The positive and negative signs are used to indicate the relative electronegativities as defined by Kharasch [22] and are not intended to indicate ionization. The addition of these two fragments to the double bond of a nonactivated molecule of trimethylethylene would take place in accordance with the relative electronegativities as follows:

$$(CH_3)_2\overset{+}{C}=\overset{-}{C}HCH_3+CH_3^- \ ^+C(CH_3)=CHCH_3\rightarrow CH_3C(CH_3)_2CH-(CH_3)C(CH_3)=CHCH_3$$

This is one of the observed products, namely 3,4,5,5-tetramethylhexene-2. The addition of the two fragments to the double bond of 1-methyl-1-ethylethylene would take place as follows:

$$C_2H_5(CH_3)\overset{+}{C}=\overset{-}{C}H_2+CH_3^- \ ^+C(CH_3)=CHCH_3\rightarrow C_2H_5C(CH_3)_2CH_2C-(CH_3)=CHCH_3$$

[20] J. Am. Chem. Soc. **54**, 4011 (1932); **55**, 3732 (1933).
[21] J. Am. Chem. Soc. **53**, 1959 (1931).
[22] J. Am. Chem. Soc. **48**, 3130 (1926).

This is the other observed product, namely 3,5,5-trimethylheptene-2. If this mechanism is correct, trimethylethylene and 1-methyl-1-ethylethylene are produced by the dehydration of methylisopropylcarbinol in the ratio 3:1. This addition of the activated olefin molecule to a double bond is similar to the addition of RMgX to a carbonyl group $=C=O$ to yield $=C(R)-OMgX$, and to the catalyzed hydrogenation of a double bond.

3. APPLICATION OF THE ACTIVATION MECHANISM TO DIISOBUTYLENE

The products formed by the polymerization of isobutylene can be predicted by the same mechanism. From a consideration of the relative electronegativities involved or of the relative calorie strengths of the C-H and C-C bonds, isobutylene would be expected to behave as $CH_3^- \ ^+C(CH_3)=CH_2$ rather tnan $H^+ \ ^-CH=C(CH_3)_2$. The products observed in the formation of the dipolymer can be accounted for on the basis of the "activation" taking place 80 percent in the first sense and 20 percent in the second sense with subsequent addition to a molecule of isobutylene:

$$(CH_3)_2\overset{+}{C}=\overset{-}{C}H_2+CH_3^- \ ^+C(CH_3)=CH_2 \rightarrow CH_3C(CH_3)_2CH_2C(CH_3)=CH_2 \quad (10)$$

$$(CH_3)_2\overset{+}{C}=\overset{-}{C}H_2+H^+ \ ^-CH=C(CH_3)_2 \rightarrow CH_3C(CH_3)_2CH=C(CH_3)_2 \quad (11)$$

The mechanism postulated by Whitmore is rather unsatisfactory in this case, also, since to obtain the above products according to his theory it is necessary to liberate a hydrogen ion from a methyl group in preference to a neopentyl group, whereas he found in a study [23] of the dehydration of 4,4-dimethylpentanol-2 that the liberation of the hydrogen occurred from the neopentyl group rather than the methyl group in the ratio 4.5:1.

4. APPLICATION OF THE ACTIVATION MECHANISM TO TRIISOBUTYLENE

The formation of the triisobutylenes provides an interesting confirmation of the activation mechanism. In this case there are 3 olefins present which may be activated, the original isobutylene and the 2 dimers (10) and (11). Isobutylene activated as $CH_3^- \ ^+C(CH_3)=CH_2$ uniting with dimer (10) would form $CH_3C(CH_3)_2CH_2C(CH_3)_2CH_2C(CH_3)=CH_2$ (12) and with dimer (11) would form $CH_3C(CH_3)_2CH[C(CH_3)_3]C(CH_3)=CH_2$ (13). Isobutylene activated as $H^+ \ ^-CH=C(CH_3)_2$ uniting with dimer (10) would form $CH_3C(CH_3)_2CH_2C(CH_3)_2CH=C(CH_3)_2$ (14) and with dimer (11) would also form trimer (14). Dimer (10) activated as $CH_3^- \ ^+C(=CH_2)CH_2C(CH_3)_3$ uniting with isobutylene would form $CH_3C(CH_3)_2CH_2C(=CH_2)CH_2C(CH_3)_3$ (15), and activated as $H^+ \ ^-CH=C(CH_3)CH_2C(CH_3)_3$ uniting with isobutylene would form $CH_3C(CH_3)_2CH_2C(CH_3)=CHC(CH_3)_3$ (16). Dimer (11) activated as $CH_3^- \ ^+C(CH_3)=CHC(CH_3)_3$ uniting with isobutylene would form trimer (16), and activated as $H^+ \ ^-C[C(CH_3)_3]=C(CH_3)_2$ uniting with

[23] J. Am. Chem. Soc. 55,4194(1933).

isobutylene would form $CH_3C(CH_3)_2C[C(CH_3)_3]=C(CH_3)_2$ (17). Of these 6 isomers (12), (14), (15), and (16) involve the dimer which makes up 80 percent of diisobutylene and they would, therefore, be expected to predominate in triisobutylene. The presence of these 4 isomers in triisobutylene has been reported by Whitmore [24] without a statement as to the proportions of each. When it is considered that there are 2,281 isomers with the empirical formula $C_{12}H_{24}$, as calculated by Henze and Blair,[25] the value of a simple mechanism which permits the prediction of the products of polymerization of simple olefins becomes evident.

5. POSSIBLE TAUTOMERIC EQUILIBRIUM

The C-H bond is approximately 22,000 calories stronger than the C-C bond and objection may be made, therefore, to the postulation of a break in the C-H bond in isobutylene to yield 20 percent of the dimer reaction products. However, it has been suggested to us by S. F. Acree of this Bureau that a tautomeric relation may exist between dimers (10) and (11) through a shift of the double bond from the 1 to the 2 position.[26] A similar tautomeric relationship between trimers (12) and (14), and (15) and (16) is possible. Evidence of such a tautomeric equilibrium could be sought by subjecting one of the dimers to the conditions resulting in their formation from isobutylene and examining the product for the presence of the other isomer. It is recognized however, that the energy of activation present in the dimer at the instant of its formation may be a necessary factor in this shift of the double bond, and that activation of the inactive dimer molecules may not take place under the same conditions that supply the necessary energy to the smaller monomer molecules. It is noteworthy that the products of such a tautomeric shift of the double bond were not observed with the diamylenes studied by the authors and that the products found result from the breaking of C-C bonds rather than C-H bonds.

6. LABILE HYDROGEN THEORY

Attempts have been made to explain the formation of polymers of olefins on the basis of a labile hydrogen theory.[27] Thus Carothers [28] formulates the mechanism for the polymerization of vinyl compounds as follows:

$$RCH=CH_2+RCH=CH_2\rightarrow RCH_2CH_2C(R)=CH_2$$

$$RCH_2CH_2C(R)=CH_2+RCH=CH_2\rightarrow RCH_2CH_2CH(R)CH_2C(R)=CH_2, \text{ etc.}$$

However, according to our mechanism the predominant reaction in the first stage would be:

$$R\overset{+}{C}H=\overset{-}{C}H_2+R^-\,{}^+CH=CH_2\rightarrow R_2CHCH_2CH=CH_2$$

[24] Ind. Eng. Chem. 26,94(1934).
[25] J. Am. Chem. Soc. 55,685(1933).
[26] Ber. Deut. Chem. Ges. 36, 2003(1903).
[27] J. Am. Chem. Soc. 53, 356(1931).
[28] Chem. Rev. 8, 353(1931).

and in the second stage would be:

$$R_2CHCH_2\overset{+}{C}H=\overset{-}{C}H_2+R^- {}^+CH=CH_2\rightarrow R_2CHCH_2CH(R)CH_2CH=CH_2$$

Activation of the monomer as $H^+ {}^-CH=CHR$ would also be expected to a greater extent than in the case of isobutylene considered above and would give rise to the dimer $CH_3CH(R)CH=CHR$. The trimers which would probably be formed in the polymerization of such a compound can be deduced by the same procedure used for isobutylene. Propylene, $CH_3CH=CH_2$, furnishes a particularly advantageous type compound for the study of such polymerization since it is the simplest molecule containing C-C as well as C-H linkages adjoining the double bond. We hope to present experimental evidence regarding the polymerization of propylene with sulphuric acid at a later date.

WASHINGTON, August 25, 1934.

U.S. DEPARTMENT OF COMMERCE NATIONAL BUREAU OF STANDARDS

RESEARCH PAPER RP741

Part of Journal of Research of the National Bureau of Standards, Volume 13, November 1934

COMPRESSION TESTS OF STRUCTURAL STEEL AT ELEVATED TEMPERATURES

By Prentiss D. Sale

ABSTRACT

The strength in compression and the stress-strain relations are given for structural-steel shapes and for round bars at temperatures up to 945° C (1,733° F), the slenderness ratio (l/r) for the bars being in the general range 20 to 150. One group of tests with cast-iron specimens is included for comparative purposes. Two general methods of testing are included, one in which the specimen is heated to a given temperature and then loaded to failure, and the other in which the load is maintained constant and the temperature increased until failure occurs. The results are given in tables and graphs.

For structural steel tested at temperatures of 250° C (482° F) or higher, and for cast iron at all temperatures, no well-defined yield point or yield region was developed. A strength higher than that obtained at room temperature was developed at temperatures near 250° C (482° F) in all tests except in those with the light-angle, pressed-steel, and cast-iron sections, and with round bars of smaller diameter than three-fourths inch (45 l/r). From the standpoint of variation of strength with slenderness ratio, the results are consistent with those derived from column theory. They are also in agreement with results from two series of fire tests of building columns.

CONTENTS

	Page
I. Introduction	714
II. Materials and test specimens	714
1. Shape specimens	714
2. Round steel specimens	719
III. Equipment and methods of testing	723
IV. Test results at elevated temperatures	725
1. Results with steel shapes and cast iron	726
(a) Constant-temperature tests	726
(1) Structural-steel shapes	727
(2) Cast-iron specimens	728
(3) Discussion	728
(b) Constant-load tests	730
2. Results with round-bar specimens	734
(a) Constant-temperature tests	734
(b) Constant-load tests	736
(c) Comparison of results with those derived from theory and tests of building columns	737
3. Expansion tests	740
V. Conclusions	741
1. Material, specimens, and test conditions	741
2. General conclusions	742

I. INTRODUCTION

The test conditions for the compression tests reported herein include some of those to which full-size building columns are subjected during fires. The rise in temperature of the structural-metal parts varies with the fire exposure and the protection applied on them, while the load remains constant or increases depending upon the restraint imposed on the particular member. Although the fire-protective material in the construction may take part of the load, the steel core usually is designed to carry all the load, and the protection is relied upon solely to retard temperature rise in the steel during a possible fire exposure.

Long-time creep tests have no direct application to ultimate performance of members subjected to these changing exposure conditions of relatively short duration. Representative temperature, expansion, load, and deformation measurements can be made to yield under laboratory-controlled conditions more definite data than those obtainable from full-size tests of columns conducted in accordance with the usual procedure, where the object is to obtain information on particular constructions, inclusive of the protective coverings.

A series of tests on rolled structural shapes is included to give information on local compressive buckling. Tests of round bars having slenderness ratios (l/r) in the general range 20 to 150 are included to cover the performance for a wide range of temperatures and loads.

The results of these short-time tests have been compared with data available from fire tests of columns [1] [2] for those results that were relatively free from effects of load-assistance from the protective coverings. The total number of tests reported herein is 281. Of this number, 63 were tension tests and 50 compression tests at room temperature 159 were compression tests at elevated temperatures, and 9 were expansion tests.

"Stress" as used in this paper indicates load per unit of area, P/A, where P denotes the total load and A the original cross-sectional area of the test specimen. "Strain" indicates the deformation per unit of original gage length.

II. MATERIALS AND TEST SPECIMENS

1. SHAPE SPECIMENS

The structural elements and the compression properties at room temperature for the shape specimens are given in table 1 and tensile properties and chemical analyses in table 2. Groups 1 to 9 refer to shape tests. The numbers designating the specimens used in the cold tests are the first in the individual groups, those following being for specimens used in the tests at elevated temperatures. All tension tests were made at room temperature with 2 in. by ½ in. round specimens for the round stock and with representative flat coupons from the structural-steel shapes.

[1] S. H. Ingberg, H. K. Griffin, W. C. Robinson, and R. E. Wilson, *Fire tests of building columns*, BS Techn. Pap. T184 (1921).
[2] N. D. Mitchell, *Fire tests of columns protected with gypsum*, BS J. Research **10**, 737(1933); RP563.

TABLE 1.—*Elements of structural shapes and compression properties at room temperature*

Reference			Elements of structural shape					Compression properties at room temperature					
Group	Shape	Specimen no.	Area	Thickness [1]	Least radius of gyration, r	Length, l	Slenderness ratio, l/r	Proportional limit	Modulus of elasticity	Yield point [2]	Strain at yield point	Ultimate strength	Strain at ultimate
			*In.*²	*In.*	*In.*	*In.*		*Lb/in.*²	*Million lb/in.*²	*Lb/in.*²		*Lb/in.*²	
	STRUCTURAL STEEL SHAPES												
1	3 in. I-beam, 5½ lb/ft (Mn 1.15%)	1	1.63	0.17	0.53	10.5	19.8	40,000	31.0	43,500	0.0019	67,300	0.0601
2	3 in. I-beam, 5½ lb/ft (Mn 0.81%)	25	1.67	.17	.50	10.5	19.8	-------	30.0	42,000	.0019	62,000	.0530
3	3 in. I-beam, 5½ lb/ft (Mn 0.81%) annealed	26	1.67	.17	.53	10.5	19.8	-------	30.0	33,000	.0016	53,000	.0532
		40	2.13	.32	.46	2.4	5.2	35,000	-------	37,500	.0030	67,000	.1167
4	4 in. channel, 7¼ lb/ft	41	-------	-------	-------	10.5	22.8	35,000	28.0	38,700	.0019	56,800	.0532
		42	-------	-------	-------	-------	22.8	35,000	30.0	37,000	.0017	52,200	.0497
		51	1.55	.18	.45	10.5	23.4	-------	30.0	39,600	.0018	42,640	.0427
5	4 in. channel, 5¼ lb/ft	59	-------	-------	.45	1.8	4.1	-------	-------	28,500	.0043	60,000	.1094
6	2½ by 2½ by ½ in. angle, 7.7 lb/ft	61	2.25	.50	.47	10.5	22.3	33,000	31.0	37,000	.0018	52,800	-------
		71	1.44	.25	.59	10.5	17.8	-------	31.0	37,500	.0017	39,200	.0083
7	3 by 3 by ¼ in. angle, 4.9 lb/ft	72	-------	-------	-------	-------	17.8	36,000	30.0	39,000	.0018	39,000	.0016
		73	-------	-------	-------	-------	17.8	34,000	-------	38,900	.0018	40,600	.0020
		90	.92	.06	.75	10.5	14.0	39,000	28.0	40,200	.0022	40,500	.0024
8	Pressed steel joist, 3.13 lb/ft	91	-------	-------	-------	-------	-------	34,000	30.0	37,800	.0019	38,500	.0026
	CAST IRON, OUTSIDE DIAMETER 1½ IN.; INSIDE DIAMETER ½ IN., WITH FLANGES												
9	Hollow round, 5.5 lb/ft	100	1.61	.50	.395	9.25	23.4	40,000	16.60	50,000	.0041	86,710	.0350
		100	-------	-------	-------	-------	-------	-------	-------	-------	-------	[3] 87,500	.0428

[1] Nominal web thickness for groups 1 to 5, leg thickness for groups 6 and 7, sheet thickness for group 8, wall thickness for group 9.
[2] Yield point selected at 0.0005 strain from initial modulus line, for structural steel; at 0.001 strain from initial modulus line, for cast iron.
[3] Reloaded at later date.

TABLE 2.—*Chemical analysis and tensile properties at room temperature for shapes and round specimens*

STRUCTURAL STEEL SHAPES

Reference		Chemical analysis						Tensile properties at room temperature [1]					
Group number	Shape and stock	C	Mn	P	S	Si	Other elements	Proportional limit	Modulus of elasticity	Yield point [2]	Tensile strength	Elongation in 2 in.	Reduction of area
		%	%	%	%	%	%	*Lb/in.*[2]	*Million Lb/in.*[2]	*Lb/in.*[2]	*Lb/in.*[2]	*Percent*	*Percent*
1	3 in. I-beam, 5½ lb/ft	0.21	1.15	0.016	0.034	0.025	Cr 0.06 Cu .18	Max 38,500	29.5	45,200	70,200	42.0	71.8
								Min 28,000	27.0	41,900	65,200	32.0	57.8
								Avg of 6 35,000	28.3	43,700	68,700	36.6	63.4
2	do	.21	.81	.020	.052	.030		Max 38,500	29.5	44,200	68,700	48.5	52.5
								Min 30,000	29.0	38,500	63,900	44.5	47.7
								Avg of 3 33,200	29.2	42,000	66,900	46.3	50.3
3	3 in. I-beam, 5½ lb/ft, annealed.	.21	.81	.020	.052	.030		Max 29,500	34.5	35,900	61,000	43.5	47.8
								Min 17,500	26.5	32,080	58,800	34.0	44.3
								Avg of 3 22,300	29.8	34,200	60,200	38.3	45.9
4	4 in. channel, 7¼ lb/ft	.21	.58	.011	.044	.050		Max 35,500	31.0	41,500	62,400	36.0	67.0
								Min 27,500	29.0	38,500	60,100	29.0	53.2
								Avg of 5 32,200	29.8	39,700	61,700	35.2	62.2
5	4 in. channel, 5¼ lb/ft	.17	.56	.036	.055	.040		Max 45,500	30.5	50,350	64,400	29.0	58.5
								Min 29,000	28.5	46,200	62,300	26.5	46.8
								Avg of 4 37,300	29.6	48,700	63,800	28.3	53.9
6	2½×2½×½ in. angle, 7.7 lb/ft	.20	.34	.018	.063	.050		Max 36,700	32.5	42,100	62,600	39.0	63.0
								Min 23,500	30.0	34,800	57,800	27.0	61.3
								Avg of 7 32,900	31.0	38,100	59,800	33.8	62.1
7	3×3×¼ in. angle, 4.9 lb/ft	.21	.57	.014	.035	.020		Max 35,000	30.0	43,000	62,400	47.5	64.2
								Min 24,000	27.0	37,300	55,800	29.0	57.8
								Avg of 12 32,100	28.7	39,900	58,400	37.5	60.3
8	Pressed steel joist, 3.13 lb/ft	.09	.39	.010	.020	.002	Cu .085	Max 36,500	29.1	42,500	52,900	34.0	57.0
								Min 29,200	24.0	34,200	46,800	29.0	49.6
								Avg of 5 33,900	27.4	40,100	51,500	31.0	54.1

CAST IRON, OUTSIDE DIAMETER 1½ IN., INSIDE DIAMETER ½ IN., WITH FLANGES

9	Hollow round, 5.5 lb/ft	{[3] 3.42 / [4] 3.10}	.37	.715	.115	1.580		Transverse test, 60,000 lb/in.², extreme fiber stress.						

STRUCTURAL STEEL, ROUND RODS

10 to 13	2 in. round, lot A	.20	.38	.013	.032	.010		Max	30,500	31.0	33,800	61,400	42.5	58.6
								Min	27,000	28.5	32.100	58,900	35.5	54.4
								Avg of 4	29,300	29.5	33,000	60,000	38.3	56.1
14 to 19	2 in. round, lot B	.18	.43	.008	.033	.010		Max	29,500	28.8	32,750	55,500	43.0	65.0
								Min	25,500	27.3	29,750	53,900	41.0	63.0
								Avg of 6	28,000	28.1	31,550	54,800	42.5	64.5
20	do.[5]	.18	.43	.008	.033	.010		1 test	28,000	31.0	62,650	63,550	25.0	63.3
								1 test			64,000	80,000	17.0	60.3
21	1 in. round, lot C	.10	.83	.107	.106	.04		Max	38,000	29.5	41,500	63,000	37.5	62.4
22 and 23	1 in. round, lot D	.20	.41	.014	.048	.10		Min	37,000	29.0	41,100	62,900	37.5	61.6
								Avg of 2	37,500	29.3	41,300	63,000	37.5	62.0
24	1½ in. round, lot E	.22	.36	.01	.041	.07		Max	32,700	30.6	33,000	57,300	41.0	63.8
								Min	27,400	28.7	30,900	57,200	39.0	62.9
								Avg of 3	30,200	29.8	32,200	57,250	39.7	63.3

[1] For groups 1 to 8, tension specimens were rectangular flats from ½ to 1¾ in. wide at the reduced section and were cut from webs and flanges. Rounds from ¼ to ½ in. in diameter were cut from the junction of flange and web. The length of the reduced section was about 4 in. for the flats and 2½ inches for the rounds. For groups 10 to 20 and 22 to 24, standard .505 inch diameter specimens with threaded ends were used. For group 21 the ⅜-inch round compression specimen was retested in tension.

[2] Yield point determined by "drop of beam" method.

[3] Combined carbon.

[4] Graphitic carbon.

[5] Cut from specimen no. 159 after its regular test.

The diagrams in figure 1 give the compressive stress-strain records for the specimens indicated by the underlined numbers. Duplicates and lengths shorter than the normal 10.5 in. test lengths are excluded here. These diagrams illustrate the performance for short struts. It is noted that the cast-iron specimen no. 100 exhibits no yielding without increase in load except at ultimate, while the remaining structural-steel shapes of varying symmetry yield at stresses from 45,000 to 32,000

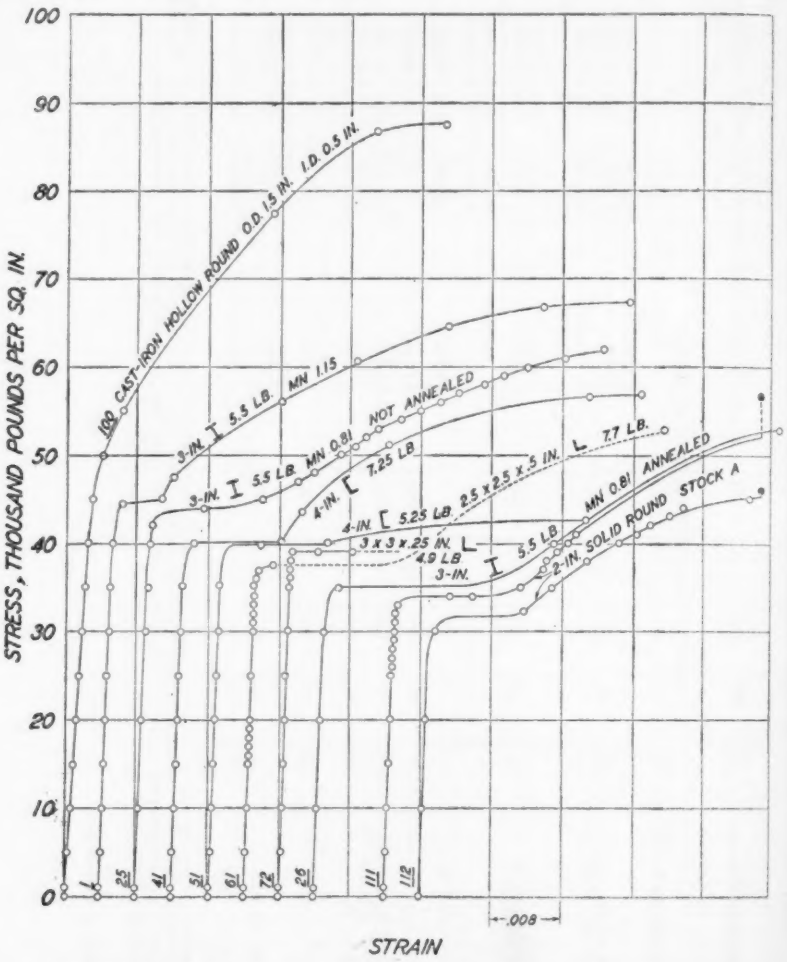

FIGURE 1.—*Stress-strain data from the shape tests at room temperature.*

lb/in². Ultimate strengths higher than the yield point are indicated, however, for all specimens except the least symmetrical and relatively thin angle section no. 72. Generally, yielding of a member beyond a certain limit disturbs seriously the distribution of stresses in the structure of which the member is a part, so an arbitrary yield point, applicable for cold tests only, has been selected from the stress-strain diagrams, as indicated in table 1, footnotes 2 and 3. The proportional limit and modulus of elasticity were estimated from plottings of the

stress-strain data to a large scale, giving due consideration to experimental errors involved. They are listed in table 1 insofar as they were obtained.

2. ROUND STEEL SPECIMENS

The round specimens were made from five lots of structural steel designated as A to E, the chemical analyses and tensile properties of which are given in table 2. The one tension test for each of groups 20 and 21 is for strain-hardened material, while the remaining tension tests identify the materials as grades of structural steel such as would be normally included by specifications for this class of material.

Table 3 gives the structural elements and compression properties at room temperature for the round specimens. The specimens, except as noted, were of 10.5 in. total length with slenderness ratios as indicated. Group 19 includes only half-length specimens and group 20 half-length strain-hardened specimens. The group values of slenderness ratio, l/r, approximate 22, 35, 45, 70, 95, and 145, where l equals the effective length of the specimen and r the least radius of gyration.

TABLE 3.—*Elements and compression properties of structural rounds at room temperature*

[Structural steel round rods, all flanged ends and reduced sections, except groups 10 and 14 and specimen no. 159 in group 19]

Reference			Elements of structural shape					Compression properties at room temperature					
Group number	Stock	Specimen number	Area	Diameter	Least radius of gyration, r	Effective length	Slenderness ratio, $l:r$	Proportional limit	Modulus of elasticity	Yield point [1]	Strain at yield point	Ultimate strength	Strain at ultimate
			Sq/in.	*In.*	*In.*	*In.*		*Lb/in.*[2]	*Million lb/in.*[2]	*Lb/in.*[2]		*Lb/in.*[2]	
10	2 in. round, lot A	111	2.763	1.88	0.470	10.50	22.4	28,000	30.0	34,000	0.0030	56,700	0.0702
		112							30.0	32,300	.0030	46,000	.0462
		113						29,000	30.0	35,000	.0030	43,000	.0203
11	do	118	.784	1.00	.250	8.61	34.4	28,000	28.0	28,000	.0010	42,000	.0375
		119						26,000	28.0	34,000	.0030	42,000	.0294
12	do	125	.440	.75	.187	8.50	45.5	26,000	28.0	30,500	.0014	35,000	.0097
		126						20,000	30.0	30,000	.0018	32,500	.0138
13	do	134	.196	.50	.125	8.53	68.3	29,500	31.0	30,000	.0017	32,500	.0034
		135						25,000	31.0	29,000	.0018	31,000	.0109
14	2 in. round, lot B	141	2.763	1.88	.470	10.50	22.4	17,000	29.0	27,000	.0037	47,000	.0584
15	do	144	.785	1.00	.250	8.91	35.6	26,000	30.0	27,000	.0015	34,700	.0292
		145						26,000	30.0	27,500	.0016	35,000	.0278
16	do	148	.442	.75	.187	8.84	47.2	26,000	30.0	27,500	.0015	28,100	.0122
17	do	152	.196	.50	.125	8.71	69.7	25,000	25.0	26,000	.0012	28,000	.0036
18	do	155	.110	.375	.094	9.26	99.0	26,000	25.0	29,000	.0016	No increase beyond yield point.	
		156						26,000	27.5	28,000	.0013		
		157	.099	.250	.062	9.29	149.1	22,000	27.5	28,000	.0011		
		158						24,000	26.5	26,000	.0016		
19	Shorts, lot B	159	2.88	1.915	1.479	5.50	11.5	15,000	25.0	28,500	.0020	69,500	.1213
		160	.196	.50	.125	4.17	33.4	20,000	29.0	28,000	.0011	37,450	.0400
		161	.110	.375	.094	4.12	43.9	25,000	31.0	29,500	.0011	30,400	.0050
		162	.049	.249	.062	4.04	64.9	25,500	31.0	29,000	.0011	29,500	.0027
		163	.049	.249	.062	4.06	65.2	25,000	29.5	28,000	.0012	28,500	.0025
20 [3]	do	164	.196	.50	.125	3.90	31.2	64,000	30.0	65,000	.0025	No increase beyond yield point.	
		165	.110	.375	.094	3.87	41.4	66,000	31.0	66,000	.0022		
		166	.049	.251	.063	3.87	61.8	66,500	31.0	66,500	.0021		

21	1 in. round, lot C	168	.109	.373	.093	8.90	95.4	61,000	31.5	61,400	.0020	do		
22	1 in. round, lot D	171	.110	.374	.093	8.92	95.5	48,900	30.2	48,900	.0016	do		
23	do	181	.049	.249	.0622	8.92	143.4	43,000	30.0	43,000	.0015	do		
		182	.049	.249	.0623	9.00	144.5	42,000	30.0	42,000	.0015			
24	1½ in. round lot E	195	.196	.499	.125	9.21	73.8		30.0				36,500	.0012
			Load dropped to 30,000 lb/in.², reloaded.											
		196	.191	.493	.123	8.80	71.5	33,500	28.5				34,400	.0018
			Load dropped to 30,100 lb/in.², reloaded.										34,500	.0012
		197	.109	.373	.093	9.02	96.7	32,000	30.6				33,000	.0012
			Load dropped to 29,100 lb/in.², reloaded.										33,500	.0011
		198	.049	.250	.0625	8.78	140.0	34,000	28.3	34,000	.0012		34,260	.0014
			.048	.247	.0618	8.91	144.2	33,000	29.6				35,000	.0014
		199	Load dropped to 30,800 lb/in.², reloaded.					31,000	31.0				33,500	.0011
													32,800	.0026

[1] Yield point selected at 0.0005 strain from initial modulus line.
[2] Shorts cut from specimen number 159 after its regular test.

The larger specimens of about 1.9 inch diameter had no flanged ends, while all smaller sizes were reduced from 2-, 1½-, or 1-inch stock to the desired diameters over the effective length, with rounded fillets at the end flanges, which were slightly smaller in diameter than the original stock. The ends were faced flat and perpendicular to the axis of the turned specimens and drilled at the center of the ends for alinement in testing.

The compression properties at room temperature given in table 3 were obtained from stress-strain records as illustrated in figures 2 and 3. Development of a yield region at nearly constant load is shown followed by increase in load for specimens of slenderness

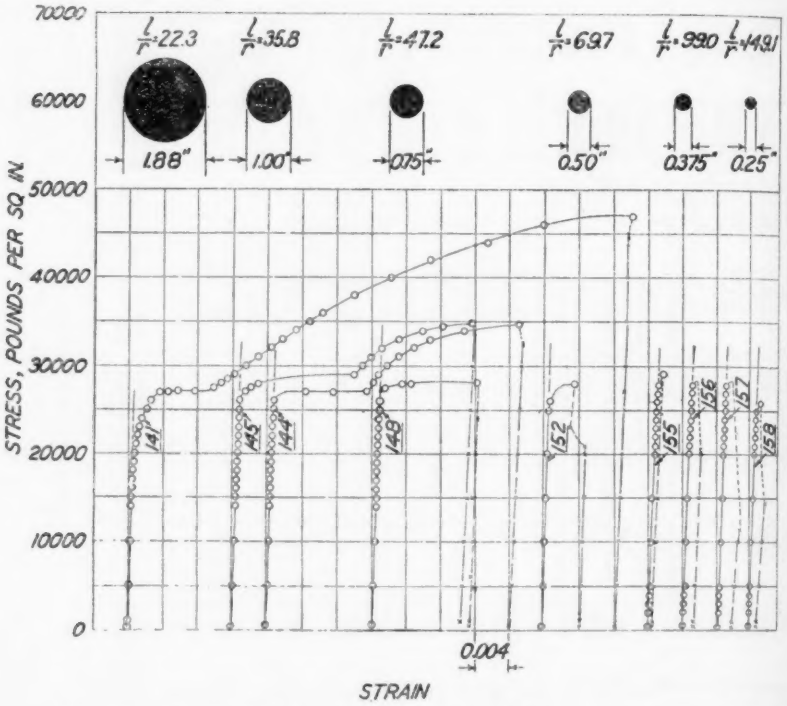

FIGURE 2.—*Stress-strain data from compression tests at room temperature of lot B specimens 141, 144, 145, 148, 152, and 155 to 158, inclusive.*

ratio less than 45, while little or no load increase is shown for specimens of greater slenderness.

Figure 3 gives results of compression tests at room temperature using half-length specimens from lot B. The first 5 tests, nos. 159 to 163, inclusive, check the performance for a given slenderness ratio with the 10.5-inch length specimens covered in figure 2. Specimens nos. 164, 165, and 166 were also from lot B, strain-hardened by compression in test no. 159, which specimen after this test was quartered to make 3 short compression specimens and 1 standard tension specimen. The stress-strain diagrams show the extent to which the strength and yield characteristics are modified due to the strain-hardened condition of the material. The properties of lots C and D

might be due to some strain-hardened conditions occurring in ordinary structural steel. Lot C was discarded as too hard for inclusion in these tests while D was retained as representative of that allowable by the upper strength limits of structural-steel specifications (see tensile properties, table 2, lots C and D). Lot E was included to supply a number of slender specimens for high-temperature tests to supplement the B series.

III. EQUIPMENT AND METHODS OF TESTING

All compression tests, except several at room temperature, were made in the machine shown in figure 4 or in the Emery testing machine shown in figure 6 equipped at the compression end for test-

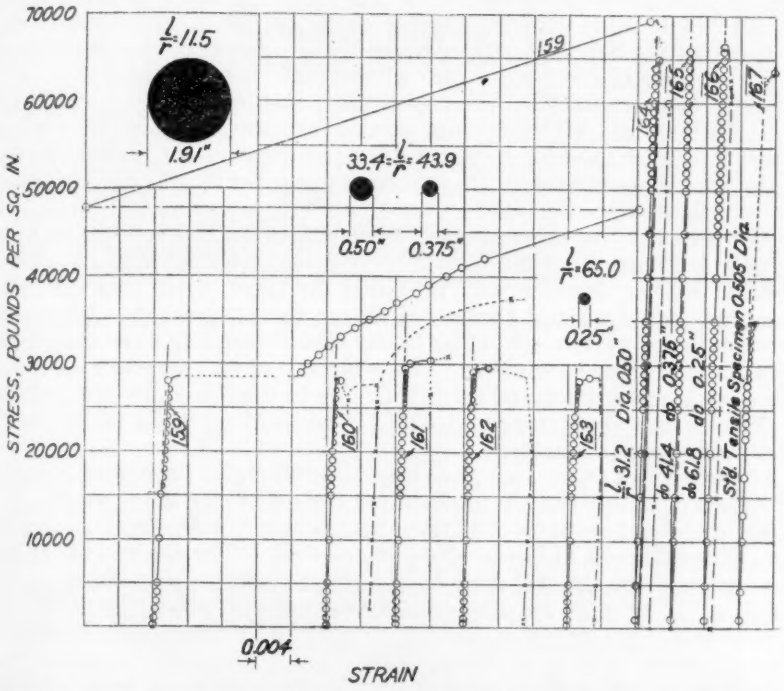

FIGURE 3.—*Stress-strain data from compression tests at room temperature of lot B specimens 159 to 167, inclusive.*

ing at elevated temperatures. Tests on shapes and the larger bars were made in the former machine, and all tests with slender specimens of lots B, C, D, and E were made in the Emery machine. All compression tests were planned for flat- or fixed-end test conditions although these conditions may not have been realized in all cases, as later indicated.

In figure 4 the main furnace, A, is shown rolled back with the specimen, B, in position for test. The load is applied from the left by the hydraulic press, C, which carries an adjustable spherical-seated block, D. Rigidly attached to the press, C, is a 1¼ in. diameter steel rod which projects through the block, D. The specimen can be positioned by means of three radial screws engaging this rod. These

parts are placed in a 260,000-pound capacity restraining frame, below which a shelf supports a mounting for two microscopes used for deformation measurements. All the movable parts, including the main furnace, are counterweighted to obviate bending stresses. Hydraulic pressure is obtained with the pump, E, and is measured by a fluid pressure scale, F. This loading equipment was calibrated before and after the series of tests by means of elastic springs and bars, which indicated an accuracy of about ± 0.2 percent for full-capacity loads and ± 5 percent for the lowest load producing failure of specimens tested in this equipment.

Uniform heating of the test specimen is obtainable by the use of three pairs of end-compensating heaters placed symmetrically with respect to the middle of the specimen. Two of the heaters at one end are shown, one at G projecting 2 inches over the end of the specimen, and one at H wound over the cast-iron bearings outside of the heat-insulating blocks, I. A third pair of separately controlled heaters is wound over the outer portions of the main furnace tube, A.

Eight iron-constantan thermocouples, insulated with flexible asbestos tubing and with hot ends peened into small drilled holes in the specimens, were used for measuring temperatures of the shapes and the larger round specimens. They were systematically distributed along the length of the specimen. For the smaller round specimens, the hot ends of the thermocouples were wrapped around the bar and the junctions bound in position with iron wire. Sufficient depth of immersion in the furnace was provided for these wires and the cold-junctions were iced and connected with a potentiometer. A temperature uniform within $\pm 3°$ C or better was obtainable over the 6-inch gage length of the specimen. The accuracy of temperature measurements was possibly limited to $\pm 5°$ C, due to the use of lot calibrations of the base-metal thermocouples and in some of the tests to the use of a portable potentiometer.

At the ends of the 6-inch gage length small metal pegs were screwed into the angle and the channel shapes for attaching wires at the centroids of the end sections. At these two points, fine annealed alloy wire were hung through tubes in the furnace wall. The lower ends of the wires were weighted and were submerged in cups of oil to dampen vibrations. For some round specimens each of the wires was supported by a wire yoke suspended from a pair of pegs screwed into the specimen at opposite ends of a horizontal diameter at each end of the gage length. For specimens of smaller diameter the loops of wire were located in shallow vertical V grooves that marked the gage length. The freely suspended but taut wires were brought into focus for observations in the microscopes K shown below the furnace.

A view of the part of the apparatus used for obtaining deformation measurements is shown in figure 5. It consists of 2 microscopes mounted in micrometer slides that are secured to 1 transverse pivoted slide, J which may be rotated by screws, R, moved laterally with the screw, L, and in the line of sight with the screw, S. This permits refocusing the microscopes on the gage wires without moving the microscopes in their tubes. During readings only one microscope was moved in its micrometer slide, the other being set on the wire by bodily movement of the supporting slide, J. The micrometer head, M, is graduated to 0.005 mm and readings were estimated to the nearest 0.001 mm.

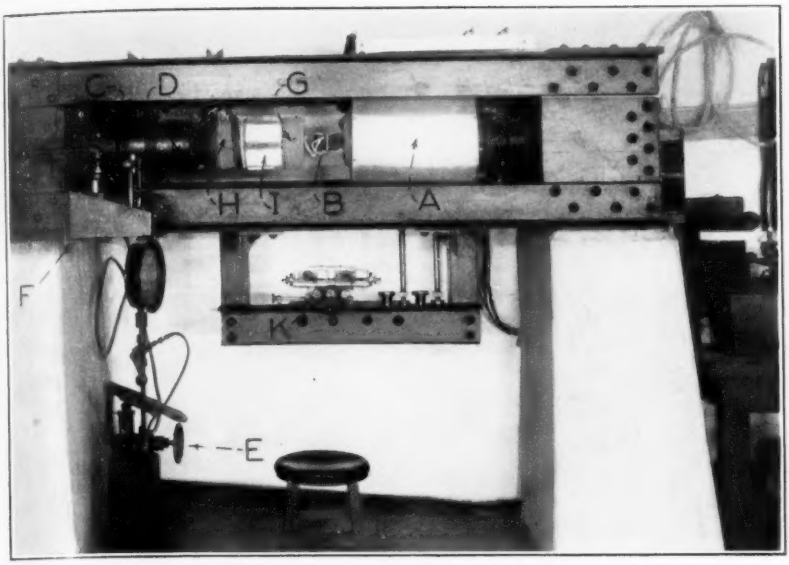

FIGURE 4.—*Equipment used for tests of shapes and of round bars of lots A and B.*

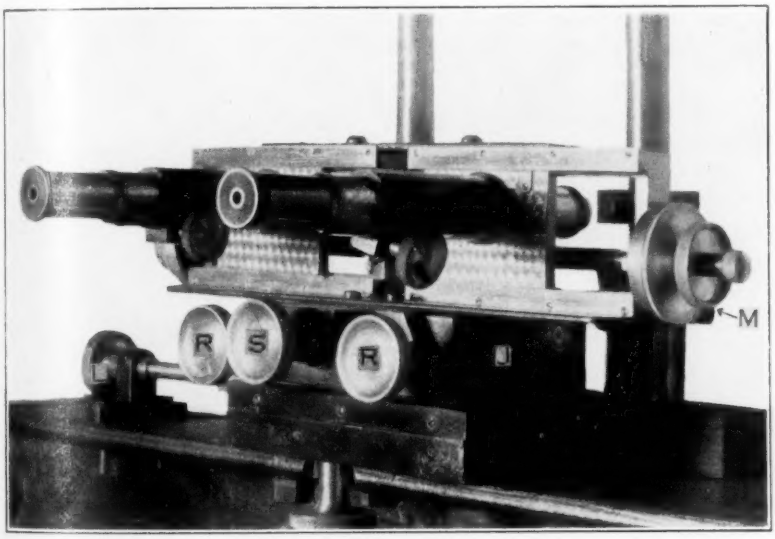

FIGURE 5.—*Apparatus for obtaining deformation measurements.*

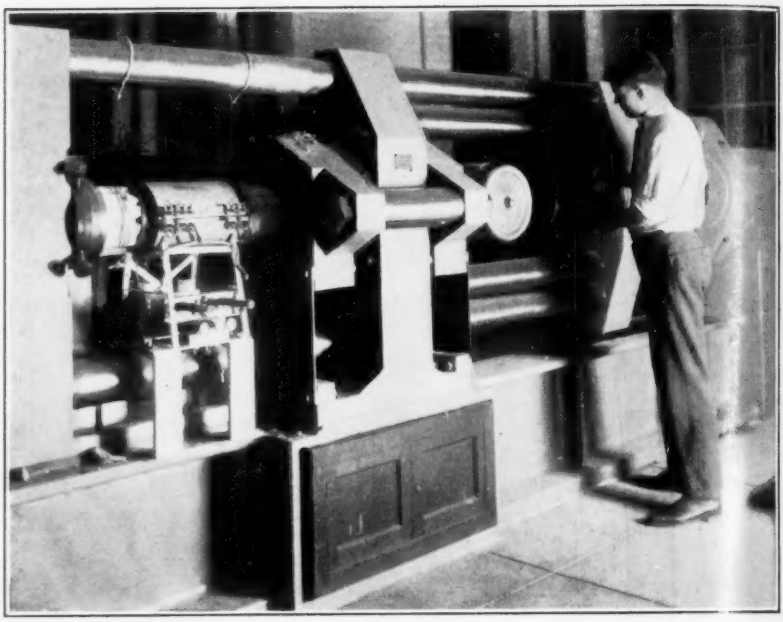

FIGURE 6.—*Equipment used for tests of slender bars of lot B and all tests of lots C, D, and E.*

The Emery testing machine, figure 6, was used for making compression tests of specimens of the higher slenderness ratios and smaller areas since greater accuracy in loading and facility of load control were desirable. In this machine use was made of the deformation equipment and some other parts employed in the original equipment. The bearing blocks were counterweighted, as before, to avoid bending stresses in the test specimen, which was supported on small pins projecting from the centers of the faces of the cast-iron bearing blocks. By use of a split furnace in this equipment the alignment of the test specimen was readily checked and the attachment of thermocouple and gage wires was greatly facilitated. The gage wires were annealed by electric heating in places after attachment in this set-up, and gave almost perfect line targets for deformation measurements. The accuracy of loading with the Emery machine was at least equal to that obtained for the larger specimens with the loading equipment previously described.

Generally, two separate testing procedures were adopted which are referred to as "constant-load" tests and "constant-temperature" tests, although these were combined in a few tests on shapes where some information on the time effect was desired.

In the constant-load test the specimen was set up as previously described and the load was applied before heating was commenced. As heat was applied and the temperature rose, the specimen expanded until the rate of expansion just equaled the rate of compressive deformation of the specimen for the load and temperature obtaining, which occurrence was termed "maximum expansion". Finally a temperature was reached beyond which full load could no longer be maintained, and further compression caused severe buckling of the specimen under decreasing load. Deformation and temperature measurements were made at intervals approximating 5 minutes and more often at critical stages of the test. Thirty tests, which included only four round specimens, were made by the constant-load method.

Most of the remaining tests were made by loading the specimen while the temperature was maintained constant. Measurements of deformation and temperature were made simultaneously for each increment of load.

IV. TEST RESULTS AT ELEVATED TEMPERATURES

Stress-strain records for all tests at elevated temperatures were obtained, but are only given in part here for the several materials tested,[3] figures 7 to 15. The specimen numbers are underlined in the diagrams to distinguish them from the indicated temperature of the test.

The performance of the shapes illustrates local bending and detail failures of columns, while that of the round bars may indicate, within limitations to be noted, primary column action for the temperature, shape, and end conditions imposed.

[3] Further data from the tests with shapes are given in "*Compressive strength and deformation of structural steel and cast iron shapes at temperatures up to 950° C (1,742° F)*", by S. H. Ingberg and P. D. Sale, Proc. ASTM, *26*, part II, 33(1926).

1. RESULTS WITH STEEL SHAPES AND CAST IRON

(a) CONSTANT-TEMPERATURE TESTS

General results of these tests are given in table 4 and figure 9, and typical stress-strain diagrams in figures 7 and 8.

TABLE 4.—*Compression properties of structural shapes at elevated temperatures from constant-temperature tests*

[All specimens are 10.5 in. long except where noted]

GROUP 1.—3 IN. I-BEAM, MANGANESE CONTENT 1.15 PERCENT

Specimen number	Elements of structural shape			Proportional limit		Modulus of elasticity		Ultimate strength		
	Thickness	Least radius of gyration (r)	Slenderness ratio l/r	Temperature	Stress	Temperature	Million lb/in.²	Temperature	Stress	Strain
	In.	*In.*		*°C*	*Lb/in.²*	*°C*		*°C*	*Lb/in.²*	
2				141	35,000	144	23.1	149	72,500	0.0486
3								248	77,500	.0488
4								306	74,000	.0540
5				348	20,000	347	22.2	360	68,500	.0513
6				463	15,000	462	17.4	468	54,500	.0525
7	0.17	0.53	19.8	514	15,000	512	17.4	521	44,500	.0600
8				553	10,000	553	24.2	560	33,650	.0399
9				601	7,000	600	11.9	608	24,400	.0990
10								705	11,000	.0538
11								797	7,500	.0598
12								916	4,800	.0670

GROUP 3.—3 in. I-BEAM, ANNEALED, MANGANESE CONTENT 0.81 PERCENT

27				183	25,000	182	24.2	190	71,500	0.0621
28								343	58,500	.0621
29								403	56,500	.0625
30								503	39,000	.0590
31								592	23,250	.0497
32				591	8,000	589	8.7	593	[2] 14,000	[3] .0692
32a [1]								594	23,000	.1142
33	0.17	0.53	19.0	603	6,000	604	10.7	595	[2] 12,000	.0751
34								702	[2] 9,000	.1222
35				709	3,000	709	5.3	705	[2] 7,000	.1342
36				691	3,500	691	4.0	702	[2] 5,000	.0961
37								732	9,000	.0484
38								828	7,800	.0577
39								910	6,900	

GROUP 4.—4 IN. 7¼ LB CHANNEL, WITH END ANGLES

43				231	20,000	231	26.3	225	63,050	0.0328
43a [1]								255	68,000	.0279
44						311	22.0	304	62,000	.0499
45								380	53,000	.0522
46	0.32	0.46	22.8	501	10,000	501	21.0	497	32,150	.0567
47						599	11.7	601	17,650	.0711
48			5.34					603	19,750	.1667
49			22.8	721	2,000	721	4.5	722	7,700	.0467
50			22.8					848	7,150	.0589

GROUP 5.—4 IN. 5¼ LB CHANNEL, WITH END ANGLES

54				99	30,000	100	31.5	99	47,000	0.0384
55				188	30,000	191	28.0	187	53,400	.0420
56			23.4					288	45,300	.0463
57								402	38,050	.0395
58	0.18	0.45		505	10,000	505	17.0	510	26,250	.0413
59a			11.83	585	4,000	584	12.7	588	17,300	.0300
59b			5.62					613	17,500	.1011
60			23.4					699	7,600	

See end of table for footnotes.

TABLE 4.—*Compression properties of structural shapes at elevated temperatures from constant-temperature tests*—Continued

GROUP 6.—2½ BY 2½ BY ½ IN. ANGLE

Specimen number	Elements of structural shape			Proportional limit		Modulus of elasticity		Ultimate strength		
	Thickness	Least radius of gyration (r)	Slenderness ratio l/r	Temperature	Stress	Temperature	Million lb/in.²	Temperature	Stress	Strain
	In.	*In.*		°C	*Lb/in.*²	°C		°C	*Lb/in.*²	
63	0.50	0.47	22.3			223	26.5	198	68,000	0.0381
63a [1]								275	59,500	
63b [1]								327	45,500	
64								406	37,500	.05
65								453	33,600	.0402
66								494	29,000	.0456
67								556	19,670	.0762
68								593	15,500	.0540
69			11.2					589	20,000	.0754
70			22.3					689	8,500	.0450

GROUP 7.—3 BY 3 BY ¼ IN. ANGLE

80	0.25	0.59	17.8	104	35,000	105	29.2	105	37,400	0.0132
81								149	37,000	.0113
82						250	21.5	248	32,400	.0155
83						308	20.2	310	29,000	.0188
84								362	27,500	.0119
85				399	10,000	399	18.0	407	27,000	.0116
86								499	20,000	.0328
87								519	19,750	.0118
88								605	11,200	.0155
89								738	5,000	.0129

GROUP 8.—3 IN. PRESSED-STEEL JOIST

94	0.069	0.75	14.0	259	23,000	258	19.4	263	37,000	0.0088
95				399	20,000	399	16.0	410	31,500	.0072
96				546	8,000	545	14.9	549	16,100	.0099
97				654	2,000	655	7.2	648	7,000	.0104
98				787	750	786	2.8	793	4,000	

GROUP 9.—CAST-IRON HOLLOW ROUND

103	0.50	0.395	[4] 23.4					250	80,000	0.0320
104								312	66,000	.0225
105								411	72,000	.0300
106				516	15,000	516	14.5	515	49,650	.0642
107								636	22,900	.0730
108								757	7,850	.0995

[1] Retest after cooling of specimen of corresponding number.
[2] Constant load and temperature maintained during these tests to obtain effect of time on yield.
[3] Maximum load and deformation not obtained.
[4] Group 9, effective length of specimen is 9.25 in.

(1) *Structural-Steel Shapes.*—Figure 7 gives results for 3-inch I-sections having manganese content of 0.81 percent, the stock having been annealed before test. In this condition the cold tensile properties, table 2, are comparable with those for a medium grade of structural steel, while in the original unannealed condition this stock was somewhat hard with properties comparable with those recorded for the higher (1.15 percent) manganese content. The symmetrical I-sections exhibited a decided yield region for test temperatures below about 250° C. The end points, indicated by solid points, are plotted

at the ultimate load obtained and the dotted connecting line indicates that the deformation is beyond the scale of the chart, but the values are given in the tables for each specimen.

Although it is generally recognized that short-time tests more closely simulate the conditions met in fire exposure of building members, some time data were obtained as indicated in figure 7, tests 31 to 37, which were run for a portion of the test at the constant loads and temperatures indicated. These come within the range of conditions that cause failure of building columns in fires.

(2) *Cast-Iron Specimens.*—In figure 8 the results of seven tests of cast-iron specimens are given for temperatures up to 757° C. These diagrams indicate the usual lower modulus of elasticity and greater

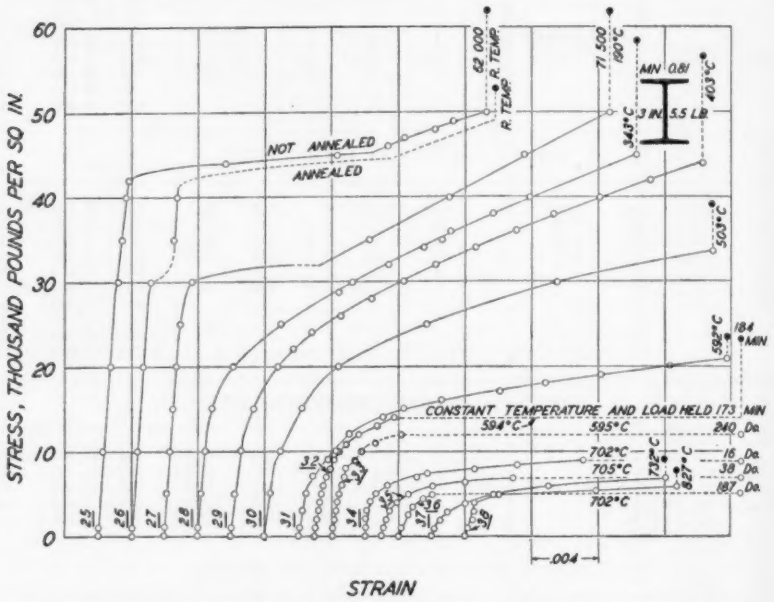

FIGURE 7.—*Stress-strain data from compression tests at elevated temperatures, of 3-in., 5.5-lb* I*-sections, annealed, manganese content of 0.81 percent.*

compressive strength at the lower temperatures for this gray cast iron compared with what is shown in the diagrams for steel.

(3) *Discussion.*—Table 4 gives the compression properties for all of the structural shapes tested at elevated temperatures by the constant-temperature method. The ultimate-strength values given cannot be taken as indicative of the properties of the metal but rather show the individual performance for shapes which differ in symmetry and stability.

Figure 9 gives the variation of compressive strengths with temperature for the 8 steel shapes and the 1 cast-iron shape tested. Here it will be noticed that an increase in strength is shown in the blue-heat range of temperature over that at room temperature, except for the cast-iron and the less stable steel sections (7 and 8). At 300 to 400° C the strength for steel sections nos. 1, 3, 4, 5, and 6 just about equals that at ordinary temperature. For higher temperatures the

strength decreases regularly as the temperature increases, the several shapes maintaining generally the same relative positions established at about 400° C. At about 750° C the symmetrical or heavy sections have nearly the same ultimate strength and the light sections, nos. 7 and 8, show only about half the strength obtained with the more stable sections. For a given stress, say 15,000 lb/in.², the temperature at

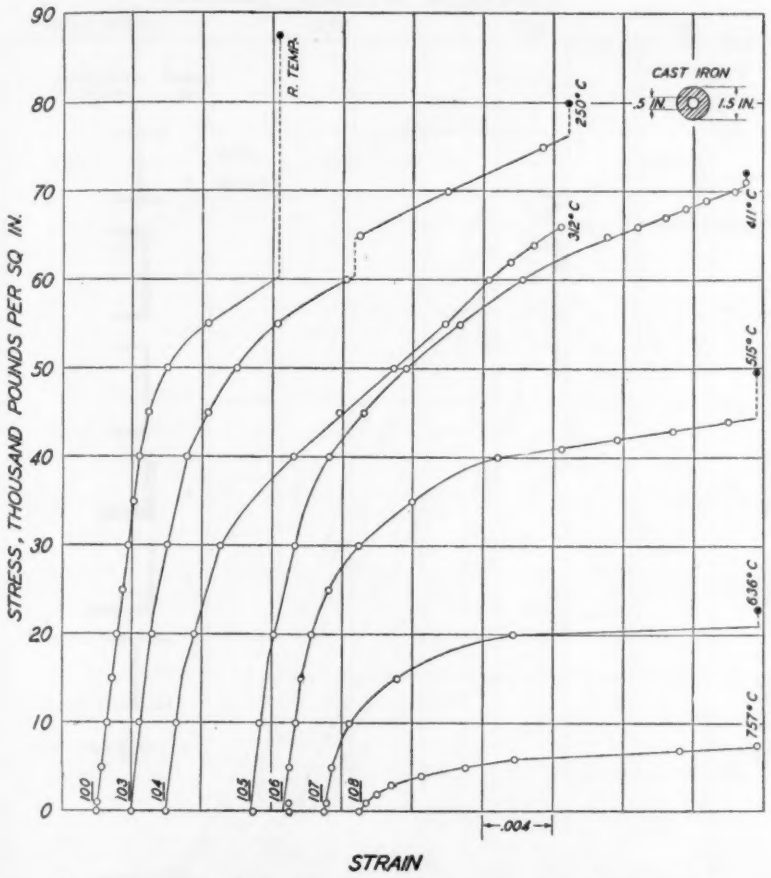

FIGURE 8.—*Stress-strain data from compression tests of hollow round cast-iron specimens at elevated temperatures.*

failure varies from about 550° C for thin-angle and pressed-steel sections (7 and 8) to 650° C for the annealed I-section having manganese content of 0.81 percent.

It will be noticed from the group headings in table 4 that the channel sections had end angles forming a part of the bearings which may have contributed some additional end restraint. The remaining sections except specimen no. 87 had no end angles and all were tested with flat ends subject to the restraint afforded by the testing equipment.

(b) CONSTANT-LOAD TESTS

The main results from the constant-load tests with shapes are given in table 5 and by the dashed lines in figure 9. Typical stress-strain-temperature relations are given in figure 10. The strain shown below the zero line at the start is due to the application of the constant load

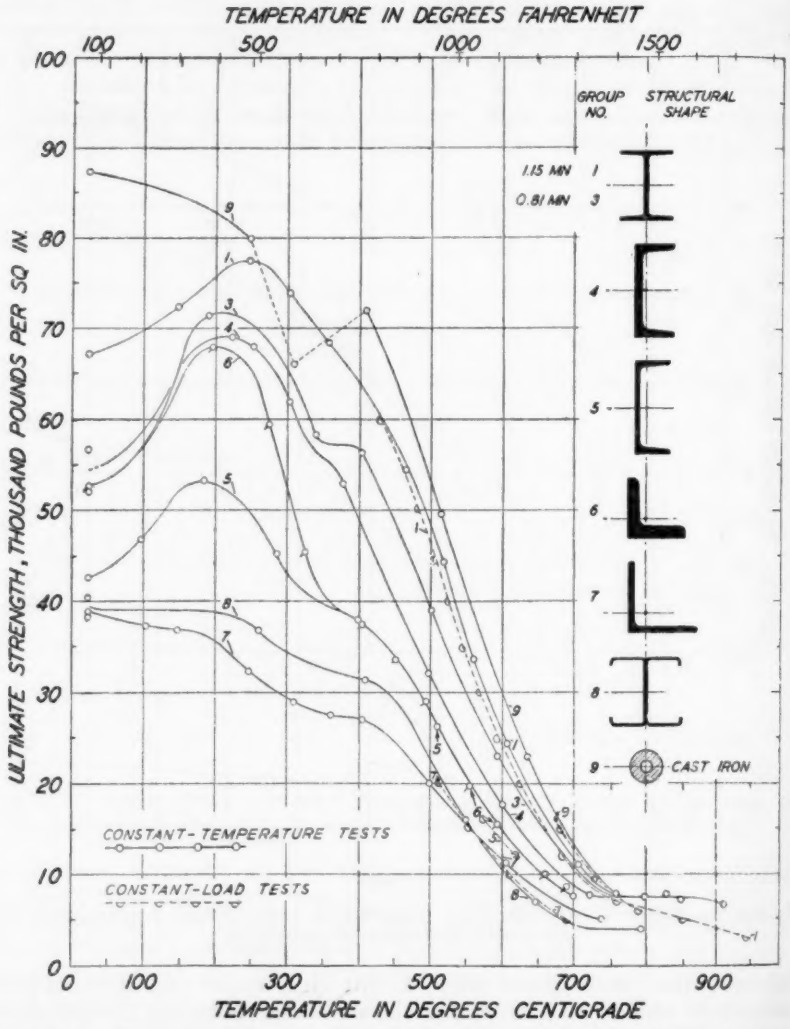

FIGURE 9.—*Compressive strength of cast-iron and structural-steel shapes at elevated temperatures.*

for the test. For group 1, I-sections (fig. 10), this load was below the yield point for applied stresses up to 40,000 lb/in^2. From this initial condition of stress and deformation the specimen expanded under the load as the temperature was raised at the approximate rate of 2 to 3° C per minute. Maximum expansion occurred at the temperatures indicated by the construction line drawn to connect

these points in the diagram, beyond which the rate of yielding exceeded the expansion. Finally failure occurred at the temperature and strain indicated by the arrows and figures. In general, the temperature at failure in the constant-load tests of I-sections was about 10° C below that for the constant-temperature test at the same

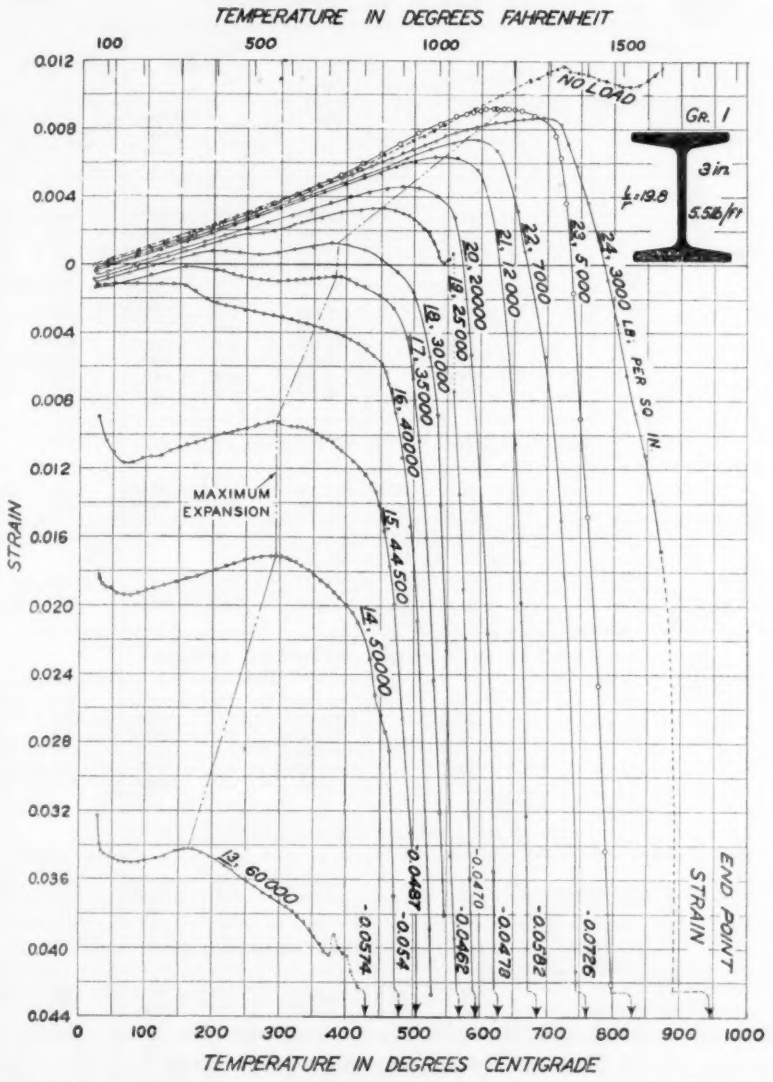

FIGURE 10.—*Data from constant-load tests of group 1,* **I***-sections, 1.15 percent manganese content.*

load, equivalent to a difference of about 1,000 lb/in.^{2} for a given temperature of failure (fig. 9). For the less symmetrical shapes and for slender bars these differences are about half the values given above. This close agreement between results obtained by the two methods of testing constitutes evidence of the reliability of the de-

terminations. The slightly lower results obtained in the constant-load tests can be attributed to the longer time of application of the load causing failure.

TABLE 5.—*Results from constant-load tests*

Group number	Specimen number	Slenderness ratio l/r	Sustained stress	Maximum expansion: Temperature	Maximum expansion: Compressive strain	Ultimate: Temperature	Ultimate: Compressive strain
			Lb/in.[2]	°C		°C	
1	13	19.8	60,000	165	0.03617	428	0.06308
	14		50,000	295	.02073	480	.06125
	15		44,500	295	.01292	502	.05550
	16		40,000	352	-------	527	.05000
	17		35,000	382	.00551	546	.04565
	18		30,000	385	.00368	569	.05422
	19		25,000	448	.00271	593	.05530
	20		20,000	490	.00207	627	.05670
	21		12,000	545	.00128	685	.06800
	22		7,000	575	.00077	758	.07255
	23		5,000	633	+.00017	851	(1)
	24		3,000	693	.00113	945	(1)
4-IN. CHANNEL, 5¼ LB, WITH END ANGLES							
5	52	23.4	16,000	458	0.00160	572	0.03451
	53	23.4	12,000	500	.00098	617	.05270
2½ BY 2½ BY ½ IN. ANGLE							
6	62	22.3	10,000	513	0.00134	659	0.06227
3 BY 3 BY ¼ IN. ANGLE, WITH END ANGLES							
7	74	17.8	20,000	440	0.00230	513	0.01838
	75		15,000	494	.00146	553	[3] .01089
	76		10,000	510	.00070	583	.04055
	77		10,000	510	.00120	608	(2)
	78		5,000	600	.00090	698	(1)
	79		2,500	719	.00055	922	(1)
3 IN. PRESSED STEEL JOISTS							
8	92	14.0	16,000	465	0.00170	531	0.01889
	93	14.0	7,000	553	.00165	646	.01965
CAST IRON, HOLLOW ROUND, FLANGED ENDS							
9	101	23.4	15,000	485	0.00285	681	0.05905
	102	23.4	6,000	610	.00088	790	(1)
LOT D, ⅜ IN. DIAMETER, FLANGED ENDS							
22	175	95.2	15,000	481	0.00126	506	0.01001
	177	95.2	9,500	523	.00105	584	.01161
LOT D, ¼ IN. DIAMETER, FLANGED ENDS							
23	185	143.2	15,000	392	0.00090	397	0.00923
	188	143.2	5,900	583	.00045	629	.01378

[1] Deformation not obtainable, wires broke or touched tubes.
[2] Preliminary loading on specimen; reduced strain otherwise available.

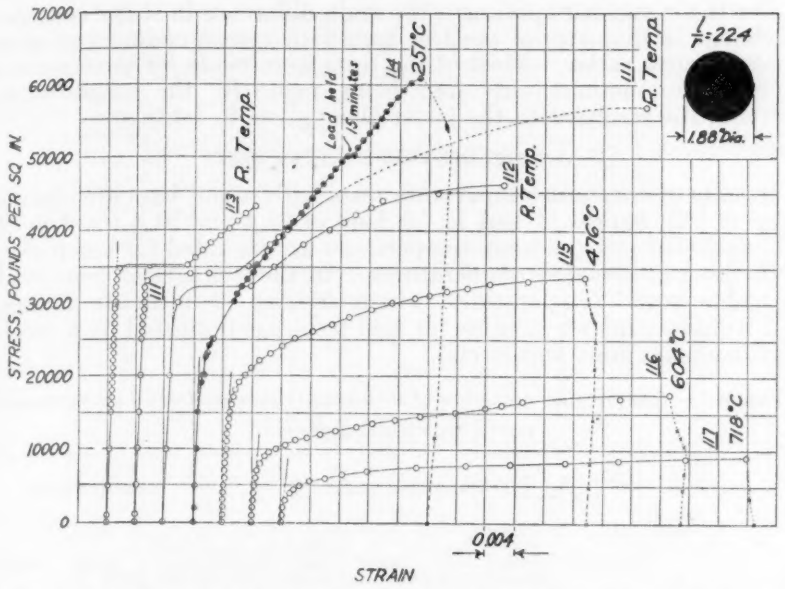

FIGURE 11.—*Stress-strain data from compression tests of 1.88 in. diameter lot A specimens at elevated temperatures.*

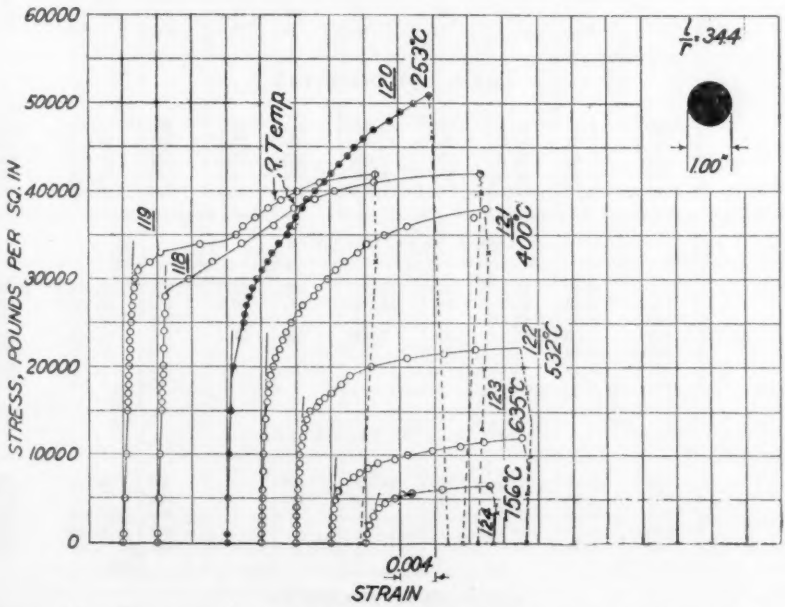

FIGURE 12.—*Stress-strain data from compression tests of 1 in. diameter lot A specimens at elevated temperatures.*

2. RESULTS WITH ROUND-BAR SPECIMENS

For the round-bar specimens the main difference in shape consisted in change in diameter of the test bars with corresponding variations in slenderness ratios. Most of the tests were made by the constant-temperature method, only four being made by the constant-load method, the results with the latter being given in table 5.

(a) CONSTANT-TEMPERATURE TESTS

Results of constant-temperature tests with round bars are given in table 6. In figures 11 and 12 for bars of 22.4 and 34.4 l/r of lot A, the results of tests at room temperature are included for comparison with those at elevated temperatures. In these diagrams tests made at "blue heat" temperatures, which develop an ultimate strength and stiffness superior to those for cold tests, are indicated by a special plotting point (dot and circle).

TABLE 6.—*Compression properties of structural rounds at elevated temperatures*

LOT A, 1⅞ IN. DIAMETER

Group number	Specimen number	Elements of structural shape		Proportional limit		Modulus of elasticity		Ultimate strength		
		Length, l	Slenderness ratio l/r	Temperature	Stress	Temperature	Million lb/in.²	Temperature	Stress	Strain
		In.		*° C*	*Lb/in.²*	*° C*			*Lb/in.²*	
10	114	10.5	23.4	254	15,000	254	27.0	251	60,600	0.0308
	115	10.5	22.4					476	33,500	.0497
	116	10.5	22.4	603	4,000	602	14.5	604	17,500	.0574
	117	10.5	22.4	715	2,000	715	10.9	718	9,000	.0638

LOT A, 1 IN. DIAMETER

11	120	8.65	34.6	255	15,000	255	28.3	253	51,000	0.0235
	121	8.64	34.6	398	12,000	397	30.0	400	38,000	.0261
	122	8.60	34.4	533	9,000	533	17.0	532	22,000	.0260
	123	8.60	34.4	635	4,500	634	8.9	635	12,000	[2].0222
	124	8.60	34.4	745	2,500	747	3.3	756	6,500	.0143

LOT A, ¾ IN. DIAMETER

12	127	8.48	45.3	226	22,000	226	26.7	225	28,000	0.0036
	[1] 127a	8.48	45.3	243	22,000	243	30.0	243	39,000	.0140
	129	8.50	45.4					398	30,000	.0096
	130	8.50	45.4	498	7,000	499	21.1	500	22,000	.0166
	[1] 130a	8.50	45.4					502	20,000	.0063
	132	8.50	45.4					631	11,750	.0153
	133	8.50	45.5					713	6,700	[2].0105

LOT A, ½ IN. DIAMETER

13	136	8.64	69.2	199	24,000	196		200	28,750	0.0021
	137	8.48	67.8	401	12,000	402	19.7	400	23,000	.0046
	138	8.50	67.9					559	15,000	.0063
	[1] 136a	8.64	69.2					633	8,750	.0074
	140	8.46	67.7					711	6,500	.0067

LOT B, 1⅞ IN. DIAMETER

14	142	10.50	22.4					238	57,250	0.0393
	143	10.50	22.4	704	2,500	704	6.8	694	9,750	.0685

[1] Retest after cooling of specimen of corresponding number.
[2] Deformation apparently not maximum obtainable.

TABLE 6.—*Compression properties of structural rounds at elevated temperatures*—Continued

LOT B, 1 IN. DIAMETER

Group number	Specimen number	Elements of structural shape		Proportional limit		Modulus of elasticity		Ultimate strength		
		Length, l	Slenderness ratio l/r	Temperature	Stress	Temperature	Million lb/in.^{2}	Temperature	Stress	Strain
		In.		°C	*Lb/in.*^{2}	°C			*Lb/in.*^{2}	
15	146	8.84	35.5	241	20,000	241	26.1	245	44,500	0.0301
	147	8.90	35.6	599	3,000	600	14.5	601	15,000	.0343
LOT B, ¾ IN. DIAMETER										
16	149	8.87	47.4	239	17,000	240	24.5	240	33,000	0.0178
	150	8.85	47.2					309	31,750	.0200
	151	8.84	47.2	601	4,000	602	11.3	604	13,150	.0219
LOT B, ½ IN. DIAMETER										
17	153	8.72	69.9	299	12,000	297	25.6	300	21,350	0.0082
	154	8.70	69.7	603	5,000	604	9.4	602	11,000	.0092
LOT C, ⅜ IN. DIAMETER (LOW CARBON CONTENT, COLD-ROLLED)										
21	169	8.90	95.4	351	45,000	356	25.2	352	48,350	0.0026
	170	8.88	95.0	606	10,000	606	15.1	607	21,500	.0080
LOT D, ⅜ IN. DIAMETER										
22	172	8.99	96.2	251	25,000	253	25.0	251	28,750	0.0039
	173	8.91	95.4	304	14,000	302	27.8	306	20,000	.0047
	174	8.90	95.2	403	11,000	401	25.0	405	19,100	.0045
	176	8.91	95.3	511	7,000	505	20.3	512	15,650	.0052
	178	8.92	95.4	599	4,500	599	12.8	597	10,850	.0092
	179	8.85	94.7	597	4,000	597	12.8	600	10,950	.0096
	180	8.91	95.4	704	1,750	702	8.0	707	5,500	.0096
LOT D, ¼ IN. DIAMETER										
23	183	8.94	143.7	175	38,500	175	28.5	175	39,300	0.0017
	184	8.94	143.6	296	15,000	293	27.5	296	18,500	.0012
	186	8.94	144.0	402	11,000	402	21.0	401	16,000	.0015
	187	8.93	143.5	560	5,000	560	14.5	561	10,300	.0030
	189	8.94	143.4	640	3,750	640	6.8	643	6,750	.0030
	190	8.85	142.4					716	4,350	.0047
LOT E, ½ IN. DIAMETER										
25a	200	9.32	75.3	495	6,000	498	16.0	501	16,500	0.0072
	201	9.14	74.2					545	14,400	.0077
	202	9.06	71.9	601	3,500	601	11.0	602	10,340	.0061
LOT E, ⅜ IN. DIAMETER										
25b	203	8.98	96.3	499	4,000	505	20.0	501	14,500	0.0030
	204	9.08	99.8	550	5,500	548	15.3	552	11,000	.0026
	[1] 204a	9.08	99.8					556	11,500	.0041
	205	9.20	103.5					550	11,500	.0051
LOT E, ¼ IN. DIAMETER										
25c	206	9.13	157.5					501	12,000	0.0012
	207	9.10	151.0	552	6,000	552	11.7	554	9,500	.0019
	208	9.15	151.5	605	3,000	605	11.7	602	7,000	.0012

[1] Retest after cooling of specimen of corresponding number.

Figures 13 and 14 give some results for lot B, which is a slightly milder grade of structural steel than lot A as indicated by tension and compression tests at room temperature.

In figure 15 is shown the variation with temperature of the ultimate compressive strength for the several qualities of steel and sizes of bars, as based on data given in table 6.

From table 6 there is seen to be a marked decrease of the strain attained at maximum load with increase of slenderness ratio, proportionately greater than the decrease in strength, as would be expected from the stress-strain relations for the material. With regard to effect of temperature, for the lower slenderness ratios, the strain developed at maximum load is somewhat smaller for tests made in the

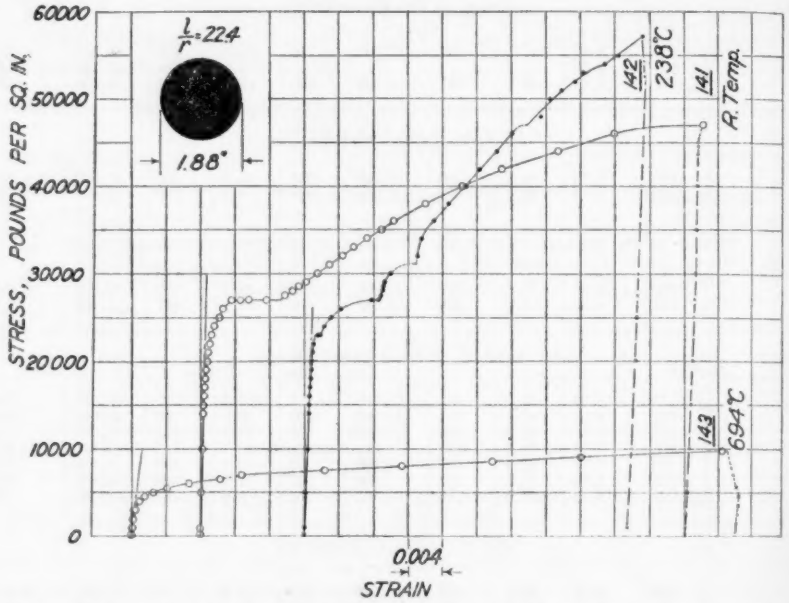

FIGURE 13.—*Stress-strain data from compression tests of 1.88 in. diameter lot B specimens at elevated temperatures.*

temperature range 250 to 300° C (482 to 572° F) than for lower or higher temperatures. Otherwise, in general, the strain at ultimate increases with the temperature of test.

The strains given in table 6 include the shortening between gage points due to the bending of the specimen near failure. Computations based on the deflections of the specimens, indicate this to be within 15 percent of the reported strain for most of the tests, although with slender specimens, where relatively small strains were developed, the percentage is larger.

(b) CONSTANT-LOAD TESTS

In this series tests of the four round bars, nos. 175 and 177 of 95.2 (l/r), and nos. 185 and 188 of 143.2 (l/r), were made of lot D by the constant-load method previously discussed, and the data included in table 5. In the constant-load tests for the slender bars of lot D

failure occurred at an average stress of 1,000 lb/in.^{2} less than that obtained in the constant-temperature test for the same temperature. This corresponds with the difference found for I-sections, discussed in section IV–1(b).

(c) COMPARISON OF RESULTS WITH THOSE DERIVED FROM THEORY AND TESTS OF BUILDING COLUMNS

The test results with round specimens have been analyzed to determine the extent to which they conform with rational column theory. Since all of these specimens failed at stresses higher than the proportional limit, the modifications of Euler's treatment that have been developed [4] to take into account the yield preceding failure, were applied, use being made of the formulas presented by Southwell for solid round sections. No results of these comparisons will be given

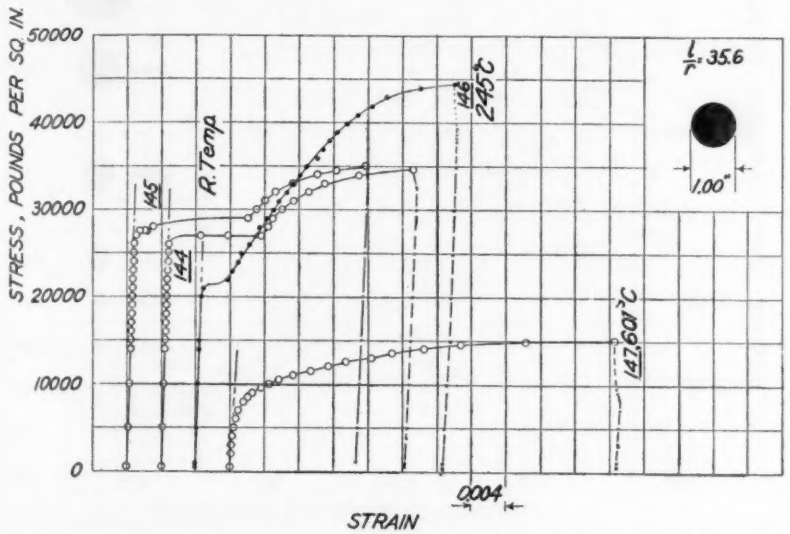

FIGURE 14.—*Stress-strain data from compression tests of 1 in. diameter lot B specimens at elevated temperatures.*

except to state that such a degree of agreement was found between experimental results and those derived from theory as to indicate from the standpoint of temperature effects that extraneous conditions such as eccentricity of load application, uneven bearings, inhomogeneity of material, and initial bends in the specimens, did not seriously affect the results.

Comparisons are made in table 7 with results from two series of tests of building columns reported in BS Technologic Paper T184 and BS Research Paper RP563, respectively. The columns included were either tested unprotected or had coverings that contributed very little to their load-carrying capacity. The temperature in the column steel was measured at 1 or more locations at each of 4 levels. In

[4] Engesser, Zeitschrift des Hannov. Arch. und Ing.—Ver., **35**, 455(1889); Schweizerische Bauzeitung, **26**, 24(1895); Zeitschrift des Vereines deutscher Ingenieure, p. 927(1898).
Considère, Résistance des Pièces Comprimées, Congrès International des Procédés de Construction, Annexe a comptes rendus, p. 382(1891).
Theo. v. Kármán, Mitteilungen über Forschungsarbeiten, Verein deutscher Ingenieure, Heft 81, Berlin, Julius Springer, 1910.
R. V. Southwell, Strength of struts, Engineering, London, **94**, 249(Aug. 23, 1912).

computing the average temperature for a section at a given level, the temperature for given locations in the section was weighted in proportion to the tributary metal area. The average of the three hottest sections is taken as the effective temperature of the column. The end restraints in the second series of tests, columns nos. *1*, *3*, *4*, *5*, and *6*, approximated the condition of 1 fixed and 1 round end, as compared with the fixed-end condition it was aimed to attain in the earlier series.

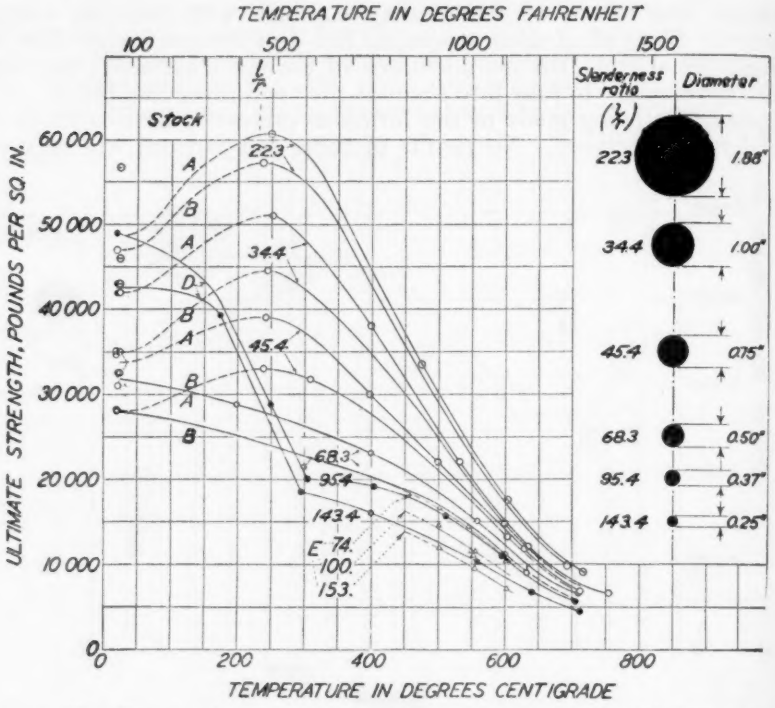

FIGURE 15.—*Compressive strength of solid round bars at elevated temperatures.*

TABLE 7.—*Temperature at failure in fire tests of full-size columns and comparable data from tests of round bars*

COLUMNS 12 FT, 8 IN. LONG WITH FLAT RESTRAINED ENDS[1]

Column number	Column section and protection	Slenderness ratio, l/r	Average load	Time of failure	Temperatures at failure					
					Maximum indicated temperature	Average for hottest section	Average of 3 hottest sections	Round bars for same P/A and l/r as columns		
								Lot A	Lots B & E	Lot D
			Lb/in.[2]	*Hr Min*	°C	°C	°C	°C	°C	°C
1	Solid rolled H, unprotected	75.6	11,750	0:11¼	624	620	588	603	580 B; 585 E	.....
2	Plate and angle, unprotected	111.8	8,900	0:19¼	672	646	624	.....	590 E	610
23	Plate and angle, 2 layers plaster on metal lath	111.8	8,900	2:52	650	634	621	.....	590 E	610

[1] Eight unprotected and 4 protected columns selected from Techn. Pap. BS **15**, (1921); T184.

TABLE 7.—*Temperature at failure in fire tests of full-size columns and comparable data from tests of round bars*—Continued

COLUMNS 12 FT, 8 IN. LONG WITH FLAT RESTRAINED ENDS—Continued

Column number	Column section and protection	Slenderness ratio, l/r	Average load	Time of failure	Temperatures at failure					
					Maximum indicated temperature	Average for hottest section	Average of 3 hottest sections	Round bars for same P/A and l/r as columns		
								Lot A	Lots B & E	Lot D
			Lb/in.[1]	*Hr Min*	°C	°C	°C	°C	°C	°C
3	Plate and channel, unprotected	64.7	12,650	0:14	632	634	622	597	582 B	------
24	Plate and channel, 2 layers of plaster on wire lath	64.7	12,650	2:24	618	615	581	597	582 B	------
4	Latticed channel, unprotected	44.0	14,250	0:11	629	602	595	600	591 B	------
5	Z-bar and plate, unprotected	81.7	11,250	0:14¼	670	613	605	602	582 B; 585 E	------
25	Z-bar and plate, 1 layer of plaster on metal lath	81.7	11,250	1:07¾	658	614	598	602	582 B; 585 E	------
6	I-beam and channel, unprotected	72.1	12,050	0:17	658	644	634	598	580 B; 579 E	------
7	Latticed angle, unprotected	40.7	14,550	0:14	620	611	587	600	593 B; 598 E	------
26	Latticed angle, 1 layer of plaster on metal lath	40.7	14,550	1:23½	605	600	583	600	593 B; 598 E	------
8	Starred angle, unprotected	108.5	9,350	0:21½	620	607	579	------	588 E	610

COLUMNS 10 FT, 4 IN. LONG WITH 1 FIXED AND 1 ROUND END[2]

1	Plate and angle, 2 in. gypsum concrete, plastered	91.2	14,100	6:54	700	620	554	------	518 E	550
2	Plate and angle, 2 in. solid gypsum block, filled and plastered	91.2	12,800	5:47	575	558	554	------	542 E	571
4	Plate and angle, 3 in. hollow gypsum block, no fill, no plaster	91.2	12,800	2:52	558	546	514	------	542 E	571
5	Plate and angle, 2 in. solid gypsum block, plastered, no fill	91.2	12,800	4:21	574	565	543	------	542 E	571
6	Plate and angle, 2 in. solid gypsum block, no fill, no plaster	91.2	12,800	2:33	587	559	508	------	542 E	571

[1] Five protected columns selected from BS J.Research **10**, 737 (1933); RP563.

The last columns in table 7 give for round bars temperatures at failure interpolated for the same load and slenderness ratio as those obtaining in the building-column test with which the comparison is made. The differences between the temperatures compared are within the limits within which the effective temperature of the columns can be considered as known. It may be of interest to note the comparison between the average temperature of 601° C (1,114° F) for the 12 columns in the first group, tested with flat ends, and the average of 594° C (1,101° F) for the round bars. In the second group the average temperature for the 5 columns, tested with end restraint approximating 1 fixed and 1 round end, is 535° C (995° F) and that for the round bars in the comparison, 552° C (1,026° F). As previously indicated, the end restraint in the tests of round bars was

probably intermediate between those obtaining for the two respective column groups.

The results with round bars in point of ultimate strength in the temperature range 450 to 600° C can be expressed approximately by the empirical formula,

$$P/A = 10{,}000 \left(\frac{1870}{T}\right)^2 \left(\frac{r}{l}\right)^{1/2},$$

where P/A is the average stress in pounds per square inch and T the average temperature at failure in degrees C. The deviation of ultimate strength obtained with the formula from individual test results is within ± 15 percent of the latter, while the maximum deviation of individual results from the general trend of results at given temperatures is about 14 percent. As applied to the results of tests with the building columns given in table 7, approximately the same maximum percentage deviations from the individual and average of test results obtains.

3. EXPANSION TESTS

The materials tested included structural steel, cast iron, and 42-percent nickel steel. Expansion bars ⅜ to 1½ inches in diameter were cut from specimens 2, 99, 127, 142, and 171 after the regular compression tests with them were completed. Expansion bars of three diameters (1½, 1, and ½ inch) were also cut from the remaining 1½-inch diameter stock of lot E. The apparatus for measuring deformation and the split furnace employed in some of the compression tests were used for the expansion tests. In all these tests expansion observations were made with fine alloy wires hung from V-grooves spaced 6 inches apart on the specimen. The wires were weighted at the free ends and annealed in place as previously described to assure the required degree of straightness.

In figure 16 the average expansion per unit length is plotted against temperature. The annealed condition was obtained by heating above the thermal critical temperature for structural steel, followed by slow cooling. The difference between data from the first run and those obtained in the subsequent annealed condition is not large. It appears that slightly larger expansion obtains for the annealed condition. The usual growth for the first runs on cast-iron specimens was obtained as shown at a temperature near 700° C. It is of interest to note the relatively low expansion of the 42 percent nickel steel.

In figure 17 the average data for all expansion tests of structural steel are given for both total expansion and corresponding average coefficient of expansion from 20° C to higher temperatures.

The expansion data indicate that structurally restrained members would bend or give evidence of initial failure after a moderate temperature rise in the steel above that of the restraining members. Fortunately structural frames do not give full restraint because of their normal elasticity, nonrigid connections, and their own expansion from the fire that causes expansion of the restrained member. Even so, the stresses thus induced, particularly in floor members, may become relatively high. For building columns, axial stresses from expansion would be induced only by differences in average temperature between columns within a building story or portion thereof.

V. CONCLUSIONS

1. MATERIAL, SPECIMENS, AND TEST CONDITIONS

The different stocks of steel included in the tests, while presenting a considerable range in properties, were identified as coming within the general range of material acceptable under current specifications for structural steel.

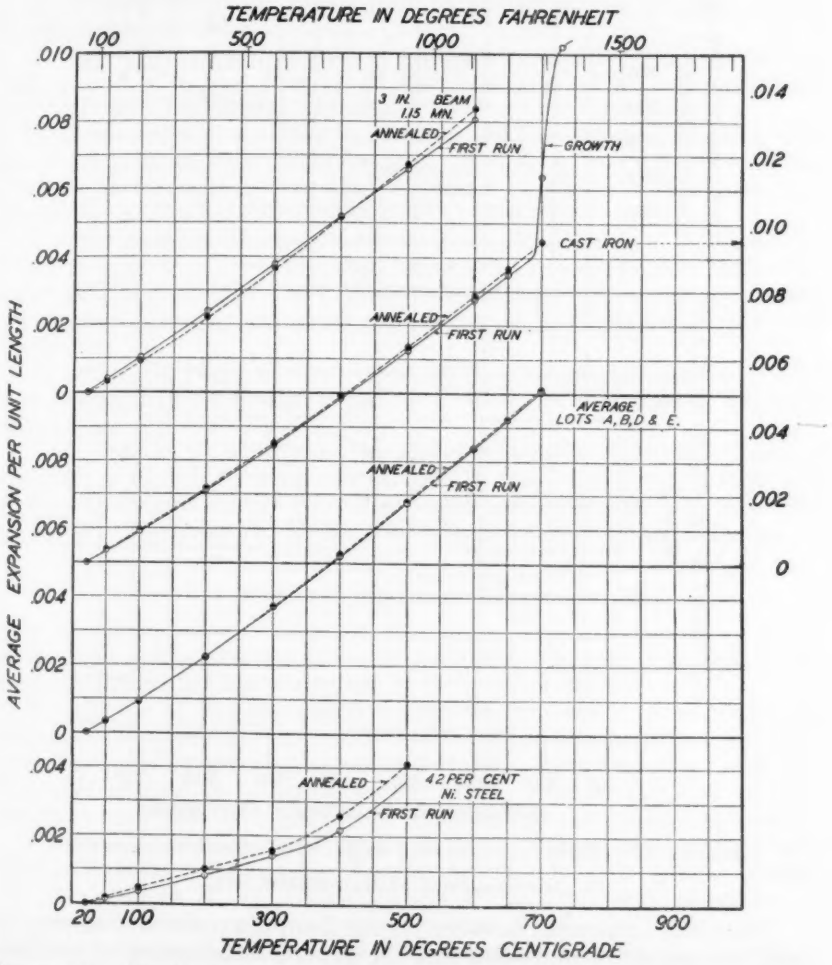

FIGURE 16.—*Average expansion per unit length above 20° C for structural steel, cast iron, and nickel steel.*

Since the compressive strength is influenced greatly by the shape of cross section and the slenderness ratio, a range in both was introduced. In point of stability, the range in specimens extended from those of relatively thin material and unsymmetrical section that failed by local buckling, to fully symmetrical sections proportioned to act as homogeneous units under load application.

The test conditions were designed in part to simulate those to which building columns are subjected when exposed to fire. While the effect of duration of load and temperature were determined from this standpoint, the results should not be taken as applicable to the design of columns to be subjected to load and high temperature for longer periods.

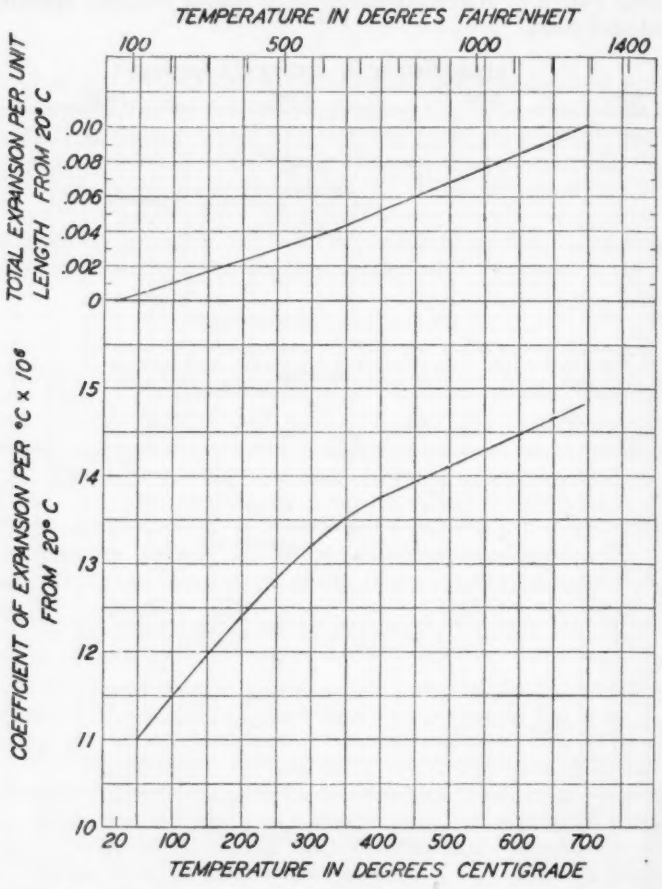

FIGURE 17.—*Total expansion and coefficient of expansion above 20° C.*

Average values for all structional-steel tests.

The good agreement between results from the constant-temperature and the constant-load tests and the general consistency of results in point of ultimate strength at given temperatures indicate that applied load and temperature were measured with the requisite accuracy.

While no great refinement is claimed for the strain measurements, the long range of the instruments permitted determinations of deformation up to the ultimate in nearly all tests.

2. GENERAL CONCLUSIONS

The variation of the compressive strength of structural steel with temperature was determined within the limits defined by the tempera-

ture range included the methods of testing, and the range in shape and proportions of specimen outlined above.

One group of tests with cast-iron specimens of low slenderness ratio was included for comparative purposes, the strength developed being a little higher than any obtained with structural steel for the same temperature and slenderness ratio.

At room temperature an ultimate strength appreciably higher than the yield point was obtained except with the light-angle and pressed-steel sections and with round bars of smaller diameter than three-fourths inch (45 l/r).

In tests with structural steel at temperatures of 250° C (482° F) or higher, and with cast iron at all temperatures, no well-defined yield point or yield region was developed.

In all tests except with the light-angle and pressed-steel sections and round bars of smaller diameter than three-fourths inch (45 l/r), an increase in strength above that obtained at room temperature was developed at temperatures near 250° C (482° F).

For specimens of the same material having symmetry and proportion of parts such that local or detail failure did not occur, the main element affecting strength at a given temperature was found to be the slenderness ratio, as would be expected with properly controlled test conditions.

Agreement in point of ultimate strength at given temperatures and slenderness ratios was also found with results of fire tests of building columns.

The variation with temperature and slenderness ratio of the ultimate strength of round, structural-steel bars in the temperature range 450 to 600° C (842 to 1,113° F) and of building columns in the range 500 to 635° C (932 to 1,175° F) is given approximately by the formula

$$P/A = 10{,}000\left(\frac{1870}{T}\right)^2\left(\frac{r}{l}\right)^{1/2}$$

where P/A is the average stress in pounds per square inch and T the temperature at failure in degrees C.

The results of the expansion determinations taken in conjunction with the stress-strain relations defined for given temperatures, indicate that if a building member is restrained by the surrounding construction and heated to a higher temperature, stresses induced by the restraint may become higher than those due to the supported load.

Acknowledgment is made to L. R. Sweetman of the engineering-mechanics section for assistance on the tests made in the Emery testing machine, and to R. M. Hamilton and F. M. Hoffheins, members of the fire-resistance section of the National Bureau of Standards, for aid in conducting the tests and reducing and verifying experimental data. The author expresses his appreciation to S. H. Ingberg, chief of the fire-resistance section, for constructive suggestions during the progress of the research project.

WASHINGTON, August 25, 1934.

U.S. DEPARTMENT OF COMMERCE NATIONAL BUREAU OF STANDARDS

RESEARCH PAPER RP742

Part of Journal of Research of the National Bureau of Standards, Volume 13, November 1934

EFFECT OF COLD-ROLLING ON THE INDENTATION HARDNESS OF COPPER

By John G. Thompson

ABSTRACT

Specimens of tough-pitch electrolytic copper, commercial oxygen-free copper, and single crystals of copper of different orientations, were subjected to severe cold-rolling to determine the effect on the properties, particularly on the hardness. In all cases the indentation hardness increased to a maximum value which was maintained during subsequent reduction until the hardness determinations became unreliable owing to the thinness of the specimens. No irregularities were encountered except in the case of very thin specimens. The results were confirmed by determinations of tensile strength of some of the specimens and by the application of Meyer's analysis to some of the data. The effect of severe cold-rolling on the indentation hardness of copper was not materially affected by the initial thickness of the specimen, the presence or absence of 0.4 percent of oxygen, the change from polycrystalline to single crystal specimens, or the orientation of the single crystals with respect to the plane of deformation.

CONTENTS

	Page
I. Introduction	745
II. Materials and procedure	746
III. Cold-rolling and hardness	748
1. Hot-rolled electrolytic copper	748
2. Commercial oxygen-free copper	751
3. Single crystals of copper	753
IV. Summary	756
V. References	756

I. INTRODUCTION

The effect of severe cold-working on the properties, particularly on the hardness, of metals such as copper has been the subject of extended discussion. It is common knowledge that moderate amounts of cold-work materially increase the hardness and tensile strength of many metals, but that an excessive amount of cold-work may result in the development of internal or external structural defects which seriously impair the mechanical properties.

Several years ago Rawdon and Mutchler (3)[1] interpreted results of hardness measurements of severely cold-rolled strips of copper as indicating the attainment of maximum hardness after a moderate amount of reduction by cold-rolling, after which further reduction was accompanied by a progressive decrease in hardness. In the discussion

[1] The figures given in parentheses here and throughout the text correspond to the numbered references, arranged in chronological order, at the end of this paper.

of their paper the reversal of hardness of copper during progressive cold-rolling was stated to be contrary to commercial experience. Subsequently, Moore (4), Fogler and Quinn (6), Hoyt and Schermerhorn (7), Malam (12), Sandifer (16), and Kawai (18) failed to find irregularities or a reversal in the hardness of copper during cold-rolling, and Harris (13) and Smith (21) found that the tensile strength of copper increased regularly with increasing amounts of cold-work. On the other hand, anomalous behavior of copper during cold-rolling was reported by Alkins (1), and subsequently by O'Neill and Cuthbertson (20) who ascribed irregularities in the ball-indentation hardness values to observational errors resulting from the ridge of metal which was extruded around the ball in the case of specimens taken during certain stages of cold-rolling when reorientation of the crystals was taking place. Johnson (2) found a reversal in hardness of copper and the results of Körber and Hoff (14) showed that both the tensile strength and Brinell hardness of cold-rolled copper rose to a maximum and subsequently declined, although the decrease was not as pronounced as was reported by Rawdon and Mutchler. In a discussion Herbert (9) reported that the hardness of a number of metals increased to a maximum and then declined, during the application of the pendulum hardness tester, although the total decrease in hardness was slight.

In addition to the illustrations cited of anomalous behavior in copper, an example of the existing uncertainty is found in the varying reports of the maximum hardness attainable through cold-rolling. For example, the maximum Brinell number for copper may be 130 according to Moore (4), 109 according to Körber and Hoff (14), or about 114 according to Smith (21). Part of these differences presumably originate in the different ball diameters and loads employed.

A number of suggestions have been offered to account for this apparently anomalous behavior of copper. Spontaneous annealing during rolling has been accepted to explain the work softening of metals such as cadmium (17) or lead alloys (11, 15, 19), but this possibility apparently did not apply to copper, as Rawdon reported additional experiments in which similar behavior was observed when the rolls and specimens were cooled with iced brine throughout the rolling operation. It was suggested that the hardness of copper after cold-rolling might be dependent upon the original thickness and hardness of the material, by the details of rolling procedure such as the roll diameter and amount of reduction per pass, and that the determinations of hardness might be influenced by the anvil effect and by sources of error inherent in the determination of ball-indentation hardness values. The use of Meyer's analysis (5) to verify the simple determinations of Brinell hardness was suggested (8). The possible effect of aging phenomena was discussed, but it was agreed (3, 6, 7) that copper does not age-harden appreciably after rolling.

The present investigation was undertaken to study the effect of some of these factors on the hardness-reduction relation for copper.

II. MATERIALS AND PROCEDURE

Cold-rolling experiments were conducted on various specimens of copper, including electrolytic copper in the cast and in the hot-rolled conditions, commercial oxygen-free copper, and single crystals of

oxygen-free copper. Specimens varying in initial thickness from 0.2 to 3.0 inches were rolled to thicknesses of 0.02 inch or less, without intermediate annealing. Three two-high rolling mills were available, equipped, respectively, with rolls 2, 5, and 16 inches in diameter. Relatively light reductions per pass were employed in all of the rolling experiments, in order to avoid heating and possible consequent annealing during the rolling operations. In spite of the light reductions, the bars frequently were warm to the touch as they emerged from the rolls, but whenever this occurred the bars were cooled in ice water after each pass through the rolls.

The 16-inch mill was used for all specimens thicker than 0.5 inch. Rolling was continued in this mill down to thicknesses of about 0.2 inch, with specimens between 0.5 and 0.2 inch in thickness receiving light finishing passes in the 5-inch mill in order to improve the surface for the hardness determinations. In addition to these finishing passes, the 5-inch mill was used for rolling specimens of 0.5 inch or less initial thickness in the annealed condition, and to complete the rolling of specimens previously reduced to about 0.2 inch in thickness in the 16-inch mill. Rolling in the 5-inch mill usually was continued until the specimens were about 0.005 inch in thickness. The 2-inch hand-operated mill was used for a few experiments on material 0.4 inch or less in initial thickness, in the soft condition.

In all cases the difficulty of rolling increased rapidly to a maximum at a reduction of approximately 50 percent from the original thickness, or at a reduction ratio [2] of about 2, and then decreased on further reduction. This difficulty in rolling was the result primarily of the tendency of the copper to curl and consequently to emerge from the rolls in a series of waves rather than in a flat strip. Subsequent determinations of hardness showed that this curling tendency was not due to the development of maximum hardness, in fact the curling was most noticeable when the material was approximately half-hard and disappeared before maximum hardness was attained. The tendency is perhaps associated with the penetration of work-hardening to the center of the specimen.

Corner cracks, which developed rather frequently during such severe cold-rolling, were removed by filing or machining before they spread across the strip.

Coupons were removed at suitable intervals during the rolling of each specimen. Hardness determinations were made on the rolled surfaces of the coupons, without additional polishing which might have influenced the results of determinations under the light loads which were used. Both Vickers and Brinell numbers were determined, each under a variety of loads. The Vickers and Brinell results in all cases yielded similar curves for the hardness-reduction relation although the Vickers numbers usually were higher than the Brinell numbers for the same specimen. For the sake of brevity only the Vickers results are discussed in this paper.

The Vickers numbers were determined by means of a diamond pyramid indenter under loads of from 5 to 30 kg, with each load

[2] In Rawdon and Mutchler's paper (3) the hardness numbers were plotted against reduction ratio instead of against percent reduction, in order to emphasize the changes which occurred at higher reductions. This reduction ratio $=\frac{To}{T}$ where To=initial thickness of specimen, and T=thickness after rolling. The use of reduction ratio rather than percent reduction has been found convenient to express results in the majority of cases throughout this paper.

applied to the indenter for a period of 10 seconds. Four or more impressions were made on each specimen; both diagonals of each impression were measured; and the eight or more measurements were averaged to obtain a single Vickers number for the specimen from the formula

$$V_N = \frac{P}{A} = \frac{2P \sin 68°}{l^2} = \frac{1.854P}{l^2}$$

where V_N = the Vickers number
P = applied load, in kg
A = area of contact between the 136° indenter and the specimen
l = length of the diagonal of the indentation, in mm

The Vickers numbers reported in this paper were obtained from specimens supported on a hard (plate glass) anvil. It is believed that these numbers were not influenced by the anvil. A study was made of the effect of the anvil, by using a soft (annealed copper) anvil in addition to the hard anvil; this study will be reported in another paper.

III. COLD-ROLLING AND HARDNESS

A few attempts were made to cold-roll electrolytic copper directly from the soft, cast condition in order to avoid any complications which might result from the customary hot-rolling of cast copper. It was soon evident, however, that the desired amount of cold-work could not be satisfactorily attained with the coarsely crystalline cast copper used.

1. HOT-ROLLED ELECTROLYTIC COPPER

A 200-pound bar of selected electrolytic copper, containing 0.40 percent oxygen, was the basic material for the next series of experiments. The bar had been reduced by hot-working to 50 percent of the thickness of the original cast bar. The Brinell number of the material, as received, was about 60 (1/16-inch ball, 15-kg load). Small bars for cold-rolling were cut from the large bar in such fashion that the planes of rolling for subsequent cold-rolling operations were the same as for the original hot-rolling. The small bars were annealed about 2½ hours at 300° C, which reduced the hardness number to about 50 without appreciably increasing the grain size.

Bars ranging from 3 to 0.2 inch in initial thickness were cold-rolled without intermediate annealing to final thicknesses between 0.02 and 0.005 inch, coupons for the determination of indentation hardness being removed at suitable intervals during the rolling operations. Representative schedules for the rolling of tough-pitch electrolytic copper and for the other forms of copper used in this investigation are shown in table 1. Both Brinell and Vickers numbers, under a variety of conditions, were determined for these coupons but the present paper is limited to a discussion of the Vickers numbers of some of the sets of coupons, selected to illustrate the hardness-reduction relations which were consistently indicated by all the data. The effect on the Vickers hardness (10-kg load) of copper of cold-rolling from initial thicknesses between 0.2 and 3 inches to final thicknesses of 0.02 inch or less, is shown in figure 1.

TABLE 1.—*Schedules of cold-rolling operations*

TABLE 1.—*Schedules of cold-rolling operations*

Tough-pitch electrolytic copper													Oxygen-free copper				Single crystals			
Coupon	Passes [1]	Reduction	Thickness	Coupon	Passes [1]	Reduction	Thickness	Coupon	Passes [1]	Reduction	Thickness	Coupon	Passes [1]	Reduction		Thickness	Coupon	Passes [1]	Reduction	Thickness
		To T	*Inches*			*To T*	*Inch*			*To T*	*Inch*			*Percent*	*To T*	*Inch*			*To T*	*Inch*
A–0	0	1.0	3.0	C–0	0	1	1.0	D–0	0	1	0.4	F–0	0	0	1.0	0.5	G–0	0	1.0	0.61
1	69	2.2	1.4	1	25	2	.494	1	18	2	.2	1	13	20	1.25	.4	1	10	1.1	.55
2	25	3.8	.792	2	21	5	.202	2	10	4	.101	2	15	40	1.7	.3	2	10	1.4	.45
3	29	10	.300	3	15	10	.100	3	1	4.4	.091	3	8	50	2.0	.25	3	15	2.1	.30
4	14	20	.149	4	6	20	.049	4	1	5	.080	4	11	60	2.5	.20	4	16	3.1	.20
5	9	30	.100	5	2	30	.033	5	1	5.7	.070	5	12	70	3.3	.15	5	14	6.1	.10
6	8	41	.073	6	2	42	.024	6	1	6.7	.060	6	10	80	5.0	.099	6	6	8.8	.07
7	4	50	.060	7	3	49	.020	7	1	8	.050	7	3	82	5.6	.089	7	8	15	.04
8	3	60	.050	8	2	57	.017	8	1	10	.040	8	4	84	6.3	.08	8	7	31	.02
9	3	75	.040	9	4	74	.013	9	2	13	.030	9	4	86	7.1	.07	9	5	62	.01
10	3	97	.031	10	5	100	.010	10	2	20	.020	10	4	88	8.3	.06	10	2	77	.008
11	3	143	.021	11	6	143	.007	11	2	36	.011	11	5	90	10	.05	11	2	102	.006
								12	1	50	.008	12	5	92	12.5	.04	12	1	123	.005
								13	1	57	.007	13	6	94	16.7	.03	13	3	154	.004
								14	1	80	.005	14	4	96	25.0	.02				
								15	2	100	.004	15	2	97	33.3	.015				
												16	4	98	50	.010				
												17	2	98.2	55.5	.009				
												18	2	98.4	62.5	.008				
												19	3	98.6	71.5	.007				
												20	4	98.8	83.3	.006				
												21	7	99.0	100	.005				
												22	5	99.3	125	.004				

[1] Each figure recorded in this column is the number of passes required to reduce the thickness from that of the preceding coupon to that of the coupon indicated.

The results indicated that the indentation hardness of copper increased rapidly and continuously during the first stages of cold-rolling, in subsequent stages the hardness continued to increase but at a slower rate until a maximum hardness was reached, after which the hardness remained constant during further reduction. The only irregularities encountered were variations in hardness of some of the coupons obtained during the stages when the specimens curled badly during rolling. The maximum hardness number in all cases was between 120 and 130 and was independent of the initial thickness of specimen used. Although the plotted results indicated some differences in the rate at which the maximum hardness was attained, in

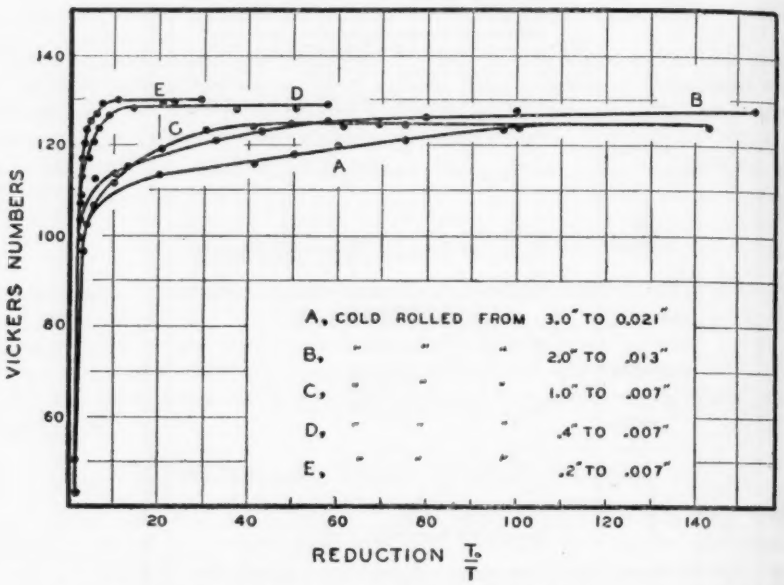

FIGURE 1.—*Effect of cold-rolling on the indentation hardness of tough-pitch electrolytic copper.*

general, variations in initial thickness of the specimen did not appear to affect materially the general characteristics of the hardness-reduction relation. Likewise, there was no material difference observed in the results obtained from rolling in the 5-inch and 16-inch mills. To study further the effect of roll diameter on the hardness of electrolytic copper, annealed bars 1 inch wide, 6 inches long, and either 0.2 or 0.4 inch thick were rolled between rolls 2 inches in diameter, in a hand-operated mill, closely approximating the conditions of Rawdon and Mutchler's experiments. Great difficulty was encountered in the operation of these hand rolls, as a result of the tendency of the specimens to curl during certain stages of reduction. This curling tendency led to inconsistent results in the determination of hardness; for example, a coupon might be five or more Brinell units harder on the convex side than on the concave surface. In general, however, the hardness-reduction relation corresponded with that of the curves in figure 1.

A number of coupons were examined for uniformity of hardness throughout the cross section. The results of the Vickers hardness determinations indicated that the center of the bar was softer than the rolled surfaces during the initial stages of reduction but that reduction of 50 percent, equivalent to a reduction ratio of 2, from initial thicknesses of 3 inches or less produced uniform hardness throughout the cross section.

2. COMMERCIAL OXYGEN-FREE COPPER

Specimens of commercial oxygen-free copper were cold-rolled to compare the hardening of this material with the results obtained for electrolytic copper. The commercial oxygen-free copper, in the form of bars 12 by 2 by 0.5 inches of hot-rolled material, was obtained through the courtesy of the United States Metals Refining Co. These bars were cold-rolled in the 5-inch mill without annealing to thicknesses of about 0.005 inch, under rolling schedules (table 1) similar to those employed for electrolytic copper. The rolling was accomplished with noticeably less difficulty than was encountered with tough-pitch electrolytic copper; the tendency to curl during rolling was less pronounced, and side splits and corner cracks were almost entirely absent.

The effect of progressive cold-rolling on the Vickers number of oxygen-free copper is shown in figure 2. The change in Vickers hardness (10-kg load) was continuous with increasing reduction until maximum hardness was reached. The initial stages of reduction were accompanied by a rapid increase in hardness until a maximum hardness number approaching 130 was reached. The maximum hardness, once attained, was maintained during further reduction until the specimens became so thin that hardness determinations were unreliable. These results are similar to those obtained for material which contained 0.4 percent oxygen; evidently the presence or absence of 0.4 percent oxygen does not affect the hardening of copper during cold-rolling.

The changes in tensile strength and in elongation, as a result of cold-rolling, also were determined on the coupons of oxygen-free copper. Flat specimens with a 2-inch gage length, 0.5 inch in width, were used; the central portion of the gage length was further reduced in width by 0.002 inch to insure breaking between the gage marks. The specimens were tested on a hydraulic-type universal testing machine at a rate of travel of the crosshead of 0.1 inch per minute. Wedge grips were used for the thicker specimens and self-alining grips for the thinner ones. Only two specimens were available for each thickness of copper but in general satisfactory duplication of results was obtained.

The results of the tensile tests, also shown in figure 2, in several respects confirmed the results of the hardness determinations. The tensile strength increased rapidly during the first reductions and less rapidly during subsequent reductions. The hardness reached a maximum and thereafter remained constant, but the tensile strength increased continuously throughout the reduction, the thinnest coupon, 0.004 inch thick, yielding the highest tensile strength, 72,000 pounds. The elongation decreased rapidly from an initial value of about 25 percent to about 3 percent and thereafter remained constant at

about 3 percent, within the limits of experimental error. These results are not in accord with results reported by Körber and Hoff (14) who found that the tensile strength and Brinell number of copper reached maxima at a thickness of 0.047 inch, representing a reduction of between 90 and 98 percent, and then decreased slightly on further

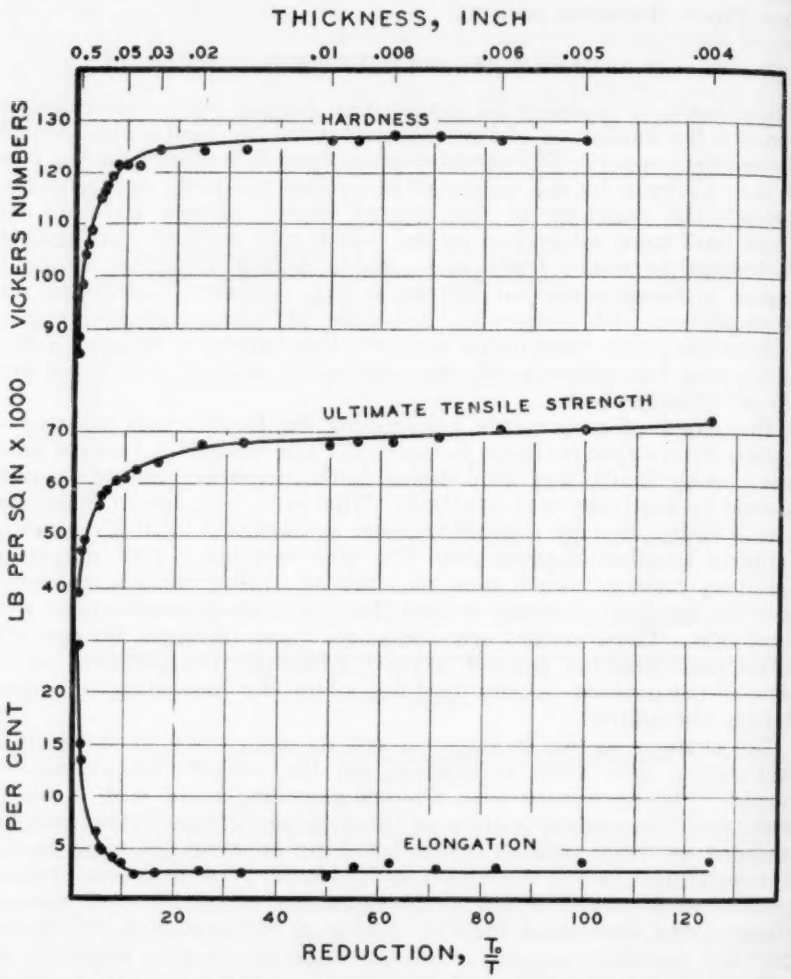

FIGURE 2.—*Effect of cold-rolling on the indentation hardness, tensile strength, and elongation of oxygen-free copper.*

reduction. In the present experiments the Vickers numbers did not fall off until specimens thinner than 0.005 inch were encountered and the tensile strength was still increasing when a specimen thickness of 0.004 inch was reached.

The application of Meyer's analysis [3] to the Vickers hardness results, under loads of from 5 to 30 kg further confirmed the fact that the indentation hardness of oxygen-free copper increased steadily with increasing reduction, at least until the thickness had been reduced to 0.005 inch. The results of Meyer's analysis have been plotted in figure 3, using percent reduction values for abscissas, to emphasize the changes during the early stages of rolling. The "a" values increased steadily to a maximum value of about 70; the "n" value was approximately 2 at 20-percent reduction, and remained constant thereafter until the thickness had been reduced to 0.005 inch. No reversal of hardness was indicated and the "n" values showed that the material was completely work-hardened to the depth affected by

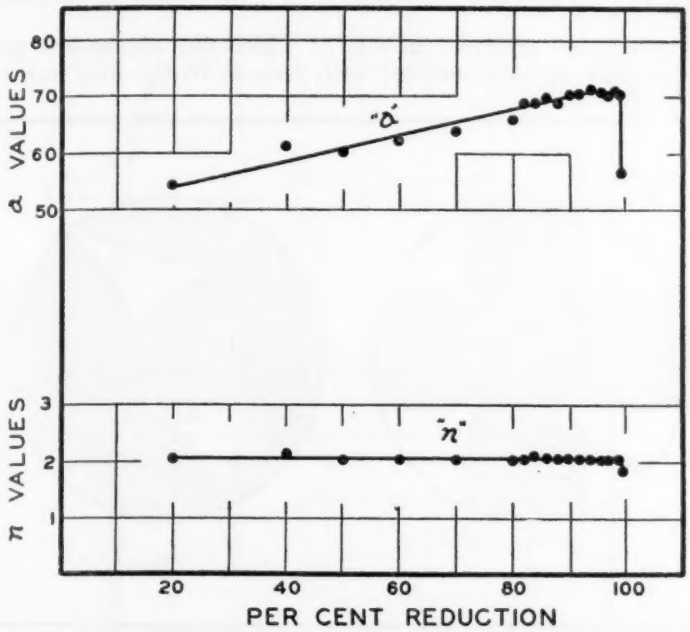

FIGURE 3.—*Meyer's analysis of the indentation-hardness determinations for oxygen-free copper.*

the Vickers indentations, by relatively slight reduction. This is in accord with the conclusions of Harris (13) regarding the skin effect in hard-drawn copper wire.

3. SINGLE CRYSTALS OF COPPER

Tough-pitch electrolytic copper was melted in an elongated graphite crucible, to form a rod about 0.6 inch in diameter and about 5 inches long. Such rods prepared in an Arsem vacuum furnace were practically oxygen free, several analyses showing that less than 0.001 percent oxygen was present. By suitable control of the rate of cooling, it

[3] See the paper by S. L. Hoyt (5) for the detailed procedure of Meyer's analysis as applied to indentation hardness impressions. Meyer's equation for the relation between load and diameter of indentation is $P=aD^n$.

Consequently his method of expressing indentation hardness requires the determination of two factors, a and n.

was possible to produce a rod the lower end of which consisted of a single crystal of copper 0.6 inch in diameter and about 3 inches in length. A number of these single crystal rods were prepared and one end of each rod was machined to a hemisphere. The hemispherical ends were blank etched [4] in 1:1 nitric acid containing a few crystals of ferric chloride, to remove the work-hardened surface resulting from the machining operation. Subsequent etching in ammonia and hydrogen peroxide developed the four-leaf clover pattern of the dodecahedral faces, from which the orientation of the single crystal with respect to the long axis of the rod was estimated. For this study accurate determinations of the crystal orientation, by means of X-ray or other precise methods, was not required; the approximate orientation established by the etching method was sufficient.

Two rods were selected, in one of which the clover-leaf pattern was approximately symmetrical with respect to the long axis of the

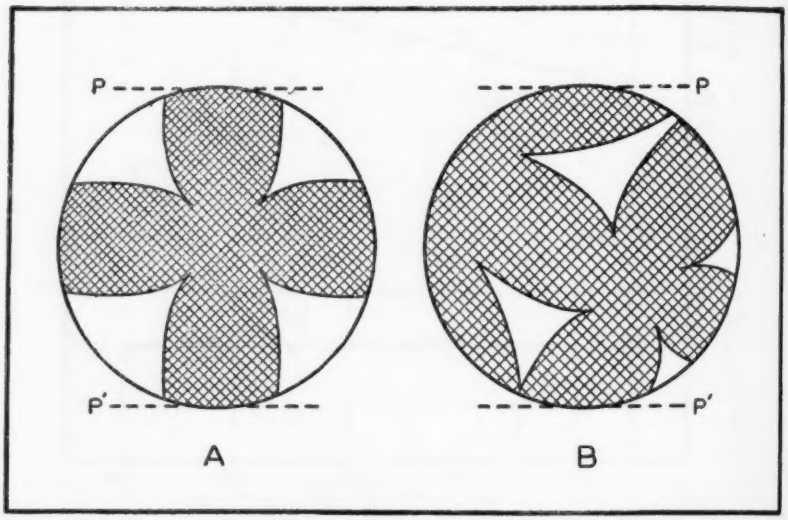

FIGURE 4.—*Etched patterns indicating the orientation in single-crystal rods of copper.*

rod, figure 4 (A), whereas in the other it was not, figure 4 (B). By selecting the proper positions on the circumference of each rod, to define the rolling planes P and P′ in figure 4, it was possible to roll one rod so that the planes of rolling coincided within about 8 degrees with the plane of a cube face; in the other rod the plane of rolling was located between and intersecting the 100 and 110 planes. The 2 rods were cold-rolled in practically identical steps, according to the schedule in table 1. There was no appreciable difference detected in the rolling characteristics of the 2 crystals; both rolled easily and satisfactorily.

Some interesting qualitative information was obtained by re-etching the hemispherical ends of the rods at different stages of the

[4] The blank etching and the selective etching to develop the pattern of the dodecahedral faces followed the procedure of Hausser and Scholz (10).

rolling operations. When the plane of rolling coincided with a cube face of the crystal, as in figure 4 (A), reductions shortened the 2 vertical leaves without affecting the 2 horizontal leaves, until a thickness of 0.2 inch was reached. The original pattern could be restored by reetching although at this point the 2 vertical leaves were almost entirely gone, and the plane of rolling was beginning to encroach upon the horizontal leaves. Etching of specimens thinner than 0.2 inch was not attempted. The survival of the horizontal leaves may indicate that this rolling procedure affected only the layers

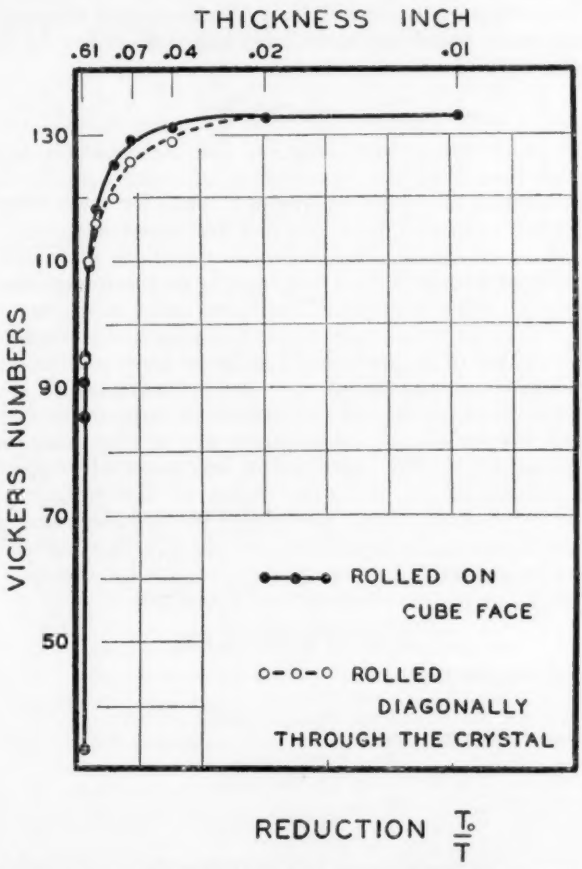

FIGURE 5.—*Effect of cold-rolling on the indentation hardness of single crystals of copper.*

of metal in contact with the rolls. On the other hand, it is possible that horizontal displacement of layers of metal could occur without destroying the etched pattern. Consequently it is not known whether the pattern developed on the end of the cold-worked rod represents the unchanged remainder of the original single crystal or whether it represents the result of a process of slippage and distortion. Somewhat similar results were obtained for the rod which was rolled diagonally through the crystal, although the etched pattern, figure 4 (B), was not as easily identified as was the symmetrical pattern of figure

4 (A). For a satisfactory explanation of these observations, a more precise study by X-ray or other methods is necessary.

Vickers numbers were determined to compare the effects of cold-rolling single-crystal and polycrystalline copper, and to see if there was any difference, on account of orientation, in the hardening of the 2 crystals by cold-work. The rate of change in hardness of the 2 crystals was almost identical as shown in figure 5. Evidently orientation did not exert a pronounced effect on the rate of hardening of copper as a result of cold-work. A comparison of the hardness-reduction curves and of the maximum-hardness numbers attained for mono and polycrystalline copper, indicated that the rate and amount of hardening by cold-work were not materially affected either by the size or number of the crystals of copper.

IV. SUMMARY

The effect of severe cold-rolling on the indentation hardness of copper was determined for specimens of tough-pitch electrolytic copper, commercial oxygen-free copper, and for two single-crystal rods of different orientations. Similar hardness-reduction relations were observed in all cases; the hardness numbers increased with reduction, rapidly at first and then less rapidly as the maximum hardness was approached. The maximum hardness once attained was maintained during further cold-work until the specimens became so thin that determinations of indentation hardness were unreliable. These conclusions were substantiated by determinations of the tensile strength of specimens of one of the grades of copper used and by the application of Meyer's analysis to some of the hardness data. The effect of cold-work on the indentation hardness of copper was not appreciably influenced by the orientation of the rolling plane with respect to the crystalline lattice structure in single-crystal specimens, by the change from single crystal to polycrystalline material, by the presence or absence of 0.4 percent oxygen, or by changes, between 0.2 and 3 inches, in initial thickness of specimen.

V. REFERENCES

1. J.Inst.Metals **23**,381(1920).
2. J.Inst.Metals **23**,443(1920).
3. Trans.Amer.Inst.Min.Met.Eng. **70**,342(1924).
4. J.Inst.Metals **32**[2],407(1924).
5. Trans.Amer.Soc.Steel Treating **6**,396(1924).
6. Trans.Amer.Inst.Min.Met.Eng. **71**,889(1925).
7. J.Inst.Metals **35**[1],231(1926).
8. Trans.Amer.Inst.Min.Met.Eng. **73**,657(1926).
9. Trans.Amer.Soc.Mech.Eng. **48**,705(1926).
10. Wiss.Veröff.a.d.Siemens-Konzern **5**[3],144(1926–27).
11. J.Inst.Metals **38**,315(1927).
12. J.Inst.Metals **40**,375(1928).
13. Proc.Amer.Inst.Min.Met.Eng.Inst.Metals Div. **78**,518(1928).
14. Mitt.K.W.Inst.Eisenforschung **10**,175(1928).
15. J.Inst.Metals **41**,257(1929).
16. J.Inst.Metals **44**,115(1930).
17. J.Inst.Metals **45**,307(1931).
18. Sci.Rep.Tohoku Imp.Univ. **20**,681(1931).
19. J.Inst.Metals **46**,139(1931).
20. J.Inst.Metals **46**,273(1931).
21. National Metals Handbook p.1186(1933 edition).

WASHINGTON, June 29, 1934.

○